ISSN 2218-4333 (online)

World Journal of *Clinical Oncology*

World J Clin Oncol 2024 March 24; 15(3): 360-463

Published by Baishideng Publishing Group Inc

World Journal of Clinical Oncology

Contents

Monthly Volume 15 Number 3 March 24, 2024

World Journal of Clinical Oncology

Monthly Volume 15 Number 3 March 24, 2024

Contents

World Journal of Clinical Oncology

Monthly Volume 15 Number 3 March 24, 2024

Contents

ABOUT COVER

Peer Reviewer of *World Journal of Clinical Oncology*, Alessandro Posa, MD, Department of Diagnostic Imaging, Oncologic Radiotherapy and Hematology, Fondazione Policlinico Universitario A. Gemelli - IRCCS, Rome 00168, RM, Italy. alessandro.posa@policlinicogemelli.it

AIMS AND SCOPE

The primary aim of *World Journal of Clinical Oncology* (*WJCO*, *World J Clin Oncol*) is to provide scholars and readers from various fields of oncology with a platform to publish high-quality basic and clinical research articles and communicate their research findings online.

WJCO mainly publishes articles reporting research results and findings obtained in the field of oncology and covering a wide range of topics including art of oncology, biology of neoplasia, breast cancer, cancer prevention and control, cancer-related complications, diagnosis in oncology, gastrointestinal cancer, genetic testing for cancer, gynecologic cancer, head and neck cancer, hematologic malignancy, lung cancer, melanoma, molecular oncology, neurooncology, palliative and supportive care, pediatric oncology, surgical oncology, translational oncology, and urologic oncology.

INDEXING/ABSTRACTING

The *WJCO* is now abstracted and indexed in PubMed, PubMed Central, Emerging Sources Citation Index (Web of Science), Reference Citation Analysis, China Science and Technology Journal Database, and Superstar Journals Database. The 2023 Edition of Journal Citation Reports® cites the 2022 impact factor (IF) for *WJCO* as 2.8; IF without journal self cites: 2.8; 5-year IF: 3.0; Journal Citation Indicator: 0.36.

RESPONSIBLE EDITORS FOR THIS ISSUE

NAME OF JOURNAL
World Journal of Clinical Oncology

ISSN
ISSN 2218-4333 (online)

LAUNCH DATE
November 10, 2010

FREQUENCY
Monthly

EDITORS-IN-CHIEF
Hiten RH Patel, Stephen Safe, Jian-Hua Mao, Ken H Young

EDITORIAL BOARD MEMBERS
https://www.wjgnet.com/2218-4333/editorialboard.htm

PUBLICATION DATE
March 24, 2024

INSTRUCTIONS TO AUTHORS
https://www.wjgnet.com/bpg/gerinfo/204

GUIDELINES FOR ETHICS DOCUMENTS
https://www.wjgnet.com/bpg/GerInfo/287

GUIDELINES FOR NON-NATIVE SPEAKERS OF ENGLISH
https://www.wjgnet.com/bpg/gerinfo/240

PUBLICATION ETHICS
https://www.wjgnet.com/bpg/GerInfo/288

PUBLICATION MISCONDUCT
https://www.wjgnet.com/bpg/gerinfo/208

ARTICLE PROCESSING CHARGE
https://www.wjgnet.com/bpg/gerinfo/242

STEPS FOR SUBMITTING MANUSCRIPTS
https://www.wjgnet.com/bpg/GerInfo/239

ONLINE SUBMISSION
https://www.f6publishing.com

World Journal of Clinical Oncology

Submit a Manuscript: https://www.f6publishing.com

World J Clin Oncol 2024 March 24; 15(3): 360-366

DOI: 10.5306/wjco.v15.i3.360

ISSN 2218-4333 (online)

EDITORIAL

Leveraging electrochemical sensors to improve efficiency of cancer detection

Li Fu, Hassan Karimi-Maleh

Specialty type: Oncology

Provenance and peer review: Invited article; Externally peer reviewed.

Peer-review model: Single blind

Peer-review report's scientific quality classification
Grade A (Excellent): A
Grade B (Very good): 0
Grade C (Good): 0
Grade D (Fair): 0
Grade E (Poor): 0

P-Reviewer: Ekine-Afolabi B, United Kingdom

Received: October 8, 2023
Peer-review started: October 8, 2023
First decision: December 6, 2023
Revised: December 14, 2023
Accepted: February 5, 2024
Article in press: February 5, 2024
Published online: March 24, 2024

Li Fu, College of Materials and Environmental Engineering, Hangzhou Dianzi University, Hangzhou 310018, Zhejiang Province, China

Hassan Karimi-Maleh, School of Resources and Environment, University of Electronic Science and Technology of China, Chengdu 611731, Sichuan Province, China

Hassan Karimi-Maleh, School of Engineering, Lebanese American University, Byblos 1102 2801, Lebanon

Corresponding author: Li Fu, PhD, Associate Professor, College of Materials and Environmental Engineering, Hangzhou Dianzi University, No. 2 Street, Xiasha Higher Education Zone, Hangzhou 310018, Zhejiang Province, China. fuli@hdu.edu.cn

Abstract

Electrochemical biosensors have emerged as a promising technology for cancer detection due to their high sensitivity, rapid response, low cost, and capability for non-invasive detection. Recent advances in nanomaterials like nanoparticles, graphene, and nanowires have enhanced sensor performance to allow for cancer biomarker detection, like circulating tumor cells, nucleic acids, proteins and metabolites, at ultra-low concentrations. However, several challenges need to be addressed before electrochemical biosensors can be clinically implemented. These include improving sensor selectivity in complex biological media, device miniaturization for implantable applications, integration with data analytics, handling biomarker variability, and navigating regulatory approval. This editorial critically examines the prospects of electrochemical biosensors for efficient, low-cost and minimally invasive cancer screening. We discuss recent developments in nanotechnology, microfabrication, electronics integration, multiplexing, and machine learning that can help realize the potential of these sensors. However, significant interdisciplinary efforts among researchers, clinicians, regulators and the healthcare industry are still needed to tackle limitations in selectivity, size constraints, data interpretation, biomarker validation, toxicity and commercial translation. With committed resources and pragmatic strategies, electrochemical biosensors could enable routine early cancer detection and dramatically reduce the global cancer burden.

Key Words: Electrochemical sensors; Cancer biomarkers; Nanomaterials; Point-of-care diagnostics; Microfabrication; Machine learning

Core Tip: Electrochemical biosensors represent a promising technology for efficient, minimally invasive, and low-cost cancer screening. Recent advances in nanomaterials, microfabrication, and analytics have enhanced sensor capabilities for detecting cancer biomarkers at ultra-low concentrations. However, challenges remain including improving selectivity in complex fluids, device miniaturization, seamless data integration, handling biomarker variability, nanotoxicity, and navigating regulatory approval. Significant interdisciplinary efforts are needed to address these limitations and facilitate clinical translation of electrochemical biosensors for transformative point-of-care cancer diagnostics. Managing expectations and developing pragmatic translational strategies will be imperative to unlock the potential of these sensors for early cancer detection and timely intervention.

Citation: Fu L, Karimi-Maleh H. Leveraging electrochemical sensors to improve efficiency of cancer detection. *World J Clin Oncol* 2024; 15(3): 360-366
URL: https://www.wjgnet.com/2218-4333/full/v15/i3/360.htm
DOI: https://dx.doi.org/10.5306/wjco.v15.i3.360

INTRODUCTION

Cancer remains one of the leading causes of death worldwide, with approximately 10 million deaths attributed to various forms of cancer in 2020 alone[1]. While cancer research has made tremendous strides over the past several decades in understanding the molecular basis of cancer and developing targeted therapies, early detection and diagnosis continues to play a pivotal role in patient survival and recovery. The stark reality is that many cancers have no overt symptoms until they have progressed to late stages, severely limiting treatment options and prognosis. There is an urgent need for efficient, affordable and accessible cancer screening techniques that would allow early detection and immediate treatment [2].

In this context, electrochemical biosensors have emerged as a promising platform technology that could potentially enable low-cost, point-of-care diagnostic tests for cancer[3-5]. Electrochemical biosensors utilize electrode interfaces to transduce molecular recognition events into readable electrical signals. They offer a number of advantageous features including rapid response times, high sensitivity, low sample volume requirements, and low cost. In recent years, there has been burgeoning interest in leveraging electrochemical biosensors for detecting cancer biomarkers-signature biomolecules that can indicate the presence of cancerous cells and tissues. Cancer biomarkers such as circulating tumor cells[6], cell-free nucleic acids[7], exosomes[8], proteins[9] and metabolites[10] can act as analyte targets for electrochemical biosensors.

A wide array of electrochemical transduction platforms have been explored for cancer biosensing, including amperometry, potentiometry, voltammetry and impedimetry[11]. Nanotechnology has unlocked further improvements in sensor performance by allowing nanoscale tailoring of electrode interfaces. For instance, nanomaterials like graphene [12,13], carbon nanotubes[14] and metal nanoparticles[15] can facilitate enhanced electron transfer kinetics and provide larger surface area for capture molecule immobilization. Electrochemical sensors have been designed to detect general cancer biomarkers such as prostate-specific antigens[16] as well as biomarkers specific to cancers such as lung[17], breast [18], ovarian[19] and colon[20].

While electrochemical biosensors represent a disruptive approach for cancer screening, several challenges need to be addressed before they can be clinically implemented. These include improving sensor selectivity in complex biological media, device miniaturization for possible implantable applications, seamless integration with data analytics, handling inter- and intra-tumor biomarker expression variability, and navigating regulatory approval pathways. That said, the field has been buoyed by exciting developments on multiple fronts: new nanomaterials to improve sensor performance, microfabrication techniques to enable miniaturization, multiplexing and array capabilities, machine learning for robust data analysis, and public-private efforts to facilitate technology translation.

In this editorial, we critically examine the prospects of electrochemical biosensors as a transformative platform for efficient, low-cost and minimally invasive cancer detection. We discuss recent technology advancements that poise these sensors on the cusp of making a tangible clinical impact. However, we also highlight lingering challenges that need to be addressed through committed interdisciplinary efforts among researchers, clinicians, regulators and the healthcare industry. Wider deployment of electrochemical biosensors could allow routine screening for early cancer detection, provide diagnostic decision support to physicians, enable therapeutic drug monitoring, and reduce the global cancer burden through timely intervention. Realizing this potential would require sustained investments, managing expectations, and pragmatic translational strategies.

ELECTROCHEMICAL SENSORS OFFER ADVANTAGES FOR CANCER DETECTION

Electrochemical sensors offer a number of compelling advantages that make them well-suited for cancer detection applic-

ations. First and foremost is their ability to provide sensitive and quantitative detection of cancer biomarkers, even at extremely low concentrations[21]. The fundamental principle behind electrochemical biosensing is the specific binding of target analytes to receptor molecules immobilized on the sensor surface, which generates detectable electrical signals. Carefully tailored electrode interfaces allow achieving detection limits as low as femto- or picomolar levels for cancer biomarkers. This is particularly important for early detection since cancer markers are typically present at very low abundances during initial stages.

Recent research has leveraged novel nanomaterials to further improve sensor performance. Nanoparticles[22], nanotubes[14], nanowires[23], graphene[12] and other nanostructures can be integrated with sensor electrodes to enhance electron transfer, provide higher surface area, and incorporate catalytic properties. For instance, gold nanoparticles have been functionalized with aptamers for electrochemical detection of exosomes[24], which are emerging biomarkers for non-invasive cancer diagnosis. The high surface area of nanoparticles increases aptamer loading, allowing ultrasensitive exosome detection down to a few hundred particles per micro liter. Creative combinations of nanomaterials have enabled detection limits that surpass conventional diagnostic modalities for cancer biomarkers by several orders of magnitude.

Apart from high sensitivity, electrochemical sensors also offer rapid response times[25]. Electron transfer reactions occur over milliseconds or shorter timescales. This allows real-time monitoring of interactions enabling quick measurements. For cancer screening applications, rapid results are indispensable to facilitate prompt confirmatory tests and immediate treatment. Lengthy assay times are unsuitable for point-of-care testing scenarios. The fast response kinetics of electrochemical sensors align well with the need for rapid cancer detection. Miniaturized designs also enable multiplexing capabilities for parallel detection of different cancer biomarkers[26].

Low cost and portability represent other major attractions of electrochemical sensors. The electrodes and measurement systems are based on relatively inexpensive materials and fabrication methods, especially compared to advanced imaging modalities used clinically for cancer detection[27]. This becomes particularly important for resource-limited settings and underserved communities. The sensing devices can be designed as portable, handheld gadgets operated with smartphones or miniaturized electronics. Such point-of-care analyzers can perform testing at the convenience of the patient's home or physician's office without needing dedicated laboratory infrastructure.

Importantly, electrochemical techniques allow non-invasive detection using easily accessible body fluids like blood, urine or saliva[28]. Cancer biomarkers shed by tumor cells circulate through the body and can be measured in these biofluids. Blood draws or urine samples present a far less invasive approach compared to tissue biopsies which are painful and have potential complications. Patient compliance is also improved with non-invasive tests. Furthermore, longitudinal monitoring can be easily performed to track biomarker trends or response to therapy.

However, realizing these advantages would require thoughtful sensor engineering and data interpretation. A persistent challenge is the variability in expression levels of cancer biomarkers between different malignancies and across patients with the same cancer type. This necessitates measuring biomarker panels rather than individual markers[29]. However, multiplexing capabilities of electrochemical sensors are still limited and need enhancement. The relevance of circulating biomarkers to primary tumors also remains unclear[30]. Meticulous clinical studies are therefore needed to correlate measurements with cancer onset and progression.

Preventing sensor fouling and degradation during use remains an engineering challenge. Electrochemical measurements in complex media like blood is fraught with artifacts. Sophisticated surface chemistries are necessary to impart specificity and prevent non-specific fouling[31]. The receptor molecules also need optimal orientation and retention of bioactivity upon immobilization. Furthermore, minimizing electrical noise, drift, and variability across fabrication batches is critical for reliable quantification[32]. There are open questions on device packaging for real-world point-of-care applications.

While nanomaterials boost sensor performance, their biocompatibility, toxicity and stability need deliberation[33]. Range of motion limitations and sizing constraints for implantable sensors also exist. Additionally, the lack of established regulatory guidelines is an impediment for commercial translation. Companies need to navigate approval pathways for screening non-Food and Drug Administration approved cancer biomarkers. Reimbursement mechanisms for new diagnostic technologies are uncertain. Hence, despite strong enthusiasm around electrochemical sensors, the path to actual clinical adoption remains strewn with major challenges.

CHALLENGES AND LIMITATIONS MUST BE ADDRESSED

While electrochemical biosensors hold promise for advancing cancer diagnostics, there are salient challenges and limitations that still need to be tackled before effective translation can occur.

One of the most pressing issues is enhancing the selectivity of electrochemical sensors. Biological fluids contain a multitude of components including proteins, metabolites, salts and cells[34]. Distinguishing the targeted cancer biomarkers from this complex milieu is extremely difficult. Non-specific adsorption and matrix effects often produce false signals leading to inaccurate results[35]. Novel surface chemistries, nanostructured coatings and creative receptor scaffolds are being explored to impart sensor selectivity[36]. But extensive optimization across diverse cancer biomarker panels will be necessary. Lack of adequate selectivity can preclude regulatory approval and clinical adoption due to concerns over false positives.

Sensor miniaturization is another aspect requiring innovation. Microfabrication and nanotechnology can enable miniaturization but biocompatibility, calibration and wireless communication become challenges at smaller dimensions [37]. Implantable sensors also require optimization of sensor surface area to avoid biofouling from nonspecific protein adsorption and immune reactions[38].

A major limitation Is the disconnect between cancer detection and data interpretation for decision making. Sensor development has outpaced diagnostics with most reports demonstrating cancer biomarker detection as a proof-of-concept. The next imperative step is rigorous analytical and clinical validation to generate actionable information. Large-scale studies are needed to understand intra- and inter-patient biomarker variability, correlate this variability with cancer risk, and set appropriate thresholds for screening. User-friendly data analytics need integration within point-of-care devices. Until statistical validation and clinical translation occurs, the true diagnostic utility of electrochemical sensors will remain uncertain regardless of their technical capabilities.

There are inherent biological complexities that electrochemical sensors need to address. Cancers are highly heterogeneous, even within the same organ. Relying on single biomarkers is unlikely to be sufficient, necessitating multiplexing capabilities. Furthermore, the relevance of circulating biomarkers *vs* primary tumor characteristics remains ambiguous. Differences between early stage, metastasized and treated cancers also need elucidation. Soluble biomarkers being shed into fluids may not comprehensively capture the tumor microenvironment. Implantable or minimally invasive sensors allowing in situ tumor analyses could be impactful.

In summary, while electrochemical biosensors enjoy tremendous advantages over conventional cancer diagnostics, their clinical translation and impact face multiple barriers. Key challenges remain in enhancing sensor specificity, enabling multiplexing, facilitating data interpretation, validating real-world performance, and easing product development. Addressing these limitations will require extensive interdisciplinary collaboration engaging scientists, engineers, clinicians, regulators, and the healthcare industry. With commitment and resources, the field can aspire to reach the lofty goal of deploying electrochemical devices for routine, non-invasive cancer screening. But expectations need calibration, and timelines should consider the arduous process of analytical validation, statistical correlation studies, and clinical trials prior to market approval.

THE PATH FORWARD

Despite existing challenges, there are promising developments across academic labs and startups to unlock the true potential of electrochemical sensors for efficient, low-cost cancer detection.

Novel nanomaterials are emerging as a tool to enhance the selectivity of electrochemical cancer biosensing. Two-dimensional nanosheets, nanoparticles, nanocomposites and other nanostructures can provide higher surface area for capture molecule loading while controlling orientation and spacing to minimize non-specific binding[8,18,20,30,39,40]. Combining synthetic receptors like aptamers with nanomaterials can further boost selectivity. Additionally, nanostructured coatings and membranes on sensor surfaces allow selectivity based on analyte size. Advancements in nanotechnology will be crucial to impart the requisite specificity.

Another area gaining traction is micro- and nanofabrication for sensor miniaturization. Techniques like micromachining, photolithography, 3D printing and etching can craft sensor components at the microscale[41-44]. Further miniaturization to the nanoscale may be possible with technologies like two-photon polymerization. Microfluidic integration would enable analysis from miniscule sample volumes. Miniaturized sensors could pave the way for implantable or ingestible devices for surgical and gastrointestinal applications.

Given the complexity of cancer, measuring panels of biomarkers rather than individual markers is imperative. Multiplexing and arrayed platforms allow concurrent analysis of different analytes using several individually addressable electrodes on the same chip. Companies are developing high-density sensor arrays with thousands of electrodes for massively parallel measurements[45]. Multiplexed data provides better predictive power but also necessitates advanced analytics. Towards this, data science approaches like machine learning and artificial intelligence are gaining importance to make sense of multifaceted sensor data[46-48]. Pattern recognition and multivariate models that can assimilate diverse datasets would aid in identifying correlations. Cloud analytics can enable decentralized testing at point-of-care with centralized data storage and analysis. Wider data sharing and open-access data repositories will facilitate large-scale validation studies.

CONCLUSION

In conclusion, the exploration of electrochemical biosensors in the field of cancer screening presents a pathway filled with both promise and challenges. These sensors, characterized by their high sensitivity, cost-effectiveness, and non-invasive nature, hold the potential to revolutionize early cancer detection. However, the journey from laboratory innovation to clinical application is not without obstacles. Critical areas requiring attention include enhancing sensor selectivity amidst complex biological fluids, developing multiplexed systems for comprehensive biomarker analysis, miniaturizing devices for wider applicability, and ensuring the safe integration of nanomaterials. Moreover, the interpretation of data generated by these sensors necessitates advanced analytical tools, and the entire process must navigate through the intricate labyrinth of regulatory approvals.

The future of electrochemical biosensors in cancer diagnostics hinges on the successful amalgamation of advancements in nanotechnology, microfabrication, and data science. This will demand sustained collaborative efforts across various domains of science and medicine. Investments in translational research and the formulation of pragmatic strategies are essential for transforming these innovative concepts into viable clinical tools. As we move forward, it is crucial to manage expectations realistically and acknowledge the timelines necessary for rigorous validation and clinical trials. With a balanced approach and dedicated resources, electrochemical biosensors could significantly impact cancer care, facilitating

early detection and potentially reducing the global burden of this disease.

FOOTNOTES

Author contributions: Fu L and Karimi-Maleh H contributed to this paper; Fu L designed the overall concept and outline of the manuscript; Karimi-Maleh H contributed to the discussion and design of the manuscript; Fu L and Karimi-Maleh H contributed to the writing and editing of the manuscript, illustrations, and review of the literature.

Conflict-of-interest statement: All the authors report no relevant conflicts of interest for this article.

Country/Territory of origin: China

ORCID number: Li Fu 0000-0002-5957-7790; Hassan Karimi-Maleh 0000-0002-1027-481X.

S-Editor: Li L
L-Editor: Filipodia
P-Editor: Zhang XD

REFERENCES

1 **Ferlay J**, Colombet M, Soerjomataram I, Parkin DM, Piñeros M, Znaor A, Bray F. Cancer statistics for the year 2020: An overview. *Int J Cancer* 2021 [PMID: 33818764 DOI: 10.1002/ijc.33588]
2 **Necula L**, Matei L, Dragu D, Neagu AI, Mambet C, Nedeianu S, Bleotu C, Diaconu CC, Chivu-Economescu M. Recent advances in gastric cancer early diagnosis. *World J Gastroenterol* 2019; **25**: 2029-2044 [PMID: 31114131 DOI: 10.3748/wjg.v25.i17.2029]
3 **Zhang Z**, Li Q, Du X, Liu M. Application of electrochemical biosensors in tumor cell detection. *Thorac Cancer* 2020; **11**: 840-850 [PMID: 32101379 DOI: 10.1111/1759-7714.13353]
4 **Karimi-Maleh H**, Khataee A, Karimi F, Baghayeri M, Fu L, Rouhi J, Karaman C, Karaman O, Boukherroub R. A green and sensitive guanine-based DNA biosensor for idarubicin anticancer monitoring in biological samples: A simple and fast strategy for control of health quality in chemotherapy procedure confirmed by docking investigation. *Chemosphere* 2022; **291**: 132928 [PMID: 34800513 DOI: 10.1016/j.chemosphere.2021.132928]
5 **Karimi-Maleh H**, Alizadeh M, Orooji Y, Karimi F, Baghayeri M, Rouhi J, Tajik S, Beitollahi H, Agarwal S, Gupta VK, Rajendran S, Rostamnia S, Fu L, Saberi-Movahed F, Malekmohammadi S. Guanine-Based DNA Biosensor Amplified with Pt/SWCNTs Nanocomposite as Analytical Tool for Nanomolar Determination of Daunorubicin as an Anticancer Drug: A Docking/Experimental Investigation. *Ind Eng Chem Res* 2021; **60**: 816-823 [DOI: 10.1021/acs.iecr.0c04698]
6 **Peng Y**, Lu B, Deng Y, Yang N, Li G. A dual-recognition-controlled electrochemical biosensor for accurate and sensitive detection of specific circulating tumor cells. *Biosens Bioelectron* 2022; **201**: 113973 [PMID: 35021133 DOI: 10.1016/j.bios.2022.113973]
7 **Yu P**, Lei C, Nie Z. Integration of electrochemical interface and cell-free synthetic biology for biosensing. *J Electroanal Chem (Lausanne)* 2022; **911**: 116209 [DOI: 10.1016/j.jelechem.2022.116209]
8 **Dezhakam E**, Khalilzadeh B, Mahdipour M, Isildak I, Yousefi H, Ahmadi M, Naseri A, Rahbarghazi R. Electrochemical biosensors in exosome analysis; a short journey to the present and future trends in early-stage evaluation of cancers. *Biosens Bioelectron* 2023; **222**: 114980 [PMID: 36521207 DOI: 10.1016/j.bios.2022.114980]
9 **Xie H**, Di K, Huang R, Khan A, Xia Y, Xu H, Liu C, Tan T, Tian X, Shen H, He N, Li Z. [Extracellular vesicles based electrochemical biosensors for detection of cancer cells: A review]. *Zhongguo hua xue kuai bao* 2020; **31**: 1737-1745 [DOI: 10.1016/j.cclet.2020.02.049]
10 **Lei L**, Ma B, Xu C, Liu H. Emerging tumor-on-chips with electrochemical biosensors. *TrAC Trends in Analytical Chemistry* 2022; **153**: 116640 [DOI: 10.1016/j.trac.2022.116640]
11 **Nemčeková K**, Labuda J. Advanced materials-integrated electrochemical sensors as promising medical diagnostics tools: A review. *Mater Sci Eng C Mater Biol Appl* 2021; **120**: 111751 [PMID: 33545892 DOI: 10.1016/j.msec.2020.111751]
12 **Tabish TA**, Hayat H, Abbas A, Narayan RJ. Graphene quantum dot-based electrochemical biosensing for early cancer detection. *Curr Opin Electrochem* 2021; **30**: 100786 [DOI: 10.1016/j.coelec.2021.100786]
13 **Fu L**, Zheng Y, Li X, Liu X, Lin CT, Karimi-Maleh H. Strategies and Applications of Graphene and Its Derivatives-Based Electrochemical Sensors in Cancer Diagnosis. *Molecules* 2023; **28** [PMID: 37764496 DOI: 10.3390/molecules28186719]
14 **Pandey RR**, Chusuei CC. Carbon Nanotubes, Graphene, and Carbon Dots as Electrochemical Biosensing Composites. *Molecules* 2021; **26** [PMID: 34771082 DOI: 10.3390/molecules26216674]
15 **Islam T**, Hasan MM, Awal A, Nurunnabi M, Ahammad AJS. Metal Nanoparticles for Electrochemical Sensing: Progress and Challenges in the Clinical Transition of Point-of-Care Testing. *Molecules* 2020; **25** [PMID: 33302537 DOI: 10.3390/molecules25245787]
16 **Traynor SM**, Pandey R, Maclachlan R, Hosseini A, Didar TF, Li F, Soleymani L. Review-Recent Advances in Electrochemical Detection of Prostate Specific Antigen (PSA) in Clinically-Relevant Samples. *J Electrochem Soc* 2020; **167**: 037551 [DOI: 10.1149/1945-7111/ab69fd]
17 **Khanmohammadi A**, Aghaie A, Vahedi E, Qazvini A, Ghanei M, Afkhami A, Hajian A, Bagheri H. Electrochemical biosensors for the detection of lung cancer biomarkers: A review. *Talanta* 2020; **206**: 120251 [PMID: 31514848 DOI: 10.1016/j.talanta.2019.120251]
18 **Mohammadpour-Haratbar A**, Zare Y, Rhee KY. Electrochemical biosensors based on polymer nanocomposites for detecting breast cancer:

Recent progress and future prospects. *Adv Colloid Interface Sci* 2022; **309**: 102795 [PMID: 36242876 DOI: 10.1016/j.cis.2022.102795]

19 **Ahmadi S**, Lotay N, Thompson M. Affinity-based electrochemical biosensor with antifouling properties for detection of lysophosphatidic acid, a promising early-stage ovarian cancer biomarker. *Bioelectrochemistry* 2023; **153**: 108466 [PMID: 37244204 DOI: 10.1016/j.bioelechem.2023.108466]

20 **Kaya SI**, Ozcelikay G, Mollarasouli F, Bakirhan NK, Ozkan SA. Recent achievements and challenges on nanomaterial based electrochemical biosensors for the detection of colon and lung cancer biomarkers. *Sens Actuators B Chem* 2022; **351**: 130856 [DOI: 10.1016/j.snb.2021.130856]

21 **Chupradit S**, Km Nasution M, Rahman HS, Suksatan W, Turki Jalil A, Abdelbasset WK, Bokov D, Markov A, Fardeeva IN, Widjaja G, Shalaby MN, Saleh MM, Mustafa YF, Surendar A, Bidares R. Various types of electrochemical biosensors for leukemia detection and therapeutic approaches. *Anal Biochem* 2022; **654**: 114736 [PMID: 35588855 DOI: 10.1016/j.ab.2022.114736]

22 **Singh S**, Gill AAS, Nlooto M, Karpoormath R. Prostate cancer biomarkers detection using nanoparticles based electrochemical biosensors. *Biosens Bioelectron* 2019; **137**: 213-221 [PMID: 31100601 DOI: 10.1016/j.bios.2019.03.065]

23 **Chang L**, Wu H, Chen R, Sun X, Yang Y, Huang C, Ding S, Liu C, Cheng W. Microporous PdCuB nanotag-based electrochemical aptasensor with Au@CuCl(2) nanowires interface for ultrasensitive detection of PD-L1-positive exosomes in the serum of lung cancer patients. *J Nanobiotechnology* 2023; **21**: 86 [PMID: 36906540 DOI: 10.1186/s12951-023-01845-y]

24 **Zhang M**, Xia L, Mei W, Zou Q, Liu H, Wang H, Zou L, Wang Q, Yang X, Wang K. One-step multiplex analysis of breast cancer exosomes using an electrochemical strategy assisted by gold nanoparticles. *Anal Chim Acta* 2023; **1254**: 341130 [PMID: 37005015 DOI: 10.1016/j.aca.2023.341130]

25 **Chen D**, Wu Y, Hoque S, Tilley RD, Gooding JJ. Rapid and ultrasensitive electrochemical detection of circulating tumor DNA by hybridization on the network of gold-coated magnetic nanoparticles. *Chem Sci* 2021; **12**: 5196-5201 [PMID: 34163756 DOI: 10.1039/d1sc01044a]

26 **Lopes LC**, Santos A, Bueno PR. An outlook on electrochemical approaches for molecular diagnostics assays and discussions on the limitations of miniaturized technologies for point-of-care devices. *Sens Actuators Rep* 2022; **4**: 100087 [DOI: 10.1016/j.snr.2022.100087]

27 **Shin Low S**, Pan Y, Ji D, Li Y, Lu Y, He Y, Chen Q, Liu Q. Smartphone-based portable electrochemical biosensing system for detection of circulating microRNA-21 in saliva as a proof-of-concept. *Sens Actuators B Chem* 2020; **308**: 127718 [DOI: 10.1016/j.snb.2020.127718]

28 **Sadighbayan D**, Sadighbayan K, Tohid-kia MR, Khosroushahi AY, Hasanzadeh M. Development of electrochemical biosensors for tumor marker determination towards cancer diagnosis: Recent progress. *Trends Analyt Chem* 2019; **118**: 73-88 [DOI: 10.1016/j.trac.2019.05.014]

29 **Kuntamung K**, Jakmunee J, Ounnunkad K. A label-free multiplex electrochemical biosensor for the detection of three breast cancer biomarker proteins employing dye/metal ion-loaded and antibody-conjugated polyethyleneimine-gold nanoparticles. *J Mater Chem B* 2021; **9**: 6576-6585 [PMID: 34279016 DOI: 10.1039/d1tb00940k]

30 **Koo KM**, Soda N, Shiddiky MJA. Magnetic nanomaterial-based electrochemical biosensors for the detection of diverse circulating cancer biomarkers. *Curr Opin Electrochem* 2021; **25**: 100645 [DOI: 10.1016/j.coelec.2020.100645]

31 **Wang J**, Wang D, Hui N. A low fouling electrochemical biosensor based on the zwitterionic polypeptide doped conducting polymer PEDOT for breast cancer marker BRCA1 detection. *Bioelectrochemistry* 2020; **136**: 107595 [PMID: 32711365 DOI: 10.1016/j.bioelechem.2020.107595]

32 **Sinha K**, Uddin Z, Kawsar HI, Islam S, Deen MJ, Howlader MMR. Analyzing chronic disease biomarkers using electrochemical sensors and artificial neural networks. *Trends Analyt Chem* 2023; **158**: 116861 [DOI: 10.1016/j.trac.2022.116861]

33 **Ghalkhani M**, Kaya SI, Bakirhan NK, Ozkan Y, Ozkan SA. Application of Nanomaterials in Development of Electrochemical Sensors and Drug Delivery Systems for Anticancer Drugs and Cancer Biomarkers. *Crit Rev Anal Chem* 2022; **52**: 481-503 [PMID: 32845726 DOI: 10.1080/10408347.2020.1808442]

34 **Díaz-Fernández A**, Lorenzo-Gómez R, Miranda-Castro R, de-Los-Santos-Álvarez N, Lobo-Castañón MJ. Electrochemical aptasensors for cancer diagnosis in biological fluids - A review. *Anal Chim Acta* 2020; **1124**: 1-19 [PMID: 32534661 DOI: 10.1016/j.aca.2020.04.022]

35 **Li Y**, Han R, Yu X, Chen M, Chao Q, Luo X. An antifouling and antibacterial electrochemical biosensor for detecting aminopeptidase N cancer biomarker in human urine. *Sens Actuators B Chem* 2022; **373**: 132723 [DOI: 10.1016/j.snb.2022.132723]

36 **Song G**, Han H, Ma Z. Anti-Fouling Strategies of Electrochemical Sensors for Tumor Markers. *Sensors (Basel)* 2023; **23** [PMID: 37299929 DOI: 10.3390/s23115202]

37 **Quinchia J**, Echeverri D, Cruz-Pacheco AF, Maldonado ME, Orozco J. Electrochemical Biosensors for Determination of Colorectal Tumor Biomarkers. *Micromachines (Basel)* 2020; **11** [PMID: 32295170 DOI: 10.3390/mi11040411]

38 **Zhao S**, Zang G, Zhang Y, Liu H, Wang N, Cai S, Durkan C, Xie G, Wang G. Recent advances of electrochemical sensors for detecting and monitoring ROS/RNS. *Biosens Bioelectron* 2021; **179**: 113052 [PMID: 33601131 DOI: 10.1016/j.bios.2021.113052]

39 **Sharifi M**, Avadi MR, Attar F, Dashtestani F, Ghorchian H, Rezayat SM, Saboury AA, Falahati M. Cancer diagnosis using nanomaterials based electrochemical nanobiosensors. *Biosens Bioelectron* 2019; **126**: 773-784 [PMID: 30554099 DOI: 10.1016/j.bios.2018.11.026]

40 **Singh S**, Numan A, Cinti S. Electrochemical nano biosensors for the detection of extracellular vesicles exosomes: From the benchtop to everywhere? *Biosens Bioelectron* 2022; **216**: 114635 [PMID: 35988430 DOI: 10.1016/j.bios.2022.114635]

41 **Liang T**, Liu B, Chen M, Lu Y, Chen J, Chen D, Wang J. A micromachined electrochemical angular accelerometer with highly integrated sensitive microelectrodes. *Microsyst Nanoeng* 2022; **8**: 100 [PMID: 36119376 DOI: 10.1038/s41378-022-00418-7]

42 **Sadrjavadi K**, Taran M, Fattahi A, Khoshroo A. A microelectrode system for simple measurement of neuron specific enolase with photolithography technique. *Microchem J* 2022; **182**: 107889 [DOI: 10.1016/j.microc.2022.107889]

43 **Cardoso RM**, Kalinke C, Rocha RG, Dos Santos PL, Rocha DP, Oliveira PR, Janegitz BC, Bonacin JA, Richter EM, Munoz RAA. Additive-manufactured (3D-printed) electrochemical sensors: A critical review. *Anal Chim Acta* 2020; **1118**: 73-91 [PMID: 32418606 DOI: 10.1016/j.aca.2020.03.028]

44 **A. Hondred J**, T. Johnson Z, C. Claussen J. Nanoporous gold peel-and-stick biosensors created with etching inkjet maskless lithography for electrochemical pesticide monitoring with microfluidics. *J Mater Chem C Mater* 2020; **8**: 11376-11388 [DOI: 10.1039/D0TC01423K]

45 **Thoeny V**, Melnik E, Asadi M, Mehrabi P, Schalkhammer T, Pulverer W, Maier T, Mutinati GC, Lieberzeit P, Hainberger R. Detection of breast cancer-related point-mutations using screen-printed and gold-plated electrochemical sensor arrays suitable for point-of-care applications. *Talanta Open* 2022; **6**: 100150 [DOI: 10.1016/j.talo.2022.100150]

46 **Rodrigues VC**, Soares JC, Soares AC, Braz DC, Melendez ME, Ribas LC, Scabini LFS, Bruno OM, Carvalho AL, Reis RM, Sanfelice RC, Oliveira ON Jr. Electrochemical and optical detection and machine learning applied to images of genosensors for diagnosis of prostate cancer with the biomarker PCA3. *Talanta* 2021; **222**: 121444 [PMID: 33167198 DOI: 10.1016/j.talanta.2020.121444]

47 **Amethiya Y**, Pipariya P, Patel S, Shah M. Comparative analysis of breast cancer detection using machine learning and biosensors. *Intell Med* 2022; **2**: 69-81 [DOI: 10.1016/j.imed.2021.08.004]

48 **Jeong HJ**, Kim K, Kim HW, Park Y. Classification between Normal and Cancerous Human Urothelial Cells by Using Micro-Dimensional Electrochemical Impedance Spectroscopy Combined with Machine Learning. *Sensors (Basel)* 2022; **22** [PMID: 36298320 DOI: 10.3390/s22207969]

World Journal of Clinical Oncology

Submit a Manuscript: https://www.f6publishing.com

World J Clin Oncol 2024 March 24; 15(3): 367-370

DOI: 10.5306/wjco.v15.i3.367

ISSN 2218-4333 (online)

EDITORIAL

Mechanisms and potential applications of COPS6 in pan-cancer therapy

Tong Wu, Miao-Rong Ji, Lian-Xiang Luo

Specialty type: Cell biology

Provenance and peer review: Invited article; Externally peer reviewed.

Peer-review model: Single blind

Peer-review report's scientific quality classification

Grade A (Excellent): 0
Grade B (Very good): B
Grade C (Good): 0
Grade D (Fair): 0
Grade E (Poor): 0

P-Reviewer: Liu JX, China

Received: November 2, 2023
Peer-review started: November 2, 2023
First decision: December 31, 2023
Revised: January 11, 2024
Accepted: February 4, 2024
Article in press: February 4, 2024
Published online: March 24, 2024

Tong Wu, Miao-Rong Ji, The First Clinical College, Guangdong Medical University, Zhanjiang 524023, Guangdong Province, China

Lian-Xiang Luo, The Marine Biomedical Research Institute, Guangdong Medical University, Zhanjiang 524000, Guangdong Province, China

Corresponding author: Lian-Xiang Luo, PhD, Associate Professor, The Marine Biomedical Research Institute, Guangdong Medical University, No. 2 Wenming East Road, Xiashan District, Zhanjiang 524000, Guangdong Province, China. luolianxiang321@gdmu.edu.cn

Abstract

The COP9 signalosome subunit 6 (COPS6) is abnormally overexpressed in many malignancies, yet its precise role in carcinogenesis is unknown. To gain a better understanding of COPS6's role, the authors conducted a pan-cancer analysis using various bioinformatics techniques such as differential expression patterns, prognostic value, gene mutations, immune infiltration, correlation analysis, and functional enrichment assessment. Results showed that COPS6 was highly correlated with prognosis, immune cell infiltration level, tumor mutation burden, and microsatellite instability in patients with a range of tumor types. This suggests that COPS6 may be a potential target for cancer treatment. Overall, this research provides insight into COPS6's role in cancer development and its potential therapeutic applications.

Key Words: COPS6; Biomarker; Tumor mutational burden; Immune infiltration; Prognostic analysis

Core Tip: COPS6 expression is often increased in malignancies, and this is associated with a poor prognosis, suggesting that it could be a potential biomarker for tumors. However, the exact role of COPS6 in different types of tumors is still unknown. This research seeks to investigate the expression of COPS6 in various tumor tissues, its prognostic value, mutations in the gene, and the correlation between expression levels and immune infiltration with different types of immune cells.

Citation: Wu T, Ji MR, Luo LX. Mechanisms and potential applications of COPS6 in pan-cancer therapy. *World J Clin Oncol* 2024; 15(3): 367-370
URL: https://www.wjgnet.com/2218-4333/full/v15/i3/367.htm
DOI: https://dx.doi.org/10.5306/wjco.v15.i3.367

INTRODUCTION

According to World Health Organization, cancer is the second biggest killer of people all around the world. While mortality due to cancer has been on a decreasing trend in recent times, the mortality rates for lung, colorectal, and female breast cancer are still increasing, proving to be an immense challenge for medical professionals attempting to treat it[1,2]. With the increasing number of cancer treatments, including chemo, radiation, surgery, and immunotherapy, many cancer patients still have a poor prognosis or treatment outcome. This makes it imperative to look for new targets for early diagnosis and tailored treatment. COP9 signalosome (CSN) has been found to be involved in a range of processes, such as protein degradation, DNA repair, cell cycle control, signal transduction, transcriptional activation, and tumorigenesis[3]. COPS6 is responsible for maintaining the structural integrity and function of the CSN complex in an MPN domain-dependent manner[4,5].Recently, COPS6 has been a subject of intense research as it has been observed to facilitate the growth of various types of cancers. In mouse experiments, COPS6 was determined to increase tumor growth by decreasing the ubiquitination of Myc and enhancing the degradation of Fbxw7. Additionally, it was seen to inhibit the P53-mediated tumor suppression by stabilizing MDM2 protein[6,7]. COPS6 has been identified to be involved in the epithelial-mesenchymal transition process in various tumors, which can lead to invasion and metastasis. For instance, the COPS6-UBR5-CDK9 axis has been found to regulate melanoma proliferation and metastasis[8]. COPS6 regulates tissue protease L expression levels through the autophagy-lysosome system, thereby promoting cervical cancer cell migration and invasion[9].

The use of multi-omics analysis has been a hot topic in tumor research in recent years. In our recently accepted paper, the authors used publicly available databases to investigate the role of COPS6 in various types of cancers, such as cervical cancer, papillary thyroid cancer, colorectal cancer, breast cancer, lung adenocarcinoma (LUAD), and glioblastoma. Our analysis included an examination of the differential expression patterns, prognostic value, gene mutations, immune penetration, correlation analyses, and functionally rich assessments of COPS6. Our findings provide initial evidence of the potential of COPS6 in cancer treatment. Several studies have used multi-omics analysis to identify targets for the treatment of LUAD in addition to anti-programmed cell death protein 1/programmed cell death ligand-1 immune checkpoints. For example, using multi-omics analysis, it was found that the catalytically active gene immunomodulatory factor TIM3, selective polyadenylation associated with mRNA maturation has a risk correlation to the immune microenvironment, biological transcription, and tumor cell resistance in lung adenocarcinoma, which affects the survival and prognosis of lung adenocarcinoma patients[10,11]. The multi-omics analysis of COPS6 and lung adenocarcinoma deserves to be investigated in depth.

The authors used R programming to analyze The Cancer Genome Atlas data and found that COPS6 expression levels were higher in hepatocellular carcinoma and renal clear cell carcinoma tissues. Further analysis of the Clinical Proteomic Tumor Analysis Consortium database, GEPIA2 website, and other websites revealed that COPS6 expression was correlated with the clinical stage of LUAD, KICH, KRIP, and LIHC. Prognostic analysis showed that, while high COPS6 expression usually indicated a poor prognosis in most tumors, it was associated with a good prognosis in KRIP, BRCA, LUSC, and PCPG.

Genetic mutations are known to be a major contributor to tumor growth. Studies of related websites and databases have revealed that missense mutations are the most common type of COPS6 mutations, with the highest frequency being found in esophageal adenocarcinoma, although they do not significantly influence the prognosis of the tumor. The progression and prognosis of esophageal adenocarcinoma and bladder cancer correlate with lncRNAs, and whether cops6 can improve the prognosis of esophageal and bladder cancers by affecting lncRNAs needs to be further investigated[12,13]. Tumor mutational load (TMB) has become a popular biomarker for immunotherapy, which is the total number of mutations present in a tumor sample. The higher the TMB, the more neoantigens are present, increasing the chances that some of the neoantigens presented by MHC proteins will be immunogenic, thus triggering a T-cell response and eliminating the cancer cells[14]. COPS6 expression levels have been seen to be linked to an increase in TMB and microsatellite instability in different types of tumors. The tumor microenvironment is composed of immune cells like T and B lymphocytes, natural killer cells, and tumor-associated macrophages, which are essential in determining the abnormal functioning of the tissue and in the progression of malignant tumors[15]. COPS6 expression has been found to affect the immune microenvironment in various types of tumors, particularly in breast cancer. It has been observed that COPS6 is a mediator of IL-6 production in the tumor microenvironment and a suppressor of CD8+ T cell tumor infiltration[16]. Research in the given paper found that the expression levels of COPS6 had a negative correlation with infiltration of CD8+ T-cells, a weak correlation with natural killer-cell infiltration, and a varying relationship with macrophage infiltration, depending on the subtype. Furthermore, correlation and enrichment analysis of COPS6 revealed that GPS1 and TCEB2 had the strongest correlation with it, implying that it could serve as a cancer biomarker and provide new insight into its molecular mechanism and potential targeted treatments. Additionally, as there is a lack of research on the role of COPS6 beyond pan-cancer, the value of lopinavir/ritonavir (LPV/r) in the treatment of SARS, MERS, and COVID-19 is instructive for a broad exploration of the role of COPS6[17].

This research provides a comprehensive analysis of COPS6 in a variety of cancers using R software and online analytical databases. The results showed that COPS6 is highly expressed in most cancers and linked to high-risk features, suggesting that it could be a potential cancer biomarker. Additionally, correlation and enrichment analyses identified two genes, GPS1 and TCEB2, associated with COPS6, which could be further explored to understand its mechanisms. Furthermore, the study revealed the effect of COPS6 on the infiltration of immune cells in different tumors, providing new insights for potential immunotherapy applications. However, further experiments are needed to validate the findings of this study.

CONCLUSION

This study is the first to investigate the role of COPS6 in pan-cancer. Results showed that COPS6 is highly expressed in many cancer types and is usually associated with a worse prognosis. Additionally, there was variability in the correlation between COPS6 expression and cancer-associated fibroblast infiltration. Furthermore, COPS6 was found to inhibit CD8+ T-cell infiltration in the tumor microenvironment, which facilitates tumor immune escape. In terms of gene expression, GPS1 and TCEB2 were significantly linked to COPS6. However, further research is needed to validate these findings as this study only used bioinformatics analysis. In conclusion, this paper provides a theoretical basis for the potential use of COPS6 as a biomarker in cancer research.

FOOTNOTES

Author contributions: Luo LX conceived and designed the editorial; Wu T and Ji MR wrote the editorial; Luo LX reviewed the paper and provided comments; All authors read and approved the final manuscript.

Conflict-of-interest statement: All authors declare that the research was conducted in the absence of any commercial or financial relationships that could be construed as a potential conflict of interest.

Country/Territory of origin: China

ORCID number: Lian-Xiang Luo 0000-0002-3391-9713.

S-Editor: Liu JH
L-Editor: A
P-Editor: Zhang XD

REFERENCES

1 **Feng R**, Su Q, Huang X, Basnet T, Xu X, Ye W. Cancer situation in China: what does the China cancer map indicate from the first national death survey to the latest cancer registration? *Cancer Commun (Lond)* 2023; **43**: 75-86 [PMID: 36397729 DOI: 10.1002/cac2.12393]
2 **Wang Y**, Yan Q, Fan C, Mo Y, Wang Y, Li X, Liao Q, Guo C, Li G, Zeng Z, Xiong W, Huang H. Overview and countermeasures of cancer burden in China. *Sci China Life Sci* 2023; **66**: 2515-2526 [PMID: 37071289 DOI: 10.1007/s11427-022-2240-6]
3 **Dubiel W**, Chaithongyot S, Dubiel D, Naumann M. The COP9 Signalosome: A Multi-DUB Complex. *Biomolecules* 2020; **10** [PMID: 32708147 DOI: 10.3390/biom10071082]
4 **Hou J**, Cui H. CSN6: a promising target for cancer prevention and therapy. *Histol Histopathol* 2020; **35**: 645-652 [PMID: 32016946 DOI: 10.14670/HH-18-206]
5 **Du W**, Zhang R, Muhammad B, Pei D. Targeting the COP9 signalosome for cancer therapy. *Cancer Biol Med* 2022; **19**: 573-590 [PMID: 35315259 DOI: 10.20892/j.issn.2095-3941.2021.0605]
6 **Chen J**, Shin JH, Zhao R, Phan L, Wang H, Xue Y, Post SM, Ho Choi H, Chen JS, Wang E, Zhou Z, Tseng C, Gully C, Velazquez-Torres G, Fuentes-Mattei E, Yeung G, Qiao Y, Chou PC, Su CH, Hsieh YC, Hsu SL, Ohshiro K, Shaikenov T, Yeung SC, Lee MH. CSN6 drives carcinogenesis by positively regulating Myc stability. *Nat Commun* 2014; **5**: 5384 [PMID: 25395170 DOI: 10.1038/ncomms6384]
7 **Zhao R**, Yeung SC, Chen J, Iwakuma T, Su CH, Chen B, Qu C, Zhang F, Chen YT, Lin YL, Lee DF, Jin F, Zhu R, Shaikenov T, Sarbassov D, Sahin A, Wang H, Lai CC, Tsai FJ, Lozano G, Lee MH. Subunit 6 of the COP9 signalosome promotes tumorigenesis in mice through stabilization of MDM2 and is upregulated in human cancers. *J Clin Invest* 2011; **121**: 851-865 [PMID: 21317535 DOI: 10.1172/JCI44111]
8 **Zhang Y**, Hou J, Shi S, Du J, Liu Y, Huang P, Li Q, Liu L, Hu H, Ji Y, Guo L, Shi Y, Cui H. CSN6 promotes melanoma proliferation and metastasis by controlling the UBR5-mediated ubiquitination and degradation of CDK9. *Cell Death Dis* 2021; **12**: 118 [PMID: 33483464 DOI: 10.1038/s41419-021-03398-0]
9 **Mao Z**, Sang MM, Chen C, Zhu WT, Gong YS, Pei DS. CSN6 Promotes the Migration and Invasion of Cervical Cancer Cells by Inhibiting Autophagic Degradation of Cathepsin L. *Int J Biol Sci* 2019; **15**: 1310-1324 [PMID: 31223289 DOI: 10.7150/ijbs.32987]

10 **Wu L**, Zhong Y, Wu D, Xu P, Ruan X, Yan J, Liu J, Li X. Immunomodulatory Factor TIM3 of Cytolytic Active Genes Affected the Survival and Prognosis of Lung Adenocarcinoma Patients by Multi-Omics Analysis. *Biomedicines* 2022; **10** [PMID: 36140350 DOI: 10.3390/biomedicines10092248]

11 **Wu L**, Zhong Y, Yu X, Wu D, Xu P, Lv L, Ruan X, Liu Q, Feng Y, Liu J, Li X. Selective poly adenylation predicts the efficacy of immunotherapy in patients with lung adenocarcinoma by multiple omics research. *Anticancer Drugs* 2022; **33**: 943-959 [PMID: 35946526 DOI: 10.1097/CAD.0000000000001319]

12 **Wu L**, Zheng Y, Ruan X, Wu D, Xu P, Liu J, Li X. Long-chain noncoding ribonucleic acids affect the survival and prognosis of patients with esophageal adenocarcinoma through the autophagy pathway: construction of a prognostic model. *Anticancer Drugs* 2022; **33**: e590-e603 [PMID: 34338240 DOI: 10.1097/CAD.0000000000001189]

13 **Liu J**, Tian C, Qiao J, Deng K, Ye X, Xiong L. m6A Methylation-Mediated Stabilization of LINC01106 Suppresses Bladder Cancer Progression by Regulating the miR-3148/DAB1 Axis. *Biomedicines* 2024; **12** [PMID: 38255219 DOI: 10.3390/biomedicines12010114]

14 **Jardim DL**, Goodman A, de Melo Gagliato D, Kurzrock R. The Challenges of Tumor Mutational Burden as an Immunotherapy Biomarker. *Cancer Cell* 2021; **39**: 154-173 [PMID: 33125859 DOI: 10.1016/j.ccell.2020.10.001]

15 **Chen F**, Zhuang X, Lin L, Yu P, Wang Y, Shi Y, Hu G, Sun Y. New horizons in tumor microenvironment biology: challenges and opportunities. *BMC Med* 2015; **13**: 45 [PMID: 25857315 DOI: 10.1186/s12916-015-0278-7]

16 **Du WQ**, Zhu ZM, Jiang X, Kang MJ, Pei DS. COPS6 promotes tumor progression and reduces CD8(+) T cell infiltration by repressing IL-6 production to facilitate tumor immune evasion in breast cancer. *Acta Pharmacol Sin* 2023; **44**: 1890-1905 [PMID: 37095198 DOI: 10.1038/s41401-023-01085-8]

17 **Wu L**, Zheng Y, Liu J, Luo R, Wu D, Xu P, Li X. Comprehensive evaluation of the efficacy and safety of LPV/r drugs in the treatment of SARS and MERS to provide potential treatment options for COVID-19. *Aging (Albany NY)* 2021; **13**: 10833-10852 [PMID: 33879634 DOI: 10.18632/aging.202860]

World Journal of Clinical Oncology

Submit a Manuscript: https://www.f6publishing.com

World J Clin Oncol 2024 March 24; 15(3): 371-374

DOI: 10.5306/wjco.v15.i3.371

ISSN 2218-4333 (online)

EDITORIAL

High-dose methotrexate and zanubrutinib combination therapy for primary central nervous system lymphoma

Budhi Singh Yadav

Specialty type: Oncology

Provenance and peer review: Invited article; Externally peer reviewed.

Peer-review model: Single blind

Peer-review report's scientific quality classification

Grade A (Excellent): 0
Grade B (Very good): 0
Grade C (Good): C
Grade D (Fair): 0
Grade E (Poor): 0

P-Reviewer: Reis F, Brazil

Received: November 23, 2023
Peer-review started: November 23, 2023
First decision: January 12, 2024
Revised: January 13, 2024
Accepted: February 20, 2024
Article in press: February 20, 2024
Published online: March 24, 2024

Budhi Singh Yadav, Department of Radiotherapy & Oncology, Post Graduate Institute of Medical Education & Research, Chandigarh 160012, India

Corresponding author: Budhi Singh Yadav, MD, Professor, Department of Radiotherapy & Oncology, Post Graduate Institute of Medical Education & Research, Regional Cancer Centre, Sector 12, Chandigarh 160012, India. drbudhi@gmail.com

Abstract

In this editorial I comment on the article, published in the current issue of the *World Journal of Clinical Oncology*. Primary central nervous system lymphoma (PCNSL) is a disease of elderly and immunocompromised patients. The authors reported clinical results of 19 patients with PCNSL treated with zanubrutinib/high dose methotrexate (HD-MTX) until disease progression. They demonstrated that the combination of zanubrutinib with HD-MTX led to a marked clinical response and tolerability among these patients. They also observed that cerebrospinal fluid liquid biopsy to detect circulating tumor DNA may be a good option for evaluating treatment response and tumor burden in patients with PCNSL. PCNSL is a challenging disease for treatment as these patients present with different neurological states and comorbidities. Treatment has evolved over the years from whole brain radiotherapy to HD-MTX followed by autologous stem cell transplant. Gradually, treatment of patients with PCNSL is going to become individualized.

Key Words: Primary central nervous system lymphoma; High dose methotrexate; Zanubrutinib; Whole brain radiotherapy; Liquid biopsy

Core Tip: Primary central nervous system lymphoma is treated with high dose methotrexate induction followed by consolidation with whole-brain radiotherapy or autologous stem cell transplant. Depending on the general condition and disease status of these patients they can be offered maintenance therapy. Zanbrutinib may be offered to these patients for maintaining the response to primary treatment.

Citation: Yadav BS. High-dose methotrexate and zanubrutinib combination therapy for primary central nervous system lymphoma. *World J Clin Oncol* 2024; 15(3): 371-374
URL: https://www.wjgnet.com/2218-4333/full/v15/i3/371.htm
DOI: https://dx.doi.org/10.5306/wjco.v15.i3.371

INTRODUCTION

This editorial is for the article "Clinical outcomes of newly diagnosed primary central nervous system lymphoma treated with zanubrutinib-based combination therapy" by Wang *et al*[1] in the current issue of *World Journal of Clinical Oncology*. In this study, the authors treated 19 patients with primary central nervous system lymphoma (PCNSL) with zanubrutinib/high dose methotrexate (HD-MTX) until disease progression. They concluded that zanubrutinib in addition with HD-MTX showed a noticeable disease response with a good toxicity profile in these patients. At a median follow-up of 14.7 months (range, 3.9–30 months), the overall response rate (ORR) was 84.2%, and progression-free survival (PFS) and overall survival (OS) rates at 2-year were 75.6% and 94.1%, respectively. They also observed that cerebrospinal fluid (CSF) liquid biopsy to detect circulating tumor DNA (ctDNA) may be a good option for evaluating treatment response and tumor burden in PCNSL. However, considering the limitations of the study such as small sample size, single institutional and retrospective by nature, it may be difficult to draw concrete conclusions from this study.

PCNSL is a relatively rare extranodal non-Hodgkin lymphoma which can manifest in the brain, leptomeninges, spinal cord or eyes. It comprises 3% of all brain malignancies[2]. PCNSL, being a disease of elderly and immunocompromised patients, poses a treatment challenge[3,4]. A few cases have also been reported in immunocompetent patients[5,6]. Age and performance status (PS) are two important prognostic factors which help in deciding the treatment strategy for these patients. Other factors such as comorbidity and organ functions also affect treatment decisions. Usually, 60 years is considered as a cutoff for young *vs* elderly patients; however, this cutoff has fluctuated between 60 to 75 years.

Conventional treatment has not improved survival in these patients[7]. In a randomized trial where whole brain radiotherapy (WBRT) was compared to chemotherapy, median PFS in the WBRT arm and the chemotherapy-only arm was 18 and 12 months, respectively (P = 0.14) and median OS was 32 months (95%CI, 26 to 39 months) *vs* 37 months (95%CI, 28 to 47 months), respectively (P = 0.71)[8]. The standard treatment for PCNSL consists of induction with combination chemotherapy followed by consolidation with WBRT or autologous stem cell transplant (ASCT). As treatment options for PCNSL have increased, OS has improved in these patients. Ferreri *et al*[8] concluded that WBRT and ASCT were both viable and effective options as consolidation therapies after HD-MTX chemotherapy for patients with PCNSL aged < 70 years. A landmark multicenter trial by DeAngelis *et al*[9] demonstrated that combination chemotherapy and radiotherapy improved survival as compared to historical reports of radiotherapy alone in patients with PCNSL. They used a higher dose of radiotherapy, 45 Gy/25#/5 wk, which may lead to increased neurotoxicity in these patients. In another multicentre study, Morris *et al*[10] used rituximab, methotrexate, procarbazine, and vincristine in sequence with consolidation reduced-dose WBRT and cytarabine in PCNSL. They demonstrated that this treatment led to high response rates, long-term disease control with minimal neurotoxicity.

HD-MTX has been the backbone of PCNSL treatment. The role of rituximab in PCNSL is controversial because of its poor CSF penetration. Multiple options are being explored to improve outcomes in these patients. Elderly patients with comorbidity are usually treated with HD-MTX and an alkylating agent. In good responders, it has been consolidated with 23.4 Gy in 13 fractions over 2.5 wk. Few elderly patients with good PS and organ functions have an option of high dose therapy followed by ASCT. Unfit patients not suitable for HD-MTX may be candidates for WBRT, which resulted in 2-year PFS of 30%, as reported by Thiel *et al*[7].

Zanubritinib is a second-generation oral Bruton tyrosin kinase (BTK) inhibitor. It has greater tyrosine kinase selectivity than ibrutinib. A twice-daily dose of 160 mg has been shown to completely occupy BTK receptors[11,12]. In patients with relapsed or refractory chronic lymphocytic leukemia or small lymphocytic lymphoma, zanubrutinib was associated with significantly better PFS and toxicity profile as compared to ibrutinib[13].

Wang *et al*[1] explored zanubrutinib with HD-MTX in newly diagnosed PCNSL patients. The ORR and PFS were comparable to those reported by Morris *et al*[10] (ORR = 84.2% *vs* 95%, respectively; 2-year PFS = 75.6% *vs* 77%, respectively). Patients in the trial by Wang *et al*[1] were younger as compared to that of by Morris *et al*[10] (median age 50 *vs* 60 years). There were no treatment-related deaths which indicates a moderate safety profile for zanubrutinib in combination with HD-MTX for patients with PCNSL.

ctDNA can be detected in CSF. It can provide diagnostic and prognostic information. It can identify potential therapeutic targets, monitor the tumour response to treatment and identify residual disease. Its level can predict resistance to treatment and help to identify tumour relapse[14]. Wang *et al*[1] demonstrated an ORR of 50%–60% by identifying different gene mutations in PCNL patients. This kind of intervention will help in providing personalized care to these patients. Although CSF analysis is less invasive than surgery, it may not be possible to do lumbar puncture in all the patients because of different medical conditions.

The tumor microenvironment in the PCNSL is different from the extra central nervous system lymphoma which makes it a difficult disease to treat. There are many target receptors in PCNSL apart from B-cell antigen receptor and Toll-like receptor signaling, such as programmed cell death-1 (PD-1)/PD-1 Ligand and immune activation shown by presence of tumor infiltrating lymphocytes. So, targeting one pathway may not be sufficient to treat such a debilitating disease[15,16]. CSF analysis may not provide information about the tumor microenvironment.

CONCLUSION

Zanubrutinib combined with HD-MTX might be an option for patients with PCNSL. However, cost of the treatment remains a concern with this therapy. Other concerns are that it needs to be tested in a large cohort from multiple centers to see whether these results are reproducible.

FOOTNOTES

Author contributions: Yadav BS contributed to concept design, literature review, manuscript writing, revision, final approval.

Conflict-of-interest statement: All the authors report no relevant conflicts of interest for this article.

Country/Territory of origin: India

ORCID number: Budhi Singh Yadav 0000-0001-6185-4139.

S-Editor: Li L
L-Editor: A
P-Editor: Zhao S

REFERENCES

1 **Wang N**, Chen FL, Pan L, Teng Y, Wei XJ, Guo HG, Jiang XM, Huang L, Liu SC, Liang ZL, Li WY. Clinical outcomes of newly diagnosed primary central nervous system lymphoma treated with zanubrutinib-based combination therapy. *World J Clin Oncol* 2023; **14**: 606-619 [PMID: 38179402 DOI: 10.5306/wjco.v14.i12.606]

2 **Ferreri AJM**. Therapy of primary CNS lymphoma: role of intensity, radiation, and novel agents. *Hematology Am Soc Hematol Educ Program* 2017; **2017**: 565-577 [PMID: 29222306 DOI: 10.1182/asheducation-2017.1.565]

3 **Radotra BD**, Parkhi M, Chatterjee D, Yadav BS, Ballari NR, Prakash G, Gupta SK. Clinicopathological features of primary central nervous system diffuse large B cell lymphoma: Experience from a Tertiary Center in North India. *Surg Neurol Int* 2020; **11**: 424 [PMID: 33365186 DOI: 10.25259/SNI_314_2020]

4 **Makhdoomi R**, Nayil K, Rayees A, Kirmani A, Ramzan A, Khalil MB, Dhar A, Besina S, Chanda N, Lone AR, Qadiri S, Maqbool M. Primary CNS lymphoma in immunocompetent: a review of literature and our experience from Kashmir. *Turk Neurosurg* 2011; **21**: 39-47 [PMID: 21294090 DOI: 10.5137/1019-5149.JTN.3100-10.2]

5 **Beraldo GL**, Brito ABC, Delamain MT, Souza CA, Lima CSP, Bonfitto JFL, Queiroz LS, Reis F. Primary infratentorial diffuse large b-cell lymphoma: a challenging diagnosis in an immunocompetent patient. *Rev Assoc Med Bras (1992)* 2019; **65**: 136-140 [PMID: 30892435 DOI: 10.1590/1806-9282.65.2.136]

6 **Yadav BS**, Mahajan R, Sharma SC, Gupta A, Kumar S. Primary central nervous system lymphoma: an experience of a Regional Cancer Center from India. *J Radiat Cancer Res* 2019; **10**: 104-107 [DOI: 10.4103/jrcr.jrcr_15_19]

7 **Thiel E**, Korfel A, Martus P, Kanz L, Griesinger F, Rauch M, Röth A, Hertenstein B, von Toll T, Hundsberger T, Mergenthaler HG, Leithäuser M, Birnbaum T, Fischer L, Jahnke K, Herrlinger U, Plasswilm L, Nägele T, Pietsch T, Bamberg M, Weller M. High-dose methotrexate with or without whole brain radiotherapy for primary CNS lymphoma (G-PCNSL-SG-1): a phase 3, randomised, non-inferiority trial. *Lancet Oncol* 2010; **11**: 1036-1047 [PMID: 20970380 DOI: 10.1016/S1470-2045(10)70229-1]

8 **Ferreri AJM**, Cwynarski K, Pulczynski E, Fox CP, Schorb E, La Rosée P, Binder M, Fabbri A, Torri V, Minacapelli E, Falautano M, Ilariucci F, Ambrosetti A, Roth A, Hemmaway C, Johnson P, Linton KM, Pukrop T, Sønderskov Gørløv J, Balzarotti M, Hess G, Keller U, Stilgenbauer S, Panse J, Tucci A, Orsucci L, Pisani F, Levis A, Krause SW, Schmoll HJ, Hertenstein B, Rummel M, Smith J, Pfreundschuh M, Cabras G, Angrilli F, Ponzoni M, Deckert M, Politi LS, Finke J, Reni M, Cavalli F, Zucca E, Illerhaus G; International Extranodal Lymphoma Study Group (IELSG). Whole-brain radiotherapy or autologous stem-cell transplantation as consolidation strategies after high-dose methotrexate-based chemoimmunotherapy in patients with primary CNS lymphoma: results of the second randomisation of the International Extranodal Lymphoma Study Group-32 phase 2 trial. *Lancet Haematol* 2017; **4**: e510-e523 [PMID: 29054815 DOI: 10.1016/S2352-3026(17)30174-6]

9 **DeAngelis LM**, Seiferheld W, Schold SC, Fisher B, Schultz CJ; Radiation Therapy Oncology Group Study 93-10. Combination chemotherapy and radiotherapy for primary central nervous system lymphoma: Radiation Therapy Oncology Group Study 93-10. *J Clin Oncol* 2002; **20**: 4643-4648 [PMID: 12488408 DOI: 10.1200/JCO.2002.11.013]

10 **Morris PG**, Correa DD, Yahalom J, Raizer JJ, Schiff D, Grant B, Grimm S, Lai RK, Reiner AS, Panageas K, Karimi S, Curry R, Shah G, Abrey LE, DeAngelis LM, Omuro A. Rituximab, methotrexate, procarbazine, and vincristine followed by consolidation reduced-dose whole-brain radiotherapy and cytarabine in newly diagnosed primary CNS lymphoma: final results and long-term outcome. *J Clin Oncol* 2013; **31**: 3971-3979 [PMID: 24101038 DOI: 10.1200/JCO.2013.50.4910]

11 **Tam CS**, Trotman J, Opat S, Burger JA, Cull G, Gottlieb D, Harrup R, Johnston PB, Marlton P, Munoz J, Seymour JF, Simpson D, Tedeschi A, Elstrom R, Yu Y, Tang Z, Han L, Huang J, Novotny W, Wang L, Roberts AW. Phase 1 study of the selective BTK inhibitor zanubrutinib in B-cell malignancies and safety and efficacy evaluation in CLL. *Blood* 2019; **134**: 851-859 [PMID: 31340982 DOI: 10.1182/blood.2019001160]

12 **Ou YC**, Tang Z, Novotny W, Cohen A, Wang K, Liu L, Gao Y, Sahasranaman S. Rationale for once-daily or twice-daily dosing of zanubrutinib in patients with mantle cell lymphoma. *Leuk Lymphoma* 2021; **62**: 2612-2624 [PMID: 34159878 DOI: 10.1080/10428194.2021.1929961]

13 **Brown JR**, Eichhorst B, Hillmen P, Jurczak W, Kaźmierczak M, Lamanna N, O'Brien SM, Tam CS, Qiu L, Zhou K, Simkovic M, Mayer J, Gillespie-Twardy A, Ferrajoli A, Ganly PS, Weinkove R, Grosicki S, Mital A, Robak T, Osterborg A, Yimer HA, Salmi T, Wang MD, Fu L, Li J, Wu K, Cohen A, Shadman M. Zanubrutinib or Ibrutinib in Relapsed or Refractory Chronic Lymphocytic Leukemia. *N Engl J Med* 2023; **388**: 319-332 [PMID: 36511784 DOI: 10.1056/NEJMoa2211582]

14 **Bobillo S**, Crespo M, Escudero L, Mayor R, Raheja P, Carpio C, Rubio-Perez C, Tazón-Vega B, Palacio C, Carabia J, Jiménez I, Nieto JC, Montoro J, Martínez-Ricarte F, Castellvi J, Simó M, Puigdefàbregas L, Abrisqueta P, Bosch F, Seoane J. Cell free circulating tumor DNA in cerebrospinal fluid detects and monitors central nervous system involvement of B-cell lymphomas. *Haematologica* 2021; **106**: 513-521 [PMID: 32079701 DOI: 10.3324/haematol.2019.241208]

15 **Parkhi M**, Chatterjee D, Bal A, Vias P, Yadav BS, Prakash G, Gupta SK, Radotra BD. Prognostic implications of the tumor immune microenvironment and immune checkpoint pathway in primary central nervous system diffuse large B-cell lymphoma in the North Indian population. *APMIS* 2022; **130**: 82-94 [PMID: 34862664 DOI: 10.1111/apm.13195]

16 **Parkhi M**, Chatterjee D, Radotra BD, Bal A, Yadav BS, Tripathi M. Double-hit and double-expressor primary central nervous system lymphoma: Experience from North India of an infrequent but aggressive variant. *Surg Neurol Int* 2023; **14**: 172 [PMID: 37292392 DOI: 10.25259/SNI_307_2023]

World Journal of Clinical Oncology

Submit a Manuscript: https://www.f6publishing.com

World J Clin Oncol 2024 March 24; 15(3): 375-377

DOI: 10.5306/wjco.v15.i3.375

ISSN 2218-4333 (online)

EDITORIAL

Role of targeting ferroptosis as a component of combination therapy in combating drug resistance in colorectal cancer

Xiao-Ting Xie, Qiang-Hu Pang, Lian-Xiang Luo

Specialty type: Cell biology

Provenance and peer review: Invited article; Externally peer reviewed.

Peer-review model: Single blind

Peer-review report's scientific quality classification

Grade A (Excellent): 0
Grade B (Very good): B
Grade C (Good): 0
Grade D (Fair): 0
Grade E (Poor): 0

P-Reviewer: Vynios D, Greece

Received: December 8, 2023
Peer-review started: December 8, 2023
First decision: December 18, 2023
Revised: December 27, 2023
Accepted: February 25, 2024
Article in press: February 25, 2024
Published online: March 24, 2024

Xiao-Ting Xie, Qiang-Hu Pang, The First Clinical College, Guangdong Medical University, Zhanjiang 524023, Guangdong Province, China

Lian-Xiang Luo, The Marine Biomedical Research Institute, Guangdong Medical University, Zhanjiang 524023, Guangdong Province, China

Corresponding author: Lian-Xiang Luo, PhD, Associate Professor, The Marine Biomedical Research Institute, Guangdong Medical University, No. 2 Wenming East Road, Xiashan District, Zhanjiang 524023, Guangdong Province, China. lulianxiang321@gdmu.edu.cn

Abstract

Colorectal cancer (CRC) is a form of cancer that is often resistant to chemotherapy, targeted therapy, radiotherapy, and immunotherapy due to its genomic instability and inflammatory tumor microenvironment. Ferroptosis, a type of non-apoptotic cell death, is characterized by the accumulation of iron and the oxidation of lipids. Studies have revealed that the levels of reactive oxygen species and glutathione in CRC cells are significantly lower than those in healthy colon cells. Erastin has emerged as a promising candidate for CRC treatment by diminishing stemness and chemoresistance. Moreover, the gut, responsible for regulating iron absorption and release, could influence CRC susceptibility through iron metabolism modulation. Investigation into ferroptosis offers new insights into CRC pathogenesis and clinical management, potentially revolutionizing treatment approaches for therapy-resistant cancers.

Key Words: Colorectal cancer; Ferroptosis; Immunotherapy; Drug resistance; Chemotherapy; Nanodrug delivery systems

Core Tip: Drug resistance poses a challenge to the treatment of colorectal cancer (CRC). In this paper, we offer novel perspectives on tackling this issue by focusing on ferroptosis in CRC cells. This approach holds promise in overcoming tumor cell resistance caused by CRC genome instability and changes in the tumor microenvironment, thereby providing innovative therapeutic strategies to break through the clinical drug resistance in CRC.

Citation: Xie XT, Pang QH, Luo LX. Role of targeting ferroptosis as a component of combination therapy in combating drug resistance in colorectal cancer. *World J Clin Oncol* 2024; 15(3): 375-377
URL: https://www.wjgnet.com/2218-4333/full/v15/i3/375.htm
DOI: https://dx.doi.org/10.5306/wjco.v15.i3.375

INTRODUCTION

Colorectal cancer (CRC) is a serious and aggressive form of cancer. Unfortunately, the majority of patients are diagnosed at advanced stages, with 50% of cases being prone to liver metastasis, leading to a poor prognosis and high mortality rate. The inflammatory tumor microenvironment (TME) and genomic instability in CRC make it resistant to existing treatments such as chemotherapy, targeted therapy, and immunotherapy. Ferroptosis emerges as a novel type of programmed cell death that is dependent on iron-induced lipid peroxidation. Cancer cells can evade ferroptosis signaling pathways, resulting in uncontrolled disease progression and drug resistance. Recently, ferroptosis has been proposed as a potential solution to the issue of cancer cells bypassing apoptosis and anti-apoptosis-induced drug resistance and metastasis[1].

The adenomatous polyposis coli (APC) tumor suppressor protein, forming a complex with GSK-3β and AXIN1, plays a significant role in the frequent mutation occurrence in CRC. Deactivation of this protein stands as a common CRC trigger. Studies indicate that pretreating HeLa cells with a GSK-3β inhibitor can thwart erastin-induced ferroptosis[2]. AMER1 is recognized as part of a complex that recruits AXIN1, β-TrCP, and APC to facilitate β-catenin ubiquitination and degradation. In CRC cells with wild-type status, AMER1 binds to SLC7A11 or FTL, recruiting β-TrCP1/2 to expedite FTL and SLC7A11 ubiquitination and degradation. This leads to an escalation in the labile free iron pool and a decline in cystine uptake, causing reactive oxygen species (ROS) overload and ferroptosis induction. However, AMER1 absence *in vivo* shields metastatic CRC cells from ferroptosis triggered by elevated blood oxygen levels, fostering CRC cell metastasis. This underscores a correlation between AMER1 mutations and CRC metastasis[3]. Studies have showed that KRAS mutations are one of the most common mutations in CRC. A recent study found that in male CRC patients, untargeted metabolomics data revealed that tumors with KRAS mutations have several pathways that inhibit ferroptosis. Furthermore, targeted metabonomics of RSL3 MC38 cells harboring KRAS mutations confirmed this finding by identifying iron metabolite precipitation. Inadequate administration of cetuximab to KRAS mutant cell lines can increase lipid peroxides or induce ferroptosis. Additionally, when used in combination with cetuximab and RSL3, cetuximab increases ROS production and the malondialdehyde enhanced RSL3 cytotoxic effect[4]. This suggests the clinical potential of ferroptosis inducers as a component of combination therapies to target tumor antioxidant status and treat CRC.

Chemotherapy is widely used in the clinical treatment of CRC. Oxaliplatin (OXA), as a chemotherapeutic drug, is frequently used in the treatment of CRC, but patients frequently develop drug resistance, which limits its therapeutic effect. Some studies have found that cyclin dependent kinase 1 (CDK1) may be a key factor in OXA resistance. The mRNA and protein levels of CDK1 were significantly up-regulated in OXA-resistant CRC tissues, while the number of clones formed by CDK1 knockout cells treated with OXA was decreased, indicating that the depletion of CDK1 could overcome OXA resistance in CRC patients. Moreover, the physical interaction of CDK1 with ACSL4 led to ACSL4 degradation in OXA-resistant CRC cells, thwarting tumor cell ferroptosis. Thus, inhibiting ACSL4 lipid peroxidation and promoting ferroptosis through CDK1 inhibition create essential conditions for managing OXA-resistant CRC patients. CDK1 inhibitors synergistically enhance the anti-tumor effect of OXA in OXA-resistant CRC[5]. Additionally, research has unveiled that the ferrophilic short-chain fatty acid butyrate can enhance the ferrophilic ability of OXA and induce ferroptosis in CRC. Butyrate can also inhibit xCT mediated ferroptosis resistance by inducing c-Fos expression, reverse the resistance of cancer stem cells to ferroptosis, and promote the occurrence of ferroptosis[6].

The conventional treatment of metastatic CRC, however, is still limited by the adverse reactions associated with chemotherapy drugs and the biological characteristics of tumors. Immune checkpoint blockade holds considerable promise in malignancy treatment. Regrettably, immunotherapy achieves notable curative outcomes only in a minority of patients with high microsatellite instability, with most patients displaying a certain level of resistance. Research indicates that CYP1B1 enhances tumor cell resistance to ferroptosis by increasing ACSL4 ubiquitination and promoting its degradation, and the therapeutic effect of anti-PD-1 therapy may be enhanced by inhibiting CYP1B1[7]. Moreover, through *in vivo* analysis, some researchers have identified the role of the APOL3-LDHA axis in promoting CRC cell ferroptosis and enhancing CD8+ T cell cytotoxicity by increasing IFNγ levels and reducing lactate concentration in the TME[8]. These findings suggest that targeting ferroptosis in CRC cells might effectively combat immune checkpoint blockade resistance.

Because targeting ferroptosis has shown great potential in CRC treatment, enhancing the selectivity of ferroptosis inducers and mitigating unnecessary side effects emerge as pressing concerns in clinical transformation. In this regard, the development of nanotechnology provides new possibilities for ferroptosis induction in cancer treatment. Nanodrug delivery systems (nano-DDSs) leverage the unique physical and chemical properties of nanomaterials for efficient targeted drug delivery to achieve more precise therapeutic effects[9]. Zhang *et al*[10] coordinated and assembled ions with 6-[2-(3-methyl)-naphthoquinyl]-hexanoic acid (NQA), a derivative of vitamin K3, to obtain multifunctional Fe-NQA nanopolymer particles, which reduced Fe^{3+} to Fe^{2+} while producing a large amount of ROS. In addition, the Fenton reaction occurred and ferroptosis was induced. The nano-DDS exhibited remarkable tumor inhibitory effect and inhibited tumor metastasis in the CT26 mouse tumor model. Most importantly, some studies have suggested that nano-DDSs may improve the multidrug resistance of CRC cells and the treatment effect in CRC patients[11]. These findings proved that

nano-therapy has great potential in targeting ferroptosis in CRC cells. However, since nano-DDSs are still in the emerging stage of research, more clinical studies are needed to further explore their efficacy.

CONCLUSION

This editorial emphasizes the potential of targeting ferroptosis in CRC cells to reduce the drug resistance of tumor cells due to CRC genomic instability and inflammatory TME, and presents a potential new approach for the treatment of this malignancy by combining ferroptosis targeting with chemotherapy, targeted therapy, radiotherapy, and immunotherapy.

FOOTNOTES

Author contributions: Xie XT, Pang QH, and Luo LX wrote the editorial; Luo LX conceived and designed the editorial, reviewed the paper, and provided comments; all authors read and approved the final manuscript.

Conflict-of-interest statement: All authors declare no conflicts of interest for this article.

Country/Territory of origin: China

ORCID number: Lian-Xiang Luo 0000-0002-3391-9713.

S-Editor: Zhang H
L-Editor: Wang TQ
P-Editor: Zhao S

REFERENCES

1 **Yan H**, Talty R, Aladelokun O, Bosenberg M, Johnson CH. Ferroptosis in colorectal cancer: a future target? *Br J Cancer* 2023; **128**: 1439-1451 [PMID: 36703079 DOI: 10.1038/s41416-023-02149-6]
2 **Wang L**, Ouyang S, Li B, Wu H, Wang F. GSK-3β manipulates ferroptosis sensitivity by dominating iron homeostasis. *Cell Death Discov* 2021; **7**: 334 [PMID: 34732689 DOI: 10.1038/s41420-021-00726-3]
3 **Lei S**, Chen C, Han F, Deng J, Huang D, Qian L, Zhu M, Ma X, Lai M, Xu E, Zhang H. AMER1 deficiency promotes the distant metastasis of colorectal cancer by inhibiting SLC7A11- and FTL-mediated ferroptosis. *Cell Rep* 2023; **42**: 113110 [PMID: 37682704 DOI: 10.1016/j.celrep.2023.113110]
4 **Yang J**, Mo J, Dai J, Ye C, Cen W, Zheng X, Jiang L, Ye L. Cetuximab promotes RSL3-induced ferroptosis by suppressing the Nrf2/HO-1 signalling pathway in KRAS mutant colorectal cancer. *Cell Death Dis* 2021; **12**: 1079 [PMID: 34775496 DOI: 10.1038/s41419-021-04367-3]
5 **Zeng K**, Li W, Wang Y, Zhang Z, Zhang L, Zhang W, Xing Y, Zhou C. Inhibition of CDK1 Overcomes Oxaliplatin Resistance by Regulating ACSL4-mediated Ferroptosis in Colorectal Cancer. *Adv Sci (Weinh)* 2023; **10**: e2301088 [PMID: 37428466 DOI: 10.1002/advs.202301088]
6 **He Y**, Ling Y, Zhang Z, Mertens RT, Cao Q, Xu X, Guo K, Shi Q, Zhang X, Huo L, Wang K, Guo H, Shen W, Shen M, Feng W, Xiao P. Butyrate reverses ferroptosis resistance in colorectal cancer by inducing c-Fos-dependent xCT suppression. *Redox Biol* 2023; **65**: 102822 [PMID: 37494767 DOI: 10.1016/j.redox.2023.102822]
7 **Chen C**, Yang Y, Guo Y, He J, Chen Z, Qiu S, Zhang Y, Ding H, Pan J, Pan Y. CYP1B1 inhibits ferroptosis and induces anti-PD-1 resistance by degrading ACSL4 in colorectal cancer. *Cell Death Dis* 2023; **14**: 271 [PMID: 37059712 DOI: 10.1038/s41419-023-05803-2]
8 **Lv Y**, Tang W, Xu Y, Chang W, Zhang Z, Lin Q, Ji M, Feng Q, He G, Xu J. Apolipoprotein L3 enhances CD8+ T cell antitumor immunity of colorectal cancer by promoting LDHA-mediated ferroptosis. *Int J Biol Sci* 2023; **19**: 1284-1298 [PMID: 36923931 DOI: 10.7150/ijbs.74985]
9 **Qiao C**, Wang H, Guan Q, Wei M, Li Z. Ferroptosis-based nano delivery systems targeted therapy for colorectal cancer: Insights and future perspectives. *Asian J Pharm Sci* 2022; **17**: 613-629 [PMID: 36382305 DOI: 10.1016/j.ajps.2022.09.002]
10 **Zhang Z**, Ding Y, Li J, Wang L, Xin X, Yan J, Wu J, Yuan A, Hu Y. Versatile iron-vitamin K3 derivative-based nanoscale coordination polymer augments tumor ferroptotic therapy. *Nano Res* 2021; **14**: 2398-2409 [DOI: 10.1007/s12274-020-3241-7]
11 **Kang XJ**, Wang HY, Peng HG, Chen BF, Zhang WY, Wu AH, Xu Q, Huang YZ. Codelivery of dihydroartemisinin and doxorubicin in mannosylated liposomes for drug-resistant colon cancer therapy. *Acta Pharmacol Sin* 2017; **38**: 885-896 [PMID: 28479604 DOI: 10.1038/aps.2017.10]

World Journal of Clinical Oncology

Submit a Manuscript: https://www.f6publishing.com

World J Clin Oncol 2024 March 24; 15(3): 378-380

DOI: 10.5306/wjco.v15.i3.378

ISSN 2218-4333 (online)

EDITORIAL

Approaches and challenges in cancer immunotherapy pathways

Maria Kapritsou

Specialty type: Immunology

Provenance and peer review: Invited article; Externally peer reviewed.

Peer-review model: Single blind

Peer-review report's scientific quality classification

Grade A (Excellent): 0
Grade B (Very good): 0
Grade C (Good): C, C
Grade D (Fair): D, D
Grade E (Poor): 0

P-Reviewer: Pan ZY, China; Wu L, China; Zhang J, China

Received: December 16, 2023
Peer-review started: December 16, 2023
First decision: January 10, 2024
Revised: January 23, 2024
Accepted: February 23, 2024
Article in press: February 23, 2024
Published online: March 24, 2024

Maria Kapritsou, Pathological Sector, Hellenic Anticancer Institute, "Saint Savvas" Hospital, Athens 11522, Greece

Corresponding author: Maria Kapritsou, MSc, MSHCM, PhD, RN, Chief Nurse, Pathological Sector, Hellenic Anticancer Institute, "Saint Savvas" Hospital, Av Alexandras 171, Athens 11522, Greece. mariakaprit@gmail.com

Abstract

Cancer immunotherapy is an effective with critical approaches in the treatment of oncological patients. Whilst numerous research and clinical trials are underway to develop endogenous immunotherapy approaches, it is necessary to focus on fundamental issues and identify barriers to basic clinical progress. Addressing these challenges and the new pathways will require researchers and clinicians to join forces to accelerate the understanding of the complex interactions between cancer and the immune system and focus resources on developing better treatments for patients.

Key Words: Immunotherapy; Oncological patients; Immune response; Target therapies; Cancer vaccinations

Core Tip: Immunotherapy has emerged as a potent treatment for specific cancer types, which evokes enduring reactions and sometimes even induces remission. Nevertheless, the efficiency of this method relies both on the type of malignancy involved and individual patient traits. Additionally, it is administered in tandem with surgical interventions or chemotherapy/radiation regimens. It holds promise but could not act as a panacea; ongoing studies focus on enhancing its efficacy levels while comprehending underlying mechanisms more precisely.

Citation: Kapritsou M. Approaches and challenges in cancer immunotherapy pathways. *World J Clin Oncol* 2024; 15(3): 378-380
URL: https://www.wjgnet.com/2218-4333/full/v15/i3/378.htm
DOI: https://dx.doi.org/10.5306/wjco.v15.i3.378

INTRODUCTION

Currently, among available cancer treatment methods, including traditional chemotherapy, radiation therapy, and surgery, immunotherapy is regarded as the fourth option. Over the last decade, immunotherapy has received significant attention due to its ability to enhance overall survival rates in a subset of patients considered untreatable. The recent advances made by biotechnology have led to several developments in cancer treatment and care, such as immune checkpoint inhibition (ICI), chimeric antigen receptor T cell therapy (CAR-T), and various forms of vaccination for cancer [1].

Although these methods are frequently successful, with most cases claiming defeat against specific tumor subtypes, some treatments, such as ipilimumab, a melanoma anti-CTLA4 antibody, show remarkable improvement beyond other therapies in squamous cell carcinoma of the head and neck management. Thus, although immunotherapeutics, such as anti-PD1 nivolumab, have gained aberrant FDA approval status designations, they still encounter unignorable financial challenges called impediments. Hence, facing countless issues without a complete understanding of how reversal treatment works requires experts to work even harder to design innovative, effective, evidence-based approaches. Therefore, new insights are needed. Although scientists broadly understand host-tumor interactions, they continue finding new data through well-articulated, detailed reviews and studying ICI-adoptive CAR T cell treatment and vaccines at a broad scope. Thus, they guide the prioritized simultaneous implementation of tools used in various fields, thereby providing future chances of success based on accurate, evidence-based updates[2,3].

Further research into checkpoint inhibitory pathways could aid ICI treatment and help combat tumor escape mechanisms alongside the suppressive effects of tumor microenvironment on the immune response. CAR-T yields good outcomes only in certain hematological malignancies, requiring an enhancement of its effectiveness by countering tumor-associated macrophages as an immunosuppressive component. Trials combining all these treatment modalities might be beneficial, given an improved response in terms of targeting alternative pathways through ICIs[4].

Tumor mutation burden plays an important role as a target for treatment to impair tumor immunity, inhibit tumor growth, and restore therapeutic efficacy. However, personalized differences influence drug reactions, making predictions uncertain despite notable success rates of PD-1/PDL1 or anti-CTLA4 therapy above 15%-25%, ensuring patient variability [3,4].

Biotherapy options include inducing immunologic responses that engage checkpoint inhibitors and improve targeted antibodies. Hence, adoptive cell transplants allow for controlled cancer management tactics against various malignancies without suffering radiation or chemotherapy side effects due to the accurate selection process. This development relies heavily on immuno-oncology studies fundamental to current achievements in this field, inspiring further global progress in combating cancer through biotherapy innovations, starting with novel immune-based approaches stemming from new technologies. Moreover, experimental neogenic vaccines focused primarily on pinpointing tumor mutation burden can lead to discoveries, significantly improving patient outcomes and, ultimately, accelerating research progression. Consequently, considering basic knowledge of therapeutically applied oncology, advancements in continuously updating areas aimed at better cancer control will ensure the constant development of oncology in the future[5].

Despite new approaches to boost immune cell sensitivity and activity against tumor cells, such as cancer vaccines and chemokine treatment, immunotherapy has presented major challenges. First, some oncological patients have experienced a dramatic response. Unfortunately, while scientists hope to develop an effective therapy for various patients, immunotherapy has proven successful for only a small proportion of malignancies. Furthermore, these successful cases are often the minority. Second, discovering biomarkers and cancer pathways is important for immunotherapy success. Moreover, chemotherapy and radiotherapy are performed before immunotherapy, possibly impeding the improvement in cancer immunotherapy efficacy. Therefore, cancer immunotherapy is currently not generally recommended as a first-line therapy and is typically given to patients whose immune system is already weakened due to advanced disease or previous treatment[6].

CONCLUSION

Over the last decade, cancer immunotherapy has transformed how physicians treat cancer patients. There is an impressive potential for immunotherapeutic methods in various clinical contexts—even those who previously developed resistance to treatment show promising results after such novel therapy.

FOOTNOTES

Author contributions: Kapritsou M wrote the manuscript.

Conflict-of-interest statement: All the authors report no relevant conflicts of interest for this article.

Country/Territory of origin: Greece

ORCID number: Maria Kapritsou 0000-0002-8187-4978.

S-Editor: Gong ZM
L-Editor: A
P-Editor: Zhao S

REFERENCES

1 **Faghfuri E**. Recent advances in personalized cancer immunotherapy with immune checkpoint inhibitors, T cells and vaccines. *Per Med* 2024; **21**: 45-57 [PMID: 38088165 DOI: 10.2217/pme-2023-0054]
2 **Fan T**, Zhang M, Yang J, Zhu Z, Cao W, Dong C. Therapeutic cancer vaccines: advancements, challenges, and prospects. *Signal Transduct Target Ther* 2023; **8**: 450 [PMID: 38086815 DOI: 10.1038/s41392-023-01674-3]
3 **Balachandran DD**, Bashoura L, Sheshadri A, Manzullo E, Faiz SA. The Impact of Immunotherapy on Sleep and Circadian Rhythms in Patients with Cancer. *Front Oncol* 2023; **13**: 1295267 [PMID: 38090501 DOI: 10.3389/fonc.2023.1295267]
4 **Fantini M**, Arlen PM, Tsang KY. Potentiation of natural killer cells to overcome cancer resistance to NK cell-based therapy and to enhance antibody-based immunotherapy. *Front Immunol* 2023; **14**: 1275904 [PMID: 38077389 DOI: 10.3389/fimmu.2023.1275904]
5 **Dang BN**, Kwon TK, Lee S, Jeong JH, Yook S. Nanoparticle-based immunoengineering strategies for enhancing cancer immunotherapy. *J Control Release* 2024; **365**: 773-800 [PMID: 38081328 DOI: 10.1016/j.jconrel.2023.12.007]
6 **Ventola CL**. Cancer Immunotherapy, Part 3: Challenges and Future Trends. *P T* 2017; **42**: 514-521 [PMID: 28781505]

World Journal of Clinical Oncology

Submit a Manuscript: https://www.f6publishing.com

World J Clin Oncol 2024 March 24; 15(3): 381-390

DOI: 10.5306/wjco.v15.i3.381

ISSN 2218-4333 (online)

MINIREVIEWS

Current interventional options for palliative care for patients with advanced-stage cholangiocarcinoma

Maryam Makki, Malak Bentaleb, Mohammed Abdulrahman, Amal Abdulla Suhool, Salem Al Harthi, Marcelo AF Ribeiro Jr

Specialty type: Gastroenterology and hepatology

Provenance and peer review: Invited article; Externally peer reviewed.

Peer-review model: Single blind

Peer-review report's scientific quality classification

Grade A (Excellent): 0
Grade B (Very good): B
Grade C (Good): 0
Grade D (Fair): 0
Grade E (Poor): 0

P-Reviewer: Chen SY, China

Received: December 11, 2023
Peer-review started: December 11, 2023
First decision: January 4, 2024
Revised: January 18, 2024
Accepted: February 27, 2024
Article in press: February 27, 2024
Published online: March 24, 2024

Maryam Makki, Marcelo AF Ribeiro Jr, Department of Surgery, Division of Trauma, Critical Care and Acute Care Surgery, Sheikh Shakhbout Medical City, Abu Dhabi 11001, United Arab Emirates

Malak Bentaleb, Mohammed Abdulrahman, Marcelo AF Ribeiro Jr, Department of Surgery, College of Medicine and Health Sciences, Khalifa University, Abu Dhabi 11001, United Arab Emirates

Amal Abdulla Suhool, Salem Al Harthi, Department of Surgery, Division of Hepato-Pancreato-Biliary (HPB) Surgery, Sheikh Shakhbout Medical City, Abu Dhabi 91888, United Arab Emirates

Corresponding author: Marcelo AF Ribeiro Jr, FAASLD, FACS, MD, PhD, Chief Physician, Professor, Surgeon, Department of Surgery, Division of Trauma, Critical Care and Acute Care Surgery, Sheikh Shakhbout Medical City, PO Box 11001, Abu Dhabi 11001, United Arab Emirates. drmribeiro@gmail.com

Abstract

Primary biliary tract tumors are malignancies that originate in the liver, bile ducts, or gallbladder. These tumors often present with jaundice of unknown etiology, leading to delayed diagnosis and advanced disease. Currently, several palliative treatment options are available for primary biliary tract tumors. They include percutaneous transhepatic biliary drainage (PTBD), biliary stenting, and surgical interventions such as biliary diversion. Systemic therapy is also commonly used for the palliative treatment of primary biliary tract tumors. It involves the administration of chemotherapy drugs, such as gemcitabine and cisplatin, which have shown promising results in improving overall survival in patients with advanced biliary tract tumors. PTBD is another palliative treatment option for patients with unresectable or inoperable malignant biliary obstruction. Biliary stenting can also be used as a palliative treatment option to alleviate symptoms in patients with unresectable or inoperable malignant biliary obstruction. Surgical interventions, such as biliary diversion, have traditionally been used as palliative options for primary biliary tract tumors. However, biliary diversion only provides temporary relief and does not remove the tumor. Primary biliary tract tumors often present in advanced stages, making palliative treatment the primary option for improving the quality of life of patients.

Key Words: Cholangiocarcinoma; Palliative care; Endoscopic treatment; Surgery; Complications; Interventional radiology

Core Tip: Nowadays, we still see a high incidence of primary biliary tract tumors arriving at emergency departments with a clinical picture of jaundice of unknown etiology. Unfortunately, when jaundice is diagnosed, most patients already show signs of advanced disease. It is up to the attending physician to offer the best alternatives for palliative treatment for a better quality of life of patients. The aim of this study is to evaluate the interventional palliative treatment options currently used to clinically improve symptoms and their results and related complications.

Citation: Makki M, Bentaleb M, Abdulrahman M, Suhool AA, Al Harthi S, Ribeiro Jr MA. Current interventional options for palliative care for patients with advanced-stage cholangiocarcinoma. *World J Clin Oncol* 2024; 15(3): 381-390
URL: https://www.wjgnet.com/2218-4333/full/v15/i3/381.htm
DOI: https://dx.doi.org/10.5306/wjco.v15.i3.381

INTRODUCTION

Cholangiocarcinoma (CCA) is a malignant tumor of the epithelial cells of the biliary tract[1]. CCAs can be divided into three forms: intrahepatic CCA (iCCA), distal extrahepatic CCA (eCCA), and perihilar pCCA[2,3]. Similarities exist among these three forms, but key differences lead to distinct outcomes[3]. CCA is considered a very aggressive tumor that presents with a poor prognosis by the time it is diagnosed[4]. Surgical resection is the only meaningful option for the possible treatment of CCA. Patients who are not candidates for surgery are considered for palliative care treatment[4].

The main goal of palliative care is to enhance the quality of life of patients[5]. Only a few patients who present with CCA are candidates for surgical treatment[6]. It has been reported that less than 20% of patients diagnosed with iCCA are eligible for surgical resection[7]. Appropriate palliative care treatments in CCA are influenced by the classification of the tumor[8]. Current palliative options include biliary stenting, chemotherapy, radiofrequency ablation, and photodynamic therapy[8]. Adverse effects are associated with some of these palliative treatments[8], and a full comprehensive understanding of the benefits and risks of current palliative treatment options will help clinicians determine the most appropriate course of action.

RISK FACTORS

The risk factors for the incidence of CCA include primary sclerosing cholangitis, parasitic infections, toxins, bile duct cysts, hepatolithiasis, hepatic cirrhosis, and viral hepatitis[9,10]. In addition, there may be evidence that certain genetic polymorphisms regulate the risk of CCA[10]. Diabetes and heavy alcohol ingestion may increase the risk of CCA[9]. CCA in Asian countries is significantly associated with the liver flukes Clonorchis sinensis and Opisthorchis viverrini[11]. The effects of hepatitis B and hepatitis C on the incidence of CCA have not been completely studied[11]. Surveillance of risk factors for CCA needs to be established as it may facilitate better prognosis for patients.

EPIDEMIOLOGY

The epidemiology of CCA differs depending on factors such as geography, risk factors, and age. The largest incidence of CCA is in Asia, with the highest occurring in parts of Thailand[12]. The incidence rates in Western countries are lower than those in Asian countries[12].

The prognosis of CCA is poor, with the only curative option being surgical resection in early-stage tumors[13]. The mortality rate of CCA has increased significantly in recent years, up to a 36% increase in mortality from 1999 to 2014 in a United States-based study[14]. The 5-year survival rates for certain CCAs range from 5% to 10%[15]. Some studies have described the percentage of resectable CCAs. In a cohort study describing hilar CCAs, research has shown that only 26% of hilar CCAs are resectable[16]. It has also been reported that only 15% of patients with iCCA present with a resectable tumor at the time of diagnosis[17]. Therefore, the importance of palliative care in CCA cannot be understated and must be fully explored and understood to deliver the most appropriate individualized care for each patient.

CLINICAL PRESENTATION

The clinical presentation of CCA depends on the type, stage, and location of the tumor. The most common presentation of

CCA is jaundice, which manifests as a yellowish pigmentation of the skin and mucous membranes[18]. However, in iCCA, because tumor growth is intrahepatic, patients are usually asymptomatic and jaundice only manifests at later stages because obstruction is less frequent[19]. Studies have shown that jaundice is reported as an initial symptom of iCCA in only 10%-15%[18] of cases and that the diagnosis of early-stage iCCA represents an incidental finding in almost 25% of cases[20]. Other clinical symptoms associated with the onset of iCCA are nonspecific and include the following: Malaise, cachexia, dull right upper quadrant abdominal pain, and night sweats[20]. Conversely, most eCCAs and pCCAs are associated with biliary obstruction. It has been estimated that 90% of eCCA cases present with symptoms of obstructive jaundice[21], which include jaundice, pale stools, dark urine, and pruritis. A cohort study demonstrated that bilirubin levels are significantly more elevated in eCCA and pCCAs than in iCCA because of the larger frequency of biliary obstruction[22]. During the course of the disease, patients with eCCA present with nonspecific symptoms similar to iCCA, such as weight loss, abdominal pain, night sweats, fatigue, emesis, vomiting, and loss of appetite, in addition to an increase in cholestasis laboratory findings[23].

On physical examination, eCCA is characterized by jaundice, hepatomegaly, and a palpable gallbladder (Courvoisier sign) whereas iCCA usually presents mainly with right upper quadrant tenderness[24]. CCA has also been associated with rare cutaneous manifestations, including sweet syndrome, erythema multiforme, and porphyria cutanea tarda[24]. However, these findings are nonspecific and can be found in other pathologies. Therefore, a definitive diagnosis of CCA requires further laboratory and imaging investigations.

DIAGNOSIS

The diagnosis and early detection of CCA remain challenging. It is important to check bilirubin, alkaline phosphatase (ALP), gamma-glutamyl transpeptidase (GGT), alanine transaminase (ALT), and aspartate aminotransferase (AST) levels in all suspected patients. In patients with eCCA, bilirubin, ALP, and GGT levels are elevated, whereas in patients with iCCA, ALP level is atypical, but the other values are within normal ranges[24]. In the early stages of CCA, ALT and AST levels are normal, but as the disease progresses, they increase because of the hepatocellular damage caused by cholestasis [24]. Blood biomarkers are also useful for detecting CCA. Cancer antigen 19-9 (CA 19-9) is an important prognostic factor at presentation and has been associated with poor prognosis[22]. However, the use of CA 19-9 is limited as it has low specificity in distinguishing malignant from benign pathologies, and it is absent in patients with deficient Lewis antigen [24]. Carcinoembryonic antigen and alpha fetoprotein can also be used, but both have shown limited specificity and sensitivity.

The diagnosis of CCA relies heavily on imaging modalities. Transabdominal ultrasound is often employed as an initial imaging modality for CCA diagnosis in patients with obstructive jaundice because it is beneficial for examining the origins of bile duct obstruction and characterizing liver lesions[25]. In addition to detecting CCA, this allows the exclusion of more common etiologies for obstruction jaundice such as choledocholithiasis. With new advancements in technology, the use of contrast-enhanced ultrasound has demonstrated significant potential in assessing both luminal and extraluminal masses in the diagnosis of CCA[25]. Computed tomography (CT) is conducted in 90% of cases with possible CCA diagnosis[25]. CT plays an important role during the initial evaluation of CCA: It demonstrates features such as the extent of the tumor, it ascertains the potential of surgical resectability, and it allows the estimation of prognostic pathological factors, including vascular infiltration and the presence of lymph node metastasis[25]. The two most commonly used imaging techniques after the identification of the tumor are endoscopic retrograde cholangiopancreatography (ERCP) and magnetic resonance cholangiopancreatography (MRCP)[21]. MRCP is the preferred modality because it allows the accurate assessment of tumor resectability[26]. Endoscopic ultrasound (EUS) and fine needle aspiration guided by EUS have also been reported to help with the diagnosis and staging of CCA[26]. ERCP is still widely used and preferred by some physicians and surgeons because it allows cytological sampling and histological confirmation of the malignancy[21,24].

PALLIATIVE TREATMENT DEFINITION

Palliative care is a medical holistic approach that aims to enhance the well-being of patients who are confronting challenges related to incurable life-threatening illnesses by preventing and alleviating physical, psychological, and spiritual suffering[27]. Palliative care should involve interdisciplinary teams with excellent communication skills to support patients and their families[27]. In patients with CCA with a locally advanced, unresectable, or recurrent tumor, palliative care goals are to relieve symptoms of obstructive jaundice, pain, and pruritis[26].

In this review, we summarize recent findings on interventional procedures for the palliative care management of CCA. Different interventional options that are currently available and their benefits and complications are discussed. Systemic treatment, although available, is beyond the scope of this review.

MANAGEMENT

Palliative biliary drainage is used in advanced-stage CCA to alleviate symptoms such as pain, severe pruritus, and cholangitis. Patients with jaundice who are asymptomatic and have a life expectancy of less than 3 months are generally

Table 1 Palliative treatment options for cholangiocarcinoma and their associated techniques, indications, and complications

Type	Technique	Indication	Complications
Percutaneous drainage	PTBD	Proximal malignant biliary obstructions (particularly Bismuth type III and IV perihilar CCA patients)	Catheter-related complications: wound care, hygiene maintenance, catheter dislodgement, and PTBD blockages
			Acute cholangitis, bleeding, and peri catheter leakage
	PTBS	Specific patients with malignant biliary obstruction	No catheter-related complications (due to no external drainage)
			Cholangitis, pancreatitis, bleeding, stent dysfunction, cholecystitis, duodenal perforation, stent obstruction (due to tumor overgrowth)
Endoscopic drainage	ERCP with biliary stenting	Patients with incurable conditions (*e.g.* Unresectable tumors, malignant hilar obstruction)	Stent occlusion or dysfunction (mainly due to tumor ingrowth)
	EUS-EBD	Cases where ERCP may be difficult due to anatomical variations, altered anatomy from prior surgeries or tumor infiltration	Minimal complications including pancreatitis and cholecystitis
Surgical Drainage (only considered as a final option after failure of other approaches)	Choledochojejunostomy	Distal CCA	High perioperative morbidity and mortality
	Intrahepatic bile duct bypass	Peri hilar CCA	
	Extrahepatic bile duct bypass	Distal obstruction or Bismuth type I	
	Left hepaticojejunostomy	Bismuth type IIIa	
	Right hepaticojejunostomy	Bismuth type IIIb	
	Right or left sectoral duct bypass	Bismuth type IV	High perioperative morbidity and mortality
			Frequently ineffective due to inadequacy of a single anastomosis to drain a sufficient volume of functioning liver

PTBD: Percutaneous transhepatic biliary drainage; PTBS: Percutaneous transhepatic biliary stenting; ERCP: Endoscopic retrograde cholangiopancreatography; EUS-EBD: Endoscopic ultrasound guided endoscopic biliary drainage; CCA: Cholangiocarcinoma.

not candidates for biliary drainage procedures. Other purposes of palliative biliary drainage include improving functional status and liver function to enable subsequent systemic chemotherapy. This procedure encompasses three methods: percutaneous, endoscopic, and surgical bypass (Table 1).

PERCUTANEOUS PALLIATIVE BILIARY DRAINAGE

The percutaneous method for palliative biliary drainage involves a guided puncture using ultrasonography aiming to place a catheter into the dilated bile ducts. This approach includes two techniques: percutaneous transhepatic biliary drainage (PTBD) and percutaneous transhepatic biliary stenting (PTBS). Palliative PTBD plays a crucial role in decompressing the biliary system specially in proximal obstructions, particularly in cases of Bismuth type III and IV perihilar CCA. Research suggests that PTBD has a higher success rate in therapy with fewer complications related to cholangitis compared with the endoscopic approach[28]. However, wound care, catheter displacement, blockages, and even hygiene maintenance may represent a challenge for some patients. To address these challenges, patients receive catheter care training before hospital discharge[28,29]. Complications may include acute cholangitis, bleeding, and pericatheter leakage.

Palliative PTBS is a procedure aimed at managing jaundice and serves as an optional treatment for specific patients with malignant biliary obstruction. The main advantage of this procedure is to restore the physiological pathway to the biliary drainage to the duodenum and minimize the loss of bile salts and electrolytes. This is achieved using either plastic or metallic stents. Studies have indicated that PTBS, particularly with the implantation of self-expandable metallic stents (SEMS), has better efficacy than catheter drainage. PTBS can effectively reduce complications associated with catheter usage and can improve the overall quality of life of patients by eliminating the need for external drainage. Metal stents have a larger diameter, present a better long-term patency, and are more cost-effective compared with plastic ones. In the palliative care of advanced hilar CCA (Bismuth III and IV), percutaneous stenting outcomes exceed those by endoscopy [30-33].

The PTBS procedure is performed under local anesthesia and moderate sedation. This procedure involves inserting a 0.035 in guidewire into the previously placed PTBD and then replacing the PTBD catheter with 5 French diagnostic catheters (specifically Cobra catheters). The tract passing through the obstructed region into the duodenum is cannulated using a 0.035 in guidewire, followed by the introduction of a metallic stent. Typically, pre stent dilation of malignant biliary strictures is avoided to prevent tumoral bleeding that might result in early stent blockage[34]. After stent placement, an internal-external drainage catheter (temporary close catheter hub) is inserted as a precautionary measure in case of stent malfunction. Follow-up after biliary stenting includes clinical assessment and laboratory investigations at the two-week mark. A cholangiogram through the internal-external drainage catheter is performed after two weeks to assess stent patency, followed by the removal of the internal-external drainage catheter.

The most frequent early complications after percutaneous procedures are cholangitis, pancreatitis, and bleeding. Stent dysfunction, bleeding, cholecystitis, and less frequently, duodenal perforation are usually the most frequent late ones. The major complication of biliary stenting is recurrent jaundice or cholangitis resulting from stent obstruction. Biliary sludge and tumor ingrowth through the stent are the primary causes of obstruction[35].

ENDOSCOPIC APPROACH

Selecting the type of stent for palliative drainage involves different factors to be considered, like the location of the obstruction, the patient's prognosis, the risk of potential stent complications such as blockage or movement, the preference of the endoscopist, and the availability of different stent types. In cases where hilar obstruction is presented like in hilar tumors, multidisciplinary teamwork is a must for its management. Relieve the obstruction of the bile ducts in advanced unresectable hilar tumors may be challenge and usually requires multiple endoscopic and/or percutaneous procedures[36,37].

Typically for the cases with hilar obstruction ERCP with uncovered SEMS represents the standard of care to prevent drainage blockage from the opposite biliary system. Similarly, in the treatment of hilar obstruction, the use of uncovered SEMS is recommended to prevent blockage of the left or right hepatic duct[37].

Uncovered SEMS offer notable advantages over plastic stents, primarily due to their wire mesh design that remains open and does not obstruct the side branches of the intrahepatic bile duct. They also feature a delivery system that allows passage through tight biliary strictures, such as a sharp tip, enabling the use of stents with reduced diameter sizes, which is particularly beneficial for lesions located proximally[37,38].

Several studies demonstrated that for patients with hilar obstructions SEMS provides higher clinical success rates as well as less need for reinterventions when compared to plastic stents[31,38-42]. In one trial involving 188 patients diagnosed with unresectable hilar CCA, the rates of success using SEMS comparing with plastic stents regarding drainage was 70% *vs* 46% and the authors also observed a prolonged overall survival (median 126 *vs* 49 d)[42]. Another study with 60 patients demonstrated that SEMS had superior patency rates at six months (81% *vs* 20%) and required fewer reinterventions (0.63 *vs* 1.80 interventions per patient)[39].

In cases of unresectable cancer with obstructed hilar regions, the placement of bilateral SEMS represents the standard approach when technically feasible to optimize biliary drainage, particularly when both liver lobes are affected by obstruction. Before the ERCP procedure, imaging techniques such as CT or MRCP must be available to identify the dominant biliary system, allowing the endoscopy team to plan, in case the bilateral stenting is not possible, to which of the ducts the stent should place to provide adequate bile drainage.

The efficacy of drainage is affected by the amount of drained liver volume[33,43,44]. Previously, it was commonly accepted that draining a minimum of 25% of the liver volume was required to relieve jaundice. However, recent research suggests that draining more than 50% of the total liver volume (assessed *via* CT) is associated with enhanced overall survival. If a single stent fails to alleviate symptoms by draining more than 50% of the total liver volume, the consideration of ERCP-guided bilateral stenting and/or percutaneous drainage may be warranted[44].

For certain patients, the placement of a single, unilateral stent provides adequate drainage and relief from symptoms. However, it remains uncertain whether bilateral drainage offers superior outcomes compared with unilateral placement [45-47]. A meta-analysis of seven studies involving more than 600 patients diagnosed with tumoral hilar obstruction suggested that bilateral stenting did not significantly differ from unilateral stenting in terms of clinical response rates, stent occlusion, cholangitis, or patient mortality[45]. Nevertheless, another study involving 133 patients that were treated with SEMS revealed that patients that had bilateral stents had a lower chance of failure when compared to unilateral ones. (hazard ratio, 0.30; 95%CI, 0.17-0.52)[46].

The primary long-term complication encountered after placing SEMS for malignant biliary obstruction is stent occlusion. The diagnosis of stent dysfunction typically involves the presence of two of the following three specified criteria:

Dilatation of the bile duct system demonstrated by ultrasound.

Abnormal elevation of serum bilirubin levels (≥ 2 mg/dL) with an increase of ≥ 1 mg/dL compared with the value following the initial successful drainage.

Increase in ALP/gamma-glutamyl transferase to more than double the upper limit of normal values with an increase of at least 30 U/L.

Manifestations of cholangitis[47]

Tumor ingrowth represents the main reason for stent occlusion and it is more related to uncovered SEMS[42]. Furthermore, this overgrowth, will involves the blockage of the stent's proximal or distal ends, contributes to long-term

stent occlusion. Occasionally, obstruction due to sludge, mucus, or debris may occur, but it typically occurs together with the progression of the tumor itself.

The average functional duration of this prothesis ranges between 5 and 6 months[48,49] before obstruction occurs. Managing occluded stents involves various methods such as balloon mechanical cleaning, placement of plastic or metallic stents, and endobiliary radiofrequency ablation. Mechanical cleaning is suitable for debris occlusion but should be combined with other procedures when tumor ingrowth is present. Placement of a second plastic stent has a shorter patency period, typically lasting 60-90 d, compared with the patency period of 100 d for second SEMS placements[42]. Endobiliary radiofrequency ablation is an innovative intervention used to safely ablate ingrown tumors within the stent lumen, leading to long-term patency comparable to SEMS placement[49]. The advantage of this procedure is to not compromise the stent lumen and represents a benefit comparing to the placement of a second stent that may decrease its diameter.

Retrospective studies that compare the safety and effectiveness of percutaneous treatment *vs* endoscopic treatment for obstructed hilar bile ducts have shown that percutaneous interventions lead to a faster therapeutic decrease in bilirubin levels, fewer instances of infections, and reduced need for repeated drainage procedures[50-53]. Among patients with tumors in the hilar region who undergo endoscopic treatment, those who receive a unilateral stent-particularly when both sides of the liver's bile ducts have been visualized with contrast-experience notably poorer survival rates compared to patients with bilateral stents[54]. Furthermore, the risk of post endoscopy cholangitis increases with the extent of isolation caused by the hilar tumor, with Bismuth I patients having only a 4% risk and Bismuth III and IV patients having a nearly 60% risk[55]. Another study comparing the outcome of endoscopic *vs* percutaneous drainage in patients with advanced type III or IV hilar CCA concluded that the percutaneous SEMS group exhibited a notably higher success rate in biliary decompression compared to the endoscopic SEMS group (92.7% *vs* 77.3%, respectively, $P = 0.049$). Although the overall occurrence of procedure-related complications was comparable between both groups, one fatality resulting from biliary sepsis was recorded in the endoscopic SEMS group. Patients who initially achieved successful biliary drainage, regardless of the procedure used, experienced substantially longer median survival than those for whom biliary drainage failed (8.7 *vs* 1.8 months, respectively, $P < 0.001$). Once successful biliary decompression was attained, and the median survival and duration of stent patency were similar in both study groups[52].

In cases of advanced malignant hilar strictures (Bismuth III and IV), the percutaneous method for biliary drainage is favored over the endoscopic approach because of its notably higher success rate (93% compared to 77%, with a P value of 0.049) and reduced incidence of cholangitis related to the procedure. In addition, the percutaneous approach enables the precise selection of the affected lobe for drainage[52].

EUS GUIDED ENDOSCOPIC BILIARY DRAINAGE

EUS provides real-time imaging with high resolution and has the ability to visualize the bile ducts and adjacent structures in great detail. EUS guided endoscopic biliary drainage (EUS-EBD) combines the advantages of EUS and biliary drainage, allowing the accurate placement of stents or drainage catheter under direct visualization. This technique is valuable in cases where conventional ERCP may be challenging because of anatomical variations, altered anatomy from prior surgeries, or tumor infiltration.

The EUS-EBD procedure involves passing an echoendoscope through the gastrointestinal tract to access the duodenum and visualize the biliary tree using ultrasound. Once the target area is identified, a guidewire is advanced through the obstructed bile duct under EUS guidance. Following successful guidewire placement, a biliary stent or drainage catheter is deployed to relieve the obstruction and alleviate symptoms such as jaundice and pruritus. The main benefits of EUS-EBD are improved visualization, precise guidance, real-time ultrasound guidance, enhanced precision of wire placement, reduced risk of complications, overcoming anatomical challenges, and permitting navigation through anatomical variations or distorted anatomy caused by the tumor, making it a valuable option in complex cases.

Several studies have demonstrated the efficacy and safety of EUS-EBD in the palliative care of patients with advanced CCA. Notable outcomes include successful drainage, symptom relief, and improved quality of life. Comparative studies have shown that EUS-EBD can be as effective as or even superior to traditional ERCP in certain cases[56,57].

Surgical approach

Surgical bypass procedures have demonstrated a significant increase in perioperative mortality, ranging from 0% to 17%, and morbidity, with rates between 17% and 55%[58]. Nowadays the surgical approach will only be considered if other options like percutaneous and/or endoscopic treatments are not available or fail. In instances where laparotomy reveals distant metastases, surgical bypass may be considered. Choledochojejunostomy is a feasible surgical bypass procedure for distal obstructions, whereas intrahepatic bile duct bypass is appropriate for perihilar CCA. Extrahepatic bile duct bypass, although technically less challenging, is associated with lower morbidity and is suitable for distal obstructions or Bismuth type I in the perihilar region. Palliative surgical bypass for perihilar CCA involves intricate surgeries tailored to each tumor type. According to the location of the tumoral obstruction, left or right main ducts, the surgeon will proceed with either a left of right hepaticojejunostomy. Bismuth type IV may requires right or left sectoral duct bypass. However, surgical bypass for this type of tumors are often ineffective because of the inadequacy of a single anastomosis to drain a sufficient volume of functioning liver. Therefore, in cases of Bismuth IV, a bilateral hepaticojejunostomy bypass should be considered with exceptional selectivity[58].

Three randomized trials[59-61] that compared surgical bypass to endoscopic drainage demonstrated similar effectiveness in alleviating symptoms. However, endoscopic drainage exhibited fewer early complications, whereas surgical

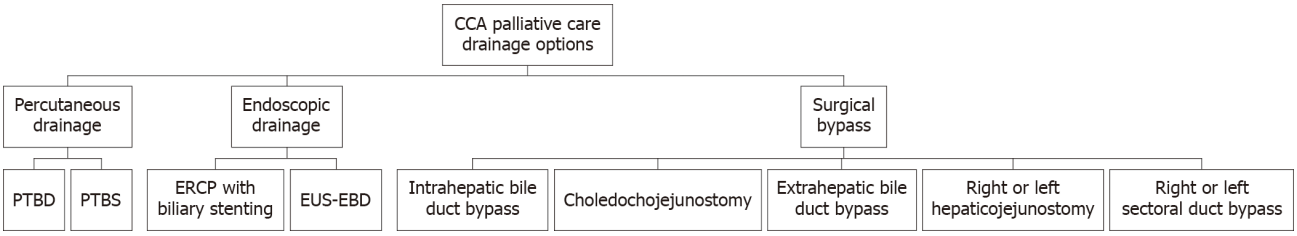

Figure 1 Current management options for palliative care of advanced cholangiocarcinoma. PTBD: Percutaneous transhepatic biliary drainage; PTBS: Percutaneous transhepatic biliary stenting; ERCP: Endoscopic retrograde cholangiopancreatography; EUS-EBD: Endoscopic ultrasound guided endoscopic biliary drainage; CCA: Cholangiocarcinoma.

bypass presented fewer late complications. It is important to note that these trials focused on patients with a lower end block caused by pancreatic and periampullary carcinoma, which limits the direct extrapolation of these findings to patients with a hilar block. In the case of locally advanced gallbladder cancer with an average survival of 3-6 months, nonoperative methods might be more effective in alleviating symptoms[62]. Two randomized trials evaluated endoscopic and percutaneous drainage methods for malignant biliary obstruction[62,63]. Speer *et al*[63] demonstrated that endoscopic drainage surpassed percutaneous drainage in terms of successful drainage (81% *vs* 61%) and lower 30-d mortality (15% *vs* 33%). This trial included 75 patients, but only 29 had a hilar block. However, the less favorable outcomes associated with percutaneous stenting might be attributed to the use of a rigid external percutaneous transhepatic catheter for drainage, leading to increased morbidity and mortality. By contrast, Piñol *et al*[64] showed different results with higher successful drainage (71% *vs* 42%, $P = 0.03$) but more complications (61% *vs* 35%) with PTBD compared to endoscopic drainage. The median survival time significantly favored the PTBD group (3.7 *vs* 2 months, $P = 0.02$). In addition, they compared a metal stent placed percutaneously with a plastic stent placed endoscopically (Figure 1).

CONCLUSION

The basis for the palliative treatment of advanced CCA relies on the alleviation of the obstructive symptoms related to the drainage of the biliary tract. Proper management must be defined by a multidisciplinary team that considers the radiological features of the tumor and the resources available in the institution. The results of systemic treatment for palliative care can be improved if the patient's biliary tract has been properly drained using one of the presented techniques.

FOOTNOTES

Author contributions: Ribeiro Jr MA supervise the project and analyzed the data; Makki M, Bentaleb M, and Abdulrahman M contributed equally to this work; Ribeiro Jr MA designed the research study; Makki M, Bentaleb M, and Abdulrahman M performed the research; Suhool AA, Al Harthi S contributed reviewing the data and performing critical analysis; Makki M, Bentaleb M, Abdulrahman M wrote the manuscript; All authors have read and approve the final manuscript.

Conflict-of-interest statement: All the authors report no relevant conflicts of interest for this article.

Country/Territory of origin: United Arab Emirates

ORCID number: Marcelo AF Ribeiro Jr 0000-0001-9826-4722.

S-Editor: Li L
L-Editor: A
P-Editor: Yuan YY

REFERENCES

1 **Ustundag Y**, Bayraktar Y. Cholangiocarcinoma: a compact review of the literature. *World J Gastroenterol* 2008; **14**: 6458-6466 [PMID: 19030196 DOI: 10.3748/wjg.14.6458]

2 **Halder R**, Amaraneni A, Shroff RT. Cholangiocarcinoma: a review of the literature and future directions in therapy. *Hepatobiliary Surg Nutr* 2022; **11**: 555-566 [PMID: 36016753 DOI: 10.21037/hbsn-20-396]

3 **Banales JM**, Cardinale V, Carpino G, Marzioni M, Andersen JB, Invernizzi P, Lind GE, Folseraas T, Forbes SJ, Fouassier L, Geier A, Calvisi DF, Mertens JC, Trauner M, Benedetti A, Maroni L, Vaquero J, Macias RI, Raggi C, Perugorria MJ, Gaudio E, Boberg KM, Marin JJ, Alvaro D. Expert consensus document: Cholangiocarcinoma: current knowledge and future perspectives consensus statement from the European Network for the Study of Cholangiocarcinoma (ENS-CCA). *Nat Rev Gastroenterol Hepatol* 2016; **13**: 261-280 [PMID: 27095655 DOI: 10.1038/nrgastro.2016.51]

4 **Zamani Z**, Fatima S. Biliary Tract Cancer. Treasure Island (FL): StatPearls Publishing, 2023

5 **Teoli D**, Schoo C, Kalish VB. Palliative Care. Treasure Island (FL): StatPearls Publishing, 2023

6 **Patel T**. Cholangiocarcinoma--controversies and challenges. *Nat Rev Gastroenterol Hepatol* 2011; **8**: 189-200 [PMID: 21460876 DOI: 10.1038/nrgastro.2011.20]

7 **Bath NM**, Pawlik TM. Narrative review: current management and novel targeted therapies in intrahepatic cholangiocarcinoma. *Chin Clin Oncol* 2023; **12**: 5 [PMID: 36922354 DOI: 10.21037/cco-22-109]

8 **Mohammad T**, Kahaleh M. Comparing palliative treatment options for cholangiocarcinoma: photodynamic therapy vs. radiofrequency ablation. *Clin Endosc* 2022; **55**: 347-354 [PMID: 35578751 DOI: 10.5946/ce.2021.274]

9 **Tyson GL**, El-Serag HB. Risk factors for cholangiocarcinoma. *Hepatology* 2011; **54**: 173-184 [PMID: 21488076 DOI: 10.1002/hep.24351]

10 **Khan SA**, Tavolari S, Brandi G. Cholangiocarcinoma: Epidemiology and risk factors. *Liver Int* 2019; **39**: 19-31 [PMID: 30851228 DOI: 10.1111/liv.14095]

11 **Shin HR**, Oh JK, Masuyer E, Curado MP, Bouvard V, Fang YY, Wiangnon S, Sripa B, Hong ST. Epidemiology of cholangiocarcinoma: an update focusing on risk factors. *Cancer Sci* 2010; **101**: 579-585 [PMID: 20085587 DOI: 10.1111/j.1349-7006.2009.01458.x]

12 **Qurashi M**, Vithayathil M, Khan SA. Epidemiology of cholangiocarcinoma. *Eur J Surg Oncol* 2023; 107064 [PMID: 37709624 DOI: 10.1016/j.ejso.2023.107064]

13 **Mosconi S**, Beretta GD, Labianca R, Zampino MG, Gatta G, Heinemann V. Cholangiocarcinoma. *Crit Rev Oncol Hematol* 2009; **69**: 259-270 [PMID: 18977670 DOI: 10.1016/j.critrevonc.2008.09.008]

14 **Yao KJ**, Jabbour S, Parekh N, Lin Y, Moss RA. Increasing mortality in the United States from cholangiocarcinoma: an analysis of the National Center for Health Statistics Database. *BMC Gastroenterol* 2016; **16**: 117 [PMID: 27655244 DOI: 10.1186/s12876-016-0527-z]

15 **Garikipati SC**, Roy P. Biliary Tract Cholangiocarcinoma. Treasure Island (FL): StatPearls Publishing, 2023

16 **Ruys AT**, van Haelst S, Busch OR, Rauws EA, Gouma DJ, van Gulik TM. Long-term survival in hilar cholangiocarcinoma also possible in unresectable patients. *World J Surg* 2012; **36**: 2179-2186 [PMID: 22569746 DOI: 10.1007/s00268-012-1638-5]

17 **Buettner S**, van Vugt JL, IJzermans JN, Groot Koerkamp B. Intrahepatic cholangiocarcinoma: current perspectives. *Onco Targets Ther* 2017; **10**: 1131-1142 [PMID: 28260927 DOI: 10.2147/OTT.S93629]

18 **Forner A**, Vidili G, Rengo M, Bujanda L, Ponz-Sarvisé M, Lamarca A. Clinical presentation, diagnosis and staging of cholangiocarcinoma. *Liver Int* 2019; **39**: 98-107 [PMID: 30831002 DOI: 10.1111/liv.14086]

19 **Zori AG**, Yang D, Draganov PV, Cabrera R. Advances in the management of cholangiocarcinoma. *World J Hepatol* 2021; **13**: 1003-1018 [PMID: 34630871 DOI: 10.4254/wjh.v13.i9.1003]

20 **Cardinale V**, Bragazzi MC, Carpino G, Di Matteo S, Overi D, Nevi L, Gaudio E, Alvaro D. Intrahepatic cholangiocarcinoma: review and update. *Hepatoma Res* 2018; **4**: 20 [DOI: 10.20517/2394-5079.2018.46]

21 **Vasilieva L**, Papadhimitriou SI, Alexopoulou A, Kostopoulos I, Papiris K, Pavlidis D, Xinopoulos D, Romanos A, Dourakis SP. Clinical presentation, diagnosis, and survival in cholangiocarcinoma: A prospective study. *Arab J Gastroenterol* 2016; **17**: 181-184 [PMID: 27914884 DOI: 10.1016/j.ajg.2016.10.003]

22 **Singal AG**, Rakoski MO, Salgia R, Pelletier S, Welling TH, Fontana RJ, Lok AS, Marrero JA. The clinical presentation and prognostic factors for intrahepatic and extrahepatic cholangiocarcinoma in a tertiary care centre. *Aliment Pharmacol Ther* 2010; **31**: 625-633 [PMID: 20003093 DOI: 10.1111/j.1365-2036.2009.04218.x]

23 **Plentz RR**, Malek NP. Clinical presentation, risk factors and staging systems of cholangiocarcinoma. *Best Pract Res Clin Gastroenterol* 2015; **29**: 245-252 [PMID: 25966425 DOI: 10.1016/j.bpg.2015.02.001]

24 **Shin DW**, Moon SH, Kim JH. Diagnosis of Cholangiocarcinoma. *Diagnostics (Basel)* 2023; **13** [PMID: 36673043 DOI: 10.3390/diagnostics13020233]

25 **Olthof SC**, Othman A, Clasen S, Schraml C, Nikolaou K, Bongers M. Imaging of Cholangiocarcinoma. *Visc Med* 2016; **32**: 402-410 [PMID: 28229074 DOI: 10.1159/000453009]

26 **Tantau AI**, Mandrutiu A, Pop A, Zaharie RD, Crisan D, Preda CM, Tantau M, Mercea V. Extrahepatic cholangiocarcinoma: Current status of endoscopic approach and additional therapies. *World J Hepatol* 2021; **13**: 166-186 [PMID: 33708349 DOI: 10.4254/wjh.v13.i2.166]

27 **Raksasataya A**, Ahooja A, Krangbunkrong V, Jareanrat A, Titapun A, Khuntikeo N. Palliative Care in Cholangiocarcinoma. In: Khuntikeo N, Andrews RH, Petney TN, Khan SA, editors. Liver Fluke, Opisthorchis viverrini Related Cholangiocarcinoma. *Cham: Springer International Publishing* 2023; 245-267

28 **Zhao XQ**, Dong JH, Jiang K, Huang XQ, Zhang WZ. Comparison of percutaneous transhepatic biliary drainage and endoscopic biliary drainage in the management of malignant biliary tract obstruction: a meta-analysis. *Dig Endosc* 2015; **27**: 137-145 [PMID: 25040581 DOI: 10.1111/den.12320]

29 **Zhang GY**, Li WT, Peng WJ, Li GD, He XH, Xu LC. Clinical outcomes and prediction of survival following percutaneous biliary drainage for malignant obstructive jaundice. *Oncol Lett* 2014; **7**: 1185-1190 [PMID: 24944690 DOI: 10.3892/ol.2014.1860]

30 **Bai AG**, Zheng CS, Zhou GF, Liang HM, Feng GS. Comparison of the therapeutic effects of PTBD and PTBS in treatment of malignant obstructive jaundice. *Zhonghua Zhong Liu Za Zhi* 2010; **32**: 456-458 [PMID: 20819490]

31 **Sangchan A**, Kongkasame W, Pugkhem A, Jenwitheesuk K, Mairiang P. Efficacy of metal and plastic stents in unresectable complex hilar cholangiocarcinoma: a randomized controlled trial. *Gastrointest Endosc* 2012; **76**: 93-99 [PMID: 22595446 DOI: 10.1016/j.gie.2012.02.048]

32 **Sangchan A**, Chaiyakunapruk N, Supakankunti S, Pugkhem A, Mairiang P. Cost utility analysis of endoscopic biliary stent in unresectable hilar cholangiocarcinoma: decision analytic modeling approach. *Hepatogastroenterology* 2014; **61**: 1175-1181 [PMID: 25436278]

33 **Rerknimitr R**, Angsuwatcharakon P, Ratanachu-ek T, Khor CJ, Ponnudurai R, Moon JH, Seo DW, Pantongrag-Brown L, Sangchan A, Pisespongsa P, Akaraviputh T, Reddy ND, Maydeo A, Itoi T, Pausawasdi N, Punamiya S, Attasaranya S, Devereaux B, Ramchandani M, Goh KL; Asia-Pacific Working Group on Hepatobiliary Cancers. Asia-Pacific consensus recommendations for endoscopic and interventional

management of hilar cholangiocarcinoma. *J Gastroenterol Hepatol* 2013; **28**: 593-607 [PMID: 23350673 DOI: 10.1111/jgh.12128]

34 **Inal M**, Aksungur E, Akgül E, Oguz M, Seydaoglu G. Percutaneous placement of metallic stents in malignant biliary obstruction: one-stage or two-stage procedure? *Cardiovasc Intervent Radiol* 2003; **26**: 40-45 [PMID: 12491022 DOI: 10.1007/s00270-002-2647-9]

35 **Sohn SH**, Park JH, Kim KH, Kim TN. Complications and management of forgotten long-term biliary stents. *World J Gastroenterol* 2017; **23**: 622-628 [PMID: 28216968 DOI: 10.3748/wjg.v23.i4.622]

36 **Dumonceau JM**, Tringali A, Papanikolaou IS, Blero D, Mangiavillano B, Schmidt A, Vanbiervliet G, Costamagna G, Devière J, García-Cano J, Gyökeres T, Hassan C, Prat F, Siersema PD, van Hooft JE. Endoscopic biliary stenting: indications, choice of stents, and results: European Society of Gastrointestinal Endoscopy (ESGE) Clinical Guideline - Updated October 2017. *Endoscopy* 2018; **50**: 910-930 [PMID: 30086596 DOI: 10.1055/a-0659-9864]

37 **Lee TH**, Moon JH, Park SH. Biliary stenting for hilar malignant biliary obstruction. *Dig Endosc* 2020; **32**: 275-286 [PMID: 31578770 DOI: 10.1111/den.13549]

38 **Perdue DG**, Freeman ML, DiSario JA, Nelson DB, Fennerty MB, Lee JG, Overby CS, Ryan ME, Bochna GS, Snady HW, Moore JP; ERCP Outcome Study ERCOST Group. Plastic versus self-expanding metallic stents for malignant hilar biliary obstruction: a prospective multicenter observational cohort study. *J Clin Gastroenterol* 2008; **42**: 1040-1046 [PMID: 18719507 DOI: 10.1097/MCG.0b013e31815853e0]

39 **Mukai T**, Yasuda I, Nakashima M, Doi S, Iwashita T, Iwata K, Kato T, Tomita E, Moriwaki H. Metallic stents are more efficacious than plastic stents in unresectable malignant hilar biliary strictures: a randomized controlled trial. *J Hepatobiliary Pancreat Sci* 2013; **20**: 214-222 [PMID: 22415652 DOI: 10.1007/s00534-012-0508-8]

40 **Raju RP**, Jaganmohan SR, Ross WA, Davila ML, Javle M, Raju GS, Lee JH. Optimum palliation of inoperable hilar cholangiocarcinoma: comparative assessment of the efficacy of plastic and self-expanding metal stents. *Dig Dis Sci* 2011; **56**: 1557-1564 [PMID: 21222156 DOI: 10.1007/s10620-010-1550-5]

41 **Wagner HJ**, Knyrim K, Vakil N, Klose KJ. Plastic endoprostheses versus metal stents in the palliative treatment of malignant hilar biliary obstruction. A prospective and randomized trial. *Endoscopy* 1993; **25**: 213-218 [PMID: 7686100 DOI: 10.1055/s-2007-1010295]

42 **Liberato MJ**, Canena JM. Endoscopic stenting for hilar cholangiocarcinoma: efficacy of unilateral and bilateral placement of plastic and metal stents in a retrospective review of 480 patients. *BMC Gastroenterol* 2012; **12**: 103 [PMID: 22873816 DOI: 10.1186/1471-230X-12-103]

43 **Takahashi E**, Fukasawa M, Sato T, Takano S, Kadokura M, Shindo H, Yokota Y, Enomoto N. Biliary drainage strategy of unresectable malignant hilar strictures by computed tomography volumetry. *World J Gastroenterol* 2015; **21**: 4946-4953 [PMID: 25945008 DOI: 10.3748/wjg.v21.i16.4946]

44 **Vienne A**, Hobeika E, Gouya H, Lapidus N, Fritsch J, Choury AD, Chryssostalis A, Gaudric M, Pelletier G, Buffet C, Chaussade S, Prat F. Prediction of drainage effectiveness during endoscopic stenting of malignant hilar strictures: the role of liver volume assessment. *Gastrointest Endosc* 2010; **72**: 728-735 [PMID: 20883850 DOI: 10.1016/j.gie.2010.06.040]

45 **Sawas T**, Al Halabi S, Parsi MA, Vargo JJ. Self-expandable metal stents versus plastic stents for malignant biliary obstruction: a meta-analysis. *Gastrointest Endosc* 2015; **82**: 256-267.e7 [PMID: 25982849 DOI: 10.1016/j.gie.2015.03.1980]

46 **Lee TH**, Kim TH, Moon JH, Lee SH, Choi HJ, Hwangbo Y, Hyun JJ, Choi JH, Jeong S, Kim JH, Park DH, Han JH, Park SH. Bilateral versus unilateral placement of metal stents for inoperable high-grade malignant hilar biliary strictures: a multicenter, prospective, randomized study (with video). *Gastrointest Endosc* 2017; **86**: 817-827 [PMID: 28479493 DOI: 10.1016/j.gie.2017.04.037]

47 **Schmidt A**, Riecken B, Rische S, Klinger C, Jakobs R, Bechtler M, Kähler G, Dormann A, Caca K. Wing-shaped plastic stents vs. self-expandable metal stents for palliative drainage of malignant distal biliary obstruction: a randomized multicenter study. *Endoscopy* 2015; **47**: 430-436 [PMID: 25590188 DOI: 10.1055/s-0034-1391232]

48 **Ridtitid W**, Rerknimitr R. Management of an occluded biliary metallic stent. *World J Gastrointest Endosc* 2012; **4**: 157-161 [PMID: 22624066 DOI: 10.4253/wjge.v4.i5.157]

49 **Kang H**, Chung MJ, Cho IR, Jo JH, Lee HS, Park JY, Park SW, Song SY, Bang S. Efficacy and safety of palliative endobiliary radiofrequency ablation using a novel temperature-controlled catheter for malignant biliary stricture: a single-center prospective randomized phase II TRIAL. *Surg Endosc* 2021; **35**: 63-73 [PMID: 32488654 DOI: 10.1007/s00464-020-07689-z]

50 **Saluja SS**, Gulati M, Garg PK, Pal H, Pal S, Sahni P, Chattopadhyay TK. Endoscopic or percutaneous biliary drainage for gallbladder cancer: a randomized trial and quality of life assessment. *Clin Gastroenterol Hepatol* 2008; **6**: 944-950.e3 [PMID: 18585976 DOI: 10.1016/j.cgh.2008.03.028]

51 **Kloek JJ**, van der Gaag NA, Aziz Y, Rauws EA, van Delden OM, Lameris JS, Busch OR, Gouma DJ, van Gulik TM. Endoscopic and percutaneous preoperative biliary drainage in patients with suspected hilar cholangiocarcinoma. *J Gastrointest Surg* 2010; **14**: 119-125 [PMID: 19756881 DOI: 10.1007/s11605-009-1009-1]

52 **Paik WH**, Park YS, Hwang JH, Lee SH, Yoon CJ, Kang SG, Lee JK, Ryu JK, Kim YT, Yoon YB. Palliative treatment with self-expandable metallic stents in patients with advanced type III or IV hilar cholangiocarcinoma: a percutaneous versus endoscopic approach. *Gastrointest Endosc* 2009; **69**: 55-62 [PMID: 18657806 DOI: 10.1016/j.gie.2008.04.005]

53 **Walter T**, Ho CS, Horgan AM, Warkentin A, Gallinger S, Greig PD, Kortan P, Knox JJ. Endoscopic or percutaneous biliary drainage for Klatskin tumors? *J Vasc Interv Radiol* 2013; **24**: 113-121 [PMID: 23182938 DOI: 10.1016/j.jvir.2012.09.019]

54 **Chang WH**, Kortan P, Haber GB. Outcome in patients with bifurcation tumors who undergo unilateral versus bilateral hepatic duct drainage. *Gastrointest Endosc* 1998; **47**: 354-362 [PMID: 9609426 DOI: 10.1016/s0016-5107(98)70218-4]

55 **Rerknimitr R**, Kladcharoen N, Mahachai V, Kullavanijaya P. Result of endoscopic biliary drainage in hilar cholangiocarcinoma. *J Clin Gastroenterol* 2004; **38**: 518-523 [PMID: 15220688 DOI: 10.1097/01.mcg.0000123204.36471.be]

56 **Khashab MA**, Valeshabad AK, Afghani E, Singh VK, Kumbhari V, Messallam A, Saxena P, El Zein M, Lennon AM, Canto MI, Kalloo AN. A comparative evaluation of EUS-guided biliary drainage and percutaneous drainage in patients with distal malignant biliary obstruction and failed ERCP. *Dig Dis Sci* 2015; **60**: 557-565 [PMID: 25081224 DOI: 10.1007/s10620-014-3300-6]

57 **Artifon EL**, Aparicio D, Paione JB, Lo SK, Bordini A, Rabello C, Otoch JP, Gupta K. Biliary drainage in patients with unresectable, malignant obstruction where ERCP fails: endoscopic ultrasonography-guided choledochoduodenostomy versus percutaneous drainage. *J Clin Gastroenterol* 2012; **46**: 768-774 [PMID: 22810111 DOI: 10.1097/MCG.0b013e31825f264c]

58 **Witzigmann H**, Lang H, Lauer H. Guidelines for palliative surgery of cholangiocarcinoma. *HPB (Oxford)* 2008; **10**: 154-160 [PMID: 18773044 DOI: 10.1080/13651820801992567]

59 **Shepherd HA**, Royle G, Ross AP, Diba A, Arthur M, Colin-Jones D. Endoscopic biliary endoprosthesis in the palliation of malignant obstruction of the distal common bile duct: a randomized trial. *Br J Surg* 1988; **75**: 1166-1168 [PMID: 2466520 DOI: 10.1002/bjs.1800751207]

60 **Smith AC**, Dowsett JF, Russell RC, Hatfield AR, Cotton PB. Randomised trial of endoscopic stenting versus surgical bypass in malignant low bileduct obstruction. *Lancet* 1994; **344**: 1655-1660 [PMID: 7996958 DOI: 10.1016/s0140-6736(94)90455-3]

61 **Andersen JR**, Sørensen SM, Kruse A, Rokkjaer M, Matzen P. Randomised trial of endoscopic endoprosthesis versus operative bypass in malignant obstructive jaundice. *Gut* 1989; **30**: 1132-1135 [PMID: 2475392 DOI: 10.1136/gut.30.8.1132]

62 **Lai EC**, Chu KM, Lo CY, Fan ST, Lo CM, Wong J. Choice of palliation for malignant hilar biliary obstruction. *Am J Surg* 1992; **163**: 208-212 [PMID: 1371206 DOI: 10.1016/0002-9610(92)90102-w]

63 **Speer AG**, Cotton PB, Russell RC, Mason RR, Hatfield AR, Leung JW, MacRae KD, Houghton J, Lennon CA. Randomised trial of endoscopic versus percutaneous stent insertion in malignant obstructive jaundice. *Lancet* 1987; **2**: 57-62 [PMID: 2439854 DOI: 10.1016/s0140-6736(87)92733-4]

64 **Piñol V**, Castells A, Bordas JM, Real MI, Llach J, Montañà X, Feu F, Navarro S. Percutaneous self-expanding metal stents versus endoscopic polyethylene endoprostheses for treating malignant biliary obstruction: randomized clinical trial. *Radiology* 2002; **225**: 27-34 [PMID: 12354980 DOI: 10.1148/radiol.2243011517]

World Journal of Clinical Oncology

Submit a Manuscript: https://www.f6publishing.com

World J Clin Oncol 2024 March 24; 15(3): 391-410

DOI: 10.5306/wjco.v15.i3.391

ISSN 2218-4333 (online)

ORIGINAL ARTICLE

Retrospective Study

Ferroptosis biomarkers predict tumor mutation burden's impact on prognosis in HER2-positive breast cancer

Jin-Yu Shi, Xin Che, Rui Wen, Si-Jia Hou, Yu-Jia Xi, Yi-Qian Feng, Ling-Xiao Wang, Shi-Jia Liu, Wen-Hao Lv, Ya-Fen Zhang

Specialty type: Oncology

Provenance and peer review: Unsolicited article; Externally peer reviewed.

Peer-review model: Single blind

Peer-review report's scientific quality classification

Grade A (Excellent): 0
Grade B (Very good): 0
Grade C (Good): C
Grade D (Fair): 0
Grade E (Poor): 0

P-Reviewer: Bansal C, India

Received: October 17, 2023
Peer-review started: October 17, 2023
First decision: December 31, 2023
Revised: January 14, 2024
Accepted: February 3, 2024
Article in press: February 3, 2024
Published online: March 24, 2024

Jin-Yu Shi, Shi-Jia Liu, Wen-Hao Lv, Ya-Fen Zhang, Department of Breast Surgery, The Fifth Hospital of Shanxi Medical University, Taiyuan 030000, Shanxi Province, China

Jin-Yu Shi, Xin Che, Ling-Xiao Wang, Shi-Jia Liu, Wen-Hao Lv, The Fifth Clinical Medical College, Shanxi Medical University, Taiyuan 030000, Shanxi Province, China

Xin Che, Ling-Xiao Wang, Department of Colorectal Surgery, The Fifth Hospital of Shanxi Medical University, Taiyuan 030000, Shanxi Province, China

Rui Wen, College of Pharmacy, Shanxi Medical University, Taiyuan 030000, Shanxi Province, China

Si-Jia Hou, Department of Neurology, The First Hospital of Shanxi Medical University, Taiyuan 030000, Shanxi Province, China

Yu-Jia Xi, Department of Urology, The Second Hospital of Shanxi Medical University, Taiyuan 030000, Shanxi Province, China

Yi-Qian Feng, Department of Breast Surgery, The First Hospital of Shanxi Medical University, Taiyuan 030000, Shanxi Province, China

Corresponding author: Ya-Fen Zhang, MD, Chief Doctor, Department of Breast Surgery, The Fifth Hospital of Shanxi Medical University, Shuangta West Street, Yingze District, Taiyuan 030000, Shanxi Province, China. cocoren2005@163.com

Abstract

BACKGROUND

Ferroptosis has recently been associated with multiple degenerative diseases. Ferroptosis induction in cancer cells is a feasible method for treating neoplastic diseases. However, the association of iron proliferation-related genes with prognosis in HER2+ breast cancer (BC) patients is unclear.

AIM

To identify and evaluate fresh ferroptosis-related biomarkers for HER2+ BC.

METHODS

First, we obtained the mRNA expression profiles and clinical information of HER2+ BC patients from the TCGA and METABRIC public databases. A four-

gene prediction model comprising *PROM2*, *SLC7A11*, *FANCD2*, and *FH* was subsequently developed in the TCGA cohort and confirmed in the METABRIC cohort. Patients were stratified into high-risk and low-risk groups based on their median risk score, an independent predictor of overall survival (OS). Based on these findings, immune infiltration, mutations, and medication sensitivity were analyzed in various risk groupings. Additionally, we assessed patient prognosis by combining the tumor mutation burden (TMB) with risk score. Finally, we evaluated the expression of critical genes by analyzing single-cell RNA sequencing (scRNA-seq) data from malignant *vs* normal epithelial cells.

RESULTS

We found that the higher the risk score was, the worse the prognosis was ($P < 0.05$). We also found that the immune cell infiltration, mutation, and drug sensitivity were different between the different risk groups. The high-risk subgroup was associated with lower immune scores and high TMB. Moreover, we found that the combination of the TMB and risk score could stratify patients into three groups with distinct prognoses. HRisk-HTMB patients had the worst prognosis, whereas LRisk-LTMB patients had the best prognosis ($P < 0.0001$). Analysis of the scRNA-seq data showed that *PROM2*, *SLC7A11*, and *FANCD2* were significantly differentially expressed, whereas *FH* was not, suggesting that these genes are expressed mainly in cancer epithelial cells ($P < 0.01$).

CONCLUSION

Our model helps guide the prognosis of HER2+ breast cancer patients, and its combination with the TMB can aid in more accurate assessment of patient prognosis and provide new ideas for further diagnosis and treatment.

Key Words: HER2+ breast cancer; Ferroptosis; Tumor mutation burden; Single-cell RNA sequencing; Prognosis

Core Tip: A prognostic model constructed with four ferroptosis-related genes (*PROM2, SLC7A11, FANCD2*, and *FH*) combined with tumor mutation burden can be used to evaluate the prognosis of patients with HER2-positive breast cancer more accurately.

Citation: Shi JY, Che X, Wen R, Hou SJ, Xi YJ, Feng YQ, Wang LX, Liu SJ, Lv WH, Zhang YF. Ferroptosis biomarkers predict tumor mutation burden's impact on prognosis in HER2-positive breast cancer. *World J Clin Oncol* 2024; 15(3): 391-410
URL: https://www.wjgnet.com/2218-4333/full/v15/i3/391.htm
DOI: https://dx.doi.org/10.5306/wjco.v15.i3.391

INTRODUCTION

Breast cancer (BC) is the most prevalent malignancy in the world and the primary cause of cancer-related deaths in women[1]. As a highly heterogeneous disease, BC has four molecular subtypes: Basal/triple-negative, luminal A, luminal B, and HER2-positive[2]. HER2 is an orphan tyrosine kinase receptor that regulates cell proliferation and survival when activated. Located at chromosome 17q12, the HER2 oncogene is amplified in 15-20% of all BCs[3]. The primary and essential mechanism of HER2 receptor overexpression is amplification[4,5]. Due to its role in cell proliferation, invasion, and survival, this mechanism confers a poor prognosis. Standard treatment modalities include surgery combined with chemotherapy, radiotherapy, endocrine therapy, and HER2-targeted therapy which are widely used in clinical practice [5]. For the HER2-positive subtype, HER2-targeted treatments, such as trastuzumab, pertuzumab, T-DM1, DS8201, and tyrosine kinase inhibitors (TKIs), can significantly improve disease-free survival and overall survival (OS)[6,7]. Notably, not all patients derive equal benefits from existing anti-HER2 therapies, and HER2-positive BC is inherently heterogeneous. Although numerous studies have focused on investigating the prognostic significance of ferroptosis-related genes in BC[8-10], analyses specific to BC subtypes are lacking. A more comprehensive understanding of tumor biology and the HER2 signaling pathway is essential for advancing novel strategies to improve patient outcomes.

A new type of controlled cell death known as ferroptosis differs from apoptosis, necrosis, and autophagy in morphology, biochemistry, and genetics[11]. It is characterized by disruption of the intracellular redox balance and nonapoptotic cell death. Previous studies revealed that the NAD (P)H/FSP1/CoQ10 and cyst (e)ine/GSH/glutathione peroxidase 4 (GPX4) signaling pathways control ferroptosis. Ferroptosis is caused by the buildup of lipid peroxidation products and reactive oxygen species generated from iron metabolism. Increasing evidence suggests that ferroptosis is closely related to many diseases, especially HER2+ BC[12]. Thus, ferroptosis has gained popularity as a potential therapeutic strategy to promote cancer cell death. Various studies have reported ferroptosis induction by afatinib and lapatinib[13]. However, the association between iron proliferation-related genes and prognosis in HER2+ BC patients has yet to be determined, hindering practical clinical assessment before treatment.

This research systematically analyzed HER2+ BC expression data and clinical information from the TCGA and METABRIC cohorts. Furthermore, we identified genes associated with ferroptosis that were differentially expressed in patient tissues compared with normal tissues, screened four signatures related to survival, and constructed a consistent prediction model. We also explored the associations of ferroptosis with immune cell infiltration, mutations, and immune checkpoints in HER2+ BC patients. These results provide a foundation for developing comprehensive therapeutic strategies for HER2+ BC patients.

MATERIALS AND METHODS

Data collection

We used HER2+ BC datasets downloaded from the TCGA (https://protal.gdc.cancer.gov/repository) and the METABRIC databases (www.cbioportal.org/). The downloaded data were filtered using the following criteria: (1) Histologically diagnosed with malignant BC; (2) complete corresponding clinical data; and (3) available OS data for more than 90 d. Additional average breast tissue mRNA expression data (n = 91) were obtained from GTEx (https://gtexportal.org/home/datasets). The final sample included 168 patients from the TCGA cohort and 126 patients from the METABRIC cohort with complete follow-up information. A total of 259 genes associated with ferroptosis were retrieved from the FerrDb website (http://www.zhounan.org/ferrdb/current/) and are reported in Supplementary Table 1 (marker: 111; Driver: 108; suppressor: 69). The single-cell RNA sequencing (scRNA-seq) dataset was assessed from the Gene Expression Omnibus (GEO) database (http://www.ncbi.nlm.nih.gov/geo).

Construction of a prognostic ferroptosis-related gene signature

The TCGA and METABRIC cohorts were selected as training and validation sets, respectively. First, the log2 transformation approach was used after the raw count data had been normalized using the transcripts per million method. The number of DEGs was calculated using the "DESeq2" package ($P < 0.05$) in R. Venn was used to identify DEGs associated with ferroptosis. Univariate Cox regression analysis was performed to identify ferroptosis-related prognostic genes, and relevant genes were selected using a cutoff of $P < 0.05$. In total, 18 genes were chosen for the minor absolute shrinkage and selection operator (LASSO) Cox regression. Multivariate Cox regression analysis was subsequently applied to further assess the significant factors. We used lasso-penalized Cox regression analysis with the "glmnet" package in R to choose prognostic ferroptosis-related genes and construct a predictive model. The following formula was used to generate the risk score: Risk score = sum (corresponding coefficient × expression level of the gene). The expression levels of the genes were normalized, and the regression coefficients were calculated from the training set. Patients were then categorized into high- or low-risk groups according to the median risk score. The "Rtsne" package was used to run t-SNE to investigate the distribution of various groups. Using the "survminer" package in R, Kaplan-Meier (K-M) curves were created to predict OS. The "survival receiver operating characteristic (ROC)" package in R was used to run a time-dependent ROC curve analysis to evaluate the ability of the signature genes to predict survival.

Integrated analysis of combined clinical and multiomics data from the risk-scoring model

To determine the relevant immune cell infiltration patterns and immunological characteristics, the CIBERSORT algorithm was used. The "ESTIMATE" program was applied to estimate the tumor purity scores. We examined the expression of immune-related signal transduction pathway components in various risk groups. We compared the estimated immune and stromal scores between the high- and low-risk groups. We also examined the underlying mechanisms in two risk subgroups using TCGA gene mutation data. The "MAFtools" package of R was used to evaluate SNP mutations and visualize the results. The tumor mutation burden (TMB) was subsequently determined. Patients were separated into two groups based on the median TMB value: The high TMB group and the low TMB group. Subsequently, the TMB score was combined with the risk score to form a new subgroup.

Our study included specific well-known immune checkpoint genes to evaluate gene expression levels across various risk score groups. Drug susceptibility was predicted using information from the GDSC database (https://www.cancerrxgene.org/celllines). The half-maximal inhibitory concentration (IC_{50}) indicated the patient's drug response and was calculated using the "pRRophetic" package.

Hub gene mRNA expression validation in the scRNA-seq data

scRNA-seq data (GSE161529) from 6 HER2-positive BC patients and 13 healthy controls were obtained from the GEO database (https://www.ncbi.nlm.nih.gov/geo/). Subsequently, low-quality cells were removed using the following criteria: (1) Had a number of expressed genes lower than 500; (2) Had a number of expressed genes higher than 2500; or (3) Had a proportion of mitochondria larger than 10%. The R "Seurat" package was used for cell cluster analysis. Cellular regions were manually annotated based on marker gene expression patterns and cell subset grouping patterns. The expression levels of the hub genes were subsequently displayed in each cell subset. Additionally, we validated the differential expression profiles of prognostic genes in the epithelial cells of patients and healthy controls using the tool "FindMarkers."

Statistical analysis

R 4.1.0 was used to perform all the statistical analyses. A log-rank test and K-M analysis were used to compare OS among various risk subgroups. The primary prognostic variables connected to OS were identified using univariate and

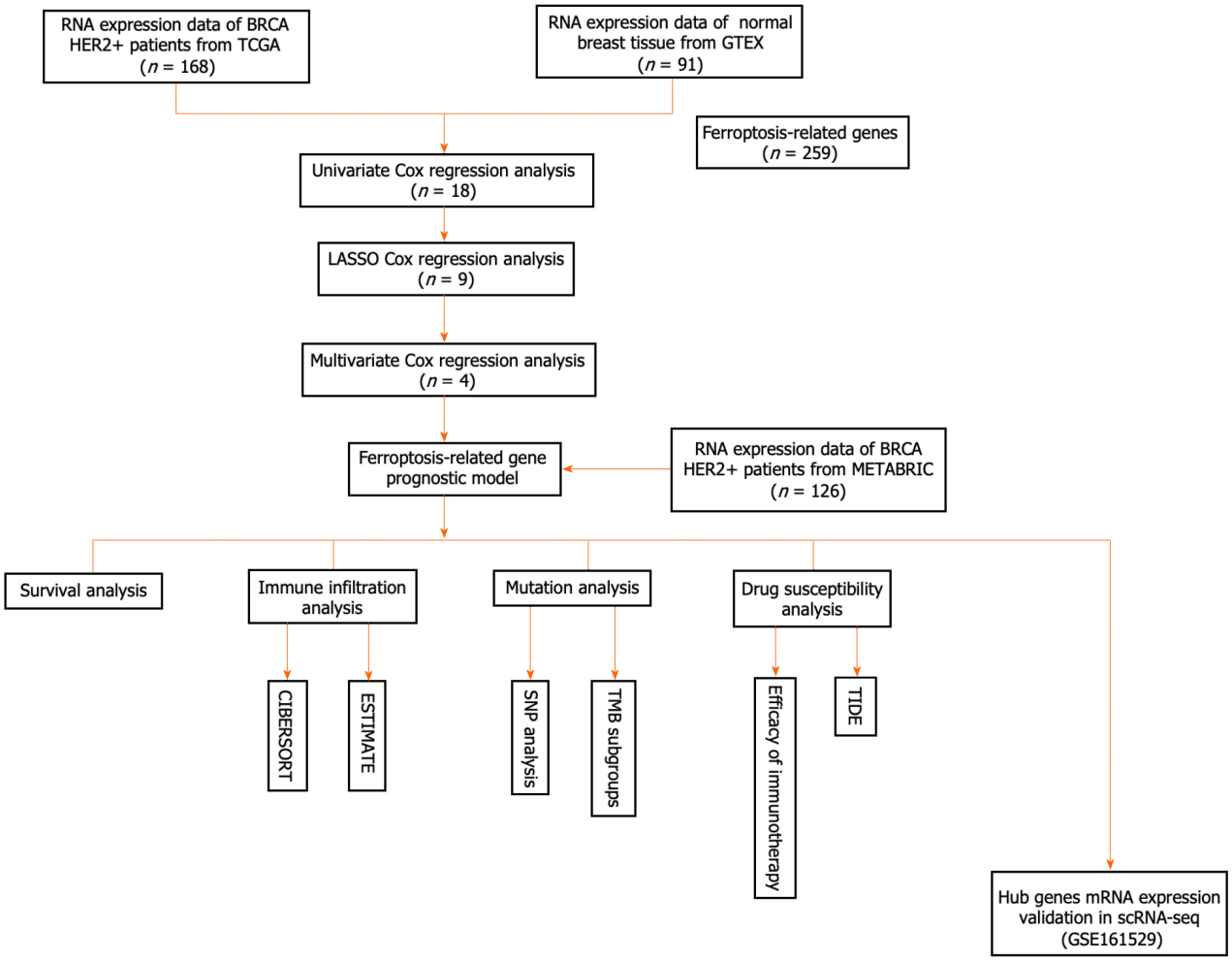

Figure 1 Flowchart for collecting and analyzing data from TCGA and METABRIC databases. scRNA-seq: Single-cell RNA sequencing; TMB: Tumor mutation burden.

multivariate Cox regression analyses. Continuous and categorical variables were compared in the training and verification sets using Spearman correlation analysis. Unless otherwise stated, all the statistical tests were two-sided, and values with $P < 0.05$ were considered to indicate statistical significance.

RESULTS

A flowchart of our research is shown below (Figure 1). In this study, 168 patients with the HER2+ subtype of BC from the TCGA database served as the training cohort, whereas 126 patients from the METABRIC cohort were enrolled as the validation cohort. Supplementary Table 2 summarizes the clinical features of the two cohorts.

Characterization of the ability of the ferroptosis risk score to predict HER2+ BC prognosis

The ferroptosis-related gene expression profiles of the patients in the high- and low-risk groups are displayed in a heatmap (Figure 2A). In addition, the volcano plot showed 5481 upregulated genes and 3766 downregulated genes in tumor tissues (Figure 2B; $P < 0.05$). A total of 128 genes were differentially expressed in ferroptosis and tumor tissues (Figure 2C). Of the 128 ferroptosis-related genes, 18 were identified using the univariate Cox regression model as significantly associated with patient OS ($P < 0.05$). The results are shown as forest plots (Figure 2D). Lasso-penalized Cox regression analysis was further conducted to limit the scope of the gene screening (Figure 3A). The nine candidate gene markers had the best lambda values (Figure 3B). Finally, multivariate regression analysis revealed that four DEGs were significantly correlated with OS.

With respect to the TCGA cohort, a risk score was developed to determine the predictive power of the 4 genes associated with ferroptosis. The risk score was calculated using the formula below: Risk score = 1.05 × expression level of *PROM2* + 0.532 × *SLC7A11* + 0.447 × *FANCD2* + 0.453 × *FH*. Patients were classified into high-risk (n = 84) and low-risk (n = 84) groups based on the median risk score cutoff (Figure 3C; Table 1).

Table 1 Clinical characteristics of patients in different risk groups in TCGA and METABRIC cohorts, *n* (%)

	TCGA			Metabric		
	High risk group, *n* = 84	Low risk group, *n* = 84	*P* value	High risk group, *n* = 54	Low risk group, *n* = 72	*P* value
Age						
< 60	38 (0.45)	40 (0.48)	0.003	34 (0.63)	41 (0.57)	0.606
≥ 60	46 (0.55)	44 (0.52)		20 (0.37)	31 (0.43)	
Stage						
I/II	59 (0.70)	58 (0.69)	0.033	40 (0.74)	60 (0.83)	0.101
III/IV	25 (0.30)	26 (0.31)		14 (0.26)	12 (0.17)	
Radio therapy						
Yes	3 (0.04)	5 (0.06)	0.293	41 (0.76)	49 (0.68)	0.548
No	7 (0.08)	6 (0.07)		13 (0.24)	23 (0.32)	
Unknown	74 (0.88)	73 (0.87)		0	0	

According to K-M curves, patients in the TCGA cohort with lower risk scores had better prognoses (Figure 3D; $P < 0.05$). Using time-dependent ROC curve analysis, the area under the curve (AUC) was evaluated. The AUCs of the four ferroptosis-related genes at 3, 5, and 8 years were 0.797, 0.770, and 0.664, respectively (Figure 3E), with the third year having the most significant AUC. These four genes are anticipated to be associated with OS. Patients in different risk groups were dispersed in both directions according to the t-distributed stochastic neighbor embedding (t-SNE) analysis (Figure 3F).

External validation of the prognostic gene signature

We chose the independent database METABRIC for validation to confirm the ability of the four-gene signature to predict survival. The patients were divided into high-risk and low-risk groups using the same algorithm used for the TCGA cohort (Table 1, Supplementary Figure 1A). Those in the high-risk group demonstrated significantly worse OS than did those in the low-risk group (Supplementary Figure 1B, $P < 0.05$), consistent with the findings in the TCGA cohort. The AUC for 3-, 5-, and 8-year OS were 0.653, 0.648, and 0.560, respectively (Supplementary Figure 1C). Additionally, T-SNE analysis verified that the two patient subgroups spread in opposite directions (Supplementary Figure 1D). These findings showed that the four-gene signature could accurately predict OS in patients with the HER2+ subtype of BC.

Independent prognostic role of the gene signature

Patients with complete data, including age, stage, radiation therapy, and risk score, were enrolled for additional analysis. The risk score was identified as a significant prognostic risk factor in the TCGA cohort [$P < 0.001$, hazard ratio (HR) = 2.72, 95%CI = 1.889-3.912] and in the METABRIC cohort ($P < 0.001$, HR = 1.17, 95%CI = 1.024-1.337) by univariate Cox analysis (Figure 4A). The risk score was also found to be an independent predictive factor for OS in the TCGA cohort ($P < 0.001$, HR = 2.62, 95%CI = 1.815-3.785) and the METABRIC cohort ($P < 0.001$, HR = 1.16, 95%CI = 1.011-1.322) according to multivariate Cox regression analysis (Figure 4B). Consequently, the risk score derived from the four-gene profile was an independent prognostic factor.

Constructing and validating a predictive nomogram

We subsequently developed a nomogram employing three independent prognostic parameters, cancer stage, age, and risk score, to predict 3-, 5-, and 8-year OS in 168 HER2+ BC patients (Figure 5A). The calibration plot showed that the nomogram might under- or overestimate mortality (Figure 5B). The C-index of the model, which considered risk score, age, and stage, was 0.87 (Figure 5C). In addition, we repeated these steps in the METABRIC cohort to validate the efficacy of the training cohort. It is important to note that there was significant agreement between the predicted and observed survival rates, suggesting that the nomogram has excellent predictive value (Supple-mentary Figure 2).

Immune-related characteristics in the low- and high-risk score groups

The four-gene signature may be correlated with the immunological characteristics of cancer patients, providing future guidance for immunotherapy for HER2+ BC patients. A significant association between the risk score and essential immune cell infiltration or immunological aspects was assessed using the CIBERSORT algorithm. We discovered that the high- and low-risk groups had distinct immune cell infiltration rates. The infiltration of M2-type macrophages, activated dendritic cells, and eosinophils was greater than that of CD8+ T cells and resting mast cells in the high-risk group (Figure 6A). We also constructed heatmaps to evaluate the correlation between immune cells and prognostic genes (Figure 6B). In the present analysis, the ESTIMATE score also revealed higher immune, stromal, and ESTIMATE scores in the low-risk subgroup than in the high-risk subgroup (Figure 6C-E). In addition, the distribution of immune-related

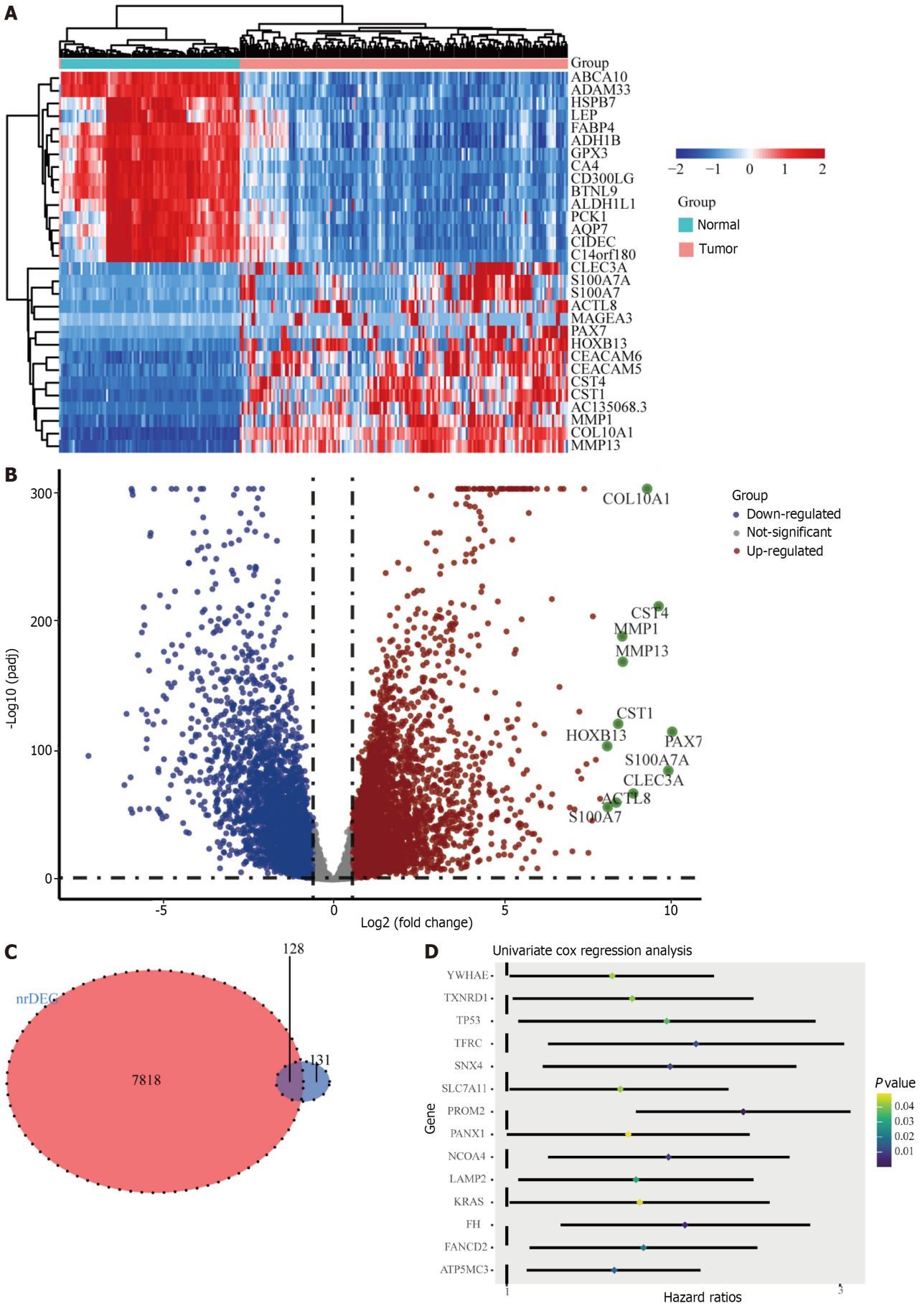

Figure 2 Identification of candidate genes associated with ferroptosis in the TCGA cohort. A: Heatmap of candidate gene expression differences

between tumor and normal tissues; B: Volcano map showing up-regulated and down-regulated genes; C: A Venn diagram to identify differentially expressed genes associated with ferroptosis between tumor and normal tissues; D: Forest plot showing univariate Cox regression analysis results of correlation between candidate gene expression and overall survival.

signal transduction pathways was significantly different between the two risk subgroups, with lower infiltration of cytokine receptors, cytokines, the BCR signaling pathway, interleukin receptors, antimicrobials, chemokines, interleukins, T cell receptor signal transduction pathways and tumor necrosis factor receptors in the high-risk subgroup(Figure 6F).

Our analysis also included genes related to immune checkpoints, PD-1 (PDCD1), BTLA, TIGIT, GZMA, HLA-DRA, HLA-DPB1, and CD40. The expression of these seven well-known immune checkpoint genes varied between the low- and high-risk groups. Figure 6G indicates that immune checkpoint mRNA expression was decreased in HER2+ BC patients with higher risk scores. In addition, there was a significant positive correlation between the mRNA levels of the seven immune checkpoint receptors (Figure 6H).

Relationships between risk groups and mutation profiles

SNP analysis was performed on 155 samples comprising 80 samples in the high-risk group and 75 samples in the low-risk group, with significant mutation frequency genes screened out using the "MAFtools" package. Supplementary Figure 3A and B lists the top 10 mutated genes in samples from the high- and low-risk groups, with TTN and TP53 mutations being the most frequent in the two groups. Supplementary Figure 3C and D lists the top 20 genes in the sample, revealing that the most significant mutation types were missense, nonsense, missense, and multihit mutations. In patients, TP53, PIK3CA, and TTN were strongly associated with the development of HER2+ BC.

We also extracted the TMB subgroups in the high-risk and low-risk groups. We found a positive correlation between risk score and TMB ($P < 0.01$; Figure 7A and B). However, there was no significant difference in the TMB between the two risk groups (Figure 7C). Therefore, to explore whether combining the TMB and risk score provides better predictive ability, we combined the TMB and risk score to form a new subgroup. Kaplan-Meier survival curves for the new subset revealed significant differences in survival outcomes. The prognosis was worst for patients with HRisk-HTMB but best for those with LRisk-LTMB ($P < 0.0001$; Figure 7D).

Drug sensitivity analysis

We then extracted data on 138 drugs from the GDSC database and analyzed patient sensitivities to 138 medications between the high- and low-risk cancer groups. We found 13 drugs with significantly different sensitivities between the two risk groups (Supplementary Figure 4; $P < 0.05$).

Hub gene mRNA expression validation via scRNA-seq

The scRNA-seq dataset (GSE161529) was used to characterize HER2+ BC heterogeneity from the GEO database. After gene filtering and normalization, the "Seurat" package of the FindCluster function was used to cluster cells into 42 clusters (Figure 8A and B). The identified clusters were labeled as cell types using marker genes (Supplementary Table 3). We ultimately annotated these clusters into three main clusters (Figure 8C, Supplementary Table 4), and Figure 8D shows the proportions of cell types in patients and healthy individuals. According to the scRNA-seq analysis, Figure 8E-H demonstrates that the identified prognostic genes were primarily expressed in epithelial cells. Differences in the expression of the four marker genes between healthy controls and patients were further verified in epithelial cells. Specifically, *PROM2*, *SLC7A11*, and *FANCD2* but not *FH* were significantly differentially expressed, indicating that these genes were expressed in cancer epithelial cells (Table 2). However, the *SLC7A11* results did not correspond to the trend observed *via* Bulk RNA-seq. This difference is most likely related to the somewhat small sample size.

Table 2 Hub gene differentially expressed between normal and cancer epithelial cells

Gene	*P* value	Avg_log2FC	Pct.1	Pct.2	*P* value adjustment
PROM2	9.48E-134	0.115125977	0.096	0.017	1.98E-129
SLC7A11	2.96E-77	-0.101678852	0.016	0.08	6.18E-73
FANCD2	4.01E-27	0.028728862	0.025	0.006	8.38E-23

DISCUSSION

Ferroptosis is a type of cell death distinguished by iron-dependent lipid peroxidation. It interferes with the progression of tumors, neurological diseases, and chronic inflammatory diseases. There has been much research recently on the role and mechanisms of ferroptosis under various conditions, particularly in the tumor research and treatment domains. Ferroptosis pathway activation increases the susceptibility of cancer cells to chemotherapy. One study demonstrated the importance of ferroptosis in tumor therapy by showing that combining the ferroptosis inducer erastin with cisplatin can significantly boost antitumor efficacy[14]. Using ferrostatin-1 (a ferroptosis inhibitor) knockdown, Chen *et al*[15] reported that cystine (Cys) starvation induces ferroptosis in TNBC cells[15]. Therefore, ferroptosis could advance our under-

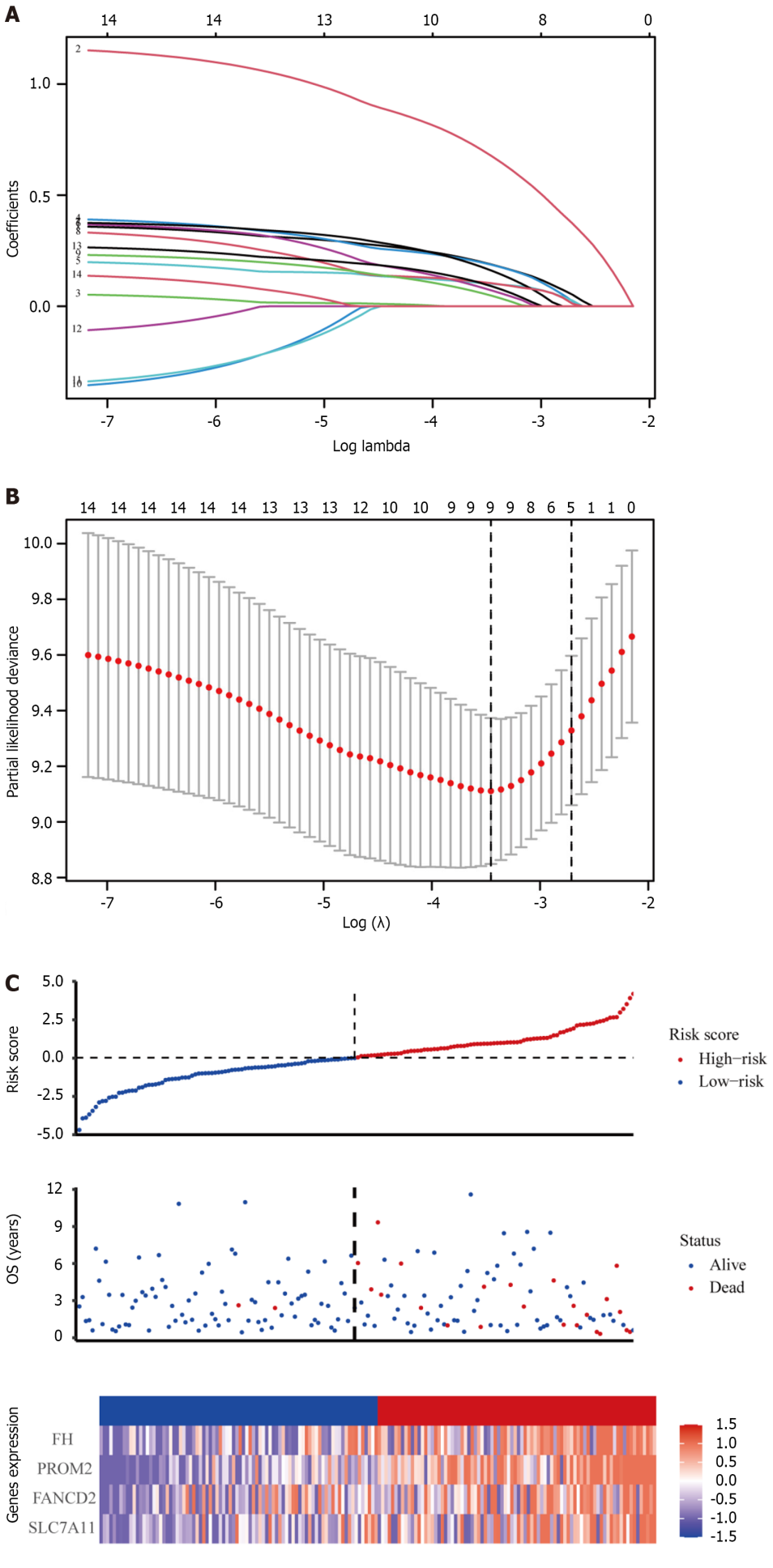
A
Coefficients
Log lambda
B
Partial likelihood deviance
Log (λ)
C
Risk score
High−risk
Low−risk
OS (years)
Status
Alive
Dead
Genes expression
FH
PROM2
FANCD2
SLC7A11

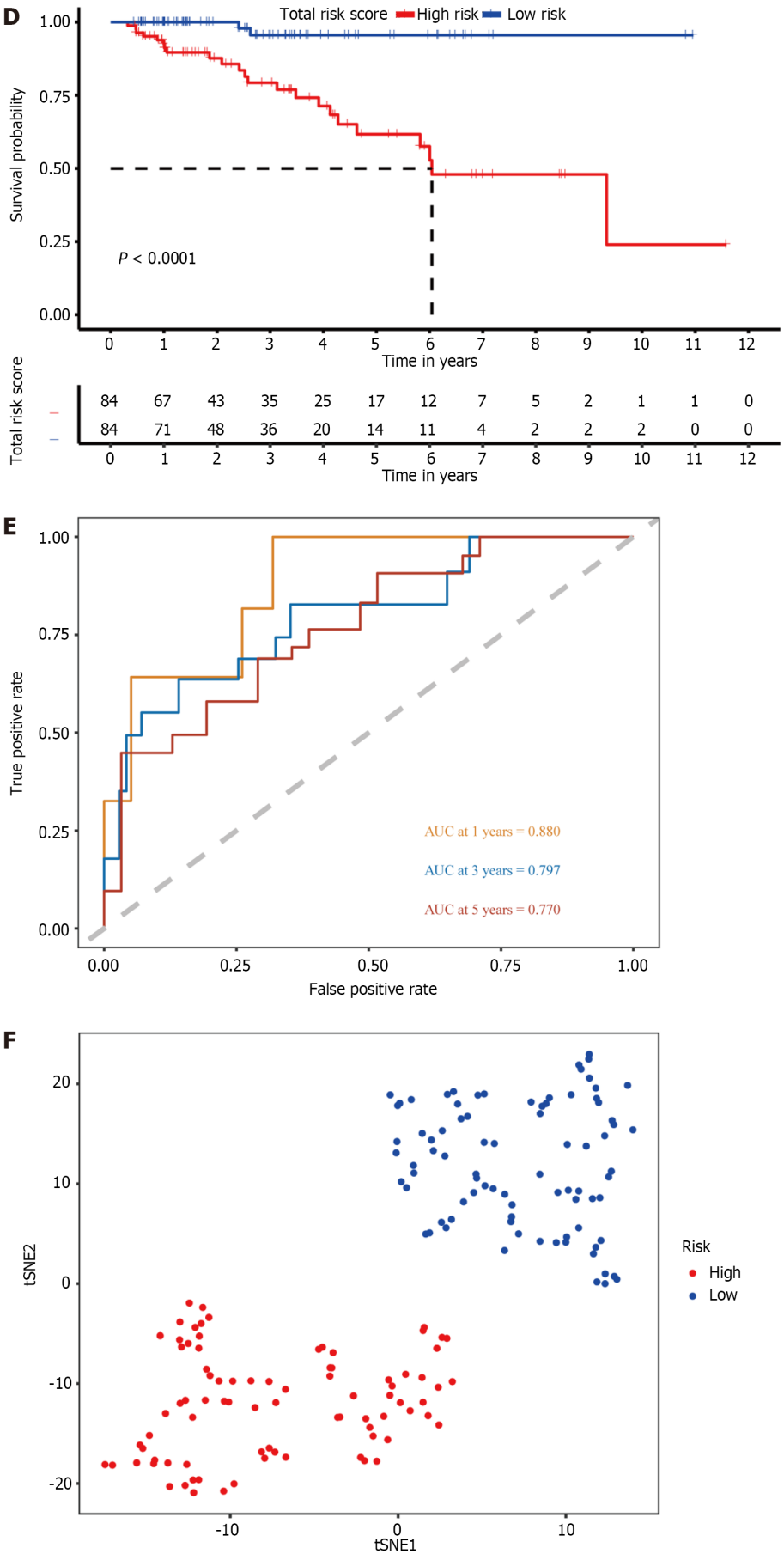

Figure 3 Prognostic analysis of four ferroptosis-related gene signature models in the TCGA cohort. A: The optimal lambda resulted in nine nonzero coefficients; B: The partial likelihood deviation curve was plotted *vs* lambda; C: Risk curves were plotted in the TCGA cohort; D: Kaplan–Meier curves for the

overall survival of patients in the high-risk and low-risk groups in the TCGA cohort; E: The area under the curves of time-dependent receiver operating characteristic curves verified the prognostic performance of the risk score in the TCGA cohort; F: T-SNE analysis of the TCGA cohort. OS: Overall survival.

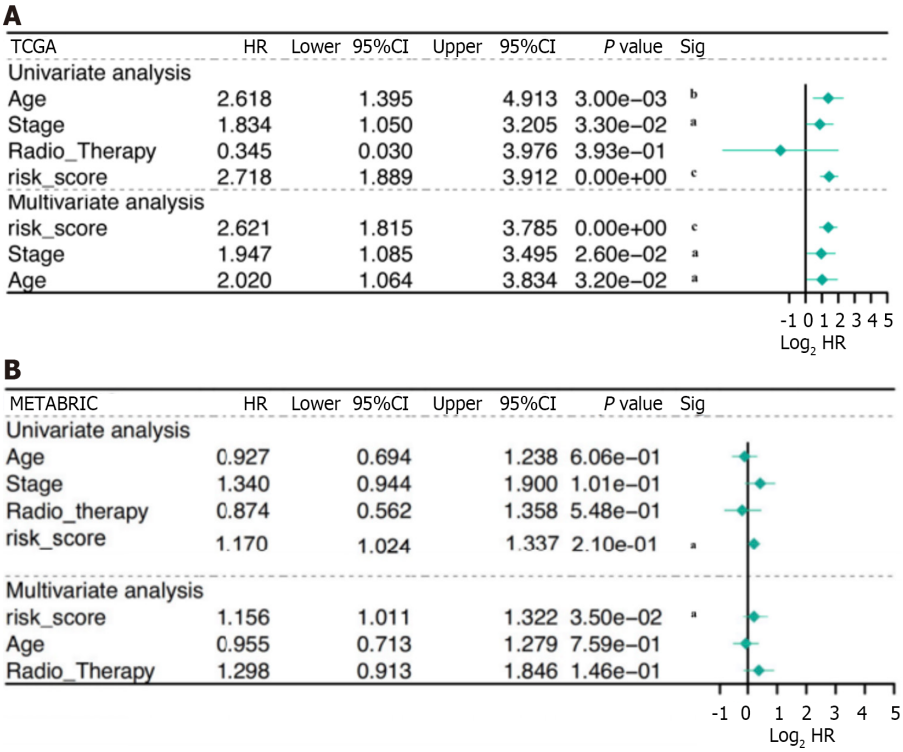

Figure 4 Results of univariate and multivariate Cox regression analyses. A: Results of the univariate and multivariate Cox analyses of overall survival (OS) in the TCGA derivation cohort; B: Results of univariate and multivariate Cox analyses of OS in the METABRIC derivation cohort. [a]*P* < 0.05, [b]*P* < 0.01, [c]*P* < 0.001. HR: Hazard ratio.

standing of tumor suppressors and reveal new therapeutic targets. From the perspective of different BC subtypes, the incidence of HER2+ BC varies little among different ethnic groups. Therefore, the results of this study have particular applicability to various ethnic groups[16]. Systematic and comprehensive analyses of ferroptosis are lacking to support malignant progression and treatment elucidating strategies for HER2+ BC.

This study systematically investigated the potential mechanisms of action of 259 iron death-associated genes in HER2+ BC patients. Four ferroptosis-related genes were included in the new prognostic model, and the validity of the model was tested in an external cohort. The association of these genes with OS was also explored. In addition, the immune microenvironment and mutations were enriched in our study. Nearly half of the iron apoptosis-related genes (129/259) were differentially expressed between 91 normal cells and 168 HER2+ cells, 18 of which were associated with OS according to univariate Cox regression analysis. Finally, a four-gene signature was obtained from the model using LASSO regression analysis and multivariate Cox regression analysis. These results demonstrated that iron-induced cell death plays a significant role in HER2+ BC patients, and prognostic features based on iron-induced cell death-related genes could be constructed.

Four ferroptosis-related genes were included in the prognostic model in this investigation. *PROM2*, *SLC7A11*, *FANCD2,* and *FH* were highly expressed in HER2+ BC patients. The expression levels of these genes were positively correlated with patient survival risk. Previous studies have shown that iron, lipid, and antioxidative metabolism are the three key pathways regulating iron-related apoptosis[17]. In addition, energy metabolism is associated with iron-related apoptosis. Consistent with our four-gene prognostic model, *PROM2*, *SLC7A11*, and *FANCD2* were previously reported to be involved in iron metabolism[18,19]. The *PROM2* gene is significantly upregulated in tumor tissues. *PROM2* contributes to iron transport and the inhibition of iron death by forming iron-containing multivesicular bodies and exosomes in BC cells[11,20]. *SLC7A11* is an essential component of the glutamate/Cys antiporter (also known as xCT). *SLC7A11* increases glutathione production and Cys absorption, reducing oxidative stress and iron cell death[21]. Depletion of *SLC7A11* significantly reduces glutathione concentrations and triggers iron-related apoptosis. In addition, *SLC7A11* is a central target of iron death regulation, and at high concentrations, it downregulates sensitivity to iron death in cancer cells[22,23]. Both *PROM2* and *SLC7A11* are regulated by GPX4, which increases the amount of peroxyl radicals required for lipid peroxidation, causing iron death. The regulation of *FANCD2* gene expression helps maintain normal DNA replication, which prevents cancer progression by influencing the iron-related death process[24,25]. *FANCD2* expression correlated with the characteristics of aggressive cancer: HER2 amplification, hormone receptor negativity, elevated p53 expression, proliferation, and high grade[26]. Several studies have demonstrated the positive association

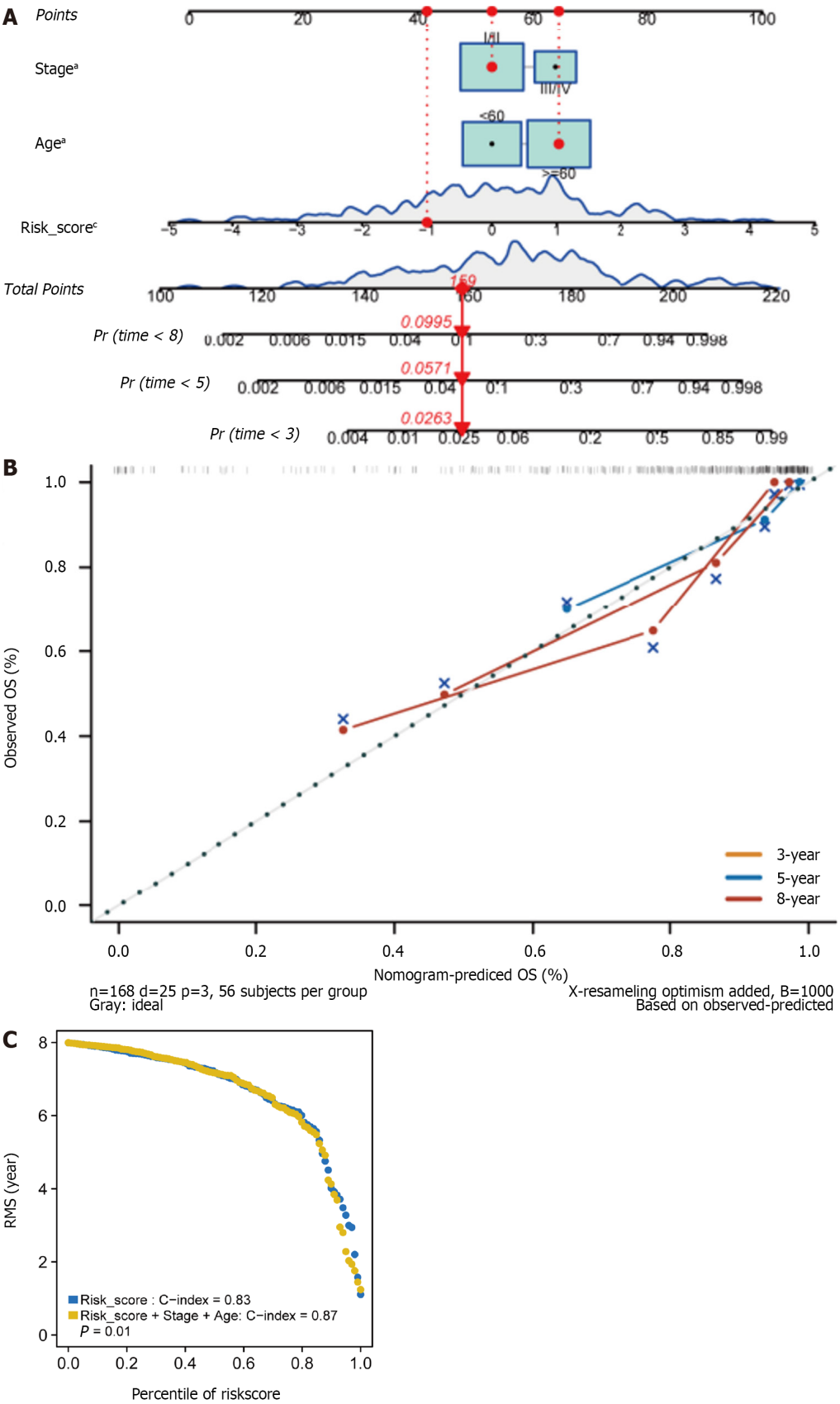

Figure 5 The four ferroptosis-related prognostic gene signature models for predicting 3-, 5-, and 8-year overall survival in HER2+ breast cancer patients. A: Independent risk factors were used to build a risk estimation nomogram to predict the probability of overall survival in HER2+ breast cancer patients; B: Calibration plots for 3-, 5-, and 8-year survival probabilities in the TCGA cohort; C: Restricted mean survival time Curve in the TCGA cohort. [a]$P < 0.05$, [b]$P < 0.01$, [c]$P < 0.001$. OS: Overall survival; RMS time: Restricted mean survival time.

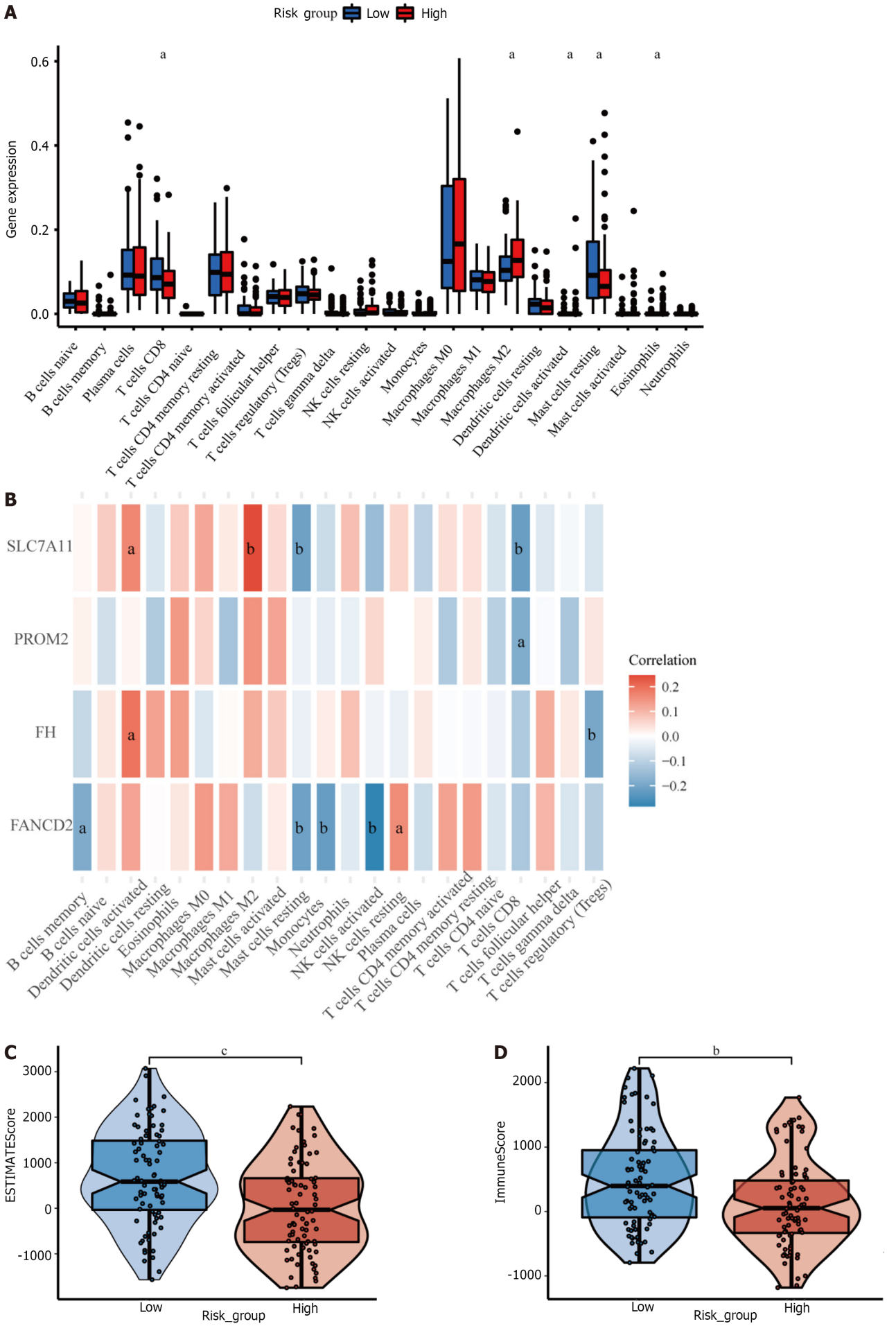
A
Risk group Low High
Gene expression
B cells naive
B cells memory
Plasma cells
T cells CD8
T cells CD4 naive
T cells CD4 memory resting
T cells CD4 memory activated
T cells follicular helper
T cells regulatory (Tregs)
T cells gamma delta
NK cells resting
NK cells activated
Monocytes
Macrophages M0
Macrophages M1
Macrophages M2
Dendritic cells resting
Dendritic cells activated
Mast cells resting
Mast cells activated
Eosinophils
Neutrophils
B
SLC7A11
PROM2
FH
FANCD2
Correlation
C
ESTIMATEScore
Low
Risk_group
High
D
ImmuneScore
Low
Risk_group
High

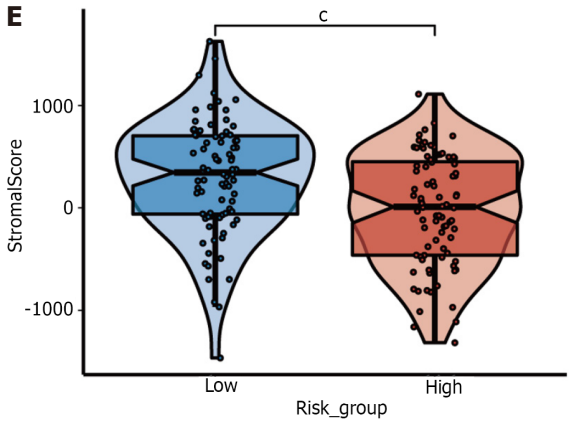
E
c
1000
0
-1000
StromalScore
Low
High
Risk_group

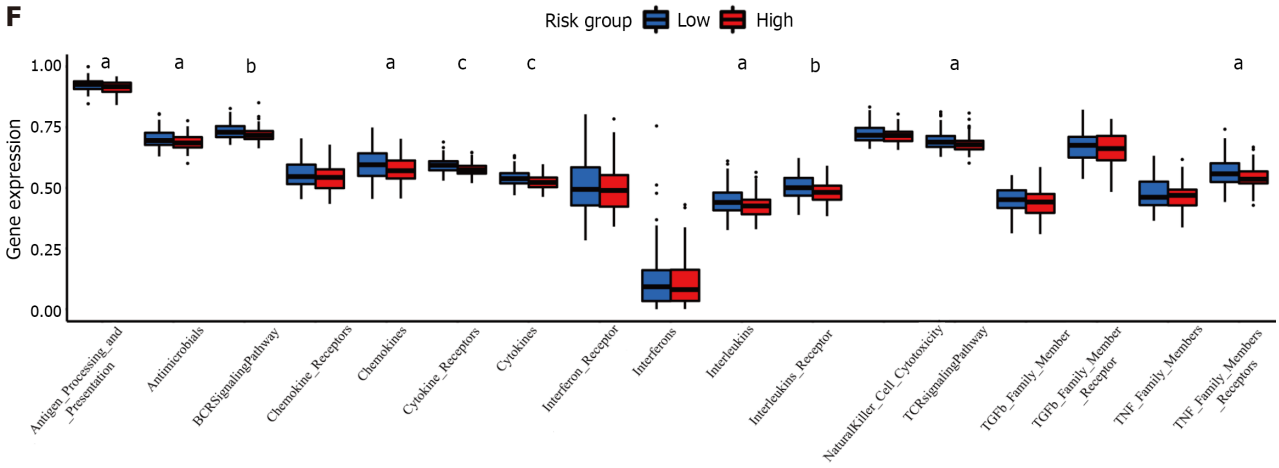
F
Risk group Low High
1.00
0.75
0.50
0.25
0.00
Gene expression
a a b a c c a b a a
Antigen_Processing_and_Presentation
Antimicrobials
BCRSignalingPathway
Chemokine_Receptors
Chemokines
Cytokine_Receptors
Cytokines
Interferon_Receptor
Interferons
Interleukins
Interleukins_Receptor
NaturalKiller_Cell_Cytotoxicity
TCRsignalingPathway
TGFb_Family_Member
TGFb_Family_Member_Receptor
TNF_Family_Members
TNF_Family_Members_Receptors

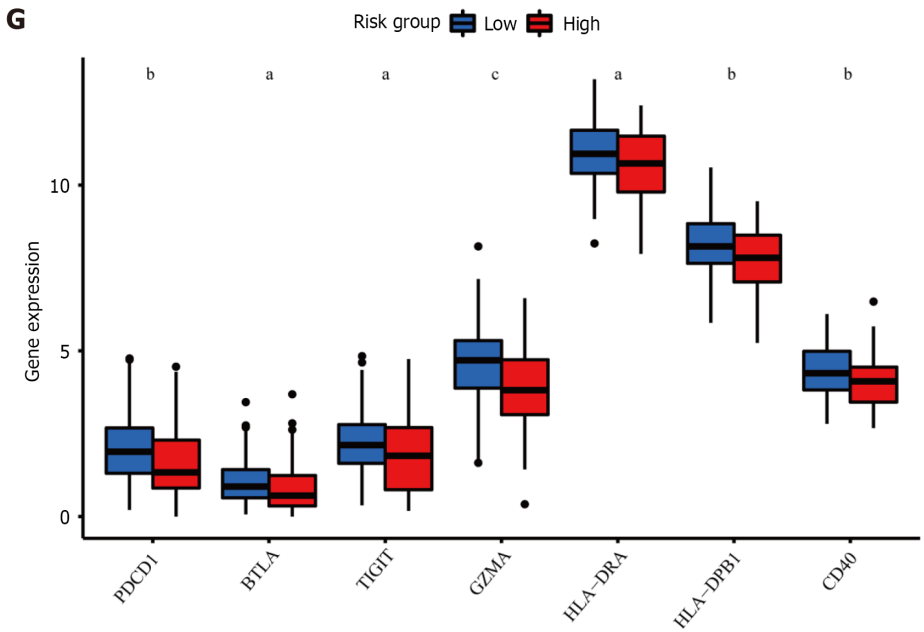
G
Risk group Low High
b a a c a b b
10
5
0
Gene expression
PDCD1
BTLA
TIGIT
GZMA
HLA-DRA
HLA-DPB1
CD40

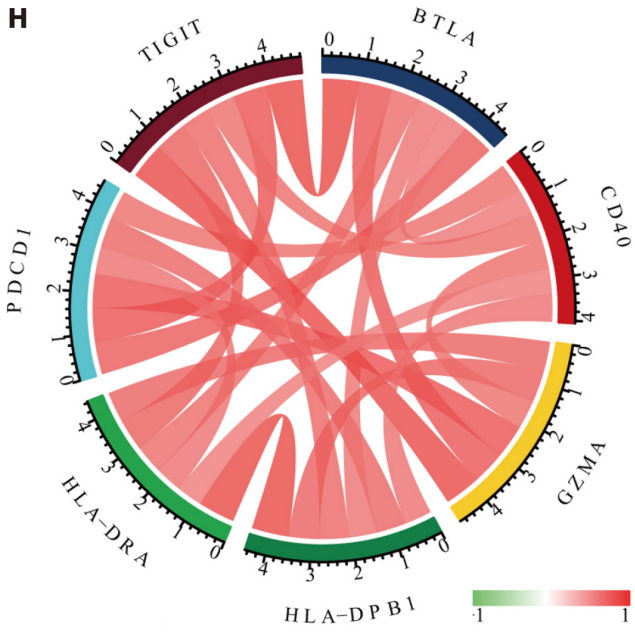

Figure 6 The immune-related analysis of the four ferroptosis-related prognostic gene signature models in HER2+ breast cancer. A: The Immune cells infiltration of differential risk groups in TCGA; B: Heatmaps represent the correlation between immune cells and prognostic genes; C-E: The immune, stromal, and estimate scores were significantly distinct statistically between low- and high-risk subgroups; F: Expression of immune cell pathways in low- and high-risk subgroups; G:The seven well-known immune checkpoint genes were differentially expressed between low- and high-risk subgroups; H: Correlation chord diagram of 7 immune checkpoints. $^{a}P < 0.05$, $^{b}P < 0.01$, $^{c}P < 0.001$.

between *FANCD2* and Ki-67 expression in BC cells[27]. Furthermore, high *FANCD2* expression could independently predict a poor prognosis in patients in the sporadic BC cohort[28]. The fumarate complex enzyme *FH* belongs to three TCA cycle enzyme families. Some studies have indicated that the *FH* double allele is inactivated in BC patients and that mutations in the *FH* gene may affect the progression of BC[29,30]. The role of these genes in inducing iron-related death in HER2+ BC patients needs further investigation, as few relevant studies have reported the regulatory function of these genes. Moreover, the patterns of the relationships among TMB, risk score, and the combination of TMB grouping and risk grouping indicated the synergistic effect of TMB and the risk score in prognostic stratification. These findings may provide new insight into cancer prognosis.

The treatment landscape for HER2-positive BC has undergone significant advancements in recent years. A comprehensive understanding of tumor biology and the intricate signaling pathways associated with HER2 has played a pivotal role in developing novel therapeutic strategies to improve patient outcomes. Prominent among these emerging approaches is dual-HER2 inhibition utilizing monoclonal antibodies, exemplified by the combination of trastuzumab and pertuzumab. Additionally, antibody–drug conjugates, including T-DM1 and trastuzumab–deruxtecan[31], and TKIs, such as tucatinib and neratinib, have emerged as promising therapeutic options[32,33]. In this study, we selected 13 drugs from a list of 138 drugs by analyzing and visualizing their IC_{50}s in high-risk and low-risk groups; these drugs included bibw2992 (afatinib) and ABT.263 (navitoclax), which have been previously reported to be effective treatments for HER2 + BC[34,35]. Bibw2992 (afatinib) is a tyrosine kinase and an irreversible blocker of the ErbB family[36]. It has been reported to be necessary for treating HER2+ BC[34,37]. Abt.263 (navitoclax) is a small molecule Bcl-2 inhibitor that induces apoptosis and treats HER2+ BC by blocking the interaction of Bcl-2 and Bcl XL with apoptotic precursor proteins[35]. Vinorelbine is an antimitotic semisynthetic drug that acts primarily by binding to tubulin, causing cells to become disorganized within microtubules during mitosis. It has been reported in the relevant literature that this approach is an effective treatment for metastatic BC. Vinorelbine is commonly used in combination therapy with trastuzumab and pyrotinib in HER2+ BC[38,39]. A-443654 is a potent pan-Akt inhibitor that has been reported to prolong survival in patients with HER2+ BC when combined with other medicines[40]. A c-Jun N-terminal kinase inhibitor called JNK.Inhibitor. VIII (TCS JNK 6o) inhibits invasive BC by reducing JNK activity. It can be used in combination with lapatinib[41].

CONCLUSION

In conclusion, our study developed a novel, previously unreported four-gene signature-associated prognostic model, which may be a useful prognostic classification tool for HER2+ BC patients. These genes were correlated with OS in the training cohort, and the association was confirmed in the validation cohort. A nomogram that combined our predictive signature with traditional clinical factors such as age and clinical stage performed noticeably better. As a result, the nomogram we developed can successfully direct clinical practice and help build a more individualized clinical follow-up approach.

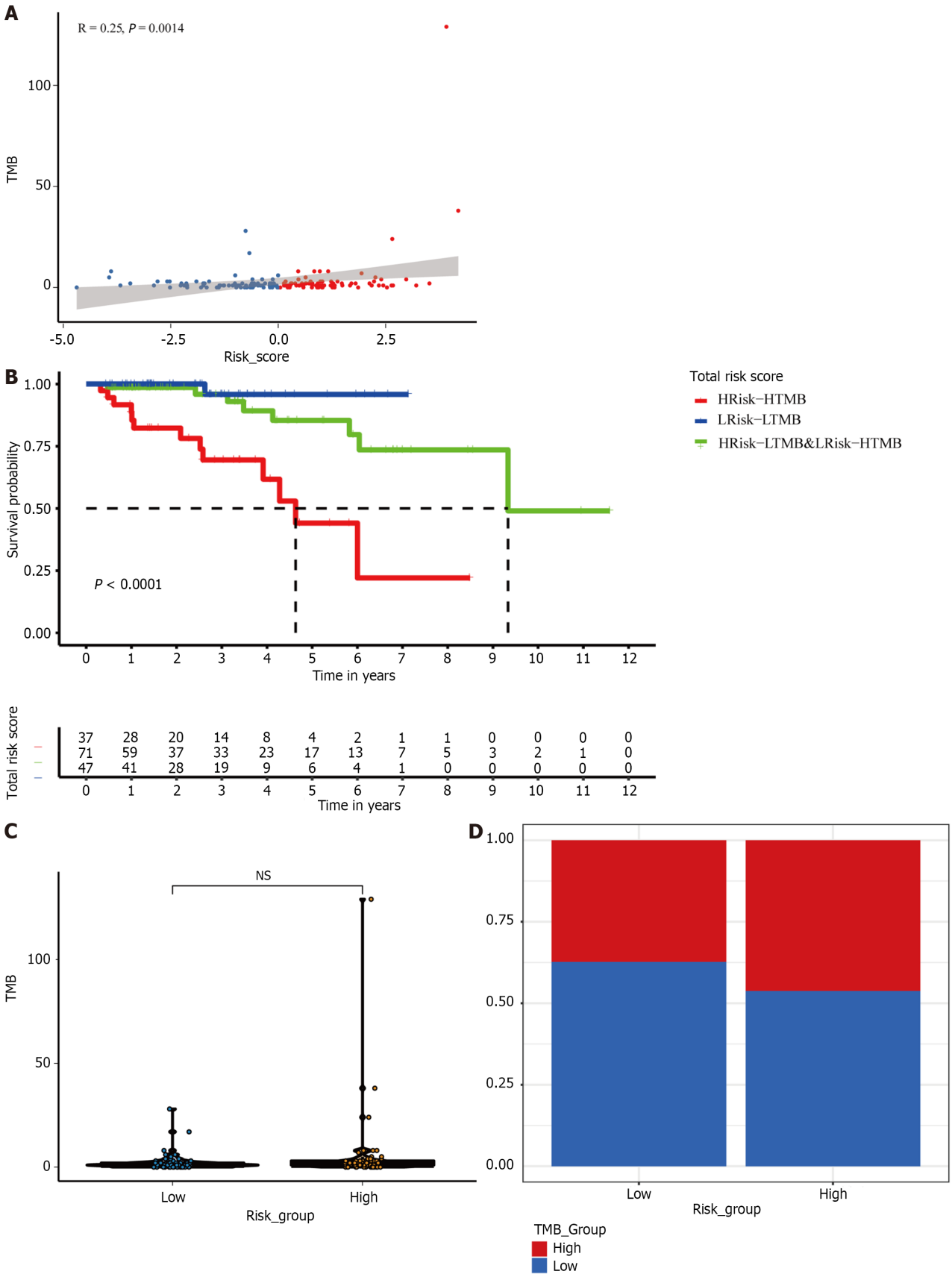

Figure 7 The mutation profile of different subgroups in the TCGA cohort. A: Relationship between tumor mutation burden (TMB) and risk scores; B: Relationship between TMB groups and risk groups; C: TMB in low- and high-risk subgroups; D: Kaplan–Meier survival analysis of a new subset in a cohort of HER2+ breast cancer patients combined with the risk group and TMB. TMB: Tumor mutation burden; NS: Not significant; BC: Breast cancer.

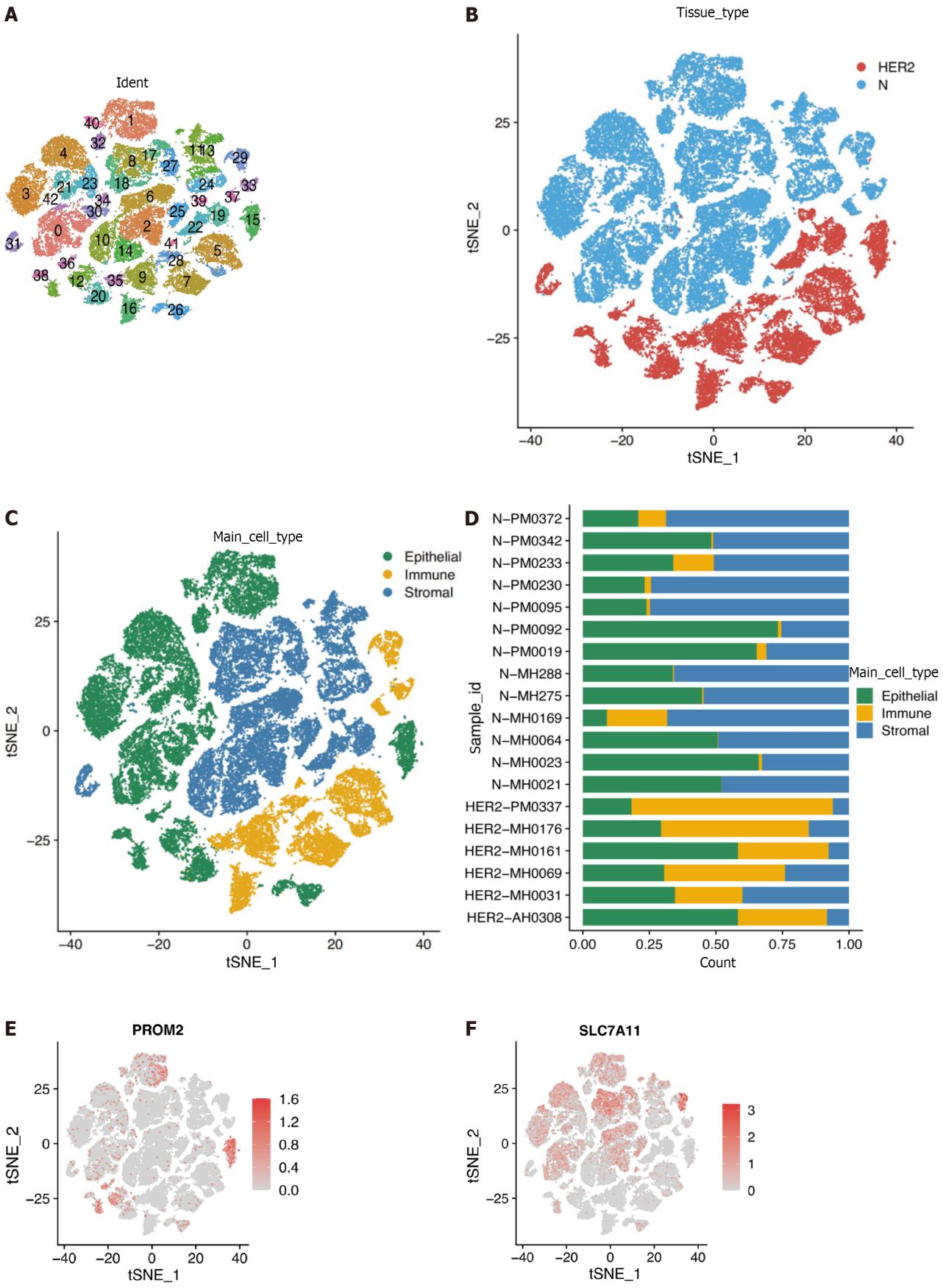
A
Ident
B
Tissue_type
HER2
N
tSNE_2
tSNE_1
C
Main_cell_type
Epithelial
Immune
Stromal
D
Sample_id
N–PM0372
N–PM0342
N–PM0233
N–PM0230
N–PM0095
N–PM0092
N–PM0019
N–MH288
N–MH275
N–MH0169
N–MH0064
N–MH0023
N–MH0021
HER2–PM0337
HER2–MH0176
HER2–MH0161
HER2–MH0069
HER2–MH0031
HER2–AH0308
Count
E
PROM2
F
SLC7A11

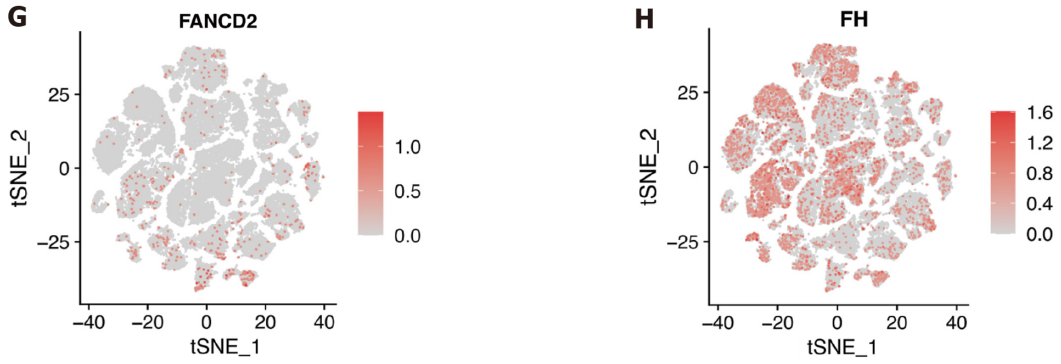

Figure 8 Overview of single cells from tumor samples and standard samples. A: Umap of 42 cell clusters; B: Umap of two different types of samples; C: Marker genes identified cell types; D: Proportion of cell types in patients' and normal people's samples; E-H: Expression of essential marker genes.

In addition, some limitations relevant to our study should be noted. First, only four prognostic genes from the TCGA database were used to calculate the prognostic risk score; their somatic mutations or methylation status should have been considered. Second, the sample size of the single-cell expression data was relatively small; future analyses with larger sample sizes are needed to validate and explore the present results. Third, the database lacks targeted therapy information within its clinical data, limiting its contents to radiotherapy and chemotherapy information exclusively. However, the mechanism underlying the four-gene signature and its therapeutic implications for treating HER2+ BC require further study.

ARTICLE HIGHLIGHTS

Research background

Our study identified a 4-gene model that, when combined with the tumor mutation burden (TMB) score, may have critical implications for clinical medical decisions and personalized treatment of patients with HER2-positive breast cancer.

Research motivation

This study aimed to identify and evaluate fresh ferroptosis-related biomarkers for HER2+ breast cancer (BC).

Research objectives

Identifying reliable prognostic biomarkers can direct clinical practice and help develop a more individualized clinical follow-up approach.

Research methods

The prediction model was constructed using data from the TCGA and METABRIC databases. Subsequently, patients were categorized into high-risk and low-risk groups according to their median risk scores, independent predictors for overall survival (OS). We investigated immune infiltration, mutations, and drug sensitivity across risk groups. Moreover, we integrated tumor mutational burden (TMB) with risk scores to assess patient prognosis. Finally, we analyzed vital gene expression through single-cell RNA sequencing (scRNA-seq) in cancerous and normal epithelial cells.

Research results

Our model helps guide the prognosis of HER2+ breast cancer patients, and its combination with the TMB can aid in more accurate assessment of patient prognosis and provide new ideas for further diagnosis and treatment.

Research conclusions

By analyzing the RNA expression data of HER2-positive breast cancer patients, we constructed a risk score model (*PROM2*, *SLC7A11*, *FANCD2*, and *FH*) for ferroptosis and evaluated the relationship between the high-risk score and patient prognosis. We verified that the high-risk group was associated with poorer immune infiltration and a greater tumor mutation load. By combining the risk score with the TMB, we found that patients with a high TMB-score had the worst prognosis, while patients with a low TMB-score had the best prognosis.

Research perspectives

The prediction model was constructed using data from the TCGA and METABRIC cohorts. Patients were subsequently categorized into high-risk and low-risk groups according to their median risk score, an independent predictor of overall survival. We investigated immune infiltration, mutations, and drug sensitivity across risk groups. Moreover, we integrated the TMB with risk scores to assess patient prognosis. Finally, we analyzed vital gene expression through

single-cell RNA sequencing in cancerous and normal epithelial cells.

FOOTNOTES

Author contributions: All authors participated in the conception and design of the study; conceptualization: Shi JY, Zhang YF, Wang LX; Methodology: Wen R, Shi JY, Formal analysis and investigation: Wen R, Hou SJ, Shi JY, and Che X; Writing - original draft preparation: Feng YQ and Xi YJ; Writing - review and editing: Liu SJ and Lv WH; Funding acquisition: Zhang YF; Resources: Zhang YF; Supervision: Zhang YF and Wang LX; All authors read and approved the paper.

Supported by The Science and Technology Commission of Shanxi province, No. 201901D111428.

Institutional review board statement: The study was reviewed and approved by the Shanxi Provincial People's Hospital Institutional Review Board, Approval No. 2022-240.

Informed consent statement: All study participants or their legal guardians provided informed written consent before enrollment.

Conflict-of-interest statement: All the authors report no relevant conflicts of interest for this article.

Data sharing statement: The public datasets to support the results can be obtained from TCGA (https://portal.gdc.cancer.gov/), METABRIC (www.cbioportal.org/), GTEx (https://gtexportal.org/home/datasets), FerrDb (http://www.zhounan.org/ferrdb/current/), GDSC (https://www.cancerrxgene.org/celllines) and GEO database (https://www.ncbi.nlm.nih.gov/geo/).

Country/Territory of origin: China

ORCID number: Ya-Fen Zhang 0009-0003-6058-1177.

S-Editor: Li L
L-Editor: A
P-Editor: Zhang XD

REFERENCES

1 **Ferlay J**, Colombet M, Soerjomataram I, Parkin DM, Piñeros M, Znaor A, Bray F. Cancer statistics for the year 2020: An overview. *Int J Cancer* 2021 [PMID: 33818764 DOI: 10.1002/ijc.33588]
2 **Cancer Genome Atlas Network**. Comprehensive molecular portraits of human breast tumours. *Nature* 2012; **490**: 61-70 [PMID: 23000897 DOI: 10.1038/nature11412]
3 **Wolff AC**, Hammond ME, Hicks DG, Dowsett M, McShane LM, Allison KH, Allred DC, Bartlett JM, Bilous M, Fitzgibbons P, Hanna W, Jenkins RB, Mangu PB, Paik S, Perez EA, Press MF, Spears PA, Vance GH, Viale G, Hayes DF; American Society of Clinical Oncology; College of American Pathologists. Recommendations for human epidermal growth factor receptor 2 testing in breast cancer: American Society of Clinical Oncology/College of American Pathologists clinical practice guideline update. *J Clin Oncol* 2013; **31**: 3997-4013 [PMID: 24101045 DOI: 10.1200/JCO.2013.50.9984]
4 **Dowsett M**, Procter M, McCaskill-Stevens W, de Azambuja E, Dafni U, Rueschoff J, Jordan B, Dolci S, Abramovitz M, Stoss O, Viale G, Gelber RD, Piccart-Gebhart M, Leyland-Jones B. Disease-free survival according to degree of HER2 amplification for patients treated with adjuvant chemotherapy with or without 1 year of trastuzumab: the HERA Trial. *J Clin Oncol* 2009; **27**: 2962-2969 [PMID: 19364966 DOI: 10.1200/JCO.2008.19.7939]
5 **Barzaman K**, Karami J, Zarei Z, Hosseinzadeh A, Kazemi MH, Moradi-Kalbolandi S, Safari E, Farahmand L. Breast cancer: Biology, biomarkers, and treatments. *Int Immunopharmacol* 2020; **84**: 106535 [PMID: 32361569 DOI: 10.1016/j.intimp.2020.106535]
6 **Blumenthal GM**, Scher NS, Cortazar P, Chattopadhyay S, Tang S, Song P, Liu Q, Ringgold K, Pilaro AM, Tilley A, King KE, Graham L, Rellahan BL, Weinberg WC, Chi B, Thomas C, Hughes P, Ibrahim A, Justice R, Pazdur R. First FDA approval of dual anti-HER2 regimen: pertuzumab in combination with trastuzumab and docetaxel for HER2-positive metastatic breast cancer. *Clin Cancer Res* 2013; **19**: 4911-4916 [PMID: 23801166 DOI: 10.1158/1078-0432.CCR-13-1212]
7 **Shao Z**, Pang D, Yang H, Li W, Wang S, Cui S, Liao N, Wang Y, Wang C, Chang YC, Wang H, Kang SY, Seo JH, Shen K, Laohawiriyakamol S, Jiang Z, Li J, Zhou J, Althaus B, Mao Y, Eng-Wong J. Efficacy, Safety, and Tolerability of Pertuzumab, Trastuzumab, and Docetaxel for Patients With Early or Locally Advanced ERBB2-Positive Breast Cancer in Asia: The PEONY Phase 3 Randomized Clinical Trial. *JAMA Oncol* 2020; **6**: e193692 [PMID: 31647503 DOI: 10.1001/jamaoncol.2019.3692]
8 **Wang L**, Chen Y, Zhao J, Luo D, Tian W. Analysis and prediction model of ferroptosis related genes in breast cancer. *Transl Cancer Res* 2022; **11**: 1970-1976 [PMID: 35966288 DOI: 10.21037/tcr-21-2686]
9 **Wang D**, Wei G, Ma J, Cheng S, Jia L, Song X, Zhang M, Ju M, Wang L, Zhao L, Xin S. Identification of the prognostic value of ferroptosis-related gene signature in breast cancer patients. *BMC Cancer* 2021; **21**: 645 [PMID: 34059009 DOI: 10.1186/s12885-021-08341-2]
10 **Jin LY**, Gu YL, Zhu Q, Li XH, Jiang GQ. The role of ferroptosis-related genes for overall survival prediction in breast cancer. *J Clin Lab Anal*

2021; **35**: e24094 [PMID: 34741349 DOI: 10.1002/jcla.24094]

11 **Brown CW**, Amante JJ, Chhoy P, Elaimy AL, Liu H, Zhu LJ, Baer CE, Dixon SJ, Mercurio AM. Prominin2 Drives Ferroptosis Resistance by Stimulating Iron Export. *Dev Cell* 2019; **51**: 575-586.e4 [PMID: 31735663 DOI: 10.1016/j.devcel.2019.10.007]

12 **Stockwell BR**, Friedmann Angeli JP, Bayir H, Bush AI, Conrad M, Dixon SJ, Fulda S, Gascón S, Hatzios SK, Kagan VE, Noel K, Jiang X, Linkermann A, Murphy ME, Overholtzer M, Oyagi A, Pagnussat GC, Park J, Ran Q, Rosenfeld CS, Salnikow K, Tang D, Torti FM, Torti SV, Toyokuni S, Woerpel KA, Zhang DD. Ferroptosis: A Regulated Cell Death Nexus Linking Metabolism, Redox Biology, and Disease. *Cell* 2017; **171**: 273-285 [PMID: 28985560 DOI: 10.1016/j.cell.2017.09.021]

13 **Dixon SJ**, Lemberg KM, Lamprecht MR, Skouta R, Zaitsev EM, Gleason CE, Patel DN, Bauer AJ, Cantley AM, Yang WS, Morrison B 3rd, Stockwell BR. Ferroptosis: an iron-dependent form of nonapoptotic cell death. *Cell* 2012; **149**: 1060-1072 [PMID: 22632970 DOI: 10.1016/j.cell.2012.03.042]

14 **Sato M**, Kusumi R, Hamashima S, Kobayashi S, Sasaki S, Komiyama Y, Izumikawa T, Conrad M, Bannai S, Sato H. The ferroptosis inducer erastin irreversibly inhibits system x(c)- and synergizes with cisplatin to increase cisplatin's cytotoxicity in cancer cells. *Sci Rep* 2018; **8**: 968 [PMID: 29343855 DOI: 10.1038/s41598-018-19213-4]

15 **Chen MS**, Wang SF, Hsu CY, Yin PH, Yeh TS, Lee HC, Tseng LM. CHAC1 degradation of glutathione enhances cystine-starvation-induced necroptosis and ferroptosis in human triple negative breast cancer cells *via* the GCN2-eIF2α-ATF4 pathway. *Oncotarget* 2017; **8**: 114588-114602 [PMID: 29383104 DOI: 10.18632/oncotarget.23055]

16 **Giaquinto AN**, Sung H, Miller KD, Kramer JL, Newman LA, Minihan A, Jemal A, Siegel RL. Breast Cancer Statistics, 2022. *CA Cancer J Clin* 2022; **72**: 524-541 [PMID: 36190501 DOI: 10.3322/caac.21754]

17 **Li J**, Cao F, Yin HL, Huang ZJ, Lin ZT, Mao N, Sun B, Wang G. Ferroptosis: past, present and future. *Cell Death Dis* 2020; **11**: 88 [PMID: 32015325 DOI: 10.1038/s41419-020-2298-2]

18 **Wei W**, Hu Q, Li W, Li M, Dong S, Peng Y, Yin J, Lu Y, Liu L, Zhao Q. The Role of Ferroptosis Signature in Overall Survival and Chemotherapy of Pancreatic Adenocarcinoma. *DNA Cell Biol* 2022; **41**: 116-127 [PMID: 34898275 DOI: 10.1089/dna.2021.0594]

19 **Chen GH**, Song CC, Pantopoulos K, Wei XL, Zheng H, Luo Z. Mitochondrial oxidative stress mediated Fe-induced ferroptosis *via* the NRF2-ARE pathway. *Free Radic Biol Med* 2022; **180**: 95-107 [PMID: 35045311 DOI: 10.1016/j.freeradbiomed.2022.01.012]

20 **Luo W**, Wang J, Xu W, Ma C, Wan F, Huang Y, Yao M, Zhang H, Qu Y, Ye D, Zhu Y. LncRNA RP11-89 facilitates tumorigenesis and ferroptosis resistance through PROM2-activated iron export by sponging miR-129-5p in bladder cancer. *Cell Death Dis* 2021; **12**: 1043 [PMID: 34728613 DOI: 10.1038/s41419-021-04296-1]

21 **Koppula P**, Zhuang L, Gan B. Cystine transporter SLC7A11/xCT in cancer: ferroptosis, nutrient dependency, and cancer therapy. *Protein Cell* 2021; **12**: 599-620 [PMID: 33000412 DOI: 10.1007/s13238-020-00789-5]

22 **He J**, Ding H, Li H, Pan Z, Chen Q. Intra-Tumoral Expression of SLC7A11 Is Associated with Immune Microenvironment, Drug Resistance, and Prognosis in Cancers: A Pan-Cancer Analysis. *Front Genet* 2021; **12**: 770857 [PMID: 34938318 DOI: 10.3389/fgene.2021.770857]

23 **Sun X**, Niu X, Chen R, He W, Chen D, Kang R, Tang D. Metallothionein-1G facilitates sorafenib resistance through inhibition of ferroptosis. *Hepatology* 2016; **64**: 488-500 [PMID: 27015352 DOI: 10.1002/hep.28574]

24 **Han B**, Shen Y, Zhang P, Jayabal P, Che R, Zhang J, Yu H, Fei P. Overlooked FANCD2 variant encodes a promising, portent tumor suppressor, and alternative polyadenylation contributes to its expression. *Oncotarget* 2017; **8**: 22490-22500 [PMID: 28157704 DOI: 10.18632/oncotarget.14989]

25 **Song X**, Xie Y, Kang R, Hou W, Sun X, Epperly MW, Greenberger JS, Tang D. FANCD2 protects against bone marrow injury from ferroptosis. *Biochem Biophys Res Commun* 2016; **480**: 443-449 [PMID: 27773819 DOI: 10.1016/j.bbrc.2016.10.068]

26 **Fagerholm R**, Sprott K, Heikkinen T, Bartkova J, Heikkilä P, Aittomäki K, Bartek J, Weaver D, Blomqvist C, Nevanlinna H. Overabundant FANCD2, alone and combined with NQO1, is a sensitive marker of adverse prognosis in breast cancer. *Ann Oncol* 2013; **24**: 2780-2785 [PMID: 23897704 DOI: 10.1093/annonc/mdt290]

27 **Rudland PS**, Platt-Higgins AM, Davies LM, de Silva Rudland S, Wilson JB, Aladwani A, Winstanley JH, Barraclough DL, Barraclough R, West CR, Jones NJ. Significance of the Fanconi anemia FANCD2 protein in sporadic and metastatic human breast cancer. *Am J Pathol* 2010; **176**: 2935-2947 [PMID: 20363922 DOI: 10.2353/ajpath.2010.090779]

28 **Feng L**, Jin F. Expression and prognostic significance of Fanconi anemia group D2 protein and breast cancer type 1 susceptibility protein in familial and sporadic breast cancer. *Oncol Lett* 2019; **17**: 3687-3700 [PMID: 30881493 DOI: 10.3892/ol.2019.10046]

29 **Zhang Q**, Liang Z, Gao Y, Teng M, Niu L. Differentially expressed mitochondrial genes in breast cancer cells: Potential new targets for anti-cancer therapies. *Gene* 2017; **596**: 45-52 [PMID: 27720940 DOI: 10.1016/j.gene.2016.10.005]

30 **Schmidt C**, Sciacovelli M, Frezza C. Fumarate hydratase in cancer: A multifaceted tumour suppressor. *Semin Cell Dev Biol* 2020; **98**: 15-25 [PMID: 31085323 DOI: 10.1016/j.semcdb.2019.05.002]

31 **Fu Z**, Li S, Han S, Shi C, Zhang Y. Antibody drug conjugate: the "biological missile" for targeted cancer therapy. *Signal Transduct Target Ther* 2022; **7**: 93 [PMID: 35318309 DOI: 10.1038/s41392-022-00947-7]

32 **Jacobs AT**, Martinez Castaneda-Cruz D, Rose MM, Connelly L. Targeted therapy for breast cancer: An overview of drug classes and outcomes. *Biochem Pharmacol* 2022; **204**: 115209 [PMID: 35973582 DOI: 10.1016/j.bcp.2022.115209]

33 **Xu B**, Yan M, Ma F, Hu X, Feng J, Ouyang Q, Tong Z, Li H, Zhang Q, Sun T, Wang X, Yin Y, Cheng Y, Li W, Gu Y, Chen Q, Liu J, Cheng J, Geng C, Qin S, Wang S, Lu J, Shen K, Liu Q, Wang H, Luo T, Yang J, Wu Y, Yu Z, Zhu X, Chen C, Zou J; PHOEBE Investigators. Pyrotinib plus capecitabine *vs* lapatinib plus capecitabine for the treatment of HER2-positive metastatic breast cancer (PHOEBE): a multicentre, open-label, randomised, controlled, phase 3 trial. *Lancet Oncol* 2021; **22**: 351-360 [PMID: 33581774 DOI: 10.1016/S1470-2045(20)30702-6]

34 **Collins DM**, Madden SF, Gaynor N, AlSultan D, Le Gal M, Eustace AJ, Gately KA, Hughes C, Davies AM, Mahgoub T, Ballot J, Toomey S, O'Connor DP, Gallagher WM, Holmes FA, Espina V, Liotta L, Hennessy BT, O'Byrne KJ, Hasmann M, Bossenmaier B, O'Donovan N, Crown J. Effects of HER Family-targeting Tyrosine Kinase Inhibitors on Antibody-dependent Cell-mediated Cytotoxicity in HER2-expressing Breast Cancer. *Clin Cancer Res* 2021; **27**: 807-818 [PMID: 33122343 DOI: 10.1158/1078-0432.CCR-20-2007]

35 **Zoeller JJ**, Vagodny A, Taneja K, Tan BY, O'Brien N, Slamon DJ, Sampath D, Leverson JD, Bronson RT, Dillon DA, Brugge JS. Neutralization of BCL-2/X(L) Enhances the Cytotoxicity of T-DM1 In Vivo. *Mol Cancer Ther* 2019; **18**: 1115-1126 [PMID: 30962322 DOI: 10.1158/1535-7163.MCT-18-0743]

36 **Wecker H**, Waller CF. Afatinib. *Recent Results Cancer Res* 2018; **211**: 199-215 [PMID: 30069769 DOI: 10.1007/978-3-319-91442-8_14]

37 **Duchnowska R**, Loibl S, Jassem J. Tyrosine kinase inhibitors for brain metastases in HER2-positive breast cancer. *Cancer Treat Rev* 2018; **67**:

71-77 [PMID: 29772459 DOI: 10.1016/j.ctrv.2018.05.004]

38 **Li Y**, Qiu Y, Li H, Luo T, Li W, Wang H, Shao B, Wang B, Ge R. Pyrotinib Combined With Vinorelbine in HER2-Positive Metastatic Breast Cancer: A Multicenter Retrospective Study. *Front Oncol* 2021; **11**: 664429 [PMID: 33996589 DOI: 10.3389/fonc.2021.664429]

39 **Aitelhaj M**, Lkhoyaali S, Rais G, Boutayeb S, Errihani H. First line chemotherapy plus trastuzumab in metastatic breast cancer HER2 positive - Observational institutional study. *Pan Afr Med J* 2016; **24**: 324 [PMID: 28154679 DOI: 10.11604/pamj.2016.24.324.4058]

40 **Yndestad S**, Austreid E, Svanberg IR, Knappskog S, Lønning PE, Eikesdal HP. Activation of Akt characterizes estrogen receptor positive human breast cancers which respond to anthracyclines. *Oncotarget* 2017; **8**: 41227-41241 [PMID: 28476032 DOI: 10.18632/oncotarget.17167]

41 **Ebelt ND**, Kaoud TS, Edupuganti R, Van Ravenstein S, Dalby KN, Van Den Berg CL. A c-Jun N-terminal kinase inhibitor, JNK-IN-8, sensitizes triple negative breast cancer cells to lapatinib. *Oncotarget* 2017; **8**: 104894-104912 [PMID: 29285221 DOI: 10.18632/oncotarget.20581]

World Journal of Clinical Oncology

Submit a Manuscript: https://www.f6publishing.com

World J Clin Oncol 2024 March 24; 15(3): 411-418

DOI: 10.5306/wjco.v15.i3.411

ISSN 2218-4333 (online)

ORIGINAL ARTICLE

Observational Study

Clinical application of reserved gastric tube in neuroendoscopic endonasal surgery for pituitary tumor

Xi Chen, Long-Yao Zhang, Zhi-Feng Wang, Yi Zhang, Yu-Hua Yin, Xue-Jian Wang

Specialty type: Oncology

Provenance and peer review: Unsolicited article; Externally peer reviewed.

Peer-review model: Single blind

Peer-review report's scientific quality classification

Grade A (Excellent): 0
Grade B (Very good): B
Grade C (Good): 0
Grade D (Fair): 0
Grade E (Poor): 0

P-Reviewer: Li XD, China

Received: October 28, 2023
Peer-review started: October 28, 2023
First decision: January 12, 2024
Revised: January 19, 2024
Accepted: February 27, 2024
Article in press: February 27, 2024
Published online: March 24, 2024

Xi Chen, Department of Nursing, Affiliated Hospital 2 of Nantong University, Nantong 226000, Jiangsu Province, China

Long-Yao Zhang, Zhi-Feng Wang, Yi Zhang, Xue-Jian Wang, Department of Neurosurgery, Affiliated Hospital 2 of Nantong University, Nantong 226000, Jiangsu Province, China

Yu-Hua Yin, Department of Neurosurgery, Renji Hospital, Shanghai Jiao Tong University, Shanghai 226000, China

Corresponding author: Xue-Jian Wang, MD, PhD, Professor, Surgeon, Department of Neurosurgery, Affiliated Hospital 2 of Nantong University, No. 666 Shengli Road, Chongchuan District, Nantong 226000, Jiangsu Province, China. 6841441@163.com

Abstract

BACKGROUND

The neuroendoscopic approach has the advantages of a clear operative field, convenient tumor removal, and less damage, and is the development direction of modern neurosurgery. At present, transnasal surgery for sphenoidal pituitary tumor is widely used. But it has been found in clinical practice that some patients with this type of surgery may experience post-operative nausea and vomiting and other discomforts.

AIM

To explore the effect of reserved gastric tube application in the neuroendoscopic endonasal resection of pituitary tumors.

METHODS

A total of 60 patients who underwent pituitary adenoma resection *via* the endoscopic endonasal approach were selected and randomly divided into the experimental and control groups, with 30 in each group. Experimental group: After anesthesia, a gastric tube was placed through the mouth under direct vision using a visual laryngoscope, and the fluid accumulated in the oropharynx was suctioned intermittently with low negative pressure throughout the whole process after nasal disinfection, during the operation, and when the patient recovered from anesthesia. Control group: Given the routine intraoperative care, no gastric tube was left. The number of cases of nausea/vomiting/aspiration within 24 h post-operation was counted and compared between the two groups; the scores of pharyngalgia after waking up, 6 h post-operation, and 24 h post-

operation. The frequency of postoperative cerebrospinal fluid leakage and intracranial infection were compared. The hospitalization days of the two groups were statistically compared.

RESULTS

The times of postoperative nausea and vomiting in the experimental group were lower than that in the control group, and the difference in the incidence of nausea was statistically significant ($P < 0.05$). After the patient woke up, the scores of sore throat 6 h after the operation and 24 h after operation were lower than those in the control group, and the difference was statistically significant ($P < 0.05$). The number of cases of postoperative cerebrospinal fluid leakage and intracranial infection was higher than that of the control group, but there was no statistically significant difference from the control group ($P > 0.05$). The hospitalization days of the experimental group was lower than that of the control group, and the difference was statistically significant ($P < 0.05$).

CONCLUSION

Reserving a gastric tube in the endoscopic endonasal resection of pituitary tumors, combined with intraoperative and postoperative gastrointestinal decompression, can effectively reduce the incidence of nausea, reduce the number of vomiting and aspiration in patients, and reduce the complications of sore throat The incidence rate shortened the hospitalization days of the patients.

Key Words: Neuroendoscopy; Endonasal approach; Pituitary tumor; Reserved gastric tube; Nausea; Vomiting; Aspiration; Complications

Core Tip: Pituitary tumors are common primary intracranial tumors in clinical practice, accounting for about 10% of intracranial tumors, second only to neuroepithelial tumors and meningiomas. Neuroendoscopic approach has the advantages of clear operative field, convenient tumor removal, and less damage, and is the development direction of modern neurosurgery. It has been found in clinical practice that some patients with this type of surgery may experience Post-Operative Nausea and Vomiting and other discomforts. The main consideration is that there is a correlation with the endonasal approach surgery. Aiming at the above postoperative problems, this study adopted the intervention method of reserving gastric tube in endoscopic endonasal resection of pituitary tumors to explore the application of reserved gastric tube in patients, and achieved good results.

Citation: Chen X, Zhang LY, Wang ZF, Zhang Y, Yin YH, Wang XJ. Clinical application of reserved gastric tube in neuroendoscopic endonasal surgery for pituitary tumor. *World J Clin Oncol* 2024; 15(3): 411-418
URL: https://www.wjgnet.com/2218-4333/full/v15/i3/411.htm
DOI: https://dx.doi.org/10.5306/wjco.v15.i3.411

INTRODUCTION

Pituitary tumors are primary intracranial tumors commonly encountered in clinical practice, accounting for about 10% of intracranial tumors and second only to neuroepithelial tumors and meningiomas[1,2]. Transsphenoidal pituitary adenoma resection is a mature technique, and it has the advantages of less surgical trauma, shorter operation time, faster postoperative recovery, and fewer complications compared to traditional craniotomy[3-5]. The neuroendoscopic approach has the advantages of a clear operative field, convenient tumor removal, and less damage, and is the development direction of modern neurosurgery[6]. It has been found in clinical practice that some patients with this type of surgery may experience post-operative nausea and vomiting (PONV) and other discomforts[7]. We hypothesize is that there is a correlation with the endonasal approach surgery. Since intraoperative disinfectant, washing fluid, bleeding, and postoperative mucosal oozing flow into the stomach through the nasopharynx, it is easy to induce postoperative vomiting in patients. Additionally, because the vomit contains bloody liquid, patients and their families become emotionally stressed. At the same time, patients are prone to flatulence due to bilateral nasal congestion prompting them to open their mouths to breathe, which will also induce and aggravate nausea and vomiting after general anesthesia, increasing the possibility of aspiration. PONV is one of most frequent side effects after anesthesia[7,8], occurring in 30% of unselected patients and up to 70% of "high-risk" patients during the 24 h after emergence[9]. In severe cases, surgical wound bleeding may be induced by increased intracranial pressure and blood pressure, resulting in delayed discharge [10] and a possible unexpected admission[11,12].

In light of the aforementioned postoperative problems, this study adopted the intervention method of gastric tube application during the endoscopic endonasal resection of pituitary tumors to explore the application of reserved gastric tubes in patients, achieving promising results.

MATERIALS AND METHODS

Ethics approval and consent to participate: This study was reviewed and approved by the Ethics Committee of Affiliated 2 Hospital of Nantong University.

General information

In total, 60 patients with pituitary tumors admitted to the neurosurgery department of our hospital from February 2021 to February 2023 were selected as the research participants. According to the random number method, the patients were evenly divided into the experimental group and the control group. The experimental group consisted of 17 males and 13 females aged 39.6 ± 14.7 years, and the control group, 18 males and 12 females aged 36.72 ± 15.4 years. There was no statistically significant difference between the two groups in terms of sex, age, condition, course of disease, and other baseline information ($P > 0.05$); both groups were comparable.

Inclusion criteria: (1) Adult patients diagnosed with pituitary adenoma who underwent endoscopic transsphenoidal pituitary tumor surgery for the first time; (2) Pituitary adenoma ≤ 3 cm; (3) No surgical contraindications; (4) Participants with American Society of Anesthesiologists classification I-III; and (5) Voluntarily signed the patient's informed consent form.

Exclusion criteria: (1) Cases of pituitary adenoma combined with cerebral aneurysm and cerebrovascular malformation; (2) Mental disorders; (3) Pregnant patients; (4) Hypertrophy of the tonsils; (5) Patients with chronic pharyngitis; (6) Patients with severe heart, lung, and/or liver disease; and/or (7) Renal dysfunction.

Research methods

Surgical method: Both groups underwent neuroendoscopic endonasal pituitary tumor resection by the same medical team. Each patient was placed in the supine position, the trachea was intubated under conventional general anesthesia, and the nasal cavity and operative field were disinfected with povidone iodine. The nasal cavity was filled with epinephrine saline cotton pads to shrink the nasal mucosa. The neuroendoscope was inserted; the right middle turbinate was moved laterally under the endoscope; the pedicled mucosal flap of the right nasal septum was prepared; the back of the nasal septum and then the nasal passage were opened; the anterior wall of the sphenoid sinus was ground; the inner septum and the sphenoid sinus mucous membrane were removed; and the sellar floor, sellar tubercle, and sphenoid plateau bone were ground. The dura mater was cut to expose the tumor, the tumor boundary was separated after intratumoral decompression, and the bleeding was completely stopped after tumor resection. Autologous fat, artificial dura mater, autologous fascia, and a pedicled nasal septum mucosa flap were used to reconstruct the skull base. Naxi cotton was used to stuff the nasal cavity for support, and at this time, the lower nasal passage was kept unobstructed as much as possible[3].

Intervention method of the experimental group: After the anesthesiologist anesthetized and intubated the trachea, while inserting a No. 14 gastric tube (Fuerkai, China), the anesthesiologist and the nurse were assisted by a video laryngoscope (Zhejiang Youyi Medical, China) to confirm that the position was below the oropharynx (oropharyngeal tongue root plane). Low negative pressure control was adopted during the operation; the suction pressure of the low negative pressure suction device (Simanfeng Company, China) was 100-120 mmHg. After the operation, the esophagus and oropharynx were sucked out before the stomach tube was removed.

Intervention methods for the control group: Routine care was given, and gastric tubes were blindly inserted through the nose or through the mouth in patients with disturbance of consciousness after surgery.

Evaluation indicators

PONV times and aspiration times: The number of patients with PONV; coughing, dyspnea, blood oxygen saturation below 90%, suffocation, other symptoms during or after vomiting, or food residues that could be seen through mouth and nose suction were judged as aspiration[13].

Scoring of sore throats after the patient woke up and after the operation: The Visual Analogue Scale (VAS) was used to score the patients after they woke up as well as the ward nurse at 6 h and 24 h after the operation, respectively. To assess sore throat, the VAS is used to assess pain and is widely used clinically[14]. The basic method is to use a moving ruler of about 10 cm long, with 10 scales, on one side, and the two ends are "0" and "10." And 0 means no pain, and 10 means difficulty. The most severe pain endured. Specifically, 0 is no pain; 1-3 is mild pain; 4-6 is moderate pain; 7-10 is severe pain.

Cases of postoperative cerebrospinal fluid leakage and intracranial infection and hospitalization days of patients: The number of cases of cerebrospinal fluid leakage and intracranial infection, as well as the length of hospitalization of patients were recorded after the operation.

Statistical methods

SPSS 24.0 statistical software was used for the t and χ^2 test and Fisher's exact test.

RESULTS

Comparison of PONV times and aspiration times between the two groups

The number of nausea in the test group was less than that in the control group, and the difference was statistically significant ($P < 0.01$). The frequency of vomiting in the experimental group was less than that in the control group, but the difference was not statistically significant ($P > 0.05$). The number of aspirations in the experimental group was less than that in the control group, and the difference was not statistically significant ($P > 0.05$; Table 1).

Scores of sore throat after waking up and postoperatively

The VAS scores of patients in the experimental group after waking up were lower than that in the control group, and the difference was statistically significant ($P < 0.05$). The VAS scores of the experimental group were lower than that of the control group at six hours post-operation, and the difference was statistically significant ($P < 0.05$). The 24 h postoperative VAS score of the experimental group was lower than that of the control group, and the difference was statistically significant ($P < 0.05$; Table 2).

Comparison of postoperative cerebrospinal fluid leakage, intracranial infection, and hospitalization days between the two groups

There was one case of cerebrospinal fluid leakage in the experimental group compared to the three in the control group, though the difference was not statistically significant ($P > 0.05$). There was one case of intracranial infection in the experimental group compared to the two in the control group; the difference was statistically significant ($P > 0.05$). The experimental group had 7.91 ± 2.020 days of hospitalization compared to the control group's 8.94 ± 2.503 days; the difference was statistically significant ($P < 0.05$; Table 3).

DISCUSSION

At present, the advancement of neuroendoscopic technology has enabled this to be widely used in sellar region lesions, such as pituitary tumors. Cappabianca *et al*[15] emphasized that the important feature of endoscopic transsphenoidal surgery is that it does not use a retractor to dilate the nasal cavity and uses the endoscope as a lighting and observation device, utilizing the physiological channels of the nasal cavity to gradually shrink the nasal mucosa to expand the operation path. However, the endoscopic lens is easily covered by blood, water vapor, and other substances, which interfere with the operative field[3,4]. The surgeon needs to wash the lens and wound surface intermittently to keep the operative field clear. Therefore, it is inevitable that there will be fluid accumulation in the throat and upper gastrointestinal tract, mixed with disinfectant iodophor, blood, and other irritating liquids, which will irritate the digestive tract and cause related complications and discomfort. Therefore, it is necessary to study similar technologies to reduce related side effects, reduce the occurrence of complications, and improve patient comfort.

During endonasal neuroendoscopic surgery, there is fluid accumulation in the surgical area. Although the aspirator will suck out some bloody fluid (including blood, disinfectant, and flushing fluid), because the patient is in an unconscious state during general anesthesia, there is no throat reflex[8,9]. Due to the connection between the nasal and oral cavities through the pharynx and the impact of body position, some liquid will accumulate in the oropharynx and upper gastrointestinal tract along the posterior pharyngeal wall. During the awakening period of general anesthesia, the patient's consciousness gradually recovers, and involuntary swallowing will occur. The mouth is the only channel that can be used at this time. Postoperative nasal bleeding and frequent swallowing can cause a large amount of gas and blood to be swallowed into the digestive tract, causing gastric dilation, leading to nausea and vomiting occurrence[16,17].

At present, such factors have not been fully considered clinically, and no pharyngeal or upper gastrointestinal drainage tube was placed during the operation. In the experimental group of this study, a gastric tube was inserted after anesthesia, and the fluid was drained during the operation. After the operation, the miscellaneous fluid was sucked out and then removed. Through the study of this group, we found that intraoperative gastric tube reservation is necessary in the perioperative process of the neuroendoscopic endonasal resection of pituitary tumors.

Reserving gastric tube during operation can improve postoperative vomiting and aspiration

Postoperative nausea, vomiting and aspiration are common postoperative complications, and the incidence rate of high-risk patients with major surgery can reach 70% to 80%[7]. In addition to increasing postoperative discomfort, frequent vomiting can also lead to delayed eating time, increased wound tension, electrolyte imbalance, aspiration, and other complications, which is an important reason for prolonging the hospital stay and increasing patient satisfaction[10]. The intranasal resection of pituitary tumors may cause intraoperative bleeding to flow into the stomach through the nasopharynx, and postoperative nasal bleeding will continue to flow in, making the stomach contain more blood and irritating the gastrointestinal tract. When the patient vomits, there will be bloody fluid, emotionally aggravating the patient. These will induce and aggravate postoperative nausea and vomiting in patients and increase the incidence of aspiration. In this study, the nausea, vomiting, and aspiration in the experimental group improved correspondingly to those in the control group, and the number of nausea cases in the experimental group was significantly different from that in the control group, which was statistically significant. This study shows that the intraoperative reserved gastric tube can improve postoperative nausea symptoms.

Table 1 Comparison of postoperative nausea and vomiting aspiration between the two groups of patients (mean ± SD, *n* = 30)

Group	Number of cases of nausea	Number of cases of vomiting	Number of cases of aspiration
Experimental group	3	2	1
Control group	7	5	2
χ^2	13.315	0.6469	0
P value	0.0002	0.421	1

Table 2 Comparison of sore throat scores between the two groups after waking up, 6 hours postoperatively and 24 hours postoperatively (mean ± SD, *n* = 30)

Group	After waking up	After postoperating 6 h	After postoperating 24 h
Experimental group	3.03 ± 1.02	4.12 ± 0.83	3.26 ± 1.13
Control group	4.22 ± 0.93	4.66 ± 1.21	4.57 ± 1.11
χ^2	4.723	2.0156	4.53
P value	< 0.05	< 0.05	< 0.05

Table 3 Comparison of postoperative cerebrospinal fluid leakage (cases) and intracranial infection (cases) and hospitalization days between the two groups (mean ± SD, *n* = 30)

Group	Cerebrospinal fluid leakage (cases)	Intracranial infection (cases)	The days of hospitalization (mean ± SD)
Experimental group	1	1	7.91 ± 2.020
Control group	3	2	8.94 ± 2.503
t or χ^2	χ^2 = 0.268	χ^2 = 0	*t* = 1.754
P value	0.605	1	< 0.05

Reserving gastric tube during the operation can improve postoperative sore throat

Postoperative sore throat (POST) is one of the most common airway complications after general anesthesia. Studies have pointed out that the incidence of POST can reach 10% to 60%[18,19]. It is worth noting that severe POST may lead to dyspnea and dysphagia, reduce patient satisfaction with anesthesia, and may even prolong hospital stay. The site and position of surgery are important reasons for POST. The incidence of POST in head and neck surgery, especially in oropharyngeal surgery, is bound to be higher than that of non-neck surgery patients due to reasons such as the compromised surgical site or the surgeon pulling the airway during the operation[20,21].

For patients undergoing endonasal surgery for pituitary tumors, in addition to the discomfort caused by tracheal intubation to the throat, due to surgery in the nasopharynx, intraoperative bleeding and other stimuli will cause postoperative pharyngeal discomfort. In this study, by sucking out the effusion, reducing the stimulation of iodine and other disinfectants and blood, and other factors, the postoperative pharyngeal discomfort was improved, which had a good effect on the postoperative comfort of patients. Insertion of a gastric tube can improve postoperative discomfort for pituitary tumor removal.

Comparison of postoperative cerebrospinal fluid leakage, intracranial infection, and hospitalization days between the two groups

Since the 1990s, skull base endoscopy has allowed great progress in the clinical application of neurosurgery and has become a routine operation for pituitary tumor resection. At the same time, serious complications, such as cerebrospinal fluid leakage and intracranial infection, have gradually attracted attention[4]. Safe and effective intraoperative skull base reconstruction can reduce postoperative short-term and long-term cerebrospinal fluid leakage, thereby preventing intracranial infection.

However, postoperative behaviors, such as sneezing, coughing, expectoration, and defecation increase intracranial pressure, which can damage the sphenoid sinus and cause cerebrospinal fluid leakage[3]. In this study, the number of cases of cerebrospinal fluid leakage and brain infection in the experimental group was more than those in the control group. Although there was no statistical significance, the small number of cases may have contributed to this. However, the hospitalization days of the experimental group were statistically significantly lower than those of the control group, suggesting that the reserved gastric tube during the operation was beneficial for the patients.

CONCLUSION

Reserved gastric tube application in the resection of pituitary tumors through the endoscopic approach through the nose can predictably improve patients' postoperative pharyngeal discomfort and improve the symptoms of postoperative vomiting and aspiration. It has a high clinical application value and is suitable for all kinds of nerve promotion of the endoscopic endonasal approach in tumor resection.

ARTICLE HIGHLIGHTS

Research background

The neuroendoscopic approach has the advantages of a clear operative field, convenient tumor removal, and less damage, and is the development direction of modern neurosurgery. At present, transnasal surgery for sphenoidal pituitary tumor is widely used. But it has been found in clinical practice that some patients with this type of surgery may experience post-operative nausea and vomiting (PONV) and other discomforts.

Research motivation

At present, it has been found that some patients after endonasal endosphenoidal neuroendoscopy surgery may experience PONV and other discomforts. Whether there can be corresponding methods to avoid the occurrence of similar events is our research motivation.

Research objectives

To explore the effect of reserved gastric tube application in the neuroendoscopic endonasal resection of pituitary tumors.

Research methods

Patients who underwent pituitary adenoma resection *via* the endoscopic endonasal approach were selected and randomly divided into the experimental and control groups. Experimental group: After anesthesia, a gastric tube was placed through the mouth under direct vision using a visual laryngoscope, and the fluid accumulated in the oropharynx was suctioned intermittently with low negative pressure throughout the whole process after nasal disinfection, during the operation, and when the patient recovered from anesthesia. Control group: Given the routine intraoperative care, no gastric tube was left. The number of cases of nausea/vomiting/aspiration within 24 h post-operation was counted and compared between the two groups; the scores of pharyngalgia after waking up, 6 h post-operation, and 24 h post-operation. The frequency of postoperative cerebrospinal fluid leakage and intracranial infection were compared. The hospitalization days of the two groups were statistically compared.

Research results

The times of postoperative nausea and vomiting in the experimental group were lower than that in the control group. The number of cases of postoperative cerebrospinal fluid leakage and intracranial infection was higher than that of the control group. The hospitalization days of the experimental group was lower than that of the control group.

Research conclusions

Reserved gastric tube application in the resection of pituitary tumors through the endoscopic approach through the nose can predictably improve patients' postoperative pharyngeal discomfort and improve the symptoms of postoperative vomiting and aspiration.

Research perspectives

In the next step, we can further study the pressure attracted by the negative pressure of the reserved gastric tube and the use time of the reserved gastric tube, so as to better propose the scheme of the reserved gastric tube.

FOOTNOTES

Co-first authors: Xi Chen and Long-Yao Zhang.

Author contributions: Chen X, Wang XJ, and Yin YH treated all these patients; Zhang Y and Wang ZF collected the data; Chen X and Zhang LY analyzed the data; Wang XJ wrote the manuscript, Zhang LY and Wang XJ revised and checked this article; All authors contributed to the article and approved the submitted version.

Supported by Traditional Chinese Medicine Science and Technology Project in Jiangsu Province, No. YB2015113; the Science and Technology Program of Nantong Health Committee, No. MA2019003, No. MA2021017, No. MB2021026, and No. MB2021027; Science and Technology Program of Nantong City, No. Key003, No. MS12015016 and No. JCZ2022040; and Kangda College of Nanjing Medical University, No. KD2021JYYJYB025, No. KD2022KYJJZD019, No. KD2022KYJJZD022, and No. 2023ZC127.

Institutional review board statement: This research has been approved by the ethics committee of Affiliated Hospital 2 of Nantong

University.

Informed consent statement: Informed consent has been obtained and this investigation has been conducted according to the principles expressed in the Declaration of Helsinki.

Conflict-of-interest statement: All the authors report no relevant conflicts of interest for this article.

Data sharing statement: The original contributions presented in the study are included in the article, further inquiries can be directed to the corresponding author at 6841441@163.com.

STROBE statement: The authors have read the STROBE Statement—checklist of items, and the manuscript was prepared and revised according to the STROBE Statement—checklist of items.

Country/Territory of origin: China

ORCID number: Long-Yao Zhang 0000-0001-7460-7903; Zhi-Feng Wang 0000-0001-8154-0356; Yi Zhang 0000-0002-4618-6256; Yu-Hua Yin 0000-0003-3760-0264; Xue-Jian Wang 0000-0003-0389-5674.

Corresponding Author's Membership in Professional Societies: American Association for Peripheral Neurosurgery, 0921121.

S-Editor: Li L
L-Editor: A
P-Editor: Yuan YY

REFERENCES

1 **Yoo F**, Kuan EC, Heaney AP, Bergsneider M, Wang MB. Corticotrophic pituitary carcinoma with cervical metastases: case series and literature review. *Pituitary* 2018; **21**: 290-301 [PMID: 29404894 DOI: 10.1007/s11102-018-0872-8]
2 **Mete O**, Lopes MB. Overview of the 2017 WHO Classification of Pituitary Tumors. *Endocr Pathol* 2017; **28**: 228-243 [PMID: 28766057 DOI: 10.1007/s12022-017-9498-z]
3 **Xuejian W**, Fan H, Xiaobiao Z, Yong Y, Ye G, Tao X, Junqi G. Endonasal endoscopic skull base multilayer reconstruction surgery with nasal pedicled mucosal flap to manage high flow CSF leakage. *Turk Neurosurg* 2013; **23**: 439-445 [PMID: 24101261 DOI: 10.5137/1019-5149.JTN.6176-12.0]
4 **Wang X**, Zhang X, Hu F, Yu Y, Gu Y, Xie T, Ge J. Middle Turbinate Mucosal Flap in Endoscopic Skull Base Reconstruction. *Turk Neurosurg* 2016; **26**: 200-204 [PMID: 26956812 DOI: 10.5137/1019-5149.JTN.6250-12.0]
5 **Bou-Nassif R**, Abou-Mrad Z, El Ahmadieh TY, Tabar V, Cohen MA. Patient-Reported Outcomes in Endoscopic Endonasal Skull Base Surgery. *Endocrinol Metab Clin North Am* 2022; **51**: 727-739 [PMID: 36244689 DOI: 10.1016/j.ecl.2022.04.005]
6 **Prevedello DM**, Ditzel Filho LF, Solari D, Carrau RL, Kassam AB. Expanded endonasal approaches to middle cranial fossa and posterior fossa tumors. *Neurosurg Clin N Am* 2010; **21**: 621-635, vi [PMID: 20947031 DOI: 10.1016/j.nec.2010.07.003]
7 **Öbrink E**, Jildenstål P, Oddby E, Jakobsson JG. Post-operative nausea and vomiting: update on predicting the probability and ways to minimize its occurrence, with focus on ambulatory surgery. *Int J Surg* 2015; **15**: 100-106 [PMID: 25638733 DOI: 10.1016/j.ijsu.2015.01.024]
8 **Eberhart LH**, Högel J, Seeling W, Staack AM, Geldner G, Georgieff M. Evaluation of three risk scores to predict postoperative nausea and vomiting. *Acta Anaesthesiol Scand* 2000; **44**: 480-488 [PMID: 10757586 DOI: 10.1034/j.1399-6576.2000.440422.x]
9 **Gan TJ**. Postoperative nausea and vomiting--can it be eliminated? *JAMA* 2002; **287**: 1233-1236 [PMID: 11886298 DOI: 10.1001/jama.287.10.1233]
10 **Chung F**, Mezei G. Factors contributing to a prolonged stay after ambulatory surgery. *Anesth Analg* 1999; **89**: 1352-1359 [PMID: 10589607 DOI: 10.1097/00000539-199912000-00004]
11 **Gupta D**, Haber H. Emetogenicity-risk procedures in same day surgery center of an academic university hospital in United States: a retrospective cost-audit of postoperative nausea vomiting management. *Middle East J Anaesthesiol* 2014; **22**: 493-502 [PMID: 25137866]
12 **Dzwonczyk R**, Weaver TE, Puente EG, Bergese SD. Postoperative nausea and vomiting prophylaxis from an economic point of view. *Am J Ther* 2012; **19**: 11-15 [PMID: 20634672 DOI: 10.1097/MJT.0b013e3181e7a512]
13 **Kollmeier BR**, Keenaghan M, Doerr C. Aspiration Risk (Nursing). 2023 Mar 16. In: StatPearls [Internet]. Treasure Island (FL): StatPearls Publishing; 2024 Jan- [PMID: 33760509]
14 **Faiz KW**. VAS--visual analog scale. *Tidsskr Nor Laegeforen* 2014; **134**: 323 [PMID: 24518484 DOI: 10.4045/tidsskr.13.1145]
15 **Cappabianca P**, Cavallo LM, de Divitiis E. Endoscopic endonasal transsphenoidal surgery. *Neurosurgery* 2004; **55**: 933-40; discussion 940 [PMID: 15458602 DOI: 10.1227/01.neu.0000137330.02549.0d]
16 **Chen H**, Luo A. Safety and Efficacy Study of the Cyclooxygenase-2 Inhibitor Parecoxib Sodium Applied for Postoperative Analgesia After Endo-Nasal Operation. *Pain Pract* 2016; **16**: 467-472 [PMID: 25857847 DOI: 10.1111/papr.12294]
17 **Liu Y**, Zheng T, Lv W, Chen L, Zhao B, Jiang X, Ye L, Qu L, Zhao L, Zhang Y, Xue Y, Liu B, Wu Y, Li Z, Niu J, Li R, Qu Y, Gao G, Wang Y, He S. Ambulatory Surgery Protocol for Endoscopic Endonasal Resection of Pituitary Adenomas: A Prospective Single-arm Trial with Initial

Implementation Experience. *Sci Rep* 2020; **10**: 9755 [PMID: 32546762 DOI: 10.1038/s41598-020-66826-9]

18 **Gemechu BM**, Gebremedhn EG, Melkie TB. Risk factors for postoperative throat pain after general anaesthesia with endotracheal intubation at the University of Gondar Teaching Hospital, Northwest Ethiopia, 2014. *Pan Afr Med J* 2017; **27**: 127 [PMID: 28904657 DOI: 10.11604/pamj.2017.27.127.10566]

19 **Fan YL**, Qian JL, Ma EL, Stricker PA, Zuo YX. Incidence and Risk Factors of Postoperative Severe Discomfort After Elective Surgery Under General Anesthesia: A Prospective Observational Study. *J Perianesth Nurs* 2021; **36**: 253-261 [PMID: 33640290 DOI: 10.1016/j.jopan.2020.10.006]

20 **Piriyapatsom A**, Dej-Arkom S, Chinachoti T, Rakkarnngan J, Srishewachart P. Postoperative sore throat: incidence, risk factors, and outcome. *J Med Assoc Thai* 2013; **96**: 936-942 [PMID: 23991600]

21 **Shrestha S**, Maharjan B, Karmacharya RM. Incidence and Associated Risk Factors of Postoperative Sore Throat in Tertiary Care Hospital. *Kathmandu Univ Med J (KUMJ)* 2017; **15**: 10-13 [PMID: 29446355]

World Journal of Clinical Oncology

Submit a Manuscript: https://www.f6publishing.com

World J Clin Oncol 2024 March 24; 15(3): 419-433

DOI: 10.5306/wjco.v15.i3.419

ISSN 2218-4333 (online)

ORIGINAL ARTICLE

Prospective Study

Nomogram based on multimodal magnetic resonance combined with B7-H3mRNA for preoperative lymph node prediction in esophagus cancer

Yan-Han Xu, Peng Lu, Ming-Cheng Gao, Rui Wang, Yang-Yang Li, Rong-Qi Guo, Wei-Song Zhang, Jian-Xiang Song

Specialty type: Oncology

Provenance and peer review: Unsolicited article; Externally peer reviewed.

Peer-review model: Single blind

Peer-review report's scientific quality classification

Grade A (Excellent): 0
Grade B (Very good): B
Grade C (Good): 0
Grade D (Fair): 0
Grade E (Poor): 0

P-Reviewer: Shiryajev YN, Russia

Received: November 19, 2023
Peer-review started: November 19, 2023
First decision: January 9, 2024
Revised: January 15, 2024
Accepted: February 6, 2024
Article in press: February 6, 2024
Published online: March 24, 2024

Yan-Han Xu, Ming-Cheng Gao, Rui Wang, Yang-Yang Li, Rong-Qi Guo, Wei-Song Zhang, School of Clinical Sciences, Graduate School of Nantong University, Yancheng 226019, Jiangsu Province, China

Yan-Han Xu, Ming-Cheng Gao, Rui Wang, Yang-Yang Li, Rong-Qi Guo, Wei-Song Zhang, Jian-Xiang Song, Department of Thoracic Surgery, Yancheng Third People's Hospital, The Affiliated Hospital 6 of Nantong University, Yancheng 224000, Jiangsu Province, China

Peng Lu, Department of Imaging, Yancheng Third People's Hospital, The Affiliated Hospital 6 of Nantong University, Yancheng 224000, Jiangsu Province, China

Corresponding author: Jian-Xiang Song, MD, PhD, Chief Doctor, Chief Physician, Dean, Doctor, Surgeon, Department of Thoracic Surgery, Yancheng Third People's Hospital, The Affiliated Hospital 6 of Nantong University, No. 2 Xindu West Road, Yandu Street, Yandu District, Yancheng 224000, Jiangsu Province, China. jxsongycsy@163.com

Abstract

BACKGROUND

Accurate preoperative prediction of lymph node metastasis (LNM) in esophageal cancer (EC) patients is of crucial clinical significance for treatment planning and prognosis.

AIM

To develop a clinical radiomics nomogram that can predict the preoperative lymph node (LN) status in EC patients.

METHODS

A total of 32 EC patients confirmed by clinical pathology (who underwent surgical treatment) were included. Real-time fluorescent quantitative reverse transcription-polymerase chain reaction was used to detect the expression of B7-H3 mRNA in EC tissue obtained during preoperative gastroscopy, and its correlation with LNM was analyzed. Radiomics features were extracted from multi-modal magnetic resonance imaging of EC using Pyradiomics in Python. Feature extraction, data dimensionality reduction, and feature selection were performed using XGBoost model and leave-one-out cross-validation. Mul-

tivariable logistic regression analysis was used to establish the prediction model, which included radiomics features, LN status from computed tomography (CT) reports, and B7-H3 mRNA expression, represented by a radiomics nomogram. Receiver operating characteristic area under the curve (AUC) and decision curve analysis (DCA) were used to evaluate the predictive performance and clinical application value of the model.

RESULTS

The relative expression of B7-H3 mRNA in EC patients with LNM was higher than in those without metastasis, and the difference was statistically significant ($P < 0.05$). The AUC value in the receiver operating characteristic (ROC) curve was 0.718 (95%CI: 0.528-0.907), with a sensitivity of 0.733 and specificity of 0.706, indicating good diagnostic performance. The individualized clinical prediction nomogram included radiomics features, LN status from CT reports, and B7-H3 mRNA expression. The ROC curve demonstrated good diagnostic value, with an AUC value of 0.765 (95%CI: 0.598-0.931), sensitivity of 0.800, and specificity of 0.706. DCA indicated the practical value of the radiomics nomogram in clinical practice.

CONCLUSION

This study developed a radiomics nomogram that includes radiomics features, LN status from CT reports, and B7-H3 mRNA expression, enabling convenient preoperative individualized prediction of LNM in EC patients.

Key Words: Esophageal cancer; Radiomics; B7-H3mRNA; Multimodal magnetic resonance imaging; Lymph node metastasis; Nomogram

Core Tip: Accurate tumor-node-metastasis staging plays a critical role in devising treatment strategies for esophageal cancer (EC), particularly in assessing lymph node (LN) metastasis. Nevertheless, existing techniques for diagnosing LN in EC are currently constrained by limited accuracy. In light of this, our study endeavors to construct a clinical column chart that can enhance the assessment of LN status, furnishing a valuable point of reference for the diagnosis and treatment of EC.

Citation: Xu YH, Lu P, Gao MC, Wang R, Li YY, Guo RQ, Zhang WS, Song JX. Nomogram based on multimodal magnetic resonance combined with B7-H3mRNA for preoperative lymph node prediction in esophagus cancer. *World J Clin Oncol* 2024; 15(3): 419-433

URL: https://www.wjgnet.com/2218-4333/full/v15/i3/419.htm

DOI: https://dx.doi.org/10.5306/wjco.v15.i3.419

INTRODUCTION

According to relevant research statistics, esophageal cancer (EC) is a common malignant tumor in the field of thoracic surgery, ranking seventh in terms of incidence and sixth in terms of mortality worldwide. In Asia, the main histological type is squamous cell carcinoma[1-3]. Most EC patients require comprehensive treatment. In the early stage, surgery or endoscopic resection is the primary approach, while concurrent chemoradiotherapy is preferred for patients in the middle and late stages. The specific treatment plan should be based on the accurate staging of EC using the tumor-node-metastasis (TNM) classification system[4].

Simultaneously, in surgical treatment, due to the highly variable lymphatic spread of cancer, suspicious positive lymph nodes (LN) should be resected together with the tumor to improve patient survival. However, some studies suggest that expanding the range of LN dissection may increase postoperative complications and worsen prognosis for cancer patients [5,6]. Therefore, in the formulation of treatment strategies for EC, accurate diagnosis of LN metastasis (LNM) status is crucial[7,8].

B7-H3, also known as CD276, is a member of the B7 Ligand family and is an attractive target in antibody immunotherapy. It is overexpressed on many malignant cells and cancer stem cells but exhibits low-level expression in normal tissues[9]. Relevant studies have shown that B7-H3 primarily promotes tumor development through immune mechanisms by inhibiting specific immune responses, leading to a pro-tumoral effect[9]. Research has found associations between B7-H3 expression and clinical TNM progression and prognosis in diseases such as gastric cancer, pancreatic cancer, colorectal cancer, lung cancer, and acute myeloid leukemia[10-15]. Additionally, Arigami *et al*[16] discovered a strong correlation between B7-H3 expression and sentinel LNM and the number of LNM in their study of breast cancer. In their multivariate analysis, the mRNA expression of B7-H3 in the primary tumor significantly predicted regional LNM [16]. Furthermore, Chen *et al*[17] found a close association between B7-H3 expression in EC and aggressive biology, low tumor-infiltrating T lymphocyte density, and poor prognosis[17]. However, there is currently no relevant research proving an association between B7-H3 expression and LNM in EC.

Currently, computed tomography (CT) is commonly used to determine the preoperative LN status in EC patients, primarily relying on size-based measurements (*e.g.*, a 10 mm short-axis diameter on CT as the cutoff value for diagnosing LNM)[18]. However, relevant studies have shown that this method has an accuracy rate of less than 70% in determining LNM[19]. Positron emission tomography (PET)/CT is a rapidly developing imaging modality that combines positron emission tomography with X-ray CT. However, its application in LNM diagnosis is limited due to its high cost, low sensitivity, and high false-positive rate[20]. Meanwhile, research on positive LN detection in certain cancers suggests that magnetic resonance imaging (MRI) has higher accuracy[21,22]. However, conventional MRI of the chest is prone to motion artifacts due to respiratory motion, which can affect image quality. With the emergence of multi-sequence MRI techniques such as StarVIBE and T2TSE-BLADE, respiratory motion artifacts in non-breath-hold patients and uncooperative patients have been significantly reduced, resulting in clearer visualization of tumors and the surrounding soft tissue boundaries and improved image quality[23,24]. However, existing imaging modalities primarily rely on LN anatomy, and their assessment of LNM is based on size measurements, which are insufficient to reveal the internal structural characteristics of LN and obtain valuable tumor-related information[25].

Radiomics research involves applying computer mathematical tools to image processing, extracting radiological features such as shape, texture, or waveform, which can provide information about cancer phenotypes and the tumor microenvironment. This concept was introduced by Lambin *et al*[26] in 2012. By combining radiomics-derived data with other relevant data, accurate and reliable Clinical Decision Support Systems (CDSS) can be generated[27]. Currently, radiomics has made significant progress in the qualitative assessment of tumors, diagnosis of LNM, and prognosis prediction[28-30]. However, there is currently no research that combines radiomics with expression factors in primary tumors to elucidate their diagnostic and predictive value in cancer. This integration could contribute to a more comprehensive understanding of the biological characteristics and behavior of tumors, providing more accurate predictions for individualized treatment.

Therefore, the objective of this study is to develop a radiomics nomogram that combines radiomic features, B7-H3 mRNA expression levels, and clinical risk factors for individualized prediction of preoperative LNM in EC patients.

MATERIALS AND METHODS

Patients

Our research institution's ethics review committee (the Medical Ethics Committee of the Sixth Affiliated Hospital of Nantong University, Yancheng Third People's Hospital) has approved this research project. Considering that the relevant examinations in this study do not pose significant physical or harm to the patients' interests, the requirement for obtaining informed consent from the patients has been waived by the committee. Our study included a total of 32 EC patients (9 females and 23 males) who received treatment at our hospital from March 2022 to July 2023 and met the inclusion criteria of this study. The patients had an average age of 70.53 ± 6.41 years, with an age range of 52-84 years. The inclusion criteria were as follows: (1) All patients were over 18 years of age; (2) Standard contrast-enhanced CT and MRI examinations were performed within 10 d before treatment; (3) Patients underwent gastroscopy and pathological biopsy at our hospital, and the pathological diagnosis was confirmed as esophageal squamous cell carcinoma; (4) The surgical approach was consistent for all patients, with three-field LN dissection for EC; (5) MRI images had sufficient clarity to support radiomic feature extraction; (6) Availability of clinical and pathological information; and (7) B7-H3 mRNA expression was determined by reverse transcription-polymerase chain reaction (RT-PCR) using cancer tissue samples obtained from preoperative esophagoscopic biopsies. The exclusion criteria were as follows: (1) Patients with significant surgical contraindications; (2) Patients with concurrent other tumor diseases; and (3) Inability to undergo MRI examination or presence of contraindications for MRI examination. The patients recruitment and selection process was showed in Figure 1.

Baseline clinical information and pathological data of the patients in the study, including age, sex, tumor location, tumor size, and LN status (based on pathological results), were obtained from medical records. In addition, the enhanced CT reports of the study patients were collected, and LN with a size of ≥ 10.0 mm in the CT reports were considered as positive for LN involvement.

Image acquisition and segmentation

The patients were scanned using a 3.0T MRI scanner (MAGNETOM Skyra 3.0T, Siemens Healthcare, Germany) and an 18-channel surface phased-array coil. Prior to the examination, patients were instructed to remove any metallic objects and undergo respiratory training. The patients were positioned in a supine position with the head first, and the scanning range extended from the bilateral lung apices to 1 cm below the diaphragm. The MRI scanning sequences included T1-Star-VIBE and T2-TSE-BLADE sequences. The parameters for the T1-Star-VIBE sequence were as follows: TR/TE = 3.98/1.91 ms; voxel size = 1.0 mm × 1.0 mm × 1.0 mm; FOV = 300 mm × 300 mm; flip angle = 12°; scanning time = 309 s. The parameters for the T2-TSE-BLADE sequence were as follows: TR/TE = 5000/97 ms; voxel size = 0.9 mm × 0.9 mm × 3.0 mm; FOV = 260 mm × 260 mm; flip angle = 180°; scanning time = 360-600 s.

We retrieved the MRI images of all patients from the hospital's Picture Archiving and Communication System. Preprocessing of the acquired images was performed using Python, which included bias field correction utilizing the N4 correction algorithm and registration alignment. Subsequently, image feature segmentation and analysis were conducted. These processes aimed to extract meaningful features from the images, facilitating further analysis and the development of our study's models.

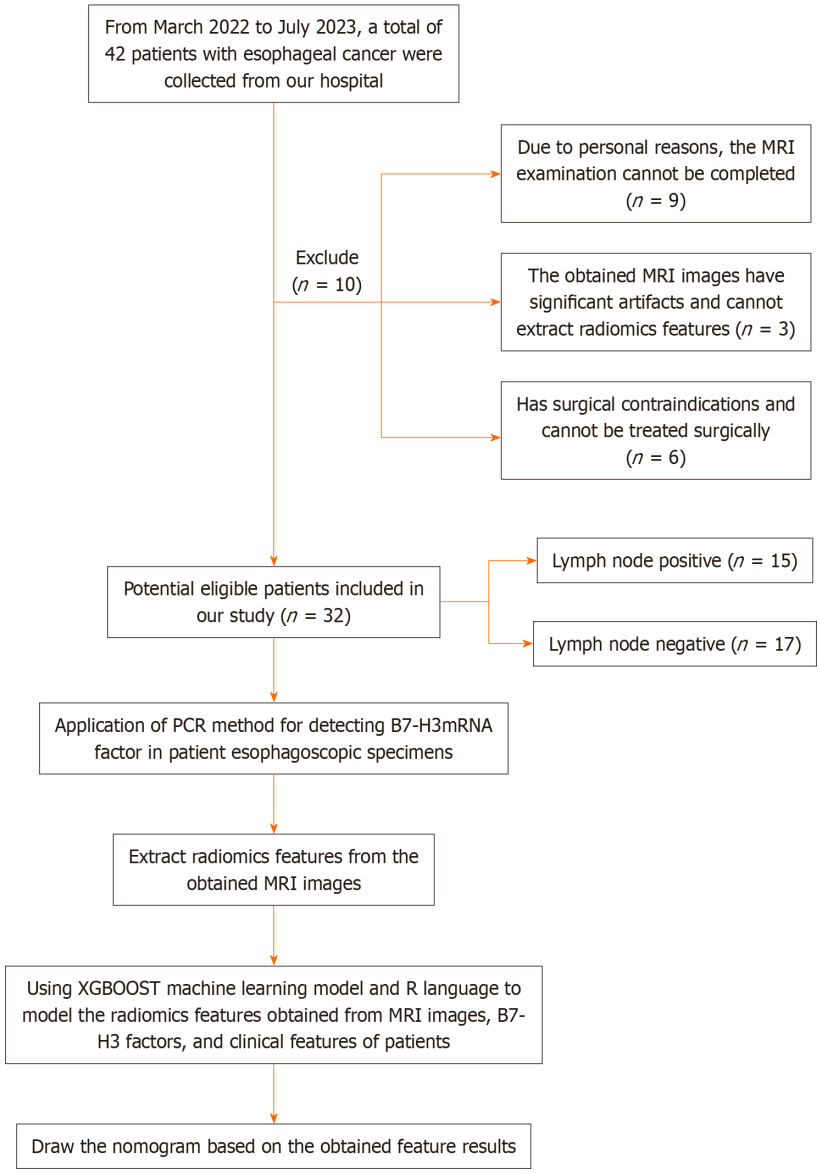

Figure 1 Recruitment and selection process of patients. MRI: Magnetic resonance imaging; PCR: Polymerase chain reaction.

The three-dimensional (3D) semi-automatic segmentation was performed by a single operator, who was a thoracic surgery graduate student, using the 3D Slicer software. The segmentation process involved the extraction of valuable regions of interest (ROIs) based on the radiologist's interpretation. The radiologist, with 10 years of experience in the field, provided the expert assessment of the images, and the operator utilized this information to guide the segmentation and extraction of the ROIs. The operator carefully followed the radiologist's findings to ensure accurate and reliable segmentation of the desired regions.

In this study, ROIs referred to the primary lesions of EC. These ROIs were manually delineated on each consecutive slice of the MRI images along the boundaries of the primary tumor lesions. The delineation process excluded adjacent air, blood vessels, fat, and normal tissues, focusing solely on the pathological features of the primary tumor. The delineation was performed by the operator using the 3D Slicer software, guided by the radiologist's interpretation and expertise.

Radiomics feature extraction and selection

We applied the PyRadiomics component in Python (https://pyradiomics.readthedocs.io/en/Latest/) to extract features from the ROI for each case. Prior to ROI processing, we performed bias field correction (N4 correction) and registration alignment on every MRI image of all sequences to mitigate the impact of varying grayscale ranges in PyRadiomics. The extracted feature categories include first-order, shape, gray level co-occurrence matrix, gray level run length matrix, gray level size zone matrix, gray level dependence matrix, and neighboring gray tone difference matrix.

Due to the limited sample size in this study, we employed the XGBoost model and leave-one-out cross-validation method to construct the radiomics features. Firstly, a *t*-test was applied to select the top 30% features that are predictive of LNM. Secondly, using the leave-one-out cross-validation method, internal cross-validation was performed to further retain features that improve diagnostic performance. Finally, the radiomics signature and its corresponding weight values were computed to obtain the consistency features in the model. The specific formula for the established and

extracted radiomics features is as follows:

Radiomics signature = Intercept + coef 1 × feature 1 + coef 2 × feature 2 + coef 3 × feature 3 + coef 4 × feature 4 + coef 5 × feature 5 + ... + coef *n* × feature *n*.

Real-time quantitative RT-PCR

Acquisition of esophageal pathological tissue under esophagoscopy: Patients diagnosed with EC were carefully screened for inclusion in the study. Under gastroscopy, specialized endoscopic forceps were used to obtain biopsy specimens from suspected cancerous lesions. Additionally, samples of normal tissue were collected from a location at least 5 cm away from the suspected cancerous area to serve as adjacent normal tissue. Following the collection of cancerous and adjacent normal tissue, the specimens were immediately immersed and washed in physiological saline solution. Subsequently, they were stored at a temperature of -80 °C in a freezer for preservation. To ensure the accuracy and reliability of the study, specimens that did not meet the predefined inclusion criteria were carefully excluded. This exclusion process was based on a combination of subsequent patient treatment and pathological diagnosis, which served as the gold standard.

RNA extraction from specimen tissue: (1) Tissue lysis: The collected specimens of EC and adjacent normal tissue were removed from the -80 °C freezer and thawed. On a sterile bench, the tissue was finely minced using sterile tissue scissors. Approximately 0.2 g of the tissue was weighed on an electronic precision balance and transferred into a grinding tube. The tissue was then washed with PBS buffer (dissolving protective reagent) for 5 min. The grinding tube containing the tissue was placed on ice.

Next, 500 μL of RNA extraction solution (*e.g.*, RNA Extrizol) was added to the grinding tube using a pipette. A handheld tissue grinder was used, adjusting it to the maximum speed, to grind the tissue in a start-stop manner. Care was taken to avoid liquid splashing during the grinding process. Grinding was continued until the tissue was completely lysed and formed a homogenized liquid. Finally, 500 μL of RNA extraction solution was added and mixed well with the lysate.

Subsequently, 200 μL of chloroform solvent (trichloromethane) was added to the tube. The tube was then placed on a shaker and shaken for 15 s. After shaking, the tube was left to stand at room temperature for 3 min.

(2) RNA Precipitation and Washing: The pre-cooled centrifuge was set to a temperature of 4 °C. The centrifuge speed was adjusted to 13000 rpm, and the centrifugation time was set to 15 min. The tubes containing the lysed tissue were placed in the centrifuge and balanced before initiating centrifugation. After 15 min of centrifugation, the top layer of liquid (approximately 400 μL) from the tube was carefully extracted using a pipette and transferred to a new tube. It is important to only aspirate the top layer of liquid, avoiding any other layered liquids to prevent contamination of chromosomal DNA.

Using a pipette, 500 μL of isopropanol was added to the tube containing the extracted liquid, and the mixture was thoroughly mixed. The tube was then left to stand at room temperature for 10 min to allow RNA precipitation.

The centrifuge process was repeated as described above (centrifuge temperature set at 4 °C, centrifuge speed at 13000 rpm, and centrifugation time of 15 min). The tube was placed in the centrifuge and balanced before initiating centrifugation. After 15 min of centrifugation, a white, flocculent precipitate could be observed at the bottom of the centrifuge tube, which represented the RNA after lysis completion. Using a pipette, the entire supernatant, excluding the flocculent precipitate, was aspirated and discarded, while retaining the RNA pellet.

To wash the RNA pellet, 1 mL of 75% ethanol solvent was added to the centrifuge tube and mixed thoroughly. The centrifuge parameters were set to a temperature of 4 °C, a speed of 750 g, and a centrifugation time of 5 min. The tube was placed in the centrifuge, balanced, and then centrifuged.

And (3) RNA resuspension and concentration measurement: Using a pipette, carefully aspirate the upper ethanol solution from the centrifuge tube, being cautious not to draw up the white precipitate at the bottom. After aspirating the ethanol solution, let the centrifuge tube air dry at room temperature. Then, add 20 μL of nuclease-free water to the dried centrifuge tube to fully dissolve the RNA.

Next, measure the concentration and purity of the RNA in the centrifuge tube using a NANODROP 2000 nucleic acid and protein analyzer. Ensure that the absorbance ratio at 260 nm and 280 nm falls within the range of 1.8-2.0 for the retained samples to ensure accuracy of the measurement results. If the ratio falls outside this range, discard the sample and repeat the experiment with a new tissue specimen. Label the centrifuge tube containing the remaining RNA and store it in a -80 °C freezer for future experiments.

mRNA real-time quantitative polymerase chain reaction experimental steps: (1) cDNA synthesis by reverse transcription: RNA extraction solution was retrieved from a -80 °C freezer and transferred to a new microcentrifuge tube. Using a pipette, 3 μg of RNA was extracted as a template and mixed with 1 μL of Oligo (dT) primer solution. Then, nuclease-free water was added to achieve a total volume of 12 μL, and the mixture was gently mixed. The mixture was centrifuged for 10 s in a microcentrifuge.

Prior to the next step, a constant temperature incubator was pre-set at 70 °C for 5 min. The microcentrifuge tube containing the mixture was heated in the incubator. After heating, the tube was immediately transferred to an icebox for cooling, followed by a brief centrifugation to collect the precipitate.

Next, the reaction mixture was prepared. Using a pipette, 4 μL of 5 × Reaction Buffer, 1 μL of RNase Inhibitor, 2 μL of 10 mmol/L dNTP Mix, and 1 μL of RevertAid M-MuLV RT were drawn. Each microcentrifuge tube was then added with 8 μL of the reaction mixture, gently mixed, and centrifuged for 5 s in a microcentrifuge.

Prior to performing the reverse transcription reaction, the polymerase chain reaction (PCR) machine was pre-set to a temperature of 42 °C, and a 6 min wait was observed. Subsequently, the reaction was incubated at 72 °C for 5 min to

terminate the reverse transcription. The microcentrifuge tubes were placed in ice, and a 1:10 dilution was performed for storage at -20 °C.

And (2) Real-time quantitative PCR amplification and analysis: Retrieve an equal volume of cDNA template from the -20 °C freezer and place it in an EP tube. Add the amplification primers to achieve a total volume of 20 μL. Transfer the mixture to the PCR machine for further reaction.

Data analysis was performed using the 2-ΔCT relative quantification method, with β-actin as the reference gene for normalization. Each group included two technical replicates, and the procedure was as follows: Retrieve the standard EP tube and sequentially add 2 μL of template, 1 μL of upstream primer (concentration of 10 μmol/L), 1 μL of downstream primer (concentration of 10 μmol/L), 12.5 μL of SYBR Green Master Mix, and 8.5 μL of double distilled water. Gently mix the solution and centrifuge for 10 s in a microcentrifuge.

Perform amplification using the PCR machine. Each group contains three samples, and the program is set as follows: Pre-denaturation at 95 °C for 10 min, followed by 40 cycles of denaturation at 95 °C for 30 s, annealing at 60 °C for 30 s, and extension at 72 °C for 40 s. Finally, terminate the reaction at 72 °C for 10 min.

After the completion of the PCR amplification, data analysis was performed based on the amplification curve and melt curve. The 2-ΔΔCt relative quantification method was used for data analysis in each group, with β-actin as the internal reference gene for normalization. Each group included four samples, and three experimental replicates were performed. The final data analysis was conducted using GraphPad Prism 5.0 software.

Model construction

We utilized the R software to perform logistic regression analysis to identify independent predictive factors, including radiomic features, B7-H3 mRNA expression level, and LN status reported by CT, in our study. A model incorporating these independent predictors was developed, and its performance was evaluated using the area under the receiver operating characteristic (ROC) curve.

Nomogram development and decision curve analysis

Nomogram development and decision curve analysis (DCA) were employed for model visualization and clinical application. To assess the additional value of radiomic features, B7-H3 mRNA, and CT in individually predicting the preoperative LN status in EC patients, four decision curves were developed based on CT reports, radiomic features of the primary lesion, B7-H3 mRNA, and a combined model (including CT reports, B7-H3 mRNA, and radiomic features). These decision curves were used to further determine the clinical utility of the plotted line chart.

RESULTS

Clinical characteristics

The study included a total of 32 EC patients, as shown in Table 1. There were no significant differences ($P > 0.05$) between the LN-positive and LN-negative groups in terms of patient age, sex, preoperative carcinoembryonic antigen (CEA) levels, preoperative squamous cell carcinoma antigen levels, pathological grade, tumor location, and tumor size. However, a statistically significant difference was observed in T stage ($P < 0.05$). In the study cohort, the LNM rate was 46.88% (15/32) based on postoperative pathological diagnosis. Regarding the subjective enhanced CT reports of LN status, 6 patients were reported as LN-negative but confirmed to have LNM, while 6 patients were reported as LN-positive but confirmed to be LN-negative. The sensitivity was 60.0%, and the specificity was 64.7% (Table 1).

The relationship between the expression level of B7-H3 mRNA and the clinical characteristics of EC patients

The correlation between B7-H3 mRNA expression levels and age, sex, T stage, and N stage (LNM) in patients with EC was analyzed separately. The T stage and N stage of EC were determined according to the International 8th edition TNM staging criteria for EC.

Among the 32 patients with EC, the average B7-H3 mRNA expression level in male patients was 2.47 ± 0.51, while in female patients, it was 2.52 ± 0.40. There was no significant statistical difference between the two groups ($P > 0.05$). The results indicate that there is no significant correlation between B7-H3 mRNA expression levels and sex in patients with EC ($P > 0.05$).

Among the 32 patients with EC, the average B7-H3 mRNA expression level in T1 stage patients was 2.23 ± 0.32, in T2 stage patients it was 2.66 ± 0.53, and in T3 stage patients it was 2.59 ± 0.12. There was a significant correlation in the average B7-H3 mRNA expression levels among the different T stages ($P < 0.05$). Furthermore, we found that the average B7-H3 mRNA expression level in the tissues of EC patients with LNM was 2.70 ± 0.53, while in patients without LNM, it was 2.29 ± 0.35. The study revealed a significant increase in B7-H3 mRNA expression levels in the tissues of EC patients with LNM compared to those without LNM ($P < 0.05$; Figure 2A).

In conclusion, the expression level of B7-H3 mRNA in EC is not significantly correlated with sex ($P > 0.05$). However, it is closely associated with T stage and LNM in EC ($P < 0.05$). The relative expression level of B7-H3 mRNA is significantly higher in LN-positive tissues of esophageal squamous cell carcinoma, indicating an upregulation of B7-H3 mRNA expression in LN-positive tissues of EC (Table 2).

Diagnostic value of B7-H3 mRNA in detecting LNM in EC

We performed quantitative analysis of B7-H3 mRNA expression in 32 EC tissues and generated a ROC curve (Figure 1) to

Table 1 Characteristics of patients in the cohort, *n* (%)

Characteristic	LN metastasis (+)	LN metastasis (-)	*P* value
Age, mean ± SD	70.18 ± 6.75	71.92 ± 7.49	0.39
Tumor size, mean ± SD	3.89 ± 1.55	3.18 ± 1.64	0.24
Sex			0.54
Male	10 (66.67)	13 (76.47)	
Female	5 (33.33)	4 (23.53)	
CEA			0.99
0-5 ng/mL	15 (99.99)	16 (94.12)	
> 5 ng/mL	0 (0.01)	1 (5.88)	
Squamous cell carcinoma antigen			0.61
0-2.7 ng/mL	12 (80.0)	14 (82.35)	
> 2.7 ng/mL	3 (20.00)	3 (17.65)	
Location			0.99
Upper mediastinal	2 (13.33)	1 (5.88)	
Middle mediastinal	6 (40.00)	8 (47.06)	
Lower mediastinal	6 (40.00)	8 (47.06)	
Abdominal	1 (6.67)	0 (0.01)	
Histologic grade			0.40
Well differentiated	0 (0.01)	2 (11.77)	
Moderately differentiated	11 (73.33)	11 (64.71)	
Poorly differentiated	4 (26.67)	4 (23.53)	
T stage			0.01
1	3 (20.00)	10 (58.82)	
2	12 (80.00)	5 (29.41)	
3	0 (0.01)	2 (11.77)	
CT-reported LN status			0.16
0-10.0 mm	6 (40.00)	11 (64.71)	
> 10.0 mm	9 (60.00)	6 (35.29)	

LN: Lymph node; T: Tumor; CEA: Carcinoembryonic antigen; CT: Computed tomography.

evaluate the diagnostic value of B7-H3 in detecting LNM in EC using clinical pathological examination as the gold standard. The area under ROC curve (AUC) for B7-H3 in detecting LNM was 0.718, with a sensitivity of 73.3% and specificity of 70.6%. The optimal diagnostic threshold for B7-H3 in identifying LNM in EC was determined to be 2.56 (Figure 2A).

Feature extraction and model construction

Using the Pyradiomics package in Python, a total of 1169 radiomic features were extracted from MRI images. The feature selection process was performed using the Leave-one-out method from the XGBoost model, resulting in the reduction of the feature set to 18 potential predictive factors (Figure 3). In the LASSO regression model, the following features were identified as having non-zero coefficients:

T1-log-sigma-2-0-mm-3D_glcm_DifferenceAverage, T1-log-sigma-5-0-mm-3D_glszm_SizeZoneNonUniformityNormalized, T1-wavelet-LLH_gldm_LargeDependenceEmphasis, T1-wavelet-LHL_firstorder_Median, T1-wavelet-LHL_firstorder_RootMeanSquared, T1-wavelet-LHH_glcm_Contrast, T1-wavelet-LHH_glcm_JointEntropy, T1-wavelet-LHH_glszm_SmallAreaHighGrayLevelEmphasis, T1-wavelet-HLH_firstorder_MeanAbsoluteDeviation, T1-wavelet-HLH_glszm_SmallAreaEmphasis, T1-wavelet-HLH_glszm_SmallAreaHighGrayLevelEmphasis, T1-wavelet-HHL_glcm_ClusterTendency, T1-wavelet-HHL_glcm_Contrast, T1-wavelet-HHL_glszm_GrayLevelNonUniformity, T1-wavelet-HHH_firstorder_InterquartileRange, T2-original_gldm_DependenceEntropy, T2-log-sigma-4-0-mm-3D_glszm_GrayLevelNonUniformity, T2-wavelet-HLH_glcm_Idn. Additionally, the optimal weight value feature was

Table 2 The relationship between B7-H3 expression and clinical characteristics of esophageal cancer patients

Clinical characteristic	Number of sample	B7-H3mRNA	Statistic	*P* value
Sex				
Male	23	2.47 ± 0.51	0.06	0.80
Female	9	2.52 ± 0.40		
T			*F* statistic	
1	13	2.23 ± 0.32	3.309	0.05
2	17	2.66 ± 0.53		
3	2	2.59 ± 0.12		
N				
0	17	2.29 ± 0.35	2.50	0.02
1-3	15	2.70 ± 0.53		

T: Tumor; N: Node.

Table 3 Values of various coefficients in the nomogram

Variables	Coef	95%CI
T1.WM	-0.5717	(-2.85, -0.25)
T1-wavelet-LHL_firstorder_Median		
T1.W.HSAHGE	0.22695	(-0.21, -2.91)
HLH_glszm_SmallAreaHighGrayLevelEmphasis		
T1.W.CT	-2.1616	(-3.72, -0.87)
T1-wavelet-HHL_gicm_ClusterTendency		
T1.W.R	0.49155	(-1.02, -3.32)
T1-wavelet		
HHH_firstorder_InterquartileRange	-4.1807	(-4.97, -0.68)
T2.O.DE		
T2-original_gldm_DependenceEntropy	47.4461	(-0.67, -3.38)
T2.W.gl		
T2-wavelet-HLH_gicm_Idn	3.69379	(0.18, -4.34)
B7.H3		
CT	1.46262	(-1.98, -4.90)

The coefficient values of individual independent factors in the developed column chart are shown in the figure. The selected radiomic features and their abbreviations in the nomogram are presented in the table. All predictive factors have a *P* value < 0.05, indicating statistical significance. CT: Computed tomography.

determined to be T1-wavelet-HLH_glcm_InverseVariance through further calculations and analysis.

Subsequently, logistic regression analysis was conducted in R language to further determine the independent predictive factors among the selected radiomic features, B7-H3 mRNA expression level, T stage, and LN status from CT reports. During the analysis, the model with the smallest Akaike information criterion (AIC) value was chosen.

The following radiomic features were further selected:

T1-wavelet-LHL_firstorder_Median, T1-wavelet-HLH_glszm_SmallAreaHighGrayLevelEmphasis, T1-wavelet-HHL_glcm_ClusterTendency, T1-wavelet-HHH_firstorder_InterquartileRange, T2-original_gldm_DependenceEntropy, T2-wavelet-HLH_glcm_Idn (the corresponding coefficient values for each independent predictive factor are detailed in Table 3).

A model incorporating these independent predictive factors was developed and presented in the form of a column chart (Figure 4).

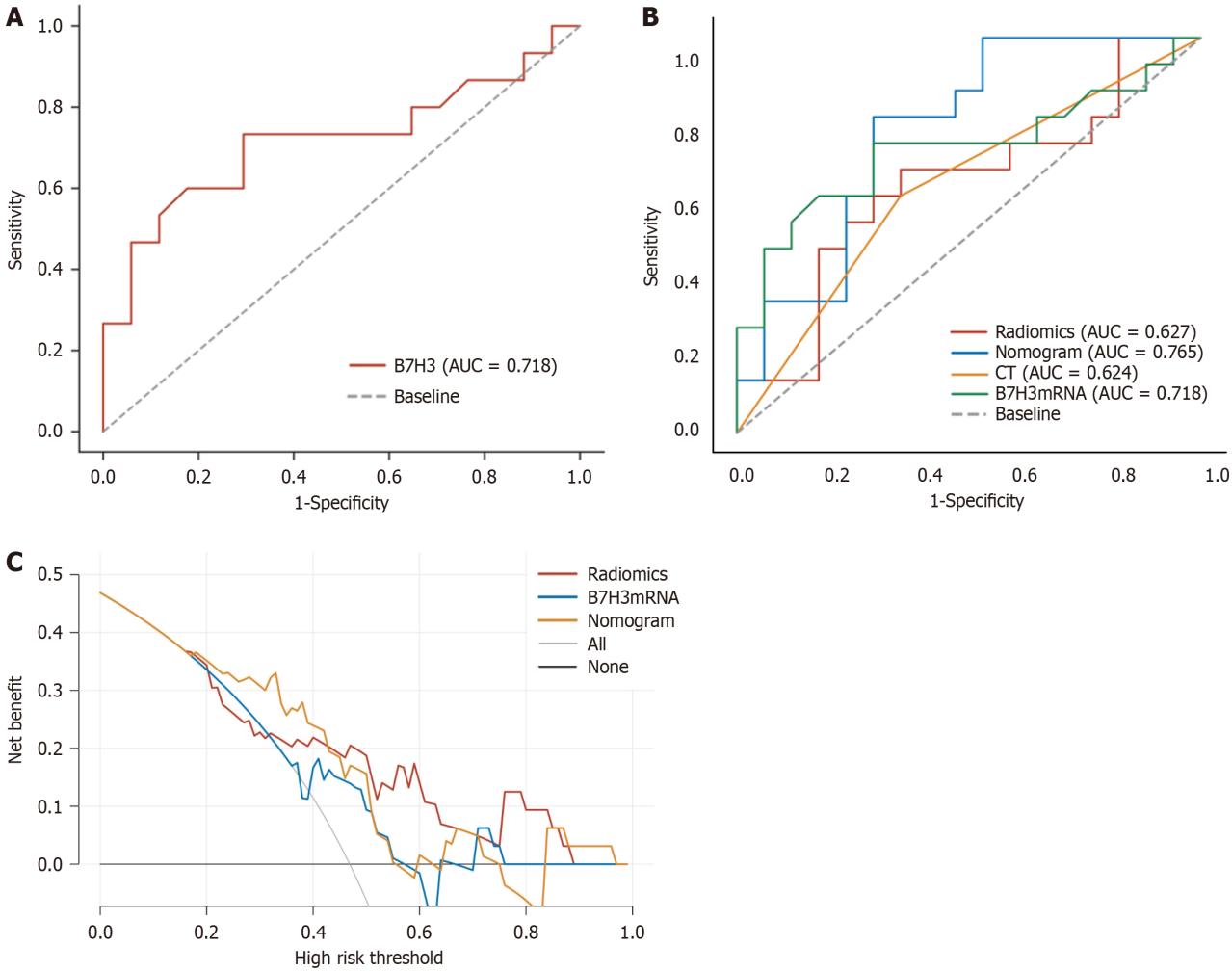

Figure 2 Receiver operating characteristic curve, the area under the receiver operating characteristic curve, and decision curve analysis. A: Receiver operating characteristic (ROC) curve of B7-H3mRNA in the study queue; B: Model performance in the study cohort. the area under the ROC curve (AUC) value increases when radiomic features are combined with B7-H3 mRNA expression compared to different feature combinations. Additionally, it can be observed that as more feature species are used, the AUC value increases, indicating better model performance; C: Decision curve analysis. The y-axis represents net benefit. The threshold probability refers to the point at which the perceived benefit of treating patients with intermediate to high-risk lymph node metastasis is considered equivalent to the harm of overtreating low-risk disease, reflecting how patients weigh the benefits and harms associated with decision-making. The higher curve at any given threshold probability represents the optimal prediction that maximizes net benefit. The decision curve indicates that the combined predictive model used provides greater net benefit compared to other models. AUC: The area under the receiver operating characteristic curve; CT: Computed tomography.

Clinical use

Using the pathological examination results as the gold standard, we calculated the diagnostic sensitivity and specificity of LN status from CT reports, B7-H3 mRNA expression, MRI radiomic features, and the combined predictive model for LNM in EC. The results are shown in Table 4. Furthermore, we plotted ROC curves (Figure 4) to illustrate the diagnostic performance of LN status from CT reports, B7-H3 mRNA expression, MRI radiomic features, and the established combined predictive model for preoperative LN diagnosis. Through comparison, we found that the combined predictive model exhibited the best discriminative power and predictive stability, with the highest AUC value (Table 4, Figure 1B).

The DCA based on combined predictive model is presented in Figure 1C. Compared to DCA using a single radiomic feature, the combined predictive model incorporating B7-H3 mRNA expression and clinical CT results demonstrates higher accuracy in predicting preoperative LN status. This indicates that the nomogram based on this predictive model is a reliable clinical tool for predicting LN status in patients with EC. The DCA suggests that within the probability threshold range of approximately 0.3 to 0.7, the nomogram based on the combined model provides additional net benefit to the "treatment" strategy.

DISCUSSION

LN status is one of the most important prognostic factors in EC, especially the number and location of metastatic LN, which are closely linked to clinical treatment decisions, including the implementation of neoadjuvant therapy, the extent of surgical LN resection, or the design of radiation therapy fields[25,31,32]. The decision of whether neoadjuvant

Table 4 Receiver operating characteristic curve of the dataset

Model	AUC (95%CI)	Sensitivity	Specificity	Youden index
Radiomics	0.627 (0.427-0.828)	0.667	0.647	0.314
Nomogram	0.765 (0.598-0.931)	0.800	0.706	0.506
CT	0.624 (0.426-0.821)	0.600	0.647	0.247
B7-H3mRNA	0.718 (0.528-0.907)	0.733	0.706	0.439

CT: Computed tomography; AUC: Area under the curve.

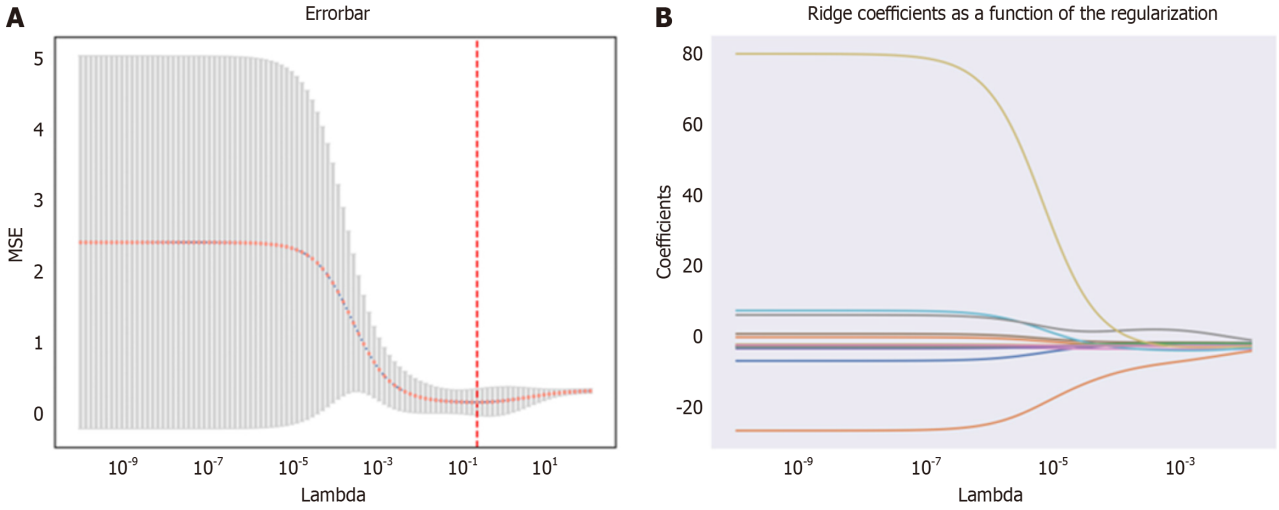

Figure 3 Texture feature selection using the Least Absolute Shrinkage and Selection Operator binary logistic regression model. A: The tuning parameter (Lambda) selection in the Least Absolute Shrinkage and Selection Operator (LASSO) model was performed using 10-fold cross-validation with the minimum criterion. The relationship curve between the mean-square error and Lambda is depicted, with a dashed line indicating the optimal value. The vertical lines represent the values selected through 10-fold cross-validation, including 18 optimized non-zero coefficients; B: LASSO coefficient profiles of 1169 texture features. The coefficient profiles were generated based on the sequence of log (Lambda). When using the value selected by 10-fold cross-validation, the optimal Lambda resulted in 18 non-zero coefficients. MSE: Mean-square error.

chemoradiotherapy is required before surgery primarily depends on the LN status. Furthermore, neoadjuvant chemoradiotherapy can target micrometastases, including LN metastases, and patients with LNM may benefit from this treatment [7,33]. However, for patients who refuse or are unable to tolerate surgery, the LN status cannot be diagnosed through postoperative biopsy. Therefore, accurate preoperative prediction of LN status is necessary and important.

With the advancement of radiomics research, an increasing number of studies are utilizing radiological features extracted from medical images, such as shape, texture, or waveform, to obtain a range of information about cancer phenotypes and the tumor microenvironment[27]. This information is distinct and complementary to other relevant data, including clinical features, treatment-related decision information, or genomic data[34]. When radiomics-derived data is combined with other relevant data and correlated with clinical disease outcomes, they can generate accurate and reliable CDSS[35,36]. These CDSS can assist clinicians in making more informed decisions regarding the diagnosis, treatment planning, and prognosis of cancer patients.

Unlike many previous studies on radiological features, which focused solely on the association of clinical and radiological features with tumor microenvironment characteristics in LNM, they neglected the impact of various proteins or tumor factors on promoting LNM[37-42]. In the study by Toiyama *et al*[43], they observed improved predictive accuracy when adding serum biomarkers to the predictive model as clinical pathological risk factors for preoperative detection of LNM in colorectal cancer patients [the area under the curve increased to 0.801 (95%CI: 0.725-0.857) with modification of the multivariate model]. Similarly, Huang *et al*[29] provided a radiomics nomogram incorporating radiomic features, LN status from CT reports, and CEA levels, which demonstrated higher accuracy in the preoperative individualized prediction of LNM in colorectal cancer patients. These studies may support the notion that considering tumor diagnostic biomarkers across different aspects is an important research approach to enhance CDSS[44].

In our previous studies, we demonstrated a close association between high expression of B7-H3 and tumor differentiation, TNM staging, and LNM in EC. In this study, we further investigated the correlation between B7-H3 mRNA expression levels and LNM in EC using the RT-PCR method. Additionally, we developed and validated a diagnostic nomogram based on radiomic features for individualized preoperative prediction of LNM in patients with EC. The nomogram incorporates three components: radiomic features, B7-H3 mRNA expression levels, and LN status from CT reports.

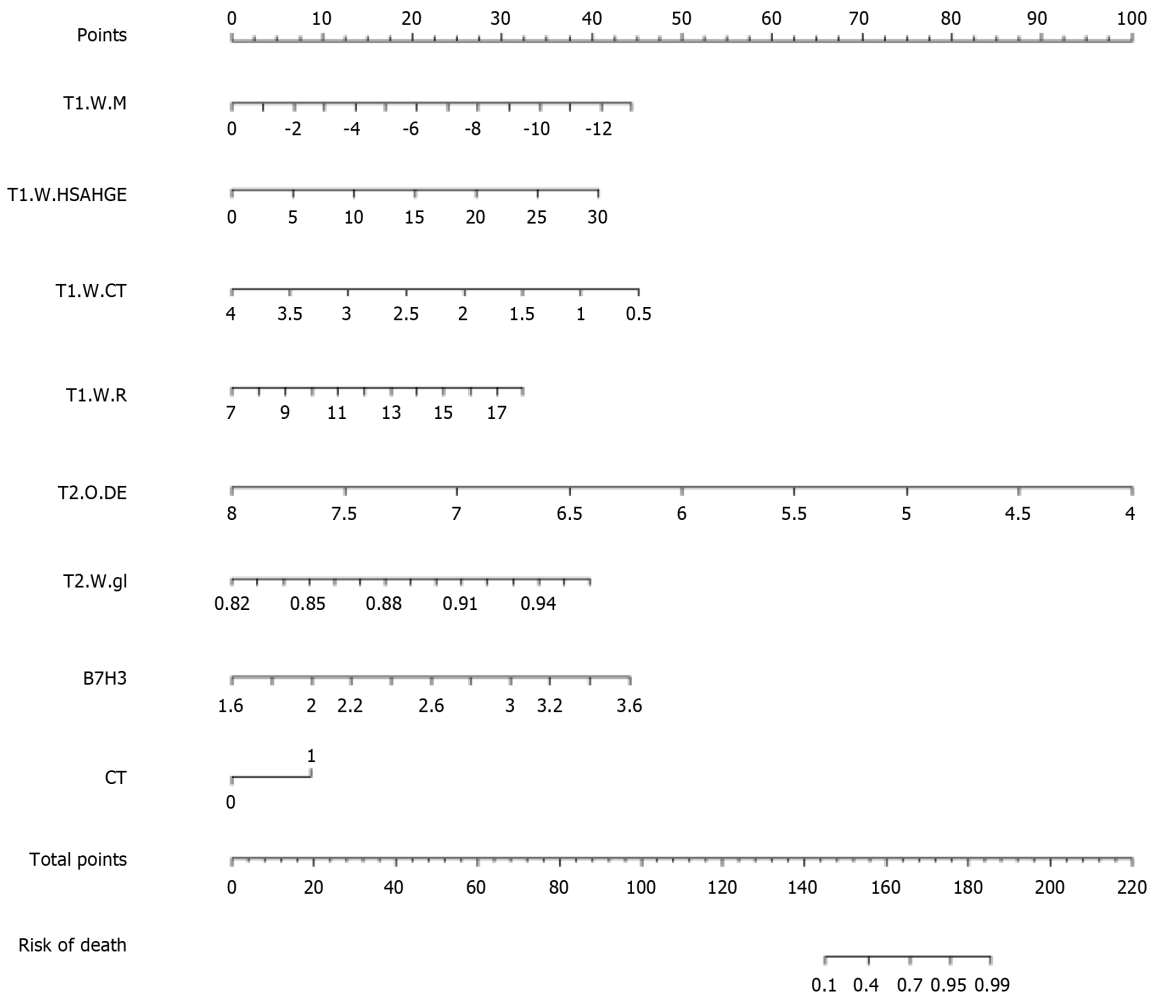

Figure 4 Developed radiomics nomogram. The radiomics nomogram was developed with the radiomics signature, B7-H3mRNA level, and computed tomography-reported lymph node status incorporated. CT: Computed tomography.

In this study, we determined the expression levels of B7-H3 mRNA in tumor tissues of EC using preoperative endoscopic biopsy. We found that the expression levels of B7-H3 mRNA were consistent with previous reports regarding LNM in EC. Additionally, our research revealed that the relative expression level of B7-H3 mRNA was significantly higher in LN-positive tissues compared to LN-negative tissues in esophageal squamous cell carcinoma. We performed ROC curve analysis and found that B7-H3 mRNA had good accuracy in predicting LNM (AUC = 0.718; 95%CI: 0.528-0.907; sensitivity: 70.3%; specificity: 70.6%). Some studies on diagnostic models have shown that relying solely on certain factors with univariate associations may not provide sufficient predictive strength[45]. However, if a factor has statistical significance, it should not be excluded from the model[46]. Therefore, in our study, we found a close association between B7-H3 and LNM, indicating the importance of B7-H3 mRNA expression in preoperative LN diagnosis.

We performed MRI image acquisition in EC patients using T2-TSE-BLADE and T1-StarVIBE sequences, which provide high image quality and anatomical details in EC and accurately depict different layers of the esophageal wall. Therefore, both T2-TSE-BLADE and T1-StarVIBE sequences are feasible for texture analysis[41]. In Python, we used the XGBoost model from the Pyradiomics package and employed leave-one-out cross-validation to extract radiomic features from the ROI in MRI. Subsequently, logistic regression analysis was conducted in R language, and based on the AIC criterion, we selected the model with the lowest entropy value. We chose six radiomic features from the extracted features, which primarily represented the tumor's texture complexity and were highly correlated with tumor heterogeneity and prognosis [47].

These extracted radiomic features, along with the B7-H3 mRNA expression and LN status from CT reports, were considered as three independent predictive factors. Subsequently, we constructed a combined prediction model using these independent risk factors. Through ROC curve analysis, our constructed combined prediction model demonstrated the highest diagnostic value in predicting LNM (AUC = 0.765; 95%CI: 0.598-0.931; sensitivity: 80.0%; specificity: 70.6%).

We applied DCA to evaluate whether the nomogram of the combined model would improve patient outcomes and thus demonstrate the clinical utility of the nomogram. DCA curves provide insights into clinical consequences based on threshold probabilities and can yield net benefits (defined as the proportion of true positives minus the proportion of false positives)[48]. Analysis of the DCA curves revealed that the combined model had higher net benefits at most threshold probabilities, suggesting that the model could be an effective approach to guide clinical decision-making and provide an accurate and reliable CDSS.

For ease of clinical application, based on the three independent risk factors from the aforementioned study, we constructed a clinical radiomic nomogram combining radiomic features, B7-H3 mRNA expression, and LN status from CT reports. This nomogram scoring system can generate the preoperative probability of LNM, enabling individualized preoperative prediction of LNM risk. Both physicians and patients can utilize the nomogram to make personalized preoperative predictions of LNM risk, aligning with the current trend of personalized medicine[49].

Certainly, this study has some limitations. Firstly, the MRI image acquisition did not include the diffusion weighted imaging (DWI) sequence, which could enrich the extracted radiomic feature library and potentially reveal more valuable radiomic features. Although DWI has demonstrated strong capabilities in distinguishing benign and malignant LN in certain cancers, the respiratory motion specific to the chest can introduce significant artifacts and affect image quality in 3.0T DWI[50]. Secondly, our study only used quantitative RT-PCR to demonstrate the mRNA expression level of B7-H3 and did not further investigate corresponding genomic features to analyze the differences between genomic and radiomic features[51]. Thirdly, although the predictive model designed in this study showed good accuracy, our sample size was relatively small, and a larger sample size would improve the confidence and performance of the LNM prediction model in EC. Fourthly, we analyzed the ROIs mainly focusing on the primary tumor and did not obtain information from the surrounding tumor-free regions, which may also contain important information. Further research is needed to address these issues.

In conclusion, a correlation was observed between B7-H3 mRNA expression levels and LNM in EC patients based on preoperative gastric endoscopic specimens. Moreover, a clinical radiomic nomogram incorporating radiomic features, B7-H3 mRNA expression levels, and LN status from CT reports was developed, enabling convenient identification of EC patients with LNM. This nomogram facilitates individualized preoperative prediction of LNM in EC patients, thereby providing guidance for the formulation of clinical treatment decisions and facilitating the selection of more rational and effective therapeutic strategies to prevent adverse patient outcomes.

CONCLUSION

This study developed a radiomics nomogram that includes radiomics features, LN status from CT reports, and B7-H3 mRNA expression, enabling convenient preoperative individualized prediction of LNM in EC patients.

ARTICLE HIGHLIGHTS

Research background

Currently, the main treatment method for esophageal cancer is surgical intervention. However, for patients with lymph node metastasis (LNM), further adjuvant chemotherapy and radiotherapy are required to support the surgical treatment. Therefore, preoperative assessment of lymph node (LN) status in esophageal cancer is of paramount importance. Currently, the preoperative diagnosis of LN status in esophageal cancer mainly relies on imaging examinations such as chest computed tomography (CT), which is limited in its diagnostic value and lacks diversity in methodology. To enhance the accurate diagnosis of preoperative LN status in esophageal cancer patients, we intend to design a clinical radiomics nomogram specifically for the diagnosis of LNM in esophageal cancer patients.

Research motivation

By developing a clinical radiomics nomogram, the preoperative LN diagnostic rate in esophageal cancer patients can be improved. This will enable a clear determination of LNM, thereby providing valuable guidance for the formulation of clinical treatment decisions. This approach aligns with the current trend in healthcare, which emphasizes the development of personalized medical treatment plans.

Research objectives

The clinical radiomics nomogram we have designed encompasses imaging radiomic features from chest magnetic resonance imaging (MRI), clinical characteristics of the patients, and the expression level of B7-H3 mRNA obtained through gastric endoscopy. All the indicators in the nomogram can be easily obtained in a clinical setting. In our study, we found that this nomogram significantly improves the diagnostic value of preoperative LN status in esophageal cancer patients compared to traditional imaging examination methods. If applied in a clinical setting in the future, it has the potential to provide valuable guidance for the formulation of clinical treatment decisions.

Research methods

In our study, we obtained esophageal cancer tissue during gastric endoscopy and used real-time quantitative polymerase chain reaction to amplify and analyze the expression level of B7-H3 mRNA. All patients underwent chest MRI examinations, and Python software packages were used to extract imaging radiomic features. Subsequently, in R language, B7-H3 mRNA, MRI radiomic features, and clinical characteristics of the patients were selected and used to construct the clinical radiomics nomogram. We further analyzed the clinical value of the nomogram using receiver operating characteristic (ROC) and decision curve analysis (DCA) curves. The results showed that the nomogram had a higher diagnostic value for preoperative LN assessment compared to traditional imaging diagnostic methods.

Research results

By quantitatively analyzing the expression of B7-H3 mRNA in 32 esophageal cancer tissues, with clinical pathological examination results as the gold standard, we plotted the ROC curve to evaluate the diagnostic value of B7-H3 for LNM in esophageal cancer. The area under the ROC curve (AUC) for B7-H3 in detecting LNM in esophageal cancer was 0.718, with a sensitivity of 73.3% and specificity of 70.6%. The optimal diagnostic threshold for B7-H3 in detecting LNM in esophageal cancer was determined to be 2.56. Using the pathological examination results as the gold standard, we calculated the LN status from CT reports, B7-H3 mRNA expression, MRI radiomic features, and a combined predictive model. Furthermore, we used ROC curves to display the diagnostic performance of CT reports, B7-H3 mRNA expression, MRI radiomic features, and the created combined predictive model for preoperative LN status. Through comparison, we found that the combined predictive model showed the best discriminative ability and predictive stability, with the highest AUC value. Based on the DCA of the combined predictive model, compared to DCA using a single radiomic feature, the addition of B7-H3 mRNA expression and clinical CT results in the combined predictive model demonstrated higher accuracy in predicting preoperative LN status. This suggests that the DCA based on this predictive model is a reliable clinical tool for predicting preoperative LN status in esophageal cancer patients. DCA indicates that the decision curve based on the combined model adds more net benefit to the "treatment" strategy when the threshold probability for patients is within the range of approximately 0.3 to 0.7.

Research conclusions

Our study has developed a clinical radiomics nomogram based on multimodal MRI, B7-H3 mRNA expression, and clinical characteristics of patients, which can be applied for preoperative LN status diagnosis in esophageal cancer patients. Compared to conventional imaging examinations, this clinical radiomics nomogram improves the accuracy of preoperative LN status diagnosis. This innovation addresses the challenge of accurately determining LN status before surgery and further facilitates optimal decision-making for the diagnosis and treatment of esophageal cancer patients. The ROC and DCA curves based on this nomogram demonstrate its significant research value in the diagnostic performance of esophageal cancer.

Research perspectives

Although the nomogram demonstrates promising diagnostic value and clinical applicability, it is important to acknowledge that the sample size in this study is relatively small. Furthermore, there was a lack of further validation cohorts to validate the nomogram. In the future, a multi-center collaborative study should be conducted to increase the sample size and design validation cohorts to confirm the effectiveness of the nomogram. Additionally, with the rapid development of genomics, integrating genomic data with radiomics may further enhance the clinical decision-making value of the designed nomogram.

FOOTNOTES

Author contributions: Xu YH performed the majority of the writing, prepared the figures and tables; Xu YH, Lu P and Gao MC performed data accusation and writing; Wang R, Li YY, Guo RQ, and Zhang WS helped proofread the abbreviations and terminology in the manuscript; Song JX provided the input in writing the paper; Xu YH and Lu P designed the outline and coordinated the writing of the paper.

Supported by The Yancheng Key Research and Development Program (Social Development), No. YCBE202324.

Institutional review board statement: The study was reviewed and approved by the Ethics Committee of Yancheng Third People's Hospital Institutional Review Board, Approval No. 2022-10.

Informed consent statement: Considering that the relevant examinations in this study do not pose significant physical or harm to the patients' interests, the requirement for obtaining informed consent from the patients has been waived by the committee.

Conflict-of-interest statement: All the authors report no relevant conflicts of interest for this article.

Data sharing statement: Technical appendix, statistical code, and dataset available from the corresponding author at jxsongycsy@163.com.

Country/Territory of origin: China

ORCID number: Yan-Han Xu 0000-0001-6230-4729; Jian-Xiang Song 0000-0003-4503-6464.

S-Editor: Li L
L-Editor: A

P-Editor: Zheng XM

REFERENCES

1 **Bray F**, Ferlay J, Soerjomataram I, Siegel RL, Torre LA, Jemal A. Global cancer statistics 2018: GLOBOCAN estimates of incidence and mortality worldwide for 36 cancers in 185 countries. *CA Cancer J Clin* 2018; **68**: 394-424 [PMID: 30207593 DOI: 10.3322/caac.21492]

2 **Chen W**, Zheng R, Baade PD, Zhang S, Zeng H, Bray F, Jemal A, Yu XQ, He J. Cancer statistics in China, 2015. *CA Cancer J Clin* 2016; **66**: 115-132 [PMID: 26808342 DOI: 10.3322/caac.21338]

3 **Smyth EC**, Lagergren J, Fitzgerald RC, Lordick F, Shah MA, Lagergren P, Cunningham D. Oesophageal cancer. *Nat Rev Dis Primers* 2017; **3**: 17048 [PMID: 28748917 DOI: 10.1038/nrdp.2017.48]

4 **Cooper JS**, Guo MD, Herskovic A, Macdonald JS, Martenson JA Jr, Al-Sarraf M, Byhardt R, Russell AH, Beitler JJ, Spencer S, Asbell SO, Graham MV, Leichman LL. Chemoradiotherapy of locally advanced esophageal cancer: long-term follow-up of a prospective randomized trial (RTOG 85-01). Radiation Therapy Oncology Group. *JAMA* 1999; **281**: 1623-1627 [PMID: 10235156 DOI: 10.1001/jama.281.17.1623]

5 **Visser E**, van Rossum PSN, Ruurda JP, van Hillegersberg R. Impact of Lymph Node Yield on Overall Survival in Patients Treated With Neoadjuvant Chemoradiotherapy Followed by Esophagectomy for Cancer: A Population-based Cohort Study in the Netherlands. *Ann Surg* 2017; **266**: 863-869 [PMID: 28742691 DOI: 10.1097/SLA.0000000000002389]

6 **Zhang HL**, Chen LQ, Liu RL, Shi YT, He M, Meng XL, Bai SX, Ping YM. The number of lymph node metastases influences survival and International Union Against Cancer tumor-node-metastasis classification for esophageal squamous cell carcinoma. *Dis Esophagus* 2010; **23**: 53-58 [PMID: 19392846 DOI: 10.1111/j.1442-2050.2009.00971.x]

7 **Rice TW**, Ishwaran H, Hofstetter WL, Schipper PH, Kesler KA, Law S, Lerut EM, Denlinger CE, Salo JA, Scott WJ, Watson TJ, Allen MS, Chen LQ, Rusch VW, Cerfolio RJ, Luketich JD, Duranceau A, Darling GE, Pera M, Apperson-Hansen C, Blackstone EH. Esophageal Cancer: Associations With (pN+) Lymph Node Metastases. *Ann Surg* 2017; **265**: 122-129 [PMID: 28009736 DOI: 10.1097/SLA.0000000000001594]

8 **Rice TW**, Lerut TE, Orringer MB, Chen LQ, Hofstetter WL, Smithers BM, Rusch VW, van Lanschot J, Chen KN, Davies AR, D'Journo XB, Kesler KA, Luketich JD, Ferguson MK, Räsänen JV, van Hillegersberg R, Fang W, Durand L, Allum WH, Cecconello I, Cerfolio RJ, Pera M, Griffin SM, Burger R, Liu JF, Allen MS, Law S, Watson TJ, Darling GE, Scott WJ, Duranceau A, Denlinger CE, Schipper PH, Ishwaran H, Apperson-Hansen C, DiPaola LM, Semple ME, Blackstone EH. Worldwide Esophageal Cancer Collaboration: neoadjuvant pathologic staging data. *Dis Esophagus* 2016; **29**: 715-723 [PMID: 27731548 DOI: 10.1111/dote.12513]

9 **Kontos F**, Michelakos T, Kurokawa T, Sadagopan A, Schwab JH, Ferrone CR, Ferrone S. B7-H3: An Attractive Target for Antibody-based Immunotherapy. *Clin Cancer Res* 2021; **27**: 1227-1235 [PMID: 33051306 DOI: 10.1158/1078-0432.CCR-20-2584]

10 **Wu CP**, Jiang JT, Tan M, Zhu YB, Ji M, Xu KF, Zhao JM, Zhang GB, Zhang XG. Relationship between co-stimulatory molecule B7-H3 expression and gastric carcinoma histology and prognosis. *World J Gastroenterol* 2006; **12**: 457-459 [PMID: 16489649 DOI: 10.3748/wjg.v12.i3.457]

11 **Loos M**, Hedderich DM, Ottenhausen M, Giese NA, Laschinger M, Esposito I, Kleeff J, Friess H. Expression of the costimulatory molecule B7-H3 is associated with prolonged survival in human pancreatic cancer. *BMC Cancer* 2009; **9**: 463 [PMID: 20035626 DOI: 10.1186/1471-2407-9-463]

12 **Bostanci O**, Sayin P, Kiziltan R, Algul S, Aydin MA, Kemik O. B7-H3: A Useful Emerging Diagnostic Marker for Colon Cancer. *Biomed Res Int* 2022; **2022**: 1523338 [PMID: 36605103 DOI: 10.1155/2022/1523338]

13 **Jin Y**, Zhang P, Li J, Zhao J, Liu C, Yang F, Yang D, Gao A, Lin W, Ma X, Sun Y. B7-H3 in combination with regulatory T cell is associated with tumor progression in primary human non-small cell lung cancer. *Int J Clin Exp Pathol* 2015; **8**: 13987-13995 [PMID: 26823710]

14 **Guery T**, Roumier C, Berthon C, Renneville A, Preudhomme C, Quesnel B. B7-H3 protein expression in acute myeloid leukemia. *Cancer Med* 2015; **4**: 1879-1883 [PMID: 26376842 DOI: 10.1002/cam4.522]

15 **Zhang T**, Jin Y, Jiang X, Li L, Qi X, Mao Y, Hua D. Clinical and Prognostic Relevance of B7-H3 and Indicators of Glucose Metabolism in Colorectal Cancer. *Front Oncol* 2020; **10**: 546110 [PMID: 33042836 DOI: 10.3389/fonc.2020.546110]

16 **Arigami T**, Narita N, Mizuno R, Nguyen L, Ye X, Chung A, Giuliano AE, Hoon DS. B7-h3 Ligand expression by primary breast cancer and associated with regional nodal metastasis. *Ann Surg* 2010; **252**: 1044-1051 [PMID: 21107115 DOI: 10.1097/SLA.0b013e3181f1939d]

17 **Chen L**, Chen J, Xu B, Wang Q, Zhou W, Zhang G, Sun J, Shi L, Pei H, Wu C, Jiang J. B7-H3 expression associates with tumor invasion and patient's poor survival in human esophageal cancer. *Am J Transl Res* 2015; **7**: 2646-2660 [PMID: 26885263]

18 **Choi J**, Kim SG, Kim JS, Jung HC, Song IS. Comparison of endoscopic ultrasonography (EUS), positron emission tomography (PET), and computed tomography (CT) in the preoperative locoregional staging of resectable esophageal cancer. *Surg Endosc* 2010; **24**: 1380-1386 [PMID: 20033712 DOI: 10.1007/s00464-009-0783-x]

19 **D'Journo XB**. Clinical implication of the innovations of the 8(th) edition of the TNM classification for esophageal and esophago-gastric cancer. *J Thorac Dis* 2018; **10**: S2671-S2681 [PMID: 30345104 DOI: 10.21037/jtd.2018.03.182]

20 **Foley K**, Findlay J, Goh V. Novel imaging techniques in staging oesophageal cancer. *Best Pract Res Clin Gastroenterol* 2018; **36-37**: 17-25 [PMID: 30551852 DOI: 10.1016/j.bpg.2018.11.009]

21 **Dappa E**, Elger T, Hasenburg A, Düber C, Battista MJ, Hötker AM. The value of advanced MRI techniques in the assessment of cervical cancer: a review. *Insights Imaging* 2017; **8**: 471-481 [PMID: 28828723 DOI: 10.1007/s13244-017-0567-0]

22 **Xu XQ**, Hu H, Su GY, Liu H, Hong XN, Shi HB, Wu FY. Utility of histogram analysis of ADC maps for differentiating orbital tumors. *Diagn Interv Radiol* 2016; **22**: 161-167 [PMID: 26829400 DOI: 10.5152/dir.2015.15202]

23 **Qu J**, Zhang H, Wang Z, Zhang F, Liu H, Ding Z, Li Y, Ma J, Zhang Z, Zhang S, Dong Y, Jiang L, Zhang W, Grimm R, Kiefer B, Kamel IR, Qin J, Li H. Comparison between free-breathing radial VIBE on 3-T MRI and endoscopic ultrasound for preoperative T staging of resectable oesophageal cancer, with histopathological correlation. *Eur Radiol* 2018; **28**: 780-787 [PMID: 28799124 DOI: 10.1007/s00330-017-4963-0]

24 **Xu YH**, Lu P, Gao MC, Wang R, Li YY, Song JX. Progress of magnetic resonance imaging radiomics in preoperative lymph node diagnosis of esophageal cancer. *World J Radiol* 2023; **15**: 216-225 [PMID: 37545645 DOI: 10.4329/wjr.v15.i7.216]

25 **Xie C**, Hu Y, Han L, Fu J, Vardhanabhuti V, Yang H. Prediction of Individual Lymph Node Metastatic Status in Esophageal Squamous Cell Carcinoma Using Routine Computed Tomography Imaging: Comparison of Size-Based Measurements and Radiomics-Based Models. *Ann Surg Oncol* 2022; **29**: 8117-8126 [PMID: 36018524 DOI: 10.1245/s10434-022-12207-7]

26 **Lambin P**, Rios-Velazquez E, Leijenaar R, Carvalho S, van Stiphout RG, Granton P, Zegers CM, Gillies R, Boellard R, Dekker A, Aerts HJ. Radiomics: extracting more information from medical images using advanced feature analysis. *Eur J Cancer* 2012; **48**: 441-446 [PMID: 22257792 DOI: 10.1016/j.ejca.2011.11.036]

27 **Lambin P**, Leijenaar RTH, Deist TM, Peerlings J, de Jong EEC, van Timmeren J, Sanduleanu S, Larue RTHM, Even AJG, Jochems A, van Wijk Y, Woodruff H, van Soest J, Lustberg T, Roelofs E, van Elmpt W, Dekker A, Mottaghy FM, Wildberger JE, Walsh S. Radiomics: the bridge between medical imaging and personalized medicine. *Nat Rev Clin Oncol* 2017; **14**: 749-762 [PMID: 28975929 DOI: 10.1038/nrclinonc.2017.141]

28 **Liu C**, Ding J, Spuhler K, Gao Y, Serrano Sosa M, Moriarty M, Hussain S, He X, Liang C, Huang C. Preoperative prediction of sentinel lymph node metastasis in breast cancer by radiomic signatures from dynamic contrast-enhanced MRI. *J Magn Reson Imaging* 2019; **49**: 131-140 [PMID: 30171822 DOI: 10.1002/jmri.26224]

29 **Huang YQ**, Liang CH, He L, Tian J, Liang CS, Chen X, Ma ZL, Liu ZY. Development and Validation of a Radiomics Nomogram for Preoperative Prediction of Lymph Node Metastasis in Colorectal Cancer. *J Clin Oncol* 2016; **34**: 2157-2164 [PMID: 27138577 DOI: 10.1200/JCO.2015.65.9128]

30 **Coroller TP**, Agrawal V, Huynh E, Narayan V, Lee SW, Mak RH, Aerts HJWL. Radiomic-Based Pathological Response Prediction from Primary Tumors and Lymph Nodes in NSCLC. *J Thorac Oncol* 2017; **12**: 467-476 [PMID: 27903462 DOI: 10.1016/j.jtho.2016.11.2226]

31 **Gabriel E**, Attwood K, Du W, Tuttle R, Alnaji RM, Nurkin S, Malhotra U, Hochwald SN, Kukar M. Association Between Clinically Staged Node-Negative Esophageal Adenocarcinoma and Overall Survival Benefit From Neoadjuvant Chemoradiation. *JAMA Surg* 2016; **151**: 234-245 [PMID: 26559488 DOI: 10.1001/jamasurg.2015.4068]

32 **Sugawara K**, Yamashita H, Uemura Y, Mitsui T, Yagi K, Nishida M, Aikou S, Mori K, Nomura S, Seto Y. Numeric pathologic lymph node classification shows prognostic superiority to topographic pN classification in esophageal squamous cell carcinoma. *Surgery* 2017; **162**: 846-856 [PMID: 28739092 DOI: 10.1016/j.surg.2017.06.013]

33 **Campbell NP**, Villaflor VM. Neoadjuvant treatment of esophageal cancer. *World J Gastroenterol* 2010; **16**: 3793-3803 [PMID: 20698042 DOI: 10.3748/wjg.v16.i30.3793]

34 **Mayerhoefer ME**, Materka A, Langs G, Häggström I, Szczypiński P, Gibbs P, Cook G. Introduction to Radiomics. *J Nucl Med* 2020; **61**: 488-495 [PMID: 32060219 DOI: 10.2967/jnumed.118.222893]

35 **Bera K**, Braman N, Gupta A, Velcheti V, Madabhushi A. Predicting cancer outcomes with radiomics and artificial intelligence in radiology. *Nat Rev Clin Oncol* 2022; **19**: 132-146 [PMID: 34663898 DOI: 10.1038/s41571-021-00560-7]

36 **Conti A**, Duggento A, Indovina I, Guerrisi M, Toschi N. Radiomics in breast cancer classification and prediction. *Semin Cancer Biol* 2021; **72**: 238-250 [PMID: 32371013 DOI: 10.1016/j.semcancer.2020.04.002]

37 **Han L**, Zhu Y, Liu Z, Yu T, He C, Jiang W, Kan Y, Dong D, Tian J, Luo Y. Radiomic nomogram for prediction of axillary lymph node metastasis in breast cancer. *Eur Radiol* 2019; **29**: 3820-3829 [PMID: 30701328 DOI: 10.1007/s00330-018-5981-2]

38 **Liu J**, Sun D, Chen L, Fang Z, Song W, Guo D, Ni T, Liu C, Feng L, Xia Y, Zhang X, Li C. Radiomics Analysis of Dynamic Contrast-Enhanced Magnetic Resonance Imaging for the Prediction of Sentinel Lymph Node Metastasis in Breast Cancer. *Front Oncol* 2019; **9**: 980 [PMID: 31632912 DOI: 10.3389/fonc.2019.00980]

39 **Qiu Q**, Duan J, Deng H, Han Z, Gu J, Yue NJ, Yin Y. Development and Validation of a Radiomics Nomogram Model for Predicting Postoperative Recurrence in Patients With Esophageal Squamous Cell Cancer Who Achieved pCR After Neoadjuvant Chemoradiotherapy Followed by Surgery. *Front Oncol* 2020; **10**: 1398 [PMID: 32850451 DOI: 10.3389/fonc.2020.01398]

40 **Yu Y**, Tan Y, Xie C, Hu Q, Ouyang J, Chen Y, Gu Y, Li A, Lu N, He Z, Yang Y, Chen K, Ma J, Li C, Ma M, Li X, Zhang R, Zhong H, Ou Q, Zhang Y, He Y, Li G, Wu Z, Su F, Song E, Yao H. Development and Validation of a Preoperative Magnetic Resonance Imaging Radiomics-Based Signature to Predict Axillary Lymph Node Metastasis and Disease-Free Survival in Patients With Early-Stage Breast Cancer. *JAMA Netw Open* 2020; **3**: e2028086 [PMID: 33289845 DOI: 10.1001/jamanetworkopen.2020.28086]

41 **Qu J**, Shen C, Qin J, Wang Z, Liu Z, Guo J, Zhang H, Gao P, Bei T, Wang Y, Liu H, Kamel IR, Tian J, Li H. The MR radiomic signature can predict preoperative lymph node metastasis in patients with esophageal cancer. *Eur Radiol* 2019; **29**: 906-914 [PMID: 30039220 DOI: 10.1007/s00330-018-5583-z]

42 **Shen C**, Liu Z, Wang Z, Guo J, Zhang H, Wang Y, Qin J, Li H, Fang M, Tang Z, Li Y, Qu J, Tian J. Building CT Radiomics Based Nomogram for Preoperative Esophageal Cancer Patients Lymph Node Metastasis Prediction. *Transl Oncol* 2018; **11**: 815-824 [PMID: 29727831 DOI: 10.1016/j.tranon.2018.04.005]

43 **Toiyama Y**, Inoue Y, Shimura T, Fujikawa H, Saigusa S, Hiro J, Kobayashi M, Ohi M, Araki T, Tanaka K, Mohri Y, Kusunoki M. Serum Angiopoietin-like Protein 2 Improves Preoperative Detection of Lymph Node Metastasis in Colorectal Cancer. *Anticancer Res* 2015; **35**: 2849-2856 [PMID: 25964566]

44 **Birkhahn M**, Mitra AP, Cote RJ. Molecular markers for bladder cancer: the road to a multimarker approach. *Expert Rev Anticancer Ther* 2007; **7**: 1717-1727 [PMID: 18062746 DOI: 10.1586/14737140.7.12.1717]

45 **Yu SC**, Qi X, Hu YH, Zheng WJ, Wang QQ, Yao HY. [Overview of multivariate regression model analysis and application]. *Zhonghua Yu Fang Yi Xue Za Zhi* 2019; **53**: 334-336 [PMID: 30841679 DOI: 10.3760/cma.j.issn.0253-9624.2019.03.020]

46 **Collins GS**, Reitsma JB, Altman DG, Moons KG. Transparent reporting of a multivariable prediction model for individual prognosis or diagnosis (TRIPOD): the TRIPOD statement. *BMJ* 2015; **350**: g7594 [PMID: 25569120 DOI: 10.1136/bmj.g7594]

47 **Yip C**, Davnall F, Kozarski R, Landau DB, Cook GJ, Ross P, Mason R, Goh V. Assessment of changes in tumor heterogeneity following neoadjuvant chemotherapy in primary esophageal cancer. *Dis Esophagus* 2015; **28**: 172-179 [PMID: 24460831 DOI: 10.1111/dote.12170]

48 **Van Calster B**, Wynants L, Verbeek JFM, Verbakel JY, Christodoulou E, Vickers AJ, Roobol MJ, Steyerberg EW. Reporting and Interpreting Decision Curve Analysis: A Guide for Investigators. *Eur Urol* 2018; **74**: 796-804 [PMID: 30241973 DOI: 10.1016/j.eururo.2018.08.038]

49 **Balachandran VP**, Gonen M, Smith JJ, DeMatteo RP. Nomograms in oncology: more than meets the eye. *Lancet Oncol* 2015; **16**: e173-e180 [PMID: 25846097 DOI: 10.1016/S1470-2045(14)71116-7]

50 **Holzapfel K**, Gaa J, Schubert EC, Eiber M, Kleeff J, Rummeny EJ, Loos M. Value of diffusion-weighted MR imaging in the diagnosis of lymph node metastases in patients with cholangiocarcinoma. *Abdom Radiol (NY)* 2016; **41**: 1937-1941 [PMID: 27271285 DOI: 10.1007/s00261-016-0791-y]

51 **Nakarai C**, Osawa K, Akiyama M, Matsubara N, Ikeuchi H, Yamano T, Hirota S, Tomita N, Usami M, Kido Y. Expression of AKR1C3 and CNN3 as markers for detection of lymph node metastases in colorectal cancer. *Clin Exp Med* 2015; **15**: 333-341 [PMID: 24934327 DOI: 10.1007/s10238-014-0298-1]

World Journal of Clinical Oncology

Submit a Manuscript: https://www.f6publishing.com

World J Clin Oncol 2024 March 24; 15(3): 434-446

DOI: 10.5306/wjco.v15.i3.434

ISSN 2218-4333 (online)

ORIGINAL ARTICLE

Clinical and Translational Research

Establishment of a prognosis predictive model for liver cancer based on expression of genes involved in the ubiquitin-proteasome pathway

Hua Li, Yi-Po Ma, Hai-Long Wang, Cai-Juan Tian, Yi-Xian Guo, Hong-Bo Zhang, Xiao-Min Liu, Peng-Fei Liu

Specialty type: Oncology

Provenance and peer review: Unsolicited article; Externally peer reviewed.

Peer-review model: Single blind

Peer-review report's scientific quality classification

Grade A (Excellent): 0
Grade B (Very good): 0
Grade C (Good): 0
Grade D (Fair): D
Grade E (Poor): 0

P-Reviewer: Rodriguez JC, Spain

Received: October 11, 2023
Peer-review started: October 11, 2023
First decision: December 7, 2023
Revised: December 27, 2023
Accepted: February 5, 2024
Article in press: February 5, 2024
Published online: March 24, 2024

Hua Li, Department of Endoscopy, Tianjin Medical University Cancer Institute and Hospital, National Clinical Research Center for Cancer, Key Laboratory of Cancer Prevention and Therapy of Tianjin, Tianjin's Clinical Research Center for Cancer, Tianjin 300060, China

Yi-Po Ma, Department of Critical Care Medicine, Dingzhou City People's Hospital, Dingzhou 073000, Hebei Province, China

Hai-Long Wang, Peng-Fei Liu, Department of Oncology, Tianjin Academy of Traditional Chinese Medicine Affiliated Hospital, Tianjin 300120, China

Cai-Juan Tian, Hong-Bo Zhang, Tianjin Marvel Medical Laboratory, Tianjin Marvelbio Technology Co., Ltd, Tianjin 300180, China

Yi-Xian Guo, Department of Intelligent Technology, Tianjin Yunquan Intelligent Technology Co., Ltd, Tianjin 300381, China

Xiao-Min Liu, Department of Oncology, Tianjin Huanhu Hospital, Tianjin 300350, China

Corresponding author: Peng-Fei Liu, MD, Chief Doctor, Surgical Oncologist, Department of Oncology, Tianjin Academy of Traditional Chinese Medicine Affiliated Hospital, No. 354 North Road, Hongqiao District, Tianjin 300120, China. liupengfeitj@163.com

Abstract

BACKGROUND

The ubiquitin-proteasome pathway (UPP) has been proven to play important roles in cancer.

AIM

To investigate the prognostic significance of genes involved in the UPP and develop a predictive model for liver cancer based on the expression of these genes.

METHODS

In this study, UPP-related E1, E2, E3, deubiquitylating enzyme, and proteasome gene sets were obtained from the Kyoto Encyclopedia of Genes and Genomes (KEGG) database, aiming to screen the prognostic genes using univariate and multivariate regression analysis and develop a prognosis predictive model based

on the Cancer Genome Atlas liver cancer cases.

RESULTS

Five genes (including autophagy related 10, proteasome 20S subunit alpha 8, proteasome 20S subunit beta 2, ubiquitin specific peptidase 17 like family member 2, and ubiquitin specific peptidase 8) were proven significantly correlated with prognosis and used to develop a prognosis predictive model for liver cancer. Among training, validation, and Gene Expression Omnibus sets, the overall survival differed significantly between the high-risk and low-risk groups. The expression of the five genes was significantly associated with immunocyte infiltration, tumor stage, and postoperative recurrence. A total of 111 differentially expressed genes (DEGs) were identified between the high-risk and low-risk groups and they were enriched in 20 and 5 gene ontology and KEGG pathways. Cell division cycle 20, Kelch repeat and BTB domain containing 11, and DDB1 and CUL4 associated factor 4 like 2 were the DEGs in the E3 gene set that correlated with survival.

CONCLUSION

We have constructed a prognosis predictive model in patients with liver cancer, which contains five genes that associate with immunocyte infiltration, tumor stage, and postoperative recurrence.

Key Words: Liver cancer; Ubiquitin-proteasome pathway; Prognosis prediction; Gene expression; Immune infiltration

Core Tip: This study unveils the crucial role of the ubiquitin-proteasome pathway (UPP) in liver cancer prognosis. Five key genes (autophagy related 10, proteasome 20S subunit alpha 8, proteasome 20S subunit beta 2, ubiquitin specific peptidase 17 like family member 2, and ubiquitin specific peptidase 8) identified from The Cancer Genome Atlas datasets constitute a robust prognostic model, accurately predicting liver cancer outcomes. Immunocyte infiltration analysis highlights associations of these genes with immune cell abundance, while clinical correlations link them to tumor stage and recurrence. Differential gene expression and pathway enrichment elucidate underlying biological processes. E3 analysis identifies specific ligases (cell division cycle 20, Kelch repeat and BTB domain containing 11, and DCAF4L2) with significant expression differences, further emphasizing the integral role of the UPP in liver cancer development and providing valuable insights for precision medicine and prognosis prediction.

Citation: Li H, Ma YP, Wang HL, Tian CJ, Guo YX, Zhang HB, Liu XM, Liu PF. Establishment of a prognosis predictive model for liver cancer based on expression of genes involved in the ubiquitin-proteasome pathway. *World J Clin Oncol* 2024; 15(3): 434-446
URL: https://www.wjgnet.com/2218-4333/full/v15/i3/434.htm
DOI: https://dx.doi.org/10.5306/wjco.v15.i3.434

INTRODUCTION

The prevalence of liver cancer has been increasing, with an annual growth rate of up to 2%-3%[1] and survival rate of 18% in 2020[2]. A total of 336400 new liver cancer cases were detected in China in 2016[3], and the sharply elevated incidence (18.0 per 100000) of liver cancer caused by sugar-sweetened food must be given extra attention[4].

Hepatitis B/C virus (HBV or HCV) infection, addiction to alcohol, liver cirrhosis, fatty hepatitis, and eating aflatoxin contaminated food are the risk factors for liver cancer[5]. Imaging examinations for liver cancer include ultrasonography, dynamic contrast-enhanced computed tomography (CT), multimodal magnetic resonance imaging, 18F-fluorodeoxyglucose positron emission tomography/CT, and so on. Virtual liver biopsy sampling pipeline for eliminating sampling bias may be the potential diagnostic method to investigate the nature of the lesions and etiology[6]. In recent years, using statistical models combined with machine learning techniques to elevate the diagnostic accuracy of serum biomarkers such as α-fetoprotein and cell-free DNA or RNA has been widely applied to the early diagnosis of hepatocellular carcinoma[7]. Additionally, surgical resection, transplantation, ablation, chemotherapy, and immunotherapy are common treatment options for liver cancer patients[8]. However, effective surveillance and prediction of the prognosis of liver cancer still face multiple challenges due to the high heterogeneity of this malignancy.

The ubiquitin-proteasome pathway (UPP) is one of the key pathways of protein selective degradation in organisms[9], which is related to cell cycle, proliferation, differentiation, apoptosis, transcription, signal transduction, immune response, stress response, and extracellular effectors[10]. The malfunction of the UPP is linked to various diseases, such as carcinogenesis, infection, autoimmunity, and inflammation. Based on The Cancer Genome Atlas (TCGA) datasets and 961 ubiquitin-proteasome system genes (UPSGs), Liu *et al*[11] found that *DDB1* and CUL4 associated factor 13 (*DCAF13*), cell division cycle 20 (*CDC20*), and proteasome 20S subunit beta 5 (*PSMB5*) have excellent performance to predict the survival of liver cancer patients. Zhang *et al*[12] identified a seven-UPSG prognostic signature, of which autophagy related 10 (*ATG10*) was found to participate in liver cancer development and prognosis through autophagy, immune response, and tumor metastasis. Therefore, proteasome inhibitors, as a class of potential and effective anti-tumor drugs, have attracted a

growing body of attention from researchers. In this study, we examined the correlation of the expression of genes involved in the UPP with the prognosis of liver cancer, to screen out some key genes and construct a prognosis predictive model, in order to provide a new horizon for the role and potential mechanism of the UPP in the development of liver cancer.

MATERIALS AND METHODS

Gene sets and data collection

The UPP-related gene set included 857 genes from the UPP-related Kyoto Encyclopedia of Genes and Genomes (KEGG) pathways[13], among which 10 was related to E1, 38 related to E2, 651 to E3, 112 to deubiquitylating enzyme (DUB), and 46 to the proteasome.

The expression data of 424 samples related to liver cancer were downloaded from The Cancer Genome Atlas (TCGA) database (https://portal.gdc.cancer.gov/). Three recurrent samples, 50 normal tissue samples, and one sample without overall survival (OS) data were deleted and the remaining 370 samples were randomly divided into a training group (n = 296) and a validation group (n = 74) in a ratio of 4:1. Another validation set (GSE54236) was downloaded from the Gene Expression Omnibus (GEO) database (http://www.ncbi.nlm.nih.gov/geo/). This data set included 162 samples, including 81 tumor samples.

Construction and validation of a prognosis predictive model

Univariate and multivariate regression analyses were performed to screen the prognostic genes in the E1, E2, DUB, and proteasome gene sets using the Survival (version 3.2-3) and Glmnet (version 4.0-2) packages in R. The threshold of univariate analysis was $P < 0.1$, and stepwise multivariate regression analysis was used to screen genes associated with OS. The risk score of the screened genes was calculated to construct a prognosis predictive model, and the prognostic ability was assessed using the receiver operating characteristic (ROC) curve drawn with Proc (version 1.16.2) package. According to the risk score, the patients were divided into either a high-risk or a low-risk group. The Maxstat (version 0.7-25) package in R was used to calculate the optimal cut-off value. The log-rank method was used to compare the difference in OS between the two groups, and the Survival (version 3.2-3) and Survminer (version 0.4.8) packages in R were used to draw the survival curve. In the validation group, the same method was used to verify the model.

Immunocyte infiltration

The abundance of 40 types of immune cells in each sample was analyzed using GVSA (version 1.32.0). The correlation analysis between the screened genes and immune-related indicators was performed using the Psych (version 2.0.8) and Corrplot (version 0.84) packages in R.

Analysis of correlation between clinical parameters and gene expression

The clinical parameters were compared between the high-risk and the low-risk groups using an independent sample t-test or two-sample Wilcoxon test, and Spearman correlation analysis was used to determine whether the gene expression and risk scores were statistically related to clinical parameters. The Psych (version 2.0.8) and Corrplot (version 0.84) packages in R were used for plotting. Univariate Cox regression analysis was used to determine the relationship between OS and clinical parameters, as well as the relationship between the gene expression and postoperative recurrence.

Identification of differentially expressed genes and enrichment analysis

The Limma package (version 3.40.2) was used to screen DEGs between the high-risk and low-risk groups, with the threshold set at $P < 0.05$ and $|\log2FC| > 1$. Then the functional enrichment analysis was carried out using the database for annotation, visualization, and integrated discovery (DAVID, https://david.ncifcrf.gov/) to identify the enriched gene ontology (GO) terms and KEGG pathways of the DEGs.

Core DEGs in E3 gene set

As a specific substrate recognition element, E3 plays an important role in the ubiquitin-mediated proteolytic cascade[14]. Because of its specificity, the relationship between the expression of genes in the E3 set and prognostic risk was analyzed separately. Similar to the screening method for DEGs, the Limma package was used to screen the DEGs in the E3 gene set between the high-risk and low-risk groups, and the screening threshold was $P < 0.05$ and $|\log2FC| > 1$.

Statistical analysis

IBM SPSS Statistics 21 and R (version 3.6.2) were used for statistical analyses. The Shapiro-Wilk test was used for normality test, and the independent sample t test or the two-sample Wilcoxon test were used to analyze the differences in variables between two groups. The chi-square test or Fisher's test was used for analysis of categorical variables. The log-rank method was used to test the significance of survival data.

Table 1 Clinical parameters of the whole samples, cases in training group, and those in validation group, *n* (%)

Parameter	Category	TCGA (*n* = 370)	Training group (*n* = 296)	Validation group (*n* = 74)
Age		59.441 ± 13.517	59.53 ± 13.71	59.081 ± 12.796
P value			0.799	
Gender	Female	121 (32.7)	101 (34.1)	20 (27)
	Male	249 (67.3)	195 (65.9)	54 (73)
P value			0.27	
Height		167.34 ± 10.7	167.32 ± 11.368	167.43 ± 7.622
P value			0.92	
Weight		72.85 ± 19.468	73.05 ± 20.571	72.07 ± 14.478
P value			0.646	
BMI		26.13 ± 8.453	26.25 ± 9.145	25.66 ± 4.909
P value			0.609	
Histological type	FLC	3 (0.8)	2 (0.7)	1 (1.4)
	HCC	360 (97.3)	287 (97)	73 (98.6)
	FLHCC	7 (1.9)	7 (2.4)	0 (0)
P value			0.35	
Stage	I/II	256 (69.2)	209 (69.6)	47 (63.5)
	III/IV	90 (24.4)	69 (23.3)	21 (28.4)
	Not available	24 (6.5)	18 (6.1)	6 (8.1)
P value			0.454	
Grade	G1/G2	232 (62.7)	180 (60.8)	52 (70.3)
	G3/G4	133 (35.9)	112 (37.9)	21 (28.4)
	Not available	5 (1.4)	4 (1.4)	1 (1.4)
P value			0.241	

P values refer to statistical results between training and validation groups. BMI: Body mass index; FLC: Fibrolamellar carcinoma; HCC: Hepatocellular carcinoma; FLHCC: Hepatocholangio carcinoma (mixed).

Table 2 The five genes significantly correlate with the prognosis of patients with liver cancer

Gene	Gene set	Coef	Hazard ratio	*Z*	*P* value
ATG10	Ubiquitin-conjugating enzyme (E2)	0.48387	1.62234	2.364	0.0181
PSMA8	Proteasome	0.20721	1.23024	1.962	0.0497
PSMB2	Proteasome	0.66763	1.94962	2.483	0.013
USP17L2	Deubiquitinating enzyme (DUB)	-2.8057	0.06046	-3.048	0.0023
USP8	Deubiquitinating enzyme (DUB)	-0.46594	0.62755	-1.701	0.0889

ATG10: Autophagy related 10; PSMA8: Proteasome 20S subunit alpha 8; PSMB2: Proteasome 20S subunit beta 2; USP17L2: Ubiquitin specific peptidase 17 like family member 2; USP8: Ubiquitin specific peptidase 8.

RESULTS

Construction of a prognosis-predicted model for liver cancer based on five genes

The clinical parameters of the whole samples, cases in the training group, and those in the validation group are listed in Table 1, with P value referring to the statistical results between the training group and the validation group. A total of five genes significantly related to prognosis were screened to construct a prognosis predictive model, including *ATG10*,

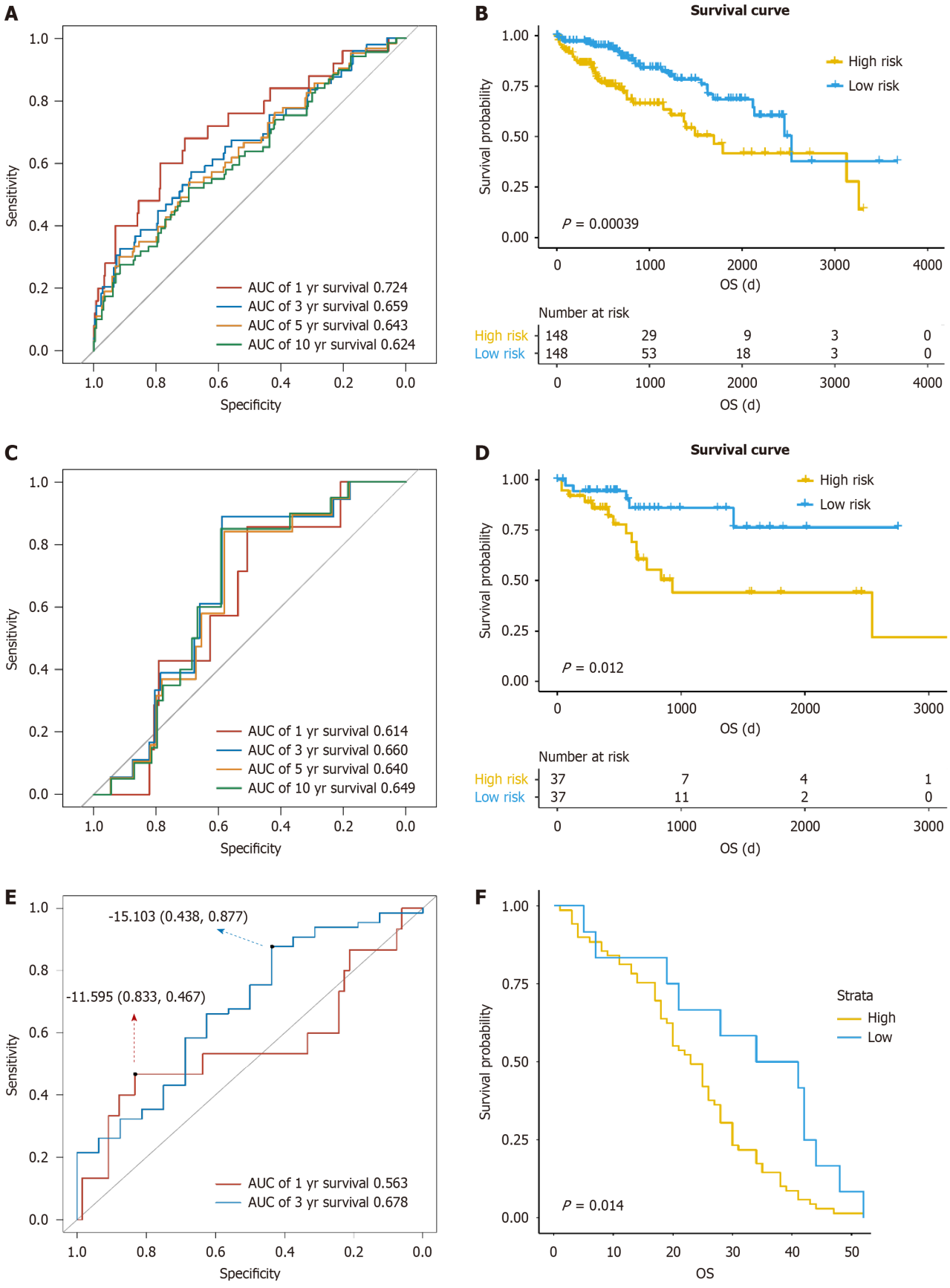

Figure 1 Prognosis predictive model for liver cancer. A: Receiver operating characteristic (ROC) curve of the model in training group; B: Survival curve of high- and low-risk patients with liver cancer in training group; C: ROC curve of the model in The Cancer Genome Atlas (TCGA) validation group; D: Survival curve of high- and low-risk patients with liver cancer in TCGA validation group; E: ROC curve of the model in gene expression comprehensive (GEO) validation group; F: Survival curve of high- and low-risk patients with liver cancer in GEO validation group. AUC: Area under the curve; OS: Overall survival.

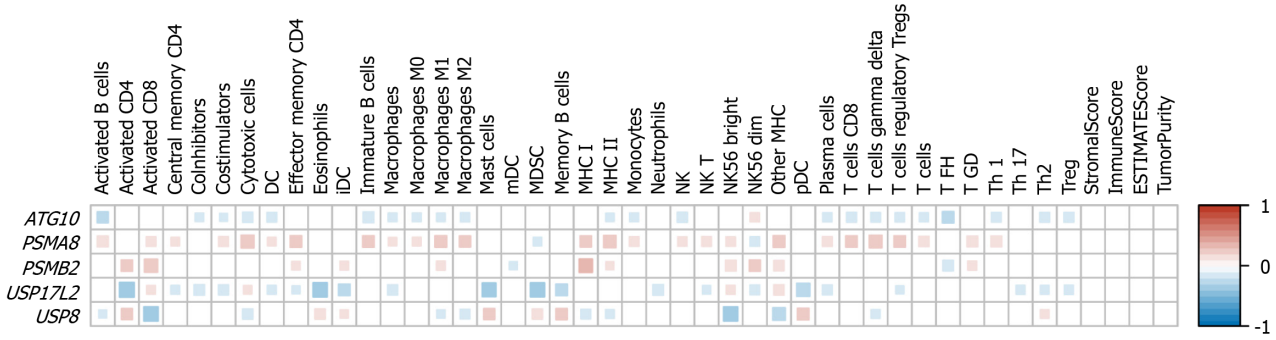

Figure 2 Immunocyte infiltration between cases with high and low expression levels of *ATG10*, *PSMA8*, *PSMB2*, *USP17L2*, and *USP8*.

proteasome 20S subunit alpha 8 (*PSMA8*), proteasome 20S subunit beta 2 (*PSMB2*), ubiquitin specific peptidase 17 like family member 2 (*USP17L2*), and ubiquitin specific peptidase 8 (*USP8*) (Table 2). In the training group, the area under the curve (AUC) values of the model for predicting 1-, 3-, 5-, and 10-year survival were 0.724, 0.659, 0.643, and 0.624, respectively (Figure 1A). All patients were classified into either a high-risk or low-risk group according to the score of risk. There was a significant difference in survival time between the high-risk and low-risk groups ($P < 0.001$, Figure 1B). In the validation group, the AUC values of the model for predicting 1-, 3-, 5-, and 10-year survival were 0.614, 0.66, 0.64, and 0.649, respectively, and the low-risk group exhibited a higher survival probability than the high-risk group ($P = 0.012$, Figure 1C and D), suggesting that the model can well predict the prognosis in liver cancer patients. In the GSE54236 data set, the AUC values of the model for predicting 1- and 3-year survival were 0.563 and 0.678, respectively, and the cases could be divided into a high-risk group and low-risk group by the risk score. There was a significantly difference in survival time between the high-risk group and low-risk group ($P = 0.014$, Figure 1E and F).

Significance of expression of the five genes in immunocyte infiltration

Through the above analysis, we found that the expression levels of the five genes can predict the prognosis of liver cancer. Because immunocyte infiltration is commonly affected by gene expression, we then studied the correlation of the expression levels of the five genes with the abundance of 40 types of immune cells. *PSMA8* was associated with the abundance of the most immune cells, and the abundance of 28 immune cell types was significantly correlated with *PSMA8* expression levels. This was followed by *USP17L2, ATG10, USP*8, and *PSMB2*, with 25, 23, 18, and 13 types of immune cells that were related to the expression levels of these genes, respectively (Figure 2). The abundance of most cells was negatively correlated with the expression levels of *ATG10, USP17L2*, and *USP8*, while *PSMA8* and *PSMB2* expression levels were positively correlated with the abundance of most cell types (Figure 2).

The five genes are associated with tumor stages and postoperative recurrence

PSMA8 and *PSMB2* expression and the risk score were significantly different between males and females (Figure 3A-C). For pathological and clinical stages, *ATG10* expression and the risk score were significantly different between T2 and T3 stages, *PSMB*2 and *USP17L2* expression was significantly different between T1 and T3 stages (Figure 3D-G), the risk score was statistically lower in N0 stage than in NX stage (Figure 3H), and the expression levels of *ATG10, PSMB2*, and *USP17L2* and the risk score were significantly different between stage I and stage II (Figure 3I-L). Moreover, *PSMA8, PSMB2, USP17L2*, and *USP8* expression was all correlated with the upper limit of albumin results, among which *PSMA8* and *USP17L2* were positively correlated, and *PSMB2* and *USP8* were negatively correlated with albumin results (Figure 3M). There was also a negative correlation between the risk score and the upper limit of albumin results, indicating that as the risk value increased, the albumin levels decreased, leading to an elevated prognosis risk for patients (Figure 3M).

Postoperative recurrence included extrahepatic recurrence, local recurrence, intrahepatic recurrence, and new primary tumor. After univariate Cox analysis, A*TG10, PSMA8*, and *USP8,* as well as the risk score, were found significantly correlated with postoperative recurrence ($P < 0.05$, Figure 3N).

DEGs between high- and low-risk groups and their enriched pathways

A total of 111 DEGs were screened out between the high-risk group and low-risk group, among which 27 were up-regulated and 84 down-regulated (Figure 4A). These DEGs were associated with 20 GO terms, comprising 9 biological processes, 6 cellular components, and 5 molecular functions (Figure 4B). Five KEGG pathways enriched were GABAergic synapse, morphine addiction, neuroactive ligand-receptor interaction, retrograde endocannabinoid signaling, and cell cycle (Figure 4C).

DEGs in the E3 gene set between the high- and low-risk groups

Between the high-risk and low-risk groups, significant differences were observed in three genes within the E3 gene set: *CDC20*, Kelch repeat and BTB domain containing 11 (*KBTBD11*), and DDB1 and CUL4 associated factor 4 like 2 (*DCAF4L2*). In the high-risk group, *CDC20* and *DCAF4L2* exhibited elevated expression levels, whereas *KBTBD11* showed higher expression in the low-risk group. This suggested a negative correlation between the expression of *CDC20* and

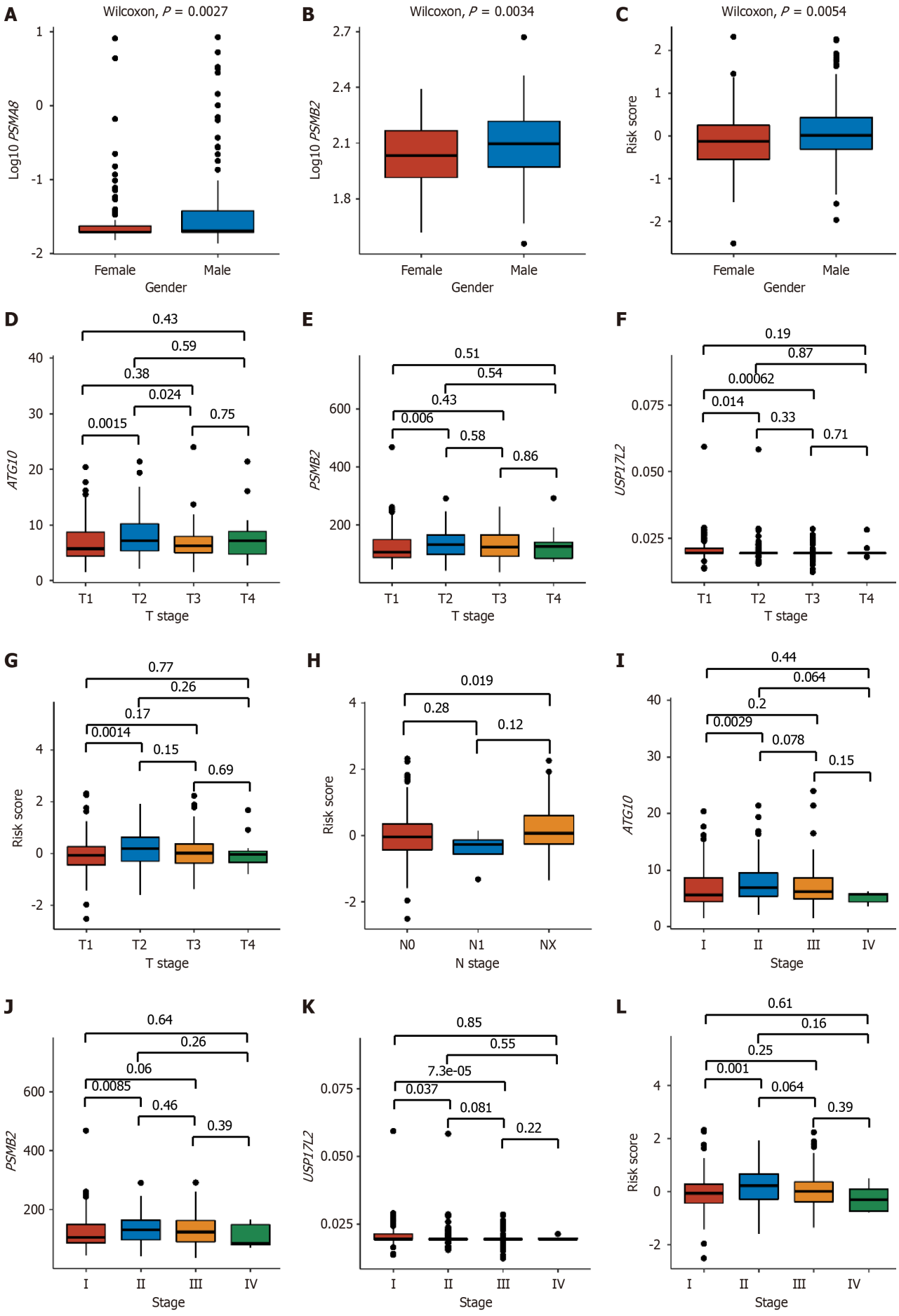
A
Wilcoxon, P = 0.0027
Log10 PSMA8
Female
Male
Gender
B
Wilcoxon, P = 0.0034
Log10 PSMB2
Female
Male
Gender
C
Wilcoxon, P = 0.0054
Risk score
Female
Male
Gender
D
ATG10
0.43
0.59
0.38
0.024
0.0015
0.75
T1
T2
T3
T4
T stage
E
PSMB2
0.51
0.54
0.43
0.006
0.58
0.86
T1
T2
T3
T4
T stage
F
USP17L2
0.19
0.87
0.00062
0.014
0.33
0.71
T1
T2
T3
T4
T stage
G
Risk score
0.77
0.26
0.17
0.0014
0.15
0.69
T1
T2
T3
T4
T stage
H
Risk score
0.019
0.28
0.12
N0
N1
NX
N stage
I
ATG10
0.44
0.064
0.2
0.0029
0.078
0.15
I
II
III
IV
Stage
J
PSMB2
0.64
0.26
0.06
0.0085
0.46
0.39
I
II
III
IV
Stage
K
USP17L2
0.85
0.55
7.3e-05
0.037
0.081
0.22
I
II
III
IV
Stage
L
Risk score
0.61
0.16
0.25
0.001
0.064
0.39
I
II
III
IV
Stage

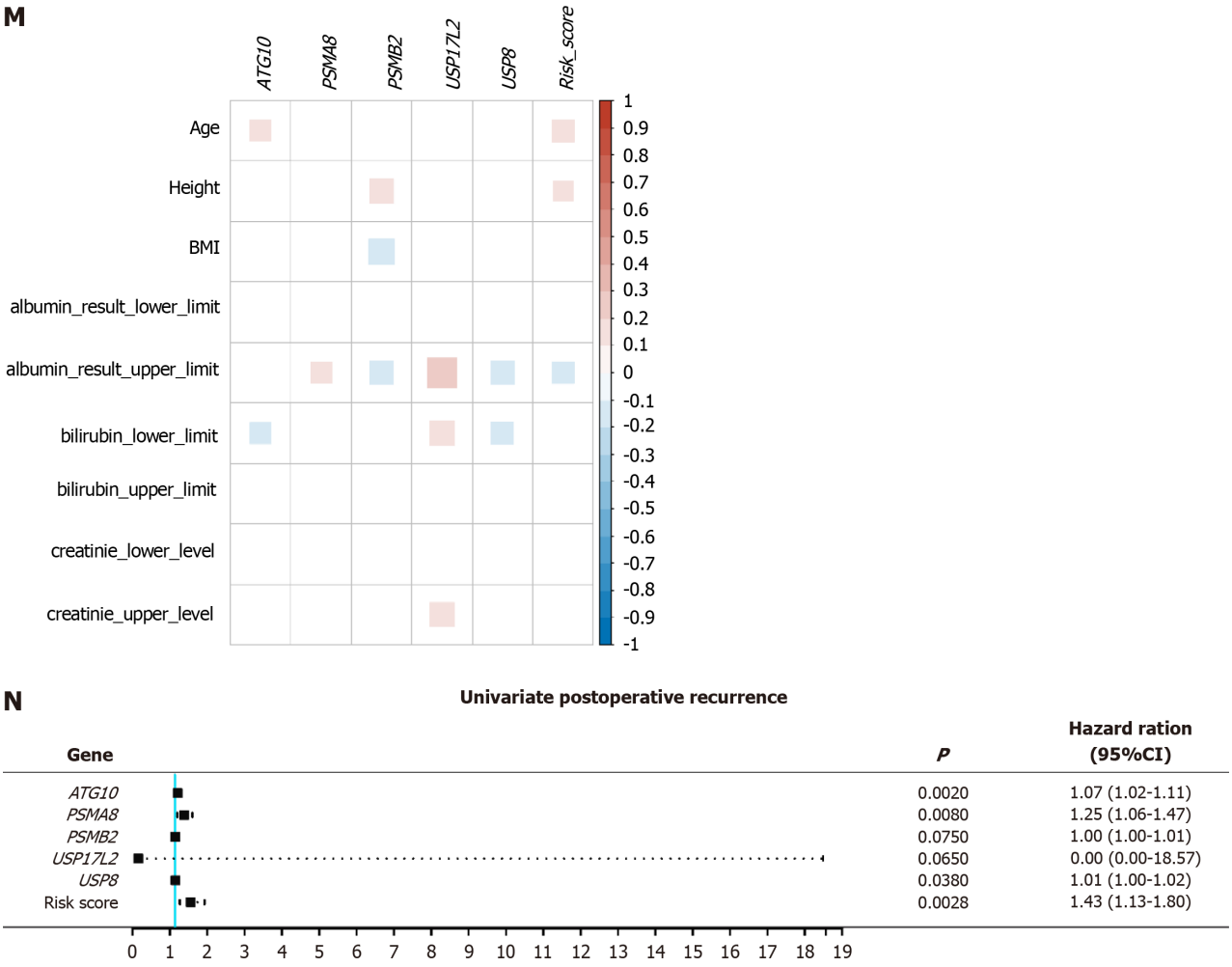

Figure 3 Correlation of expression levels of *ATG10*, *PSMA8*, *PSMB2*, *USP17L2*, and *USP8* and risk score with clinical parameters. A-C: Gene expression and risk score between genders; D-G: Gene expression and risk score among T stages; H: Risk score among N stages; I-L: Gene expression and risk score among clinical stages; M: Correlation of gene expression levels and risk score with biochemical indexes; N: Correlation of gene expression levels and risk score with postoperative recurrence in liver cancer, with a hazard ratio (HR) > 1 referring to a positive correlation and HR < 1 referring to a negative correlation. $P < 0.05$ indicated statistical significance. HR: Hazard ratio.

DCAF4L2 and survival, while *KBTBD11* displayed a positive correlation with the prognosis of liver cancer (Figure 5).

DISCUSSION

The key factor to cell survival lies in the balance of protein synthesis and decomposition. The UPP is an ATP-dependent non-lysosomal protein degradation pathway, which is important for the body to regulate the level and function of intracellular proteins, thus efficiently and selectively degrading intracellular proteins. This study showed that the expression of the UPP genes *ATG10, PSMA8, PSMB2, USP17L2*, and *USP8* was significantly correlated with the prognosis of liver cancer. The prognosis model constructed based on these five genes could accurately predict the prognosis of patients ($P < 0.001$ and $P = 0.012$ in training and validation groups, respectively, Figure 1). These genes were statistically correlated with different clinical parameters and immune cell abundance (Figures 2 and 3). The model categorized all patients into either a high-risk group or a low-risk group, and a total of 111 DEGs were screened between the two groups, which were enriched in GO terms related to protein binding, GABA-A receptor, synapse, *etc.*, and KEGG pathways of retrograde endocannabinoid signaling, neuroactive ligand-receptor interaction, morphine addiction, GABAergic synapse, and cell cycle (Figure 4).

Those five genes were found to promote the development of many malignant tumors, including liver cancer[15-22]. Our results showed that the increased expression of *ATG10*, *PSMA8*, and *PSMB2* increased the risk of death ($P = 0.018$, 0.049, and 0.013, respectively), while the increased expression of *USP17L2* and *USP8* decreased the risk of death ($P = 0.002$ and 0.089, respectively). According to previous studies, the overexpression of ATG10 and PSMB2 in tumors promoted the invasion or metastasis of tumor cells[16,18], and USP8 showed the opposite effect[21,22]. Besides, PSMA8 could affect the progression and prognosis of colorectal cancer due to its strong association with PSMB2[23]. Interestingly, higher PSMA8 expression levels were correlated with good prognoses for breast cancer through epigenetic regulation

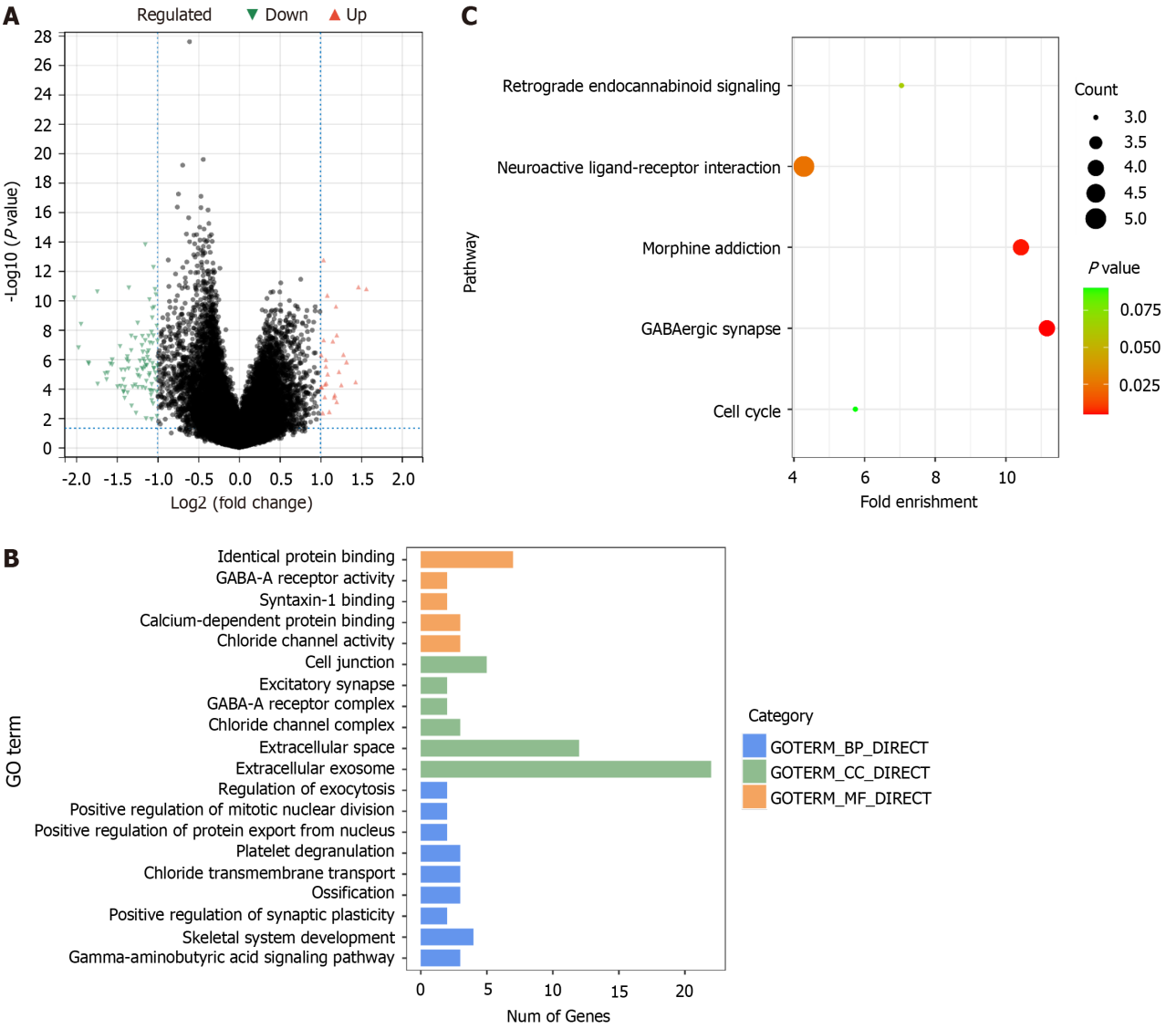

Figure 4 Enrichment analysis of differentially expressed genes between liver cancer and normal samples. A: Volcano plot of differentially expressed genes (DEGs); B: Gene ontology terms enriched by DEGs; C: Kyoto Encyclopedia of Genes and Genomes pathways enriched by DEGs. GO: Gene ontology; KEGG: Kyoto Encyclopedia of Genes and Genomes; DEGs: Differentially expressed genes.

[24]. In our study, it was found that *PSMA8* was positively correlated with the prognosis of patients with liver cancer. On the contrary, USP17L2 has been found to be overexpressed in a variety of tumors[19,20], which is similar to our results. However, recent studies have found that up-regulation of USP17L2 causes chemotherapy resistance in colorectal cancer, and knockdown of USP17L2 could overcome bromodomain and extra-terminal domain inhibitor resistance in prostate cancer cells[25,26]. Hence, the role of USP17L2 in liver cancer still requires further exploration.

The global immune system functions pose great technical challenges to the research of tumor-immune interaction[27, 28]. Because immune infiltration plays a key role in the development of liver cancer[27], we conducted a thorough correlation analysis to identify the immune cell types associated with the prognosis model. Minor alterations in the distribution of immune cells could potentially exert diverse impacts on the progression of tumors[29]. In this study, myeloid dendritic cells were the immune cell type with a significant difference in abundance only between groups with high and low expression of the *PSMB2* gene, as well as neutrophils and Th17 cells between groups with different expression of the *USP17L2* gene (Figure 2). However, no significant correlation was found between tumor-infiltrating immune cells and gene expression, and it is imperative to conduct additional confirmation and validation in an independent cohort. Furthermore, exploring the connection between the expression levels of some checkpoints and immune infiltration, as well as the tumor microenvironment, will be a hotspot for future research.

Moreover, the expression of one or more of the five genes and the risk score were different among different T, N, and clinical stages (Figure 3). It is widely known that tumor stage is a key prognostic factor for malignant tumors[30]. In addition, all genes except *ATG10* and the risk score were correlated with the upper limit of albumin results (Figure 3). The risk score was not only statistically significant in different stages, but also negatively correlated with the upper limit of albumin results and postoperative recurrence, which proves that the model developed in this study has appreciated value in clinical prediction of recurrence and prognosis.

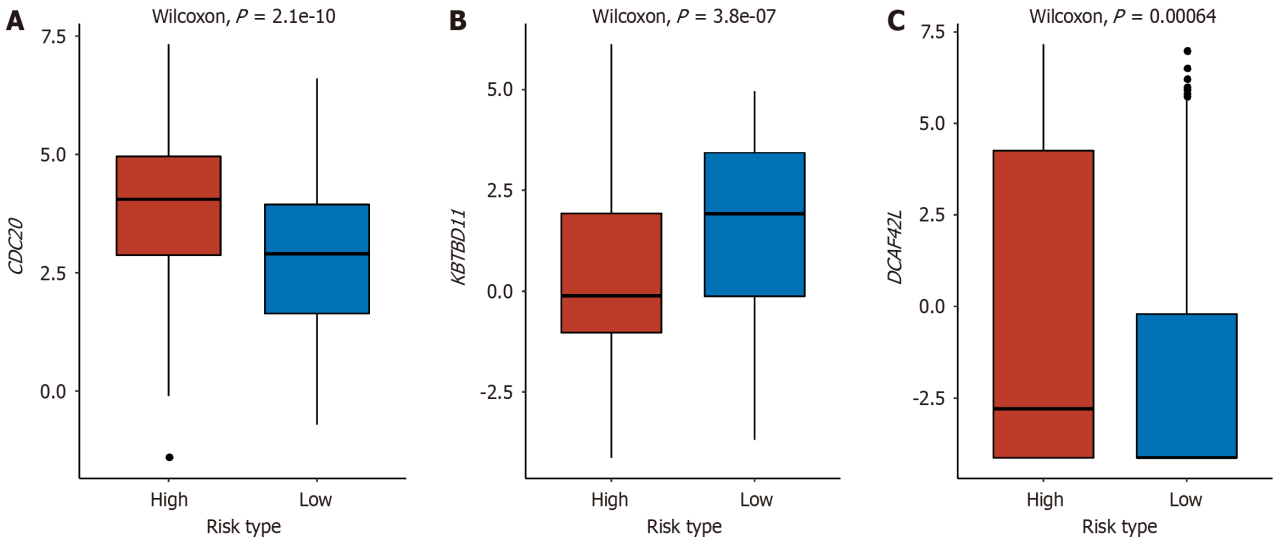

Figure 5 Differentially expressed genes in E3 gene set between high- and low-risk groups. A-C: *CDC20* (A), *KBTBD11* (B), and *DCAF4L2* (C) in E3 gene sets were significantly different between high- and low-risk groups.

E3 is the key factor in the UPP, which can specifically recognize different substrates and show high selectivity in protein degradation. Therefore, we analyzed the E3 gene set independently of E1, E2, DUB, and proteasome-related genes. Finally, the expression levels of *CDC20, KBTBD11*, and *DCAF4L2* were identified as significantly different between the high-risk and low-risk groups, which were also included in the above 111 DEGs. CDC20 plays a vital role in chromosome segregation and mitosis[31]. It regulates the stability of phosphorylated mitotic centromere-associated kinesin in metaphase-anaphase transition[32], which may play a role as a cancer protein to promote the development and progression of liver cancer. In the study of Zheng *et al*[33], CDC20, proliferating cell nuclear antigen, and minichromosome maintenance complex component 6 synergistically affect the regulation of the cell cycle and may be potential prognostic factors for liver cancer. Shi *et al*[34] found that CDC20 serves as a crucial factor in the development of hepatocellular carcinoma (HCC) by controlling the prolyl-4-hydroxylase domain 3 protein. By analyzing four expression profiles from the GEO database, it was found that the up-regulation of CDC20 in HCC tissues indicates poor OS and disease-free survival[35]. Recently, *KBTBD11* was identified as a newly discovered adipogenesis-related gene[36]. In diverse cancer types, such as colorectal cancer, HCC, and head and neck squamous cell carcinoma, the expression of KBTBD11 was significantly decreased in tumor tissues as compared to normal tissues[37]. This is consistent with our result that patients in the high-risk group had lower *KBTBD11* gene expression levels. DCAF4L2 is a member of the E3 complex, which is usually used as a mediator of protein-protein interaction and negatively regulates NF-κB signal transduction. Overexpression of DCAF4L2 has been observed in human colon cancer[38]. In a study of HCC, overexpression of DCAF4L2 is a common feature of nonalcoholic steatohepatitis-associated HCC and viral hepatitis-associated HCC, which can be used as a candidate therapeutic target for HCC[39]. We also found overexpression of *DCAF4L2* in high-risk patients, which suggested a poor prognosis in patients with liver cancer.

One of the main shortcomings of this study is the lack of clinical cases. All the data were from TCGA and GEO, resulting in the lack of clinical data for some patients, and it was unable to validate the expression of the five genes and comprehensively analyze their correlation with clinical and prognostic indicators. This is a preliminary study, and the results reported are exploratory. We intend to validate these results and the detailed mechanisms in future studies.

CONCLUSION

In conclusion, we have used gene expression data in TCGA to screen genes involved in the UPP pathway that significantly correlate with the prognosis of liver cancer. Our findings indicate that the UPP plays an important role in the development of liver cancer, which provides new insights into the early prediction of prognosis and precision medicine in liver cancer.

ARTICLE HIGHLIGHTS

Research background

The ubiquitin-proteasome pathway (UPP) is crucial for selective protein degradation, and its dysfunction is linked to various diseases, including cancer. Proteasome inhibitors are emerging as potential anti-tumor drugs. This study explored the association between UPP gene expression and liver cancer prognosis, aiming to identify key genes and develop a predictive model. By doing so, the research seeks to offer novel insights into the role and potential mechanisms

of the UPP in liver cancer development, contributing to the ongoing exploration of effective therapeutic strategies for liver cancer.

Research motivation

Due to the high tumor heterogeneity, effective surveillance and predication of the prognosis of liver cancer still face multiple challenges. This study was performed to analyze the relationship between the expression of genes in the UPP and the prognosis of liver cancer and construct a prognosis predictive model for this malignancy.

Research objectives

The study aimed to investigate the prognostic significance of genes in the UPP in liver cancer. Using gene expression data from The Cancer Genome Atlas (TCGA) and gene expression comprehensive (GEO) databases, the study identified key genes involved in the UPP, constructed a prognostic predictive model for liver cancer, and explored the associations of the model with immune cell infiltration and clinical parameters, in order to enhance liver cancer prognosis prediction and provide insights into the role and potential mechanisms of the UPP in liver cancer development, contributing valuable information for precision medicine in the context of liver cancer management.

Research methods

The research employed diverse methodologies, utilizing UPP-related gene sets and patient data from TCGA and GEO databases. A prognostic model was constructed using univariate and multivariate regression analyses, involving five key genes (ATG10, PSMA8, PSMB2, USP17L2, and USP8). The model demonstrated robust predictive abilities for liver cancer prognosis. Immunocyte infiltration analysis and correlation studies with clinical parameters provided additional insights. Differentially expressed genes and enrichment analyses shed light on relevant pathways. The study's comprehensive approach contributes a nuanced understanding of UPP gene implications in liver cancer prognosis.

Research results

This study investigated the role of the UPP in liver cancer, identifying five key genes (*ATG10, PSMA8, PSMB2, USP17L2,* and *USP8*) associated with prognosis. A predictive model was constructed and validated using TCGA and GEO datasets. The study highlighted differential gene expression between the high- and low-risk groups and enriched relevant pathways. Additionally, differentially expressed genes in the E3 gene set (*CDC20, KBTBD11,* and *DCAF4L2*) were identified as significant. The findings provide valuable insights into liver cancer prognosis, immunology, and potential therapeutic targets.

Research conclusions

We have used gene expression data in TCGA to screen genes in the UPP that significantly correlated with the prognosis of liver cancer. Our findings indicate that the UPP plays an important role in the development of liver cancer, which provides new insights into the early prediction of prognosis and precision medicine in liver cancer.

Research perspectives

This is a preliminary study, and the results reported are exploratory. We intend to validate these results and the detailed mechanisms in future studies.

FOOTNOTES

Co-first authors: Hua Li and Yi-Po Ma.

Co-corresponding authors: Xiao-Min Liu and Peng-Fei Liu.

Author contributions: Liu XM and Liu PF conceptualized and designed the research; Li H and Ma YP collected the data and wrote the manuscript; Wang HL conducted the data mining and prepared the figures; Tian CJ, Guo YX, and Zhang HB conducted the bioinformatics analysis; all authors were involved in the critical review of the results and have contributed to, read, and approved the final manuscript. Li H and Ma YP contributed equally to this work and are the co-first authors. Liu XM and Liu PF contributed equally to this study and are the co-corresponding authors. There are two primary reasons behind appointing Li H and Ma YP as co-first authors, and Liu XM and Liu PF as co-corresponding authors. First, our research was conducted through a collaborative effort, and the selection of first and corresponding authors aptly mirrors the distribution of responsibilities and the shared commitment of time and effort needed to carry out the study and produce the resulting paper. This approach ensures effective communication and facilitates the management of post-submission matters, ultimately enhancing the paper's overall quality and reliability. Second, each of these researchers made substantial and equal contributions throughout the entire research process. Designating them as co-first authors or co-corresponding authors not only acknowledges and respects their equivalent input but also highlights the spirit of teamwork and collaboration that characterized this study. In summary, the choice to designate Li H and Ma YP as co-first authors, and Liu XM and Liu PF as co-corresponding authors is appropriate for our manuscript as it accurately reflects our team's collaborative ethos and equal contributions.

Supported by the Tianjin Municipal Natural Science Foundation, No. 21JCYBJC01110.

Institutional review board statement: TCGA is a public database. The patients involved in the database have obtained ethical approval. Users can download relevant data for free for research and publish relevant articles. Our study was based on open-source data, so there

are no statements on ethics approval and consent.

Informed consent statement: Our study is based on open-source data, so there are no statements on informed consent.

Conflict-of-interest statement: All authors declare that they have no competing interests to disclose.

Data sharing statement: Publicly available datasets were analyzed in this study, and these can be found in the TCGA database (http://portal.gdc.cancer.gov/).

Country/Territory of origin: China

ORCID number: Hua Li 0000-0001-5257-889X; Xiao-Min Liu 0000-0002-7533-3809; Peng-Fei Liu 0000-0002-2971-3800.

S-Editor: Liu JH
L-Editor: Wang TQ
P-Editor: Zheng XM

REFERENCES

1 **Sung H**, Ferlay J, Siegel RL, Laversanne M, Soerjomataram I, Jemal A, Bray F. Global Cancer Statistics 2020: GLOBOCAN Estimates of Incidence and Mortality Worldwide for 36 Cancers in 185 Countries. *CA Cancer J Clin* 2021; **71**: 209-249 [PMID: 33538338 DOI: 10.3322/caac.21660]

2 **Cui Y**, Li H, Zhan H, Han T, Dong Y, Tian C, Guo Y, Yan F, Dai D, Liu P. Identification of Potential Biomarkers for Liver Cancer Through Gene Mutation and Clinical Characteristics. *Front Oncol* 2021; **11**: 733478 [PMID: 34604069 DOI: 10.3389/fonc.2021.733478]

3 **Maomao C**, He L, Dianqin S, Siyi H, Xinxin Y, Fan Y, Shaoli Z, Changfa X, Lin L, Ji P, Wanqing C. Current cancer burden in China: epidemiology, etiology, and prevention. *Cancer Biol Med* 2022; **19**: 1121-1138 [PMID: 36069534 DOI: 10.20892/j.issn.2095-3941.2022.0231]

4 **Zhao L**, Zhang X, Coday M, Garcia DO, Li X, Mossavar-Rahmani Y, Naughton MJ, Lopez-Pentecost M, Saquib N, Shadyab AH, Simon MS, Snetselaar LG, Tabung FK, Tobias DK, VoPham T, McGlynn KA, Sesso HD, Giovannucci E, Manson JE, Hu FB, Tinker LF. Sugar-Sweetened and Artificially Sweetened Beverages and Risk of Liver Cancer and Chronic Liver Disease Mortality. *JAMA* 2023; **330**: 537-546 [PMID: 37552302 DOI: 10.1001/jama.2023.12618]

5 **Zhou J**, Sun H, Wang Z, Cong W, Wang J, Zeng M, Zhou W, Bie P, Liu L, Wen T, Han G, Wang M, Liu R, Lu L, Ren Z, Chen M, Zeng Z, Liang P, Liang C, Yan F, Wang W, Ji Y, Yun J, Cai D, Chen Y, Cheng W, Cheng S, Dai C, Guo W, Hua B, Huang X, Jia W, Li Y, Liang J, Liu T, Lv G, Mao Y, Peng T, Ren W, Shi H, Shi G, Tao K, Wang X, Xiang B, Xing B, Xu J, Yang J, Yang Y, Ye S, Yin Z, Zhang B, Zhang L, Zhang S, Zhang T, Zhao Y, Zheng H, Zhu J, Zhu K, Shi Y, Xiao Y, Dai Z, Teng G, Cai J, Cai X, Li Q, Shen F, Qin S, Dong J, Fan J. Guidelines for the Diagnosis and Treatment of Hepatocellular Carcinoma (2019 Edition). *Liver Cancer* 2020; **9**: 682-720 [PMID: 33442540 DOI: 10.1159/000509424]

6 **Li Q**, Wang F, Chen Y, Chen H, Wu S, Farris AB, Jiang Y, Kong J. Virtual liver needle biopsy from reconstructed three-dimensional histopathological images: Quantification of sampling error. *Comput Biol Med* 2022; **147**: 105764 [PMID: 35797891 DOI: 10.1016/j.compbiomed.2022.105764]

7 **Johnson P**, Zhou Q, Dao DY, Lo YMD. Circulating biomarkers in the diagnosis and management of hepatocellular carcinoma. *Nat Rev Gastroenterol Hepatol* 2022; **19**: 670-681 [PMID: 35676420 DOI: 10.1038/s41575-022-00620-y]

8 **Li Y**, Zhang R, Xu Z, Wang Z. Advances in Nanoliposomes for the Diagnosis and Treatment of Liver Cancer. *Int J Nanomedicine* 2022; **17**: 909-925 [PMID: 35250267 DOI: 10.2147/IJN.S349426]

9 **Hershko A**. The ubiquitin system for protein degradation and some of its roles in the control of the cell division cycle. *Cell Death Differ* 2005; **12**: 1191-1197 [PMID: 16094395 DOI: 10.1038/sj.cdd.4401702]

10 **Staszczak M**. [Ubiquitin-proteasome pathway as a target for therapeutic strategies]. *Postepy Biochem* 2017; **63**: 287-303 [PMID: 29374430]

11 **Liu ZY**, Li YH, Zhang QK, Li BW, Xin L. Development and validation of a ubiquitin-proteasome system gene signature for prognostic prediction and immune microenvironment evaluation in hepatocellular carcinoma. *J Cancer Res Clin Oncol* 2023; **149**: 13363-13382 [PMID: 37490101 DOI: 10.1007/s00432-023-05189-w]

12 **Zhang J**, Liu L, Wang Z, Hou M, Dong Z, Yu J, Sun R, Cui G. Ubiquitin-proteasome system-based signature to predict the prognosis and drug sensitivity of hepatocellular carcinoma. *Front Pharmacol* 2023; **14**: 1172908 [PMID: 37180696 DOI: 10.3389/fphar.2023.1172908]

13 **Kanehisa M**, Furumichi M, Sato Y, Ishiguro-Watanabe M, Tanabe M. KEGG: integrating viruses and cellular organisms. *Nucleic Acids Res* 2021; **49**: D545-D551 [PMID: 33125081 DOI: 10.1093/nar/gkaa970]

14 **Sun Y**. E3 ubiquitin ligases as cancer targets and biomarkers. *Neoplasia* 2006; **8**: 645-654 [PMID: 16925947 DOI: 10.1593/neo.06376]

15 **Sun W**, Li J, Zhou L, Han J, Liu R, Zhang H, Ning T, Gao Z, Liu B, Chen X, Ba Y. The c-Myc/miR-27b-3p/ATG10 regulatory axis regulates chemoresistance in colorectal cancer. *Theranostics* 2020; **10**: 1981-1996 [PMID: 32104496 DOI: 10.7150/thno.37621]

16 **Liu P**, Ma C, Wu Q, Zhang W, Wang C, Yuan L, Xi X. MiR-369-3p participates in endometrioid adenocarcinoma *via* the regulation of autophagy. *Cancer Cell Int* 2019; **19**: 178 [PMID: 31337985 DOI: 10.1186/s12935-019-0897-8]

17 **Jiao X**, Liu W, Mahdessian H, Bryant P, Ringdahl J, Timofeeva M, Farrington SM, Dunlop M, Lindblom A. Recurrent, low-frequency coding variants contributing to colorectal cancer in the Swedish population. *PLoS One* 2018; **13**: e0193547 [PMID: 29547645 DOI: 10.1371/journal.pone.0193547]

18 **Tan S**, Li H, Zhang W, Shao Y, Liu Y, Guan H, Wu J, Kang Y, Zhao J, Yu Q, Gu Y, Ding K, Zhang M, Qian W, Zhu Y, Cai H, Chen C, Lobie PE, Zhao X, Sun J, Zhu T. NUDT21 negatively regulates PSMB2 and CXXC5 by alternative polyadenylation and contributes to hepatocellular carcinoma suppression. *Oncogene* 2018; **37**: 4887-4900 [PMID: 29780166 DOI: 10.1038/s41388-018-0280-6]

19 **Hu B**, Deng T, Ma H, Liu Y, Feng P, Wei D, Ling N, Li L, Qiu S, Zhang L, Peng B, Liu J, Ye M. Deubiquitinase DUB3 Regulates Cell Cycle Progression *via* Stabilizing Cyclin A for Proliferation of Non-Small Cell Lung Cancer Cells. *Cells* 2019; **8** [PMID: 30935108 DOI: 10.3390/cells8040297]

20 **Baohai X**, Shi F, Yongqi F. Inhibition of ubiquitin specific protease 17 restrains prostate cancer proliferation by regulation of epithelial-to-mesenchymal transition (EMT) *via* ROS production. *Biomed Pharmacother* 2019; **118**: 108946 [PMID: 31377470 DOI: 10.1016/j.biopha.2019.108946]

21 **Zhu Y**, Xu J, Hu W, Wang F, Zhou Y, Gong W, Xu W. Inhibiting USP8 overcomes hepatocellular carcinoma resistance *via* suppressing receptor tyrosine kinases. *Aging (Albany NY)* 2021; **13**: 14999-15012 [PMID: 34081623 DOI: 10.18632/aging.203061]

22 **Rong Z**, Zhu Z, Cai S, Zhang B. Knockdown of USP8 Inhibits the Growth of Lung Cancer Cells. *Cancer Manag Res* 2020; **12**: 12415-12422 [PMID: 33293867 DOI: 10.2147/IJN.S259191]

23 **Wang Z**, Huang C, Wu J, Zhang H, Shao Y, Fu Z. Analysis of the Prognostic Significance and Immune Infiltration of the Amino Acid Metabolism-Related Genes in Colon Adenocarcinoma. *Front Genet* 2022; **13**: 951461 [PMID: 36035152 DOI: 10.3389/fgene.2022.951461]

24 **Chiao CC**, Liu YH, Phan NN, An Ton NT, Ta HDK, Anuraga G, Minh Xuan DT, Fitriani F, Putri Hermanto EM, Athoillah M, Andriani V, Ajiningrum PS, Wu YF, Lee KH, Chuang JY, Wang CY, Kao TJ. Prognostic and Genomic Analysis of Proteasome 20S Subunit Alpha (PSMA) Family Members in Breast Cancer. *Diagnostics (Basel)* 2021; **11** [PMID: 34943457 DOI: 10.3390/diagnostics11122220]

25 **Zhang Q**, Zhang ZY, Du H, Li SZ, Tu R, Jia YF, Zheng Z, Song XM, Du RL, Zhang XD. DUB3 deubiquitinates and stabilizes NRF2 in chemotherapy resistance of colorectal cancer. *Cell Death Differ* 2019; **26**: 2300-2313 [PMID: 30778200 DOI: 10.1038/s41418-019-0303-z]

26 **Jin X**, Yan Y, Wang D, Ding D, Ma T, Ye Z, Jimenez R, Wang L, Wu H, Huang H. DUB3 Promotes BET Inhibitor Resistance and Cancer Progression by Deubiquitinating BRD4. *Mol Cell* 2018; **71**: 592-605.e4 [PMID: 30057199 DOI: 10.1016/j.molcel.2018.06.036]

27 **Fu Y**, Liu S, Zeng S, Shen H. From bench to bed: the tumor immune microenvironment and current immunotherapeutic strategies for hepatocellular carcinoma. *J Exp Clin Cancer Res* 2019; **38**: 396 [PMID: 31500650 DOI: 10.1186/s13046-019-1396-4]

28 **Quan Y**, Liang F, Wu D, Yao X, Hu Z, Zhu Y, Chen Y, Wu A, Tang D, Huang B, Xu R, Lyu Z, Yan Q, Luo L, Ning Z, Li Y, Xiong J. Blood Cell DNA Methylation of Aging-Related Ubiquitination Gene DZIP3 Can Predict the Onset of Early Stage Colorectal Cancer. *Front Oncol* 2020; **10**: 544330 [PMID: 33330022 DOI: 10.3389/fonc.2020.544330]

29 **Pan S**, Zhan Y, Chen X, Wu B, Liu B. Bladder Cancer Exhibiting High Immune Infiltration Shows the Lowest Response Rate to Immune Checkpoint Inhibitors. *Front Oncol* 2019; **9**: 1101 [PMID: 31737562 DOI: 10.3389/fonc.2019.01101]

30 **Piñero F**, Dirchwolf M, Pessôa MG. Biomarkers in Hepatocellular Carcinoma: Diagnosis, Prognosis and Treatment Response Assessment. *Cells* 2020; **9** [PMID: 32492896 DOI: 10.3390/cells9061370]

31 **Kapanidou M**, Curtis NL, Bolanos-Garcia VM. Cdc20: At the Crossroads between Chromosome Segregation and Mitotic Exit. *Trends Biochem Sci* 2017; **42**: 193-205 [PMID: 28202332 DOI: 10.1016/j.tibs.2016.12.001]

32 **Sanhaji M**, Ritter A, Belsham HR, Friel CT, Roth S, Louwen F, Yuan J. Polo-like kinase 1 regulates the stability of the mitotic centromere-associated kinesin in mitosis. *Oncotarget* 2014; **5**: 3130-3144 [PMID: 24931513 DOI: 10.18632/oncotarget.1861]

33 **Zheng Y**, Shi Y, Yu S, Han Y, Kang K, Xu H, Gu H, Sang X, Chen Y, Wang J. GTSE1, CDC20, PCNA, and MCM6 Synergistically Affect Regulations in Cell Cycle and Indicate Poor Prognosis in Liver Cancer. *Anal Cell Pathol (Amst)* 2019; **2019**: 1038069 [PMID: 32082966 DOI: 10.1155/2019/1038069]

34 **Shi M**, Dai WQ, Jia RR, Zhang QH, Wei J, Wang YG, Xiang SH, Liu B, Xu L. APC(CDC20)-mediated degradation of PHD3 stabilizes HIF-1a and promotes tumorigenesis in hepatocellular carcinoma. *Cancer Lett* 2021; **496**: 144-155 [PMID: 33039559 DOI: 10.1016/j.canlet.2020.10.011]

35 **Zhuang L**, Yang Z, Meng Z. Upregulation of BUB1B, CCNB1, CDC7, CDC20, and MCM3 in Tumor Tissues Predicted Worse Overall Survival and Disease-Free Survival in Hepatocellular Carcinoma Patients. *Biomed Res Int* 2018; **2018**: 7897346 [PMID: 30363964 DOI: 10.1155/2018/7897346]

36 **Watanabe K**, Yoshida K, Iwamoto S. Kbtbd11 gene expression in adipose tissue increases in response to feeding and affects adipocyte differentiation. *J Diabetes Investig* 2019; **10**: 925-932 [PMID: 30582777 DOI: 10.1111/jdi.12995]

37 **Gong J**, Tian J, Lou J, Wang X, Ke J, Li J, Yang Y, Gong Y, Zhu Y, Zou D, Peng X, Yang N, Mei S, Zhong R, Chang J, Miao X. A polymorphic MYC response element in KBTBD11 influences colorectal cancer risk, especially in interaction with an MYC-regulated SNP rs6983267. *Ann Oncol* 2018; **29**: 632-639 [PMID: 29267898 DOI: 10.1093/annonc/mdx789]

38 **Wang H**, Chen Y, Han J, Meng Q, Xi Q, Wu G, Zhang B. DCAF4L2 promotes colorectal cancer invasion and metastasis *via* mediating degradation of NFκb negative regulator PPM1B. *Am J Transl Res* 2016; **8**: 405-418 [PMID: 27158335]

39 **Tian Y**, Arai E, Makiuchi S, Tsuda N, Kuramoto J, Ohara K, Takahashi Y, Ito N, Ojima H, Hiraoka N, Gotoh M, Yoshida T, Kanai Y. Aberrant DNA methylation results in altered gene expression in non-alcoholic steatohepatitis-related hepatocellular carcinomas. *J Cancer Res Clin Oncol* 2020; **146**: 2461-2477 [PMID: 32685988 DOI: 10.1007/s00432-020-03298-4]

World Journal of Clinical Oncology

Submit a Manuscript: https://www.f6publishing.com

World J Clin Oncol 2024 March 24; 15(3): 447-455

DOI: 10.5306/wjco.v15.i3.447

ISSN 2218-4333 (online)

META-ANALYSIS

Transarterial chemoembolization plus stent placement for hepatocellular carcinoma with main portal vein tumor thrombosis: A meta-analysis

Wei-Fan Sui, Jian-Yun Li, Jian-Hua Fu

Specialty type: Oncology

Provenance and peer review: Unsolicited article; Externally peer reviewed.

Peer-review model: Single blind

Peer-review report's scientific quality classification

Grade A (Excellent): 0
Grade B (Very good): 0
Grade C (Good): 0
Grade D (Fair): D
Grade E (Poor): 0

P-Reviewer: Elshimi E, Egypt

Received: October 29, 2023
Peer-review started: October 29, 2023
First decision: December 22, 2023
Revised: January 5, 2024
Accepted: February 4, 2024
Article in press: February 4, 2024
Published online: March 24, 2024

Wei-Fan Sui, Jian-Yun Li, Jian-Hua Fu, Department of Interventional Radiology, Zhenjiang First People's Hospital, Zhenjiang 212000, Jiangsu Province, China

Corresponding author: Jian-Hua Fu, Doctor, Director, Department of Interventional Radiology, Zhenjiang First People's Hospital, No. 8 Dianli Road, Zhenjiang 212000, Jiangsu Province, China. suiweifan@126.com

Abstract

BACKGROUND

Portal vein tumor thrombus is an important indicator of poor prognosis in patients with hepatocellular carcinoma. Transarterial chemoembolization is recommended as the standard first-line therapy for unresectable hepatocellular carcinoma. Portal vein stent placement is a safe and effective therapy for promptly restoring flow and relieving portal hypertension caused by tumor thrombus.

AIM

To assess the clinical significance of transarterial chemoembolization plus stent placement for the treatment of hepatocellular carcinoma with main portal vein tumor thrombosis.

METHODS

We searched English and Chinese databases, assessed the quality of the included studies, analyzed the characteristic data, tested heterogeneity, explored heterogeneity, and tested publication bias.

RESULTS

In total, eight clinical controlled trials were included. The results showed that the pressure in the main portal vein after stent placement was significantly lower than that with no stent placement. The cumulative stent patency and survival rates at 6 and 12 months were lower in the transarterial chemoembolization + stent placement group than in the transarterial chemoembolization + stent placement + brachytherapy/radiotherapy group. The survival rates of patients treated with transarterial chemoembolization + stent placement for 6 and 12 months were higher than those of patients treated with transarterial chemoembolization alone.

CONCLUSION

For Chinese patients with hepatocellular carcinoma with main portal vein tumor

thrombosis, transarterial chemoembolization plus stenting is effective. Transarterial chemoembolization + stent placement is more effective than transarterial chemoembolization alone. Transarterial chemoembolization + stent placement + brachytherapy/radiotherapy is more effective than transarterial chemoembolization + stenting.

Key Words: Hepatocellular carcinoma; Transarterial chemoembolization; Portal vein tumor thrombus; Stent; Meta-analysis

Core Tip: Portal vein tumor thrombus (PVTT) as an important indicator of poor prognosis existed in 44% of patients with hepatocellular carcinoma (HCC). Transarterial chemoembolization (TACE) is recommended as the standard first-line therapy in unresectable hepatocellular carcinoma. Some Chinese scholars have found that TACE combined with portal vein stent placement is safe and could prolong the survival time in HCC patients with PVTT.

Citation: Sui WF, Li JY, Fu JH. Transarterial chemoembolization plus stent placement for hepatocellular carcinoma with main portal vein tumor thrombosis: A meta-analysis. *World J Clin Oncol* 2024; 15(3): 447-455
URL: https://www.wjgnet.com/2218-4333/full/v15/i3/447.htm
DOI: https://dx.doi.org/10.5306/wjco.v15.i3.447

INTRODUCTION

Hepatocellular carcinoma (HCC) is one of the most common malignancies worldwide[1]. It is the fourth most common malignant tumor and the third most common cause of cancer-related death in China[2]. Portal vein tumor thrombus (PVTT), an important indicator of poor prognosis, occurs in 44% of patients with HCC[3]. PVTT decreases the blood supply to the normal liver and cause deterioration of liver function, gastrointestinal bleeding, and tumor recurrence[4]. HCC with PVTT is regarded as technically unresectable.

Transarterial chemoembolization (TACE) is recommended as the standard first-line therapy for unresectable HCC[5]. However, PVTT limits the effect of TACE and leads to liver failure because of portal vein obstruction. Three-dimensional conformal radiotherapy (3-DCRT) and I^{125} seeds have been shown to improve survival in HCC patients with main PVTT but not in those with worsened liver function[6,7]. However, the obstruction of the portal vein cannot be relieved immediately by 3-DCRT or I^{125} seeds alone.

Portal vein stent placement is a safe and effective therapy for promptly restoring flow and relieving portal hypertension caused by tumor thrombus. It prolonged survival in patients with HCC and main PVTT[8]. Several Chinese scholars have shown that TACE combined with portal vein stent placement is safe and can prolong the survival time of HCC patients with main PVTT[9,10]. However, clinical trials with large samples for demonstrating the clinical significance of TACE plus stent placement for HCC patients with main PVTT are currently lacking, and no systematic analysis on the clinical significance of TACE plus stent placement for HCC patients with main PVTT in the Chinese population has been performed. Hence, this study aimed to carry out a meta-analysis to assess the clinical significance of TACE plus stent placement for Chinese patients with HCC and main PVTT.

MATERIALS AND METHODS

Search strategy

We performed a comprehensive literature search by using English-language databases, including PubMed, the Cochrane Library, and Excerpt Medica Database, and Chinese databases, including the Chinese National Knowledge Infrastructure (CNKI), Wanfang Data, and CQVIP, up to 2019.

We used the following search terms in the field for title/abstract and/or keywords: "Hepatocellular carcinoma", ''transarterial chemoembolization'' or ''TACE'' or "chemoembolization", "portal vein tumor thrombus", and "stent". All the data were available from published papers.

Study selection

The studies selected met the following inclusion criteria: (1) Original research; (2) human participants; (3) the study had clinical results, such as stent patency rates and survival rates; and (4) the study showed the clinical value of TACE plus stent placement for HCC patients with main PVTT.

Data extraction and study quality assessment

Two authors screened the titles and abstracts of potentially eligible studies independently and examined the full-text articles to determine whether they could be included. One author independently extracted the data, including author, country, publication year, design, treatment, and patient number. All the included studies were assessed for quality

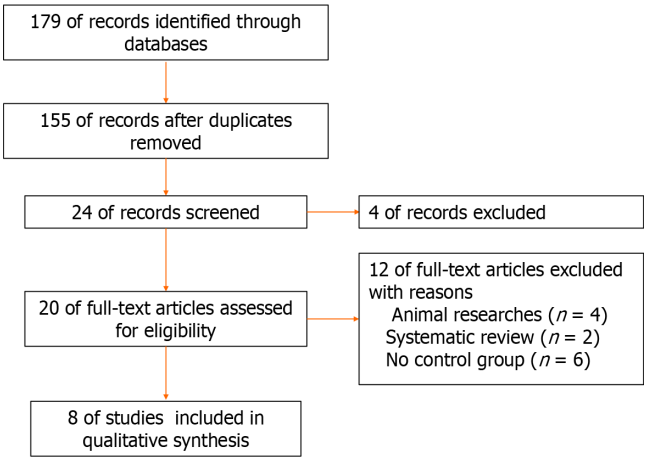

Figure 1 Flowchart of the meta-analysis.

through the Cochrane Collaboration tool[11].

Data analysis

Review Manager 5.3 was used to analyze the data. For all analyses, $P < 0.05$ was considered to indicate statistical significance. Heterogeneity was assessed by using the chi-square test and I^2 statistic[12,13]. The I^2 statistic was applied to further assess heterogeneity ($25\% \leq I^2 \leq 50\%$ indicated low heterogeneity; $50\% < I^2 \leq 75\%$ indicated moderate heterogeneity). An $I^2 \geq 75\%$ indicated significant heterogeneity.

Subgroup analysis was performed to explore the source of heterogeneity.

Publication bias was evaluated using funnel plots[13]. When a funnel plot was asymmetrical, interpretation of the results was assessed critically. Otherwise, no publication bias existed.

RESULTS

Search strategy

We included eight studies in this meta-analysis. Two studies were published in English[14,15]. Six studies were of Chinese descent[9,10,16-19] (Figure 1).

Data extraction and study quality assessment

The extracted data included author, publication year, nation, study design, number of patients, and therapies used in the experimental and control groups (Table 1).

The quality of the included studies was assessed. The tool included seven bias metrics, namely, random sequence generation (selection bias), allocation concealment (selection bias), blinding of participants and personnel (performance bias), blinding of outcome assessment (detection bias), incomplete outcome data (attrition bias), selective reporting (reporting bias), and other bias. A summary and graphs of the risk of bias were constructed based on the investigators' judgments about each risk of bias item for each included study and are presented as percentages (Figure 2).

Data analysis

We compared the changes in main portal vein pressure before and after the operation (Figure 3). The pressure in the main portal vein after stent placement was significantly lower than that before stent placement ($P < 0.00001$), suggesting that stent placement decreased the main portal vein pressure. Heterogeneity existed in these results ($I^2 = 63\%$).

We compared the cumulative stent patency rates at 6 and 12 months (Figure 4). The cumulative stent patency rates at 6 and 12 months were lower in the TACE + stent placement group than in the TACE + stent placement + brachytherapy/radiotherapy group ($P < 0.00001$), suggesting that stents without brachytherapy/radiotherapy were more obstructed by main PVTT. Heterogeneity did not exist in these results ($I^2 = 0\%$).

We also compared the survival rates at 6 and 12 months (Figure 5). The overall survival (OS) rates at 6 and 12 months were lower in the TACE + stent placement group than in the TACE + stent placement + brachytherapy/radiotherapy group ($P < 0.00001$), suggesting that TACE + stent placement + brachytherapy/radiotherapy could prolong overall survival better than TACE + stent placement. Heterogeneity existed in these results ($I^2 = 85\%, 27\%$).

To explore the source of heterogeneity, we performed a subgroup analysis of the overall survival rates at 6 and 12 months (Figure 6). The results showed that the source of heterogeneity was the different therapies: TACE + stent placement + brachytherapy/radiotherapy could prolong overall survival better than TACE + stent therapy, and TACE + stent placement could prolong overall survival better than TACE alone ($P < 0.00001$).

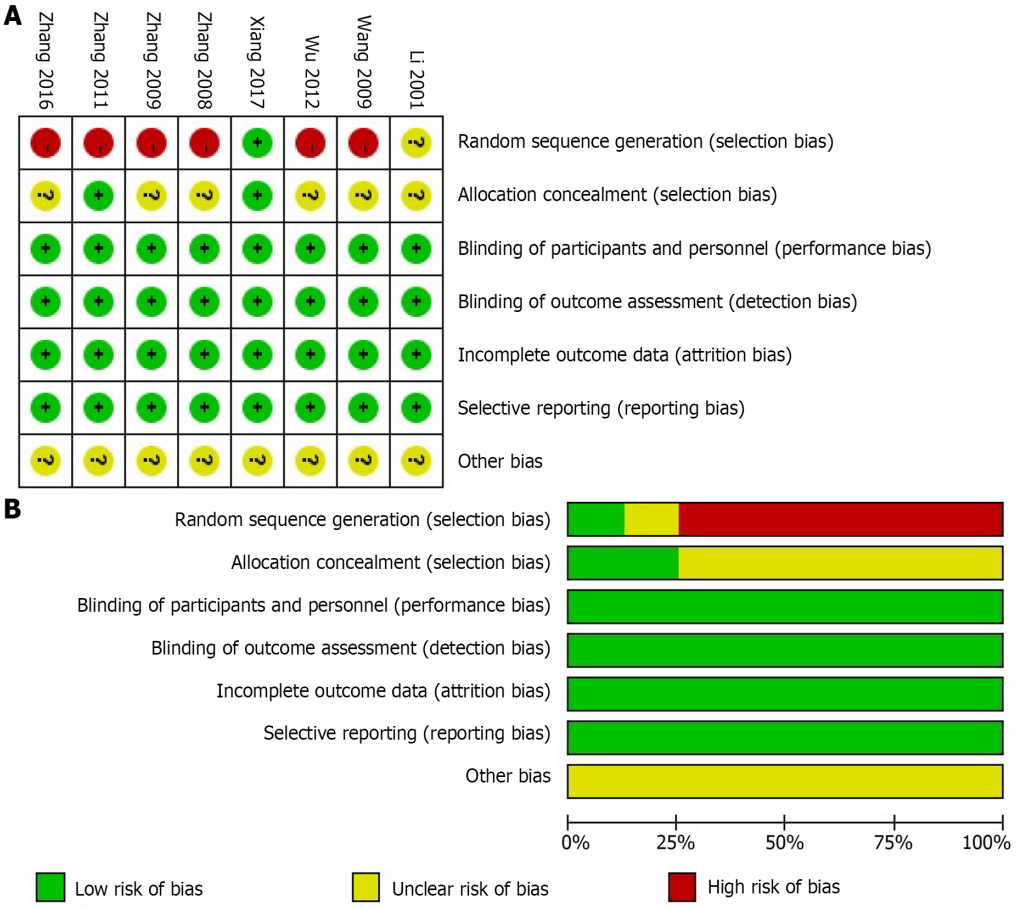

Figure 2 Risk of bias summary and bias graph. A: Review authors' judgements about each risk of bias item for each included study; B: Review authors' judgements about each risk of bias item presented as percentages across all included studies. −: High risk; +: Low risk; ?: Unclear risk.

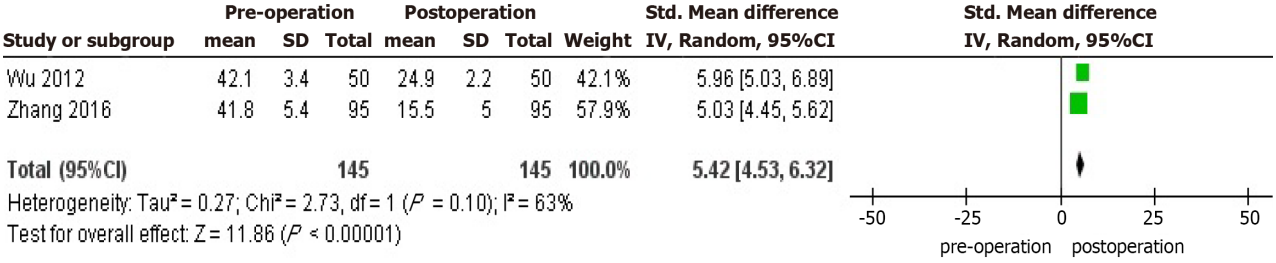

Figure 3 Forest plot of changes of main portal vein pressure.

To assess publication bias, funnel plots were generated, and no publication bias was found (Figure 7).

DISCUSSION

PVTT is recognized as one of the most significant causes of recurrence and metastasis in HCC patients. The prognosis of HCC patients with PVTT is poor. The portal vein is the main nutrient vessel for the liver. It can be invaded by a tumor thrombus, which causes extensive intrahepatic metastases. When portal vein occlusion is accompanied by tumor thrombus, liver function fails, and the possibility of esophageal gastrointestinal bleeding increases, which is lethal for HCC patients.

Surgical resection can cure PVTT, but the high rate of recurrence after surgery and the high surgical requirements limit its use[20]. 3-DCRT was also used for PVTT. The liver is sensitive to radiation and can tolerate 30 Gy/3-4 wk. However, to cure PVTT, the radiation dose must be above 40 Gy, which can cause external radiation to the liver and body[21]. Because of the tumor thrombus in the hepatic artery, TACE can lead to necrosis of the tumor and tumor thrombus. However, the effect of TACE on tumor thrombi is less than that on tumors because TACE indirectly affects tumor thrombi.

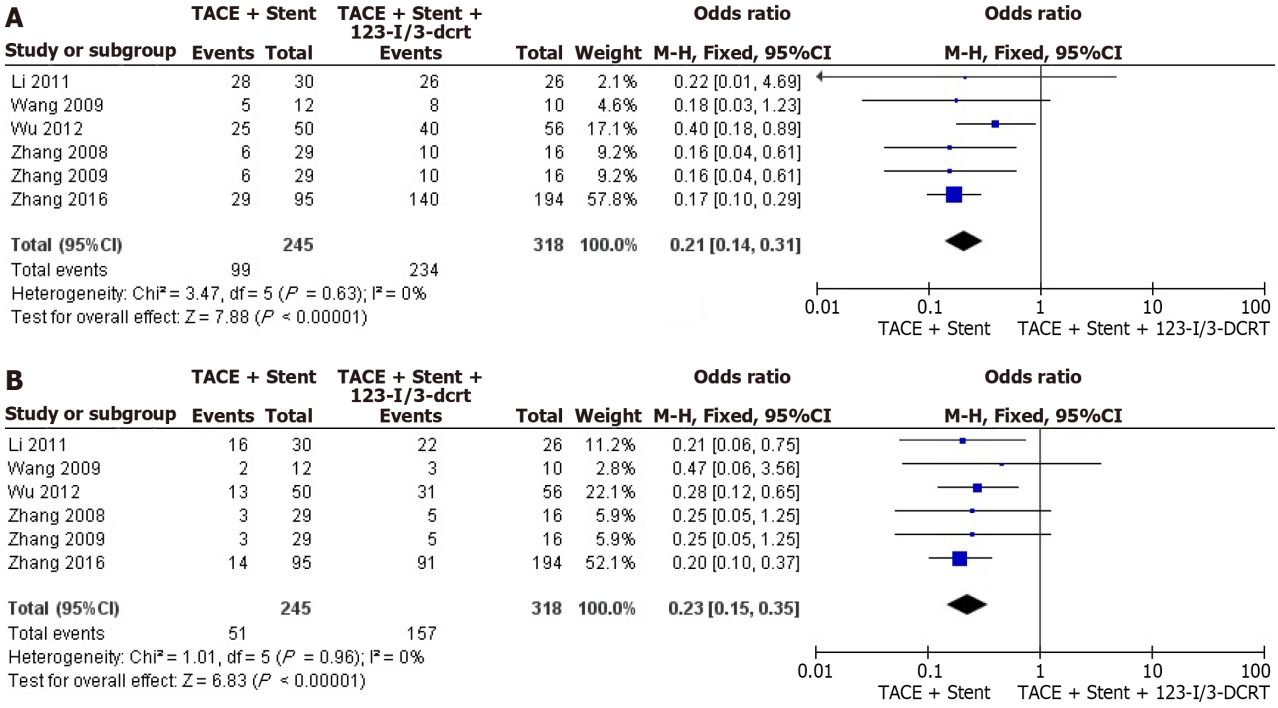

Figure 4 Forest plots of cumulative stent patency rates at 6 and 12 months. A: 6 months; B: 12 months.

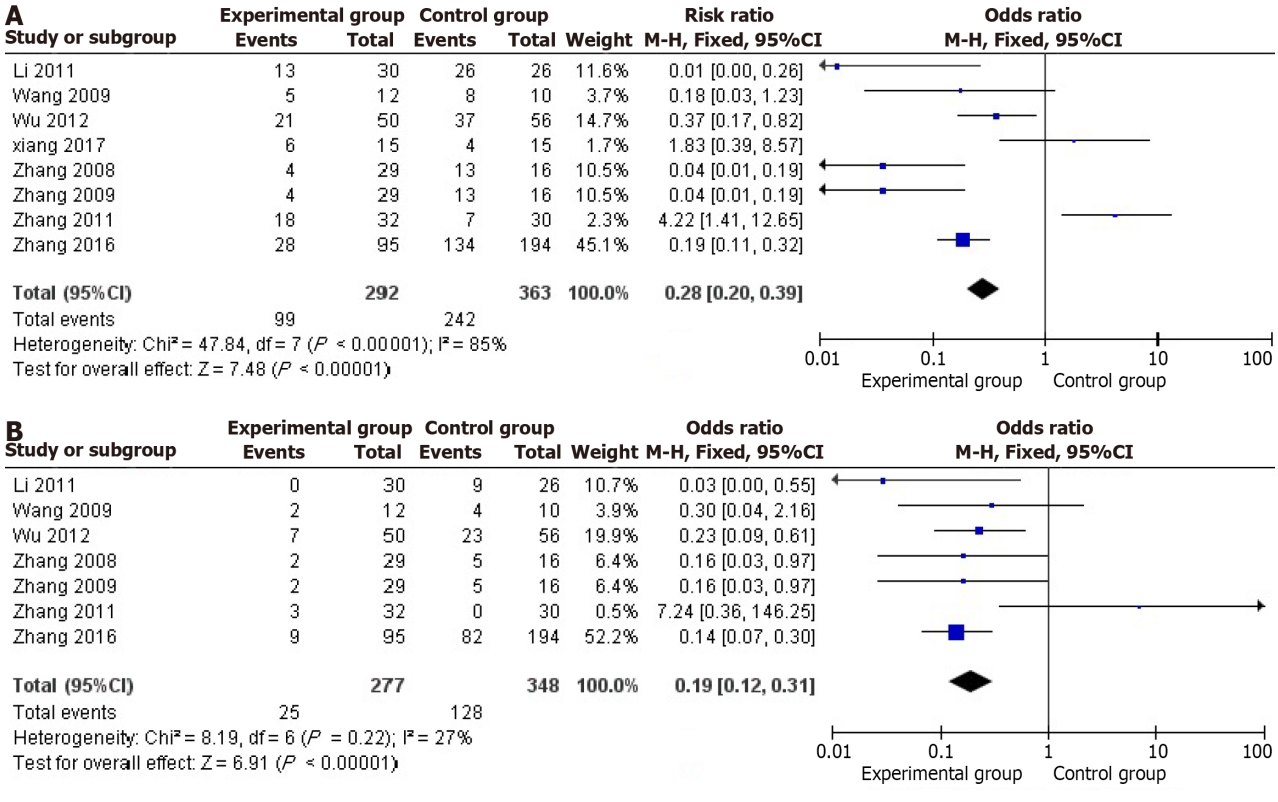

Figure 5 Forest plots of survival rates at 6 and 12 months. A: 6 months; B: 12 months.

According to our meta-analysis, TACE plus a main portal vein stent decreased the pressure in the main portal vein. Furthermore, for HCC patients with main PVTT, TACE plus portal vein stenting improved the survival rate compared with TACE alone. TACE + stent placement + brachytherapy/radiotherapy could improve the stent patency and survival rates better than TACE + stenting. Several studies have shown that portal vein stents serve as palliative remedies for malignant portal vein obstructions and could interrupt the infiltration and ingrowth of tumor thrombi in the portal vein to some degree[8,22], which is consistent with our meta-analysis. However, within a short period, owing to the mesh of the stent, the tumor thrombus might regrow into the stent, leading to reoccurrence and restenosis of the portal vein.

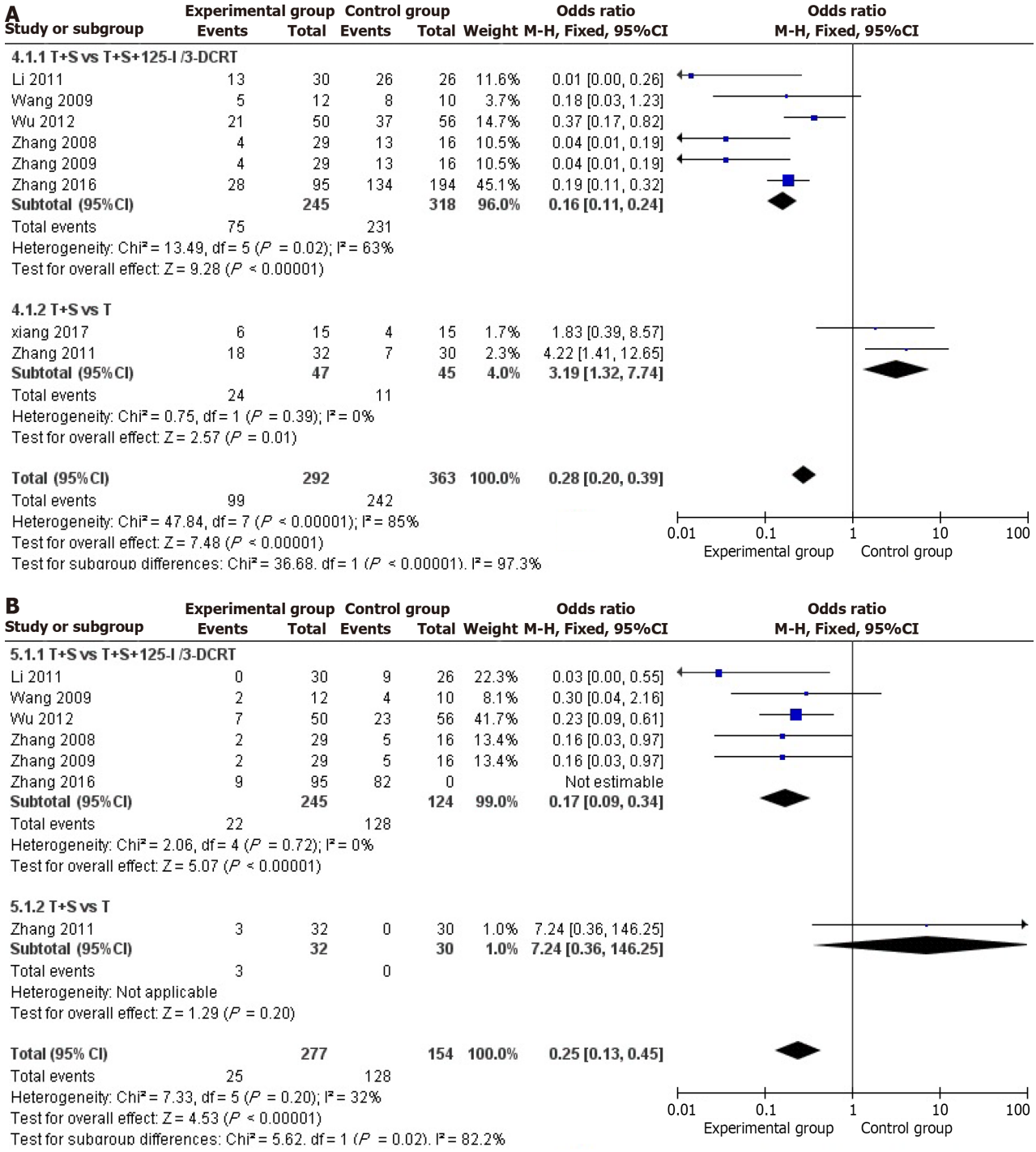

Figure 6 Forest plots of subgroup analysis. A: 6 months; B: 12 months.

Fortunately, TACE + stent placement + brachytherapy/radiotherapy is a practical superior treatment for HCC with main PVTT[14,23]. Because the stent pressed the tumor thrombus, 3-DCRT minimized the likelihood of treating PVTT exactly, which reduced the damage to the normal liver and benefited liver function. I^{125} seeds were close to the tumor tissue to deliver continuous irradiation, which restrained the ability of the tumor thrombus to proliferate by damaging the DNA tumor cells. Consequently, the efficiency of TACE + stent placement + brachytherapy/radiotherapy may be better than TACE + stenting and TACE alone for HCC patients with main PVTT. In the future, we can pay more attention to comparing the efficiency of TACE + stent placement + brachytherapy/radiotherapy and TACE + stent placement + radiotherapy for HCC patients with main PVTT.

There were several limitations in our meta-analysis: (1) Fifty randomized controlled trials were not included in the selected studies, which may have induced bias and affected our assessment of the management of HCC patients with main PVTT; (2) there was a lack of sufficient statistical data from multiple medical centers available to evaluate the efficacy of different therapies for patients with HCC and main PVTT; and (3) potential publication bias cannot be ignored, although our results showed no significant publication bias.

Table 1 Characteristics of included studies

Ref.	Nation	Design	Number of patients (M/F)		Therapy	
			Experimental group	Control group	Experimental group	Control group
Li *et al*[14], 2011	China	NG	23/7	17/9	TACE + stenting	TACE + stenting + I^{125}
Wang *et al*[16], 2009	China	Retrospective study	12/0	9/1	TACE + stenting	TACE + 3-DCRT
Wu *et al*[17], 2012	China	Retrospective study	43/7	51/5	TACE + stenting	TACE + stenting + I^{125}
Xiang *et al*[9], 2017	China	Prospective study	9/6	8/7	TACE + stenting	TACE
Zhang *et al*[18], 2008	China	Retrospective study	28/1	15/1	TACE + stenting	TACE + stenting + 3-DCRT
Zhang *et al*[15], 2009	China	Retrospective study	28/1	15/1	TACE + stenting	TACE + stenting + 3-DCRT
Zhang *et al*[10], 2011	China	Retrospective study	23/7	22/8	TACE + stenting	TACE
Zhang *et al*[19], 2016	China	Retrospective study	83/12	178/16	TACE + stenting	TACE + stenting + I^{125}

NG: Not given.

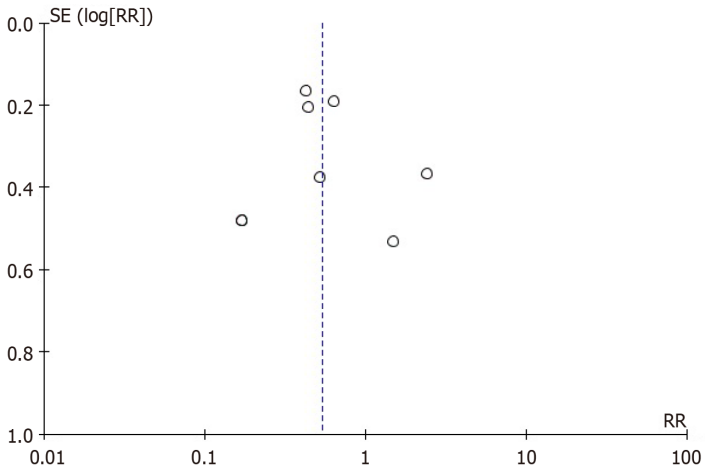

Figure 7 Funnel plot of included studies.

CONCLUSION

In summary, for HCC patients with main PVTT in the Chinese population, TACE + stent surgery is effective. The therapeutic benefits of TACE + stent placement are better than those of TACE alone. TACE + stent placement + brachytherapy/radiotherapy is more effective than TACE + stent placement.

ARTICLE HIGHLIGHTS

Research background

Portal vein tumor thrombus (PVTT) has been recognized as an important indicator of poor prognosis for hepatocellular carcinoma (HCC) patients. HCC with main PVTT limits the effect of transarterial chemoembolization (TACE).

Research motivation

Portal vein stent placement is a safe and effective therapy for promptly restoring flow and relieving portal hypertension caused by tumor thrombus. The efficacy and safety of TACE combined with portal vein stent placement have been proved by some Chinese scholars. No meta-analysis on the clinical significance of TACE plus stent placement for HCC with main PVTT was performed.

Research objectives

This study aimed to carry out a meta-analysis to assess the clinical significance of TACE plus stent placement for HCC with main PVTT.

Research methods

We searched English and Chinese databases, assessed the quality of the included studies, analyzed the characteristic data, explored heterogeneity, and tested publication bias.

Research results

The results showed that the pressure in the main portal vein after stent placement was significantly lower than that with no stent placement. The cumulative stent patency and survival rates at 6 and 12 months were lower in the transarterial chemoembolization + stent placement group than in the transarterial chemoembolization + stent placement + brachytherapy/radiotherapy group. The survival rates of patients treated with transarterial chemoembolization + stent placement for 6 and 12 months were greater than those of patients treated with transarterial chemoembolization alone.

Research conclusions

Transarterial chemoembolization + stenting is safe. Transarterial chemoembolization + stent placement is more effective than transarterial chemoembolization alone. Transarterial chemoembolization + stent placement + brachytherapy/radiotherapy is more effective than transarterial chemoembolization + stenting.

Research perspectives

Tyrosine kinase inhibitors and immune therapies have been proved safe and effective. Adding tyrosine kinase inhibitors and immune therapies will improve the value of this study.

FOOTNOTES

Author contributions: Fu JH designed the research study; Li JY and Sui WF performed the research; Sui WF analyzed the data and wrote the manuscript; all authors have read and approved the final manuscript.

Conflict-of-interest statement: All the authors report no relevant conflicts of interest for this article.

PRISMA 2009 Checklist statement: The authors have read the PRISMA 2009 Checklist, and the manuscript was prepared and revised according to the PRISMA 2009 Checklist.

Country/Territory of origin: China

ORCID number: Wei-Fan Sui 0000-0002-2732-9565; Jian-Yun Li 0000-0003-2733-9566; Jian-Hua Fu 0000-0003-4380-129X.

S-Editor: Gong ZM
L-Editor: Wang TQ
P-Editor: Zhao S

REFERENCES

1 **Torre LA**, Bray F, Siegel RL, Ferlay J, Lortet-Tieulent J, Jemal A. Global cancer statistics, 2012. *CA Cancer J Clin* 2015; **65**: 87-108 [PMID: 25651787 DOI: 10.3322/caac.21262]
2 **Chen W**, Zheng R, Baade PD, Zhang S, Zeng H, Bray F, Jemal A, Yu XQ, He J. Cancer statistics in China, 2015. *CA Cancer J Clin* 2016; **66**: 115-132 [PMID: 26808342 DOI: 10.3322/caac.21338]
3 **Kim JY**, Chung SM, Choi BO, Kay CS. Hepatocellular carcinoma with portal vein tumor thrombosis: Improved treatment outcomes with external beam radiation therapy. *Hepatol Res* 2011; **41**: 813-824 [PMID: 21696524 DOI: 10.1111/j.1872-034X.2011.00826.x]
4 **Okuda K**, Ohtsuki T, Obata H, Tomimatsu M, Okazaki N, Hasegawa H, Nakajima Y, Ohnishi K. Natural history of hepatocellular carcinoma and prognosis in relation to treatment. Study of 850 patients. *Cancer* 1985; **56**: 918-928 [PMID: 2990661 DOI: 10.1002/1097-0142(19850815)56:4<918::aid-cncr2820560437>3.0.co;2-e]
5 **Cabibbo G**, Tremosini S, Galati G, Mazza G, Gadaleta-Caldarola G, Lombardi G, Antonucci M, Sacco R. Transarterial chemoembolization and sorafenib in hepatocellular carcinoma. *Expert Rev Anticancer Ther* 2014; **14**: 831-845 [PMID: 24850249 DOI: 10.1586/14737140.2014.920694]
6 **Sugiyama S**, Beppu T, Ishiko T, Takahashi M, Masuda T, Hirata T, Imai K, Hayashi H, Takamori H, Kanemitsu K, Hirota M, Murakami R, Baba Y, Oya N, Yamashita Y, Baba H. Efficacy of radiotherapy for PV and IVC tumor thrombosis in unresectable HCC. *Hepatogastroenterology* 2007; **54**: 1779-1782 [PMID: 18019717 DOI: 10.1016/j.radonc.2007.07.005]
7 **Lee DS**, Seong J. Radiotherapeutic options for hepatocellular carcinoma with portal vein tumor thrombosis. *Liver Cancer* 2014; **3**: 18-30 [PMID: 24804174 DOI: 10.1159/000343855]
8 **Yamakado K**, Tanaka N, Nakatsuka A, Matsumura K, Takase K, Takeda K. Clinical efficacy of portal vein stent placement in patients with

hepatocellular carcinoma invading the main portal vein. *J Hepatol* 1999; **30**: 660-668 [PMID: 10207808 DOI: 10.1016/s0168-8278(99)80197-4]

9 **Xiang B**, Xiang H. Effect Analysis of TACE Combined with Portal Vein Stent Implantation Treating Primary Liver Cancer with Portal Vein Tumor Thrombus. Shiyong Aizheng Zazhi 2017; 32: 1494-1497

10 **Zhang L**, Lu LG, Li Y, Shao PJ, Hu BS, Wei ZG, He X, Yu XY, Luo XN. [Portal vein stent placement combined with TACE for the treatment of hepatocellular carcinoma associated with tumor thrombus in portal vein]. *Jieru Fangshexue Zazhi* 2011; **20**: 968-973

11 **Higgins JP**, Altman DG, Gøtzsche PC, Jüni P, Moher D, Oxman AD, Savovic J, Schulz KF, Weeks L, Sterne JA; Cochrane Bias Methods Group; Cochrane Statistical Methods Group. The Cochrane Collaboration's tool for assessing risk of bias in randomised trials. *BMJ* 2011; **343**: d5928 [PMID: 22008217 DOI: 10.1136/bmj.d5928]

12 **Higgins JP**, Thompson SG. Quantifying heterogeneity in a meta-analysis. *Stat Med* 2002; **21**: 1539-1558 [PMID: 12111919 DOI: 10.1002/sim.1186]

13 **Egger M**, Davey Smith G, Schneider M, Minder C. Bias in meta-analysis detected by a simple, graphical test. *BMJ* 1997; **315**: 629-634 [PMID: 9310563 DOI: 10.1136/bmj.315.7109.629]

14 **Chuan-Xing L**, Xu H, Bao-Shan H, Yong L, Pei-Jian S, Xian-Yi Y, Xiao-Ning L, Li-Gong L. Efficacy of therapy for hepatocellular carcinoma with portal vein tumor thrombus: chemoembolization and stent combined with iodine-125 seed. *Cancer Biol Ther* 2011; **12**: 865-871 [PMID: 22037354 DOI: 10.4161/cbt.12.10.17676]

15 **Zhang XB**, Wang JH, Yan ZP, Qian S, Du SS, Zeng ZC. Hepatocellular carcinoma with main portal vein tumor thrombus: treatment with 3-dimensional conformal radiotherapy after portal vein stenting and transarterial chemoembolization. *Cancer* 2009; **115**: 1245-1252 [PMID: 19156918 DOI: 10.1002/cncr.24139]

16 **Wang CG**, Wang XL, Gong GQ, Chen G, Zeng ZC, Qiu WL, Lin GL, Chen Y, Li GP. [The preliminary study of metallic stent implantation in combination with three-dimensional conformal radiation therapy in the treatment of hepatocellular carcinoma patients with portal vein tumor thrombus]. *Zhonghua Gan Zang Bing Za Zhi* 2009; **17**: 417-421 [PMID: 19567018 DOI: 10.21203/rs.3.rs-88313/v1]

17 **Wu LL**, Luo JJ, Yan ZP, Wang JH, Wang XL, Zhang XB, Fang ZT, Zhang W. [Comparative study of portal vein stent and TACE combined therapy with or without endovascular implantation of iodine-125 seeds strand for treating patients with hepatocellular carcinoma and main portal vein tumor thrombus]. *Zhonghua Gan Zang Bing Za Zhi* 2012; **20**: 915-919 [PMID: 23522253 DOI: 10.3760/cma.j.issn.1007-3418.2012.12.009]

18 **Zhang XB**, Wang JH, Yan ZP, Qian S, Du SS, Zeng ZC. [Hepatocellular carcinoma complicated by mare portal vein tumor thrombus:treated by portal vein slenting, transarterial chemoembolizalion and 3-dimemional conformal radiotherapy]. *Zhonghua Fangshexue Zazhi* 2008; **24**: 1311-1315 [DOI: 10.3321/j.issn:1005-1201.2008.12.018]

19 **Zhang ZH**, Liu QX, Zhang W, Ma JQ, Wang JH, Luo JJ, Liu LX, Yan ZP. Combined endovascular brachytherapy, sorafenib, and transarterial chemobolization therapy for hepatocellular carcinoma patients with portal vein tumor thrombus. *World J Gastroenterol* 2017; **23**: 7735-7745 [PMID: 29209114 DOI: 10.3748/wjg.v23.i43.7735]

20 **Shi J**, Lai EC, Li N, Guo WX, Xue J, Lau WY, Wu MC, Cheng SQ. Surgical treatment of hepatocellular carcinoma with portal vein tumor thrombus. *Ann Surg Oncol* 2010; **17**: 2073-2080 [PMID: 20131013 DOI: 10.1245/s10434-010-0940-4]

21 **Dawson LA**, Ten Haken RK, Lawrence TS. Partial irradiation of the liver. *Semin Radiat Oncol* 2001; **11**: 240-246 [PMID: 11447581 DOI: 10.1053/srao.2001.23485]

22 **Yamakado K**, Nakatsuka A, Tanaka N, Fujii A, Terada N, Takeda K. Malignant portal venous obstructions treated by stent placement: significant factors affecting patency. *J Vasc Interv Radiol* 2001; **12**: 1407-1415 [PMID: 11742015 DOI: 10.1016/s1051-0443(07)61699-6]

23 **Ishikura S**, Ogino T, Furuse J, Satake M, Baba S, Kawashima M, Nihei K, Ito Y, Maru Y, Ikeda H. Radiotherapy after transcatheter arterial chemoembolization for patients with hepatocellular carcinoma and portal vein tumor thrombus. *Am J Clin Oncol* 2002; **25**: 189-193 [PMID: 11943901 DOI: 10.1097/00000421-200204000-00019]

World Journal of Clinical Oncology

Submit a Manuscript: https://www.f6publishing.com

World J Clin Oncol 2024 March 24; 15(3): 456-463

DOI: 10.5306/wjco.v15.i3.456

ISSN 2218-4333 (online)

CASE REPORT

PD-1 antibody in combination with chemotherapy for the treatment of SMARCA4-deficient advanced undifferentiated carcinoma of the duodenum: Two case reports

Yi-Nan Shi, Xiao-Rui Zhang, Wei-Yu Ma, Jing Lian, Yan-Feng Liu, Yi-Fan Li, Wen-Hui Yang

Specialty type: Gastroenterology and hepatology

Provenance and peer review: Unsolicited article; Externally peer reviewed.

Peer-review model: Single blind

Peer-review report's scientific quality classification

Grade A (Excellent): A
Grade B (Very good): 0
Grade C (Good): 0
Grade D (Fair): D
Grade E (Poor): 0

P-Reviewer: Rizzo A, Italy

Received: January 2, 2024
Peer-review started: January 2, 2024
First decision: January 10, 2024
Revised: January 23, 2024
Accepted: February 21, 2024
Article in press: February 21, 2024
Published online: March 24, 2024

Yi-Nan Shi, Xiao-Rui Zhang, Wei-Yu Ma, Yan-Feng Liu, Wen-Hui Yang, Department of Gastroenterology and Hepatology, Shanxi Province Cancer Hospital/Shanxi Hospital Affiliated to Cancer Hospital, Chinese Academy of Medical Sciences/Cancer Hospital Affiliated to Shanxi Medical University, Taiyuan 030013, Shanxi Province, China

Jing Lian, Department of Pathology, Shanxi Province Cancer Hospital/Shanxi Hospital Affiliated to Cancer Hospital, Chinese Academy of Medical Sciences/Cancer Hospital Affiliated to Shanxi Medical University, Taiyuan 030013, Shanxi Province, China

Yi-Fan Li, Department of General Surgery, Shanxi Province Cancer Hospital/Shanxi Hospital Affiliated to Cancer Hospital, Chinese Academy of Medical Sciences/Cancer Hospital Affiliated to Shanxi Medical University, Taiyuan 030013, Shanxi Province, China

Corresponding author: Wen-Hui Yang, PhD, Associate Chief Physician, Department of Gastroenterology and Hepatology, Shanxi Province Cancer Hospital/Shanxi Hospital Affiliated to Cancer Hospital, Chinese Academy of Medical Sciences/Cancer Hospital Affiliated to Shanxi Medical University, No. 3 Zhigong Xin Street, Taiyuan 030013, Shanxi Province, China. yangwenhui-10012@163.com

Abstract

BACKGROUND

SMARCA4 is a component of chromatin remodeling of SWItch/sucrose-nonfermenting (SWI/SNF) complexes and plays an essential role in oncogenesis. SMARCA4-deficient malignancies arising from the gastrointestinal tract are rare and have a poor prognosis. There is no standard treatment for advanced and undifferentiated SMARCA4-deficient duodenal malignancies. Programmed death 1 (PD-1) antibodies, known as immune checkpoint inhibitor antibodies, potentially play a role in treating gastrointestinal tract malignancies.

CASE SUMMARY

We present two patients with SMARCA4 deficiency and *TP53* gene mutation in advanced undifferentiated carcinomas of the duodenum. For both patients, SMARCA4 deficiency was confirmed by immunohistochemical staining for the BRG1 protein, while *TP53* gene mutations were observed *via* next-generation sequencing. Both patients were administered chemotherapy in combination with an anti-PD-1 antibody. The two patients exhibited completely different responses

to treatment and had different prognoses. Case 1 experienced rapid progression after PD-1 infusion and chemotherapy, case 2 experienced a remarkable response after treatment, and the progression-free survival was more than 6 months.

CONCLUSION
This study described our clinical and pathological observations of SMARCA4-deficient advanced undifferentiated carcinoma of the duodenum. PD-1 combined with chemotherapy showed a certain efficacy in select patients, providing options for treating these highly malignant tumors. Patients with liver metastases had a worse prognosis than did those with only lymph node metastasis.

Key Words: SMARCA4 deficiency; Undifferentiated carcinomas; Chemotherapy; Programmed death 1; Immune checkpoint inhibitors; Case report

Core Tip: SMARCA4-deficient malignancies arising from the gastrointestinal tract are rare and have a poor prognosis. We present two patients diagnosed with advanced duodenal undifferentiated carcinoma by immunohistochemical staining for SMARCA4 deficiency and *TP53* gene mutations. Patients with high tumor mutational burden responded well to programmed death 1 antibodies in combination with chemotherapy, and those with liver metastases had a worse prognosis.

Citation: Shi YN, Zhang XR, Ma WY, Lian J, Liu YF, Li YF, Yang WH. PD-1 antibody in combination with chemotherapy for the treatment of SMARCA4-deficient advanced undifferentiated carcinoma of the duodenum: Two case reports. *World J Clin Oncol* 2024; 15(3): 456-463
URL: https://www.wjgnet.com/2218-4333/full/v15/i3/456.htm
DOI: https://dx.doi.org/10.5306/wjco.v15.i3.456

INTRODUCTION

The small intestine accounts for only 1%-1.4% of all gastrointestinal (GI) malignancies. The most common primary malignancy in the small bowel is adenocarcinoma, with the duodenum being the most frequently affected site. Various histological subtypes of duodenal malignancies, including adenocarcinoma, sarcoma, lymphoma, and neuroendocrine tumors, have been identified. Undifferentiated carcinoma of the duodenum, characterized by rhabdoid features, is a rare form of malignancy. A previous study revealed that, in most cases, patients with undifferentiated/rhabdoid carcinoma in the gastrointestinal tract lacked expression of at least one of the four SWItch/sucrose-nonfermenting (SWI/SNF) complex subunits, namely, SMARCB1, SMARCA2, SMARCA4, and ARID1A[1,2]. The SWI/SNF complex is an ATP-consuming multisubunit cellular machine that modulates chromatin compaction, thereby regulating DNA-related processes such as transcription, replication, and DNA repair and oncogenesis[3,4]. The absence of the key proteins INI1 and BRG1, which are encoded by SMARCB1 and SMARCA4, respectively, is commonly observed in various malignancies, including atypical teratoid/rhabdoid tumors, epithelioid sarcoma, and ovarian small-cell carcinomas of the hypercalcemic type[3,5].

Recently, investigations into SMARCA4 inactivation as a driver event in malignancies have been performed. Mutations leading to the loss of expression of these protein components have also been identified in a subset of poorly differentiated or undifferentiated carcinomas at many sites throughout the body. These include the sinonasal tract[4], lung[5], gastrointestinal tract[6,7], and uterus[8].

In this case report, we documented two patients diagnosed with duodenal SMARCA4-deficient undifferentiated carcinoma who underwent immunohistopathological tests combined with next-generation sequencing and multiplex immunofluorescence analysis. There is no current standard treatment for advanced and undifferentiated SMARCA4-deficient duodenal malignancies. Both patients were administered chemotherapy in combination with programmed death 1 (PD-1) antibody, known as immune checkpoint inhibitor (ICI). Patients with high tumor mutational burden (TMB) responded well to PD-1 antibodies in combination with chemotherapy, and those with liver metastases had a worse prognosis.

CASE PRESENTATION

Chief complaints

Case 1: A 51-year-old male patient presented to our hospital with increasing upper abdominal pain for more than one month.

Case 2: A 43-year-old female complained of intermittent upper abdominal pain for 4 months and enlargement of the left supraclavicular lymph nodes.

History of present illness

Case 1: The patient's premorbidity was good, with an Eastern Cooperative Oncology Group performance status score of 0. Gastroscopy revealed an ulcer in the descending part of the duodenum, approximately 3 cm × 3.5 cm, with irregular protrusions around the perimeter. A biopsy from the descending part of the duodenum was performed by endoscopy, and an ulcerative mass was found.

Case 2: Gastroenteroscopy was also conducted, and an ulcer in the duodenal papilla was found. Biopsy revealed undifferentiated carcinoma of the duodenum, and contrast-enhanced computed tomography (CT) indicated multiple lymph node metastases involving the retroperitoneal lymph nodes.

History of past illness

Case 1: He had no history of smoking or drinking or a significant medical history.

Case 2: She had no history of smoking or drinking or a significant medical history.

Personal and family history

Case 1: The patient had no personal or family history.

Case 2: The patient had no personal or family history.

Physical examination

Case 1: The patient had mild upper abdominal tenderness.

Case 2: A mass in the left neck was palpated.

Laboratory examinations

Case 1: All of the tumor marker results in the blood sample were negative.

Case 2: An elevated CEA level of 5.14 μg/L was observed. CA199, CA242, and CA724 were all negative.

Imaging examinations

Case 1: An initial CT scan and magnetic resonance imaging (MRI) with enhanced contrast agent injection showed abnormal wall thickening in the duodenal ampulla and multiple liver nodular masses revealing malignant metastases. Retroperitoneal lymphadenopathy was also considered (Figure 1A and B).

Case 2: Gastroenteroscopy was also conducted, and an ulcer in the duodenal papilla was found. Biopsy revealed undifferentiated carcinoma of the duodenum. Contrast-enhanced CT indicated multiple lymph node metastases involving the retroperitoneal lymph nodes (Figure 2A and B).

Further diagnostic work-up

Case 1: Histology was performed, and the epithelioid or undifferentiated tumor cells grew in cords or nests. hematoxylin-eosin staining is shown in Figure 1E. Extensive areas of necrosis were observed within the tumor. The immunohistological analysis revealed the following results: Ki-67 (approximately more than 90% positive), CK7 (-), SMARCA4 (-), and INSM1 (-) (Figure 1F). Multiplex immunofluorescence staining was also analyzed. PD-L1 expression was positive, with a CPS of 5, and microsatellite stabilization (MSS) was observed. The tumor immune microenvironment was classified as an acquired immune tolerance type according to the presence of both CD8+ tumor-infiltrated lymphocytes TILs and PD-L1-expressing cells. Notably, tertiary lymphoid structures were not found in the tumor area (Figure 1G and H). Next-generation sequencing of biopsy tissue was subsequently performed. The results revealed TP53 and CTNNB1 mutations (Table 1). However, the SMARCA4 mutation variant was not observed in this patient.

The final pathological diagnosis was duodenal SMARCA4-deficient undifferentiated carcinoma, clinical stage IV with multiple liver metastases and retroperitoneal lymph node metastases.

Case 2: Immunohistopathological staining revealed the following results: Ki-67 (90%+) and SMARCA4 (-) (Figure 2E and F). Next-generation sequencing revealed *TP53*, *NCOR1*, *MYH9*, *ERBB3*, *RAD52* and *CTNNB1* mutations (Table 1), and the TMB increased to 10.56/Mb, with a score of 6 for PD-L1 expression. MSS was observed. However, the SMARCA4 mutation variant was not observed in this patient.

FINAL DIAGNOSIS

The final pathological diagnosis was duodenal SMARCA4-deficient undifferentiated carcinoma, clinical stage IV with multiple lymph node metastases.

Table 1 Genomic profile of somatic alterations for the patients

	Gene	Transcript description	Mutant allele frequency
Case 1	*TP53*	NM_000546.5:c.742C>T(p.Arg 248Trp)	20.9%
	CTNNB1	NM_001098209.1:c.134C>T(p.Ser45Phe)	23.4%
Case 2	*TP53*	NM_000546.5: c.1024C>T(p.R342)	23.2%
	NCOR1	NM_006311.3 :c.5689T>G (p.S1897A)	18.7%
	MYH9	NM_002473.4 : c.1560C[6>7] (p.I524Hfs*44)	15.9%
	ERBB3	NM_001982.3 : c.850G>C (p.G284R)	15.0%
	RAD52	NM_134424.2 : c.779G>A (p.R260Q)	14.8%
	CTNNB1	NM_001904.3 :c.133T>C (p.S45P)	14.2%

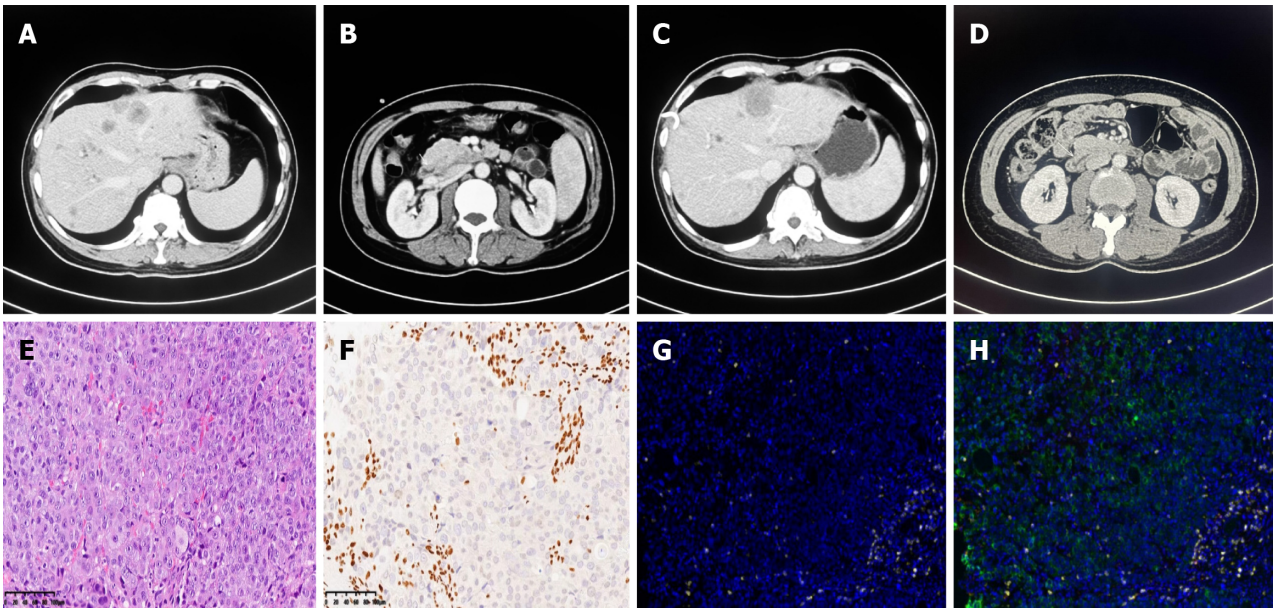

Figure 1 No response to immunochemotherapy or disease progression was confirmed by contrast computed tomography in case 1. A and B: A mass in the descending part of the duodenum and multiple liver metastases at the end of 1st-line chemotherapy; C and D: Disease progression was confirmed by enlargement of liver metastases and infusions and impaired liver function with persisting mixed jaundice even after percutaneous transhepatic cholangial drainage; E: H&E: The undifferentiated tumor cells grew in cords, nests, and diffuse sheets, and the nucleus of the tumor was vacuolated with obvious nucleoli. Mitotic images and scattered multinucleated giant cells were also observed. Extensive areas of necrosis were observed within the tumor; F: The SMARCA4 protein was negative for BRG1 according to immunohistology; G: CD8+ T-cell infiltration was assessed by multiple immunofluorescence assays; H: Tertiary lymphoid structures were not intact, and case 1 was classified as an acquired immune tolerance type by microenvironment analysis.

TREATMENT

Case 1

First, two cycles of bevacizumab in combination with the XELOX regimen were initiated on March 10, 2023 (bevacizumab, 7.5 mg/kg D1 + oxaliplatin, 130 mg/m^2 D1 + capecitabine, 1250 mg/m^2 D1-14; Q21D). However, an enlargement of liver metastases was detected, and disease progression was considered. Given the positive expression of PD-L1 and the acquired immune tolerance environment, we introduced a second-line combination therapy comprising a PD-1 antibody, nab-paclitaxel and gemcitabine (nab-paclitaxel 220 mg/m^2 D1 + gemcitabine 1000 mg/m^2 D1 and D8; Q21D), and the patient initially exhibited good tolerance. After two cycles of second-line immunotherapy-chemotherapy combination therapy, progressive disease was observed as liver-targeted lesions increased significantly after infusion (Figure 1C and D). Disease progression was considered. However, the patient refused subsequent immunochemotherapy. The timeline of the summarizing events is shown in Figure 3A.

Case 2

This patient received PD-1 antibody in combination with chemotherapy comprising nab-paclitaxel and cisplatin for six cycles (nab-paclitaxel 220 mg/m^2 D1 + cisplatin 80 mg/m^2 D1; Q21D). The patient responded positively to this combination therapy. Disease regression with extensively shrunken retroperitoneal lymph nodes was observed

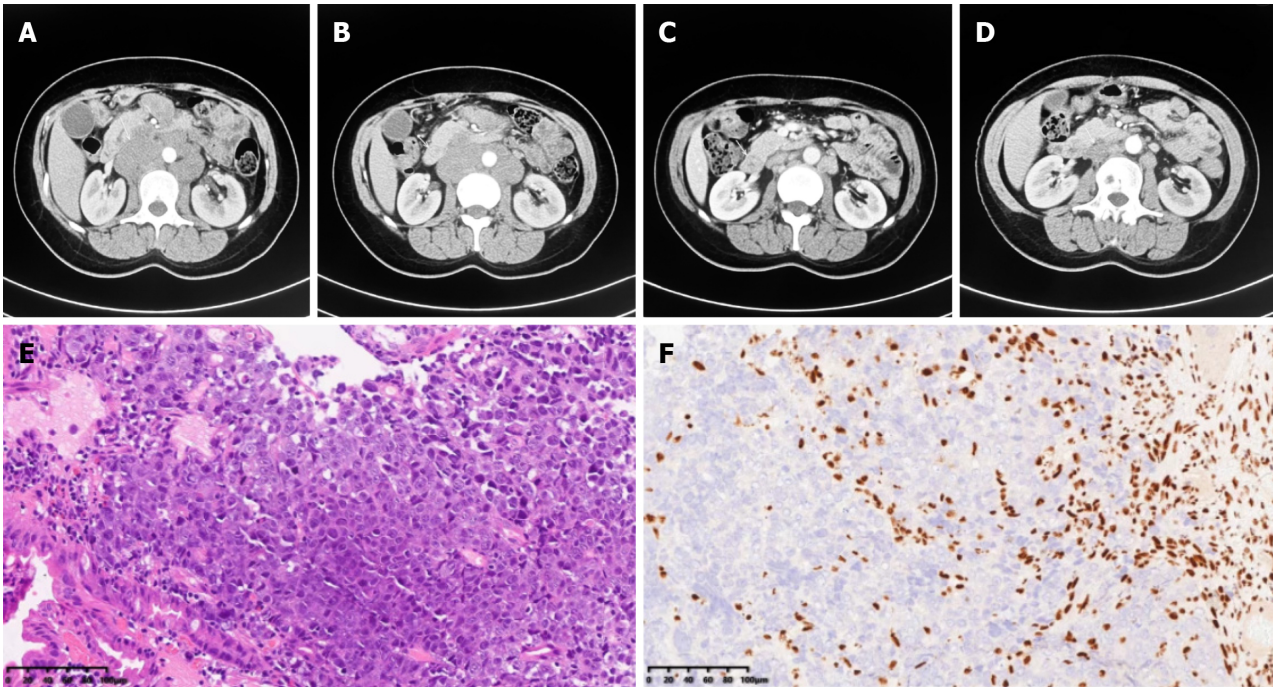

Figure 2 Major response to immunochemotherapy and disease regression in case 2. A and B: A mass in the descending part of the duodenum and multiple retroperitoneal lymph node metastases initially observed; C and D: Significant disease regression after the administration of immunochemotherapy; E: H&E: The undifferentiated tumor cells were diffusely distributed, and patchy necrosis was observed; F: The SMARCA4 protein was negative for BRG1 according to immunohistology.

(Figure 2C and D), with an improvement in the general condition of the patient. After six cycles of combination therapy, the patient started PD-1 antibody maintenance treatment, and the disease was in remission. Patients showed disease progression with liver metastases at 6 months after diagnosis, and second-line therapy was administered. The second-line therapy consisted of the XELIRI regimen and bevacizumab (bevacizumab, 7.5 mg/kg D1 + irinotecan, 180 mg/m^2 D1 + capecitabine, 1250 mg/m^2 D1-14; Q21D). The patient was administered two cycles of second-line treatment and started receiving the best supportive care for cachexia and obvious weight loss. The timeline of the summarizing events is shown in Figure 3B.

OUTCOME AND FOLLOW-UP

Case 1

The patient suffered from significant mixed jaundice and showed no improvement after supportive care. Finally, the patient died from liver failure on September 15, 2023, with an overall survival period of 6 months. The progression-free survival (PFS) times for first-line and second-line therapy were both 8 wk.

Case 2

The patient died from this malignancy on January 4, 2024.

DISCUSSION

Duodenal malignancies are uncommon but highly fatal, and undifferentiated duodenal malignancies are extremely rare. As extensive immunohistochemical profiling has been performed for malignancies such as atypical rhabdoid tumors or epithelioid sarcomas, SMARCA4-deficient malignancies are frequently observed and can be identified[1,9]. Undifferentiated carcinomas with rhabdoid cells are characteristic diagnostic clues, and SWI/SNF complex deficiencies are complex molecular events of undifferentiated carcinoma. It is highly malignant and has a short survival time, with no standard treatment at present. Several case reports and retrospective studies have analyzed SMARCA4-deficient malignancies arising from the gastrointestinal tract[1,6,7,9]. A previous study demonstrated that a small proportion of gastroesophageal carcinomas exhibit loss of SMARCA4 expression separately or with coinactivation of other subunits of SWI/SNF complexes[1]. Among the two patients, not all SMARCA4-deficient tumors harbored SMARCA4 pathological genomic variants. Although these tumors exhibit poorly differentiated and undifferentiated morphologies, they exhibit a broad range of genomic variant features[7,9,10]. First, compared with gastroesophageal adenocarcinomas, SMARCA4-deficient gastroesophageal carcinomas exhibit a similar range of somatic mutations, including enrichment of TP53, KRAS,

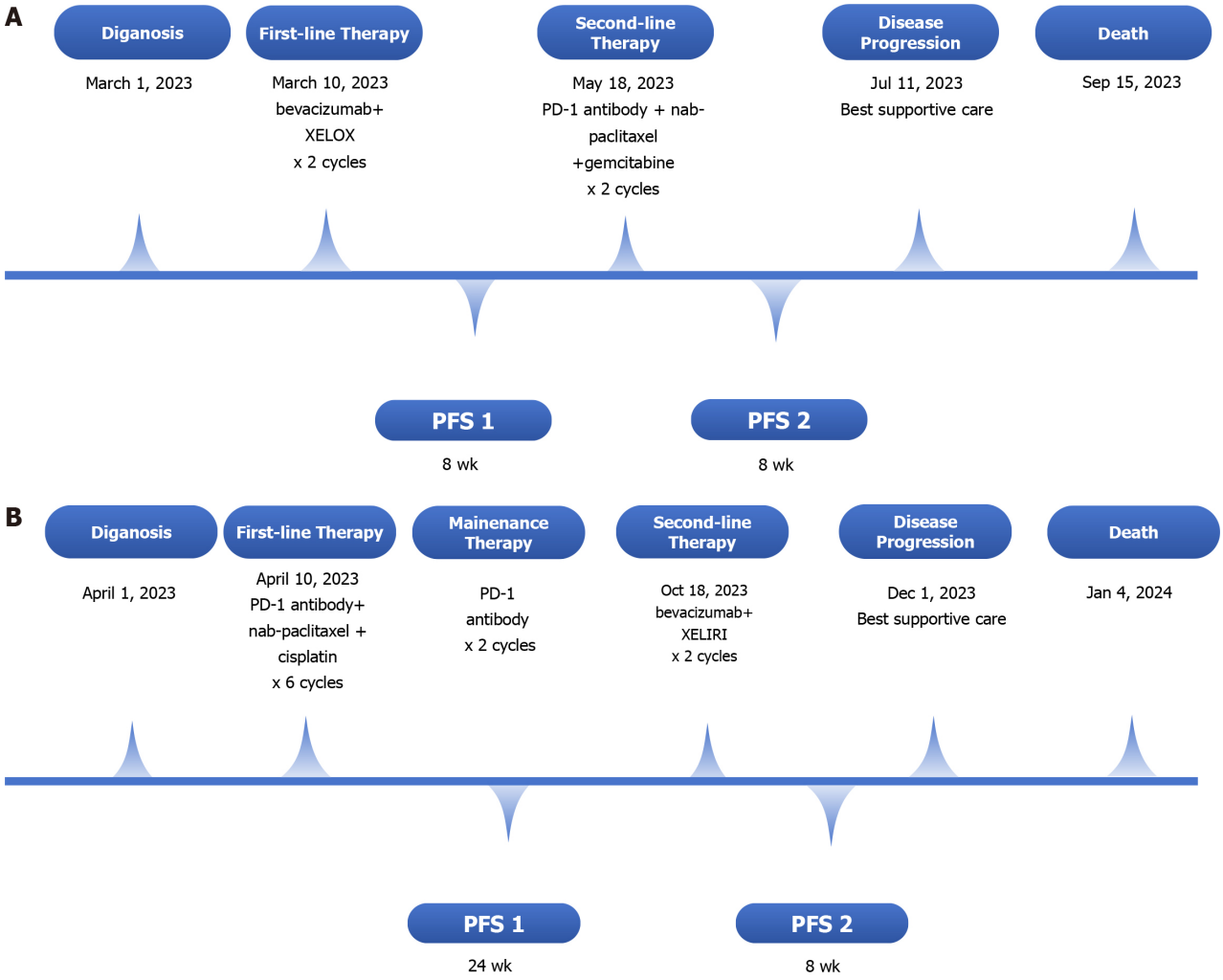

Figure 3 Timeline summarizing. A: Case 1; B: Case 2. PFS: Progression-free survival; PFS1: PFS time during first-line therapy; PFS2: PFS time during second-line therapy.

ARID1A, and APC mutations. The most common cooccurring mutations in pathogenic SMARCA4 were identified in TP53, APC, ARID1A, CDKN2A, and CTNNB1[7]. On the one hand, this difference may be attributed to the limitations of NGS in accurately detecting large deletions. Additionally, epigenetic modifications, including DNA methylation, histone modifications, and noncoding RNAs, may also contribute to deficiencies in gene expression. Therefore, some investigators have proposed that most SMARCA4-deficient gastroesophageal carcinomas are considered undifferentiated or dedifferentiated gastroesophageal adenocarcinomas rather than distinct biological entities[9,10].

Several factors, such as PD-L1 expression, tumor mutational burden, body mass index, and laboratory parameters (including the neutrophil-to-lymphocyte ratio), may predict the response to immunotherapy as well as immune chemotherapy.

As somatic mutations generate neoantigens, a high TMB is expected to induce a positive antitumor response. However, it can serve as a biomarker for predicting favorable responses to ICIs. The ability of high TMB to predict the efficacy of immunotherapy was not affected by the expression of PD-L1. Hence, some patients benefit from immunotherapy and have prolonged survival[10,11]. The infiltration of CD8+ lymphocytes and positive PD-L1 expression are also considered potential predictive biomarkers of immunotherapy response[12].

In previous studies, immunochemotherapy has been shown to have various anticancer effects, including immunogenic cell death and a reduction in the number of tumor cells that are engaged in the production of immunosuppressive substances[13,14]. Furthermore, the combination of chemotherapy and immunotherapy results in the depletion of myeloid-derived suppressor cells and regulatory T cells. Building upon these principles, the use of chemotherapy combined with immune checkpoint inhibitors (ICIs) has demonstrated synergistic effects. Over the past few years, several trials investigating combination strategies of chemotherapy and ICIs have been presented and published, leading to their approval for diverse solid tumors. Examples of these approved combinations can be found in non-small cell lung cancer, gastric cancer and urothelial carcinoma[15]. As mentioned above, in our second patient, a high TMB was associated with a major partial response to PD-1 antibodies during first-line therapy.

The clinical significance of recognizing SWI/SNF complex-deficient undifferentiated carcinoma/rhabdoid carcinoma lies in its aggressive clinical behavior and poor response to traditional chemotherapy. SMARCA4-deficient undifferentiated tumors originating from the gastrointestinal tract might have a worse prognosis than those originating from the

thorax[11,16]. Adding immunotherapy to conventional chemotherapy may improve the treatment efficacy and increase the response rate. This study was the first to describe the response of SMARCA4-deficient undifferentiated duodenal tumors to immunochemotherapy. According to our observations, case 1 did not benefit from immunotherapy as a second-line chemotherapy, while case 2 benefited from immunochemotherapy combination therapy. The differences in the response of the two patients were partially due to differences in metastatic target organs, differences in mutation genes and differences in the tumor microenvironment, which resulted in differences in tumor mutation burdens. A study reported a median progression-free survival time of 7.2 months in patients who initially presented with metastatic disease, whereas the median overall survival was 13.6 months in patients with malignancies involving the esophagogastric junction and stomach[9].

CONCLUSION

In brief, this case report presented the histopathological and clinical responses of two patients with SMARCA4-deficient advanced undifferentiated carcinoma of the duodenum. PD-1 combined with chemotherapy showed a certain efficacy in select patients, providing options for treating these highly malignant tumors. Patients with liver metastases had a worse prognosis than did those with only lymph node metastasis. Potential molecular mechanisms need to be further studied to elucidate this phenomenon.

FOOTNOTES

Author contributions: Shi YN and Zhang XR analyzed and interpreted the patient data regarding the disease and the diagnosis; Lian J performed the histological examination and diagnosis; Shi YN, Zhang XR, Ma WY and Liu YF handled the therapeutic management of the patient; Liu YF and Yang WH participated in the acquisition, analysis and drafting of the manuscript; all the authors read and approved the final manuscript.

Informed consent statement: The number of ethics approval points was JC2023012. The patients provided written informed consent to participate in this study.

Conflict-of-interest statement: All the authors report no relevant conflicts of interest for this article.

CARE Checklist (2016) statement: The authors have read the CARE Checklist (2016), and the manuscript was prepared and revised according to the CARE Checklist (2016).

Country/Territory of origin: China

ORCID number: Yi-Nan Shi 0009-0007-5660-4654; Yi-Fan Li 0000-0002-6378-7635; Wen-Hui Yang 0000-0002-1452-6789.

S-Editor: Gong ZM
L-Editor: A
P-Editor: Zhao S

REFERENCES

1 **Agaimy A**, Daum O, Märkl B, Lichtmannegger I, Michal M, Hartmann A. SWI/SNF Complex-deficient Undifferentiated/Rhabdoid Carcinomas of the Gastrointestinal Tract: A Series of 13 Cases Highlighting Mutually Exclusive Loss of SMARCA4 and SMARCA2 and Frequent Co-inactivation of SMARCB1 and SMARCA2. *Am J Surg Pathol* 2016; **40**: 544-553 [PMID: 26551623 DOI: 10.1097/PAS.0000000000000554]

2 **Mardinian K**, Adashek JJ, Botta GP, Kato S, Kurzrock R. SMARCA4: Implications of an Altered Chromatin-Remodeling Gene for Cancer Development and Therapy. *Mol Cancer Ther* 2021; **20**: 2341-2351 [PMID: 34642211 DOI: 10.1158/1535-7163.MCT-21-0433]

3 **Jelinic P**, Mueller JJ, Olvera N, Dao F, Scott SN, Shah R, Gao J, Schultz N, Gonen M, Soslow RA, Berger MF, Levine DA. Recurrent SMARCA4 mutations in small cell carcinoma of the ovary. *Nat Genet* 2014; **46**: 424-426 [PMID: 24658004 DOI: 10.1038/ng.2922]

4 **Rooper LM**, Uddin N, Gagan J, Brosens LAA, Magliocca KR, Edgar MA, Thompson LDR, Agaimy A, Bishop JA. Recurrent Loss of SMARCA4 in Sinonasal Teratocarcinosarcoma. *Am J Surg Pathol* 2020; **44**: 1331-1339 [PMID: 32520761 DOI: 10.1097/PAS.0000000000001508]

5 **Sauter JL**, Graham RP, Larsen BT, Jenkins SM, Roden AC, Boland JM. SMARCA4-deficient thoracic sarcoma: a distinctive clinicopathological entity with undifferentiated rhabdoid morphology and aggressive behavior. *Mod Pathol* 2017; **30**: 1422-1432 [PMID: 28643792 DOI: 10.1038/modpathol.2017.61]

6 **Gupta S**, Noona SW, Pambuccian SE, Robinson B, Martin LW, Williams E, Stelow EB, Raghavan SS. Malignant undifferentiated and

rhabdoid tumors of the gastroesophageal junction and esophagus with SMARCA4 loss: a case series. *Hum Pathol* 2023; **134**: 56-65 [PMID: 36549598 DOI: 10.1016/j.humpath.2022.12.008]

7 **Neil AJ**, Zhao L, Isidro RA, Srivastava A, Cleary JM, Dong F. SMARCA4 Mutations in Carcinomas of the Esophagus, Esophagogastric Junction, and Stomach. *Mod Pathol* 2023; **36**: 100183 [PMID: 37054973 DOI: 10.1016/j.modpat.2023.100183]

8 **Kolin DL**, Dong F, Baltay M, Lindeman N, MacConaill L, Nucci MR, Crum CP, Howitt BE. SMARCA4-deficient undifferentiated uterine sarcoma (malignant rhabdoid tumor of the uterus): a clinicopathologic entity distinct from undifferentiated carcinoma. *Mod Pathol* 2018; **31**: 1442-1456 [PMID: 29700418 DOI: 10.1038/s41379-018-0049-z]

9 **Chang B**, Sheng W, Wang L, Zhu X, Tan C, Ni S, Weng W, Huang D, Wang J. SWI/SNF Complex-deficient Undifferentiated Carcinoma of the Gastrointestinal Tract: Clinicopathologic Study of 30 Cases With an Emphasis on Variable Morphology, Immune Features, and the Prognostic Significance of Different SMARCA4 and SMARCA2 Subunit Deficiencies. *Am J Surg Pathol* 2022; **46**: 889-906 [PMID: 34812766 DOI: 10.1097/PAS.0000000000001836]

10 **Zhu PP**, Li XX, Liu JH, Du XL, Su HY, Wang J. [SMARCA4-deficient undifferentiated carcinoma of the gastrointestinal tract: a clinicopathological and immunohistochemical study of nine cases]. *Zhonghua Bing Li Xue Za Zhi* 2022; **51**: 868-874 [PMID: 36097904 DOI: 10.3760/cma.j.cn112151-20220226-00130]

11 **Schoenfeld AJ**, Bandlamudi C, Lavery JA, Montecalvo J, Namakydoust A, Rizvi H, Egger J, Concepcion CP, Paul S, Arcila ME, Daneshbod Y, Chang J, Sauter JL, Beras A, Ladanyi M, Jacks T, Rudin CM, Taylor BS, Donoghue MTA, Heller G, Hellmann MD, Rekhtman N, Riely GJ. The Genomic Landscape of SMARCA4 Alterations and Associations with Outcomes in Patients with Lung Cancer. *Clin Cancer Res* 2020; **26**: 5701-5708 [PMID: 32709715 DOI: 10.1158/1078-0432.CCR-20-1825]

12 **Iijima Y**, Sakakibara R, Ishizuka M, Honda T, Shirai T, Okamoto T, Tateishi T, Sakashita H, Tamaoka M, Takemoto A, Kumaki Y, Ikeda S, Miyazaki Y. Notable response to nivolumab during the treatment of SMARCA4-deficient thoracic sarcoma: a case report. *Immunotherapy* 2020; **12**: 563-569 [PMID: 32363992 DOI: 10.2217/imt-2019-0142]

13 **Rizzo A**, Ricci AD, Lanotte L, Lombardi L, Di Federico A, Brandi G, Gadaleta-Caldarola G. Immune-based combinations for metastatic triple negative breast cancer in clinical trials: current knowledge and therapeutic prospects. *Expert Opin Investig Drugs* 2022; **31**: 557-565 [PMID: 34802383 DOI: 10.1080/13543784.2022.2009456]

14 **Mollica V**, Rizzo A, Marchetti A, Tateo V, Tassinari E, Rosellini M, Massafra R, Santoni M, Massari F. The impact of ECOG performance status on efficacy of immunotherapy and immune-based combinations in cancer patients: the MOUSEION-06 study. *Clin Exp Med* 2023; **23**: 5039-5049 [PMID: 37535194 DOI: 10.1007/s10238-023-01159-1]

15 **Paz-Ares L**, Luft A, Vicente D, Tafreshi A, Gümüş M, Mazières J, Hermes B, Çay Şenler F, Csőszi T, Fülöp A, Rodríguez-Cid J, Wilson J, Sugawara S, Kato T, Lee KH, Cheng Y, Novello S, Halmos B, Li X, Lubiniecki GM, Piperdi B, Kowalski DM; KEYNOTE-407 Investigators. Pembrolizumab plus Chemotherapy for Squamous Non-Small-Cell Lung Cancer. *N Engl J Med* 2018; **379**: 2040-2051 [PMID: 30280635 DOI: 10.1056/NEJMoa1810865]

16 **Kim TK**, Herbst RS, Chen L. Defining and Understanding Adaptive Resistance in Cancer Immunotherapy. *Trends Immunol* 2018; **39**: 624-631 [PMID: 29802087 DOI: 10.1016/j.it.2018.05.001]

Published by **Baishideng Publishing Group Inc**
7041 Koll Center Parkway, Suite 160, Pleasanton, CA 94566, USA
Telephone: +1-925-3991568
E-mail: office@baishideng.com
Help Desk: https://www.f6publishing.com/helpdesk
https://www.wjgnet.com